Synthesis, Conformational Dynamics and Spectro-electrochemical Characteristics of Core-Modified Expanded Isophlorinoids

A Thesis

Submitted in Partial Fulfillment of the Requirements

for the Degree of

Doctor of Philosophy

By

UDAYA H S

20153403

INDIAN INSTITUTE OF SCIENCE EDUCATION AND RESEARCH PUNE

2023

Dedicated to,

My Doddamma…

Smt. Dhanalakshmamma K. V.

CERTIFICATE

Certified that the work incorporated in the thesis entitled ***"Synthesis, Conformational Dynamics and Spectro-electrochemical Characteristics of Core-Modified Expanded Isophlorinoids"*** Submitted by ***Mr. UDAYA H S*** was carried out by the candidate, under my supervision. The work presented here or any part of it has not been included in any other thesis submitted previously for the award of any degree or diploma from any other University or institution.

Date: 28th February 2023

Prof. V. G. Anand

Declaration

I declare that this written submission represents my ideas in my own words and where others' ideas have been included; I have adequately cited and referenced the original sources. I also declare that I have adhered to all principles of academic honesty and integrity and have not misrepresented or fabricated or falsified any idea/data/fact/source in my submission. I understand that violation of the above will be cause for disciplinary action by the Institute and can also evoke penal action from the sources which have thus not been properly cited or from whom proper permission has not been taken when needed.

Date: 28th February 2023 **UDAYA H S**

Roll No. 20153403

Acknowledgment

Accomplishment of PhD journey, not only my individual effort, it's a motivation, vision and support of so many responsible persons in my life. This is an opportunity to thankful to them individually.

First I sincerely thankful to my thesis supervisor Prof. V. G. Anand sir, it's very difficult express my sincere gratitude to you sir. Sir, you never strict professor for us but patiently taught all the basic discipline and values of life. Sir, I greatly thankful to you, now I am near to complete degree only because of the strength that you are always with me, especially in my difficult time, at my failures, at my dark days, thank you sir. In fact I am very thank and inspired by your unique ideas, unique knowledge, each and every small observations, way of interacting with students, and the respect you gave to students and their efforts and your effort to make that work to the best level and your valuable suggestions inspired to work in the right direction, thank you sir. Sir I am admirer for your soft words, kindness, smile, and your respectful behaviour with us. Sir I thankful for the continuous support and motivation and I also believe that you will be with us to motivate, strengthen and enlighten the future life. I knew sir, I made lot of mistakes knowingly and unknowingly, but you never scolded or punished us but very silently you corrected those mistakes with time, thank you sir. I always remember each and every best moment I spend with you. Finally I am too lucky, honour and I have complete satisfaction as your student, thank you sir.

My heartfelt thanks to my best teacher Prof. Ramakrishna G. Bhat sir, sir always motivates and gave the full strength throughout my degree. Sir words always energetic and motivates to work, I feel very lucky to get a teacher like you, I greatly thankful to you sir.

I would like to thank Priya ma'am and sir father, gave the homely environment with care whenever I visit to your home. Ma'am I always remember I am coming by skipping previous meal to have food, thank you ma'am and also dedicate my love and best wishes to Savi and Somu.

I thankful to my Grandmother Smt. Chikkathirumalamma and Grandfather Shri, Dassaiah, their unrestrained blessings, love and care was my strength always in life. I thankful to my Doddamma smt. Dhanalakshamamma, because of her knowledge, discipline, truthiness and firing words took me here and giving the strength to move forward. I also thankful to my Doddappa Dr. Dasappa, always motivate and pushed me towards higher education, he is

always nearest inspiration to me and also thankful to sister Komala and brother Darshan. I always thankful to my maama, Sri. Venkateshiah, Sri. Ramaswamy and Sri. Chinnagiri, they hold my hand firmly with love and care, I am lucky to have parents like you.

I thankful to my friend Syed Ibrahim, both we took the strong decision for CSIR-NET preparation at our difficult time, in fact our strong belief and our friendship made it possible. Thank you.

I am really lucky to get best friends Yogaraju, Siddu, Rudra, Raghavendra, Vinusha, Dileepa, Abhi… in fact they are with in all situation and in difficult condition. Thank you everyone.

Dr. Santhosh sir, you are unbelievable bundle of energy, your suggestion to pursue PhD in IISERP finally made it possible. You made so many lives beautiful among them I am also one of the candidates, thank you sir.

I sincerely and greatly thankful to all my best teachers give the wisdom, courage, discipline and knowledge from my childhood.

My special thanks to my botany Professor Sharvani ma'am, she believed on my strength even more than me and ma'am always pushed me towards higher level, even I was not able to imagine to do, thank you ma'am.

I also thankful to my best teachers in my Bachelor's degree Sowmya ma'am, Basavaraju sir, Chandramohan sir, Akka mahadevamma ma'am, Yashoda ma'am, Devaki ma'am…….

I greatly thankful to my Chemistry Prof. Lokanath Ri sir, your richness of knowledge made to think out of the classroom, out of the syllabus, in fact inspired me to open the text books, sir my heartiest thankful to you. I also thankful to my chemistry professors D Channegowda sir, Nagendrappa sir, Syed akhil ahmed sir. Yours knowledge, honesty, vision and motivation made us to think out of the box.

I thankful to my RAC memebers Prof. H N Gopi and Dr. Santhosh babu Sukumaran, for their valuable suggestions during my RAC meetings.

I greatly thankful to all past and present lab mates Dr. Gopalakrishna, Dr. Kiran Reddy, Dr. Santosh C. Gadekar, Dr. Santosh Panchal, Dr. Neelam Shivaran, Dr. Rasmi Nayak, Dr. Jyotsna Arora, Dr. Brijesh Chandra, Dr. Tarunpreeth singh, Dr. Sujith P. Chavan, Dr. Sunita Gadakh, Dr. Rakesh Gaur, Dr. Madan Ambhore, Dr. Ashokkumar B., Dr. Prachi Gupta,

Markose Joshi, Pragati Shukla, Vishnu Mishra, Ramesh Hiremath and Rakesh. Because of each person having different set of knowledge, skills, experimental method, dedication, learning and healthy discussions made possible to complete this journey. In all my best time and even worst time you are all with me and helped me lot, I really lucky to have wonderful labmets, thankful to each and every one. My special thanks Dr. Kiran Reddy, Dr. Gopalakrishna and Dr. Sujith P. Chavan for their valuable suggestions and valuable help at all my difficult time.

I thankful Dr. Subbuji, he taught basic theoretical calculations and inspired me lot.

I thankful to all my lovable Kannada friends Chethu, Vijendra sir, Ashok, Puneeth, Deepak, Santhosh, Mutthu, Yathish, Shambulinga, Mahesh, Chiddu, Vinay, Sarvajith, Giddirappa, Sharath, Tripura, Gaudappa, Venkanna, Shivakumar, Clifford, Naveen….. Also my love and thanks to my best friends Chandan, Sanjith, Shatrugan, Neetu, Bala, Ganesh,…….I never forget the moment I spent with you all, in fact yours presence made this journey beautiful and success.

My special thanks to my batch-mets Dheeraj, Sathish, Santhosh, Divya, Satwik, Vishal and Jyothi.

I greatly thankful to T S Mahesh sir, JK sir, Hotha sir, Bhoomi sir, Kikkeri sir, Rajesh gonade sir, Gopi sir, Ganesh sir for your help, motivation and inspiration and all also thanks to all faculties in chemistry department.

I also Thankful to administrative staffs, Thushar, Mayuresh, Ashwini, Yatish, Ganesh, Megha, Sanjay, Hemalata and all technical team Mahesh, Nitin, Ravindra, Sandeep, Jnaneshwar, Archana, Chinmay, Dipali. My special thanks to Dr. Sandeep for valuable help during NMR experiments.

Finally, I greatly thankful to IISER, for Research facility and UGC-CSIR, for the Financial support.

UDAYA H S

Contents

Synopsis 1

Publication 7

I. Introduction

I.1 Porphyrin 9

I.2 Isophlorin to Porphyrin 10

I.3 Different class of Expanded Porphyrins 11

I.4 Meso-Aryl substituted Expanded Porphyrins 15

I.5 Vinylogous Porphyrins 23

I.6 Thiophene Incorporated Porphyrinoids 26

I.7 Redox Chemistry 30

I.8 Aim of the thesis 34

I.9 References 35

II. Redox Active π-Expanded Core-Modified Isophlorinoids at Crossroads of Topology and Antiaromaticity

II.1 Introduction 41

II.2 One-pot synthesis of Cyclooligothiophenes 42

II.3.1 Isolation and Characterisation of [40]octaphyrin 44

II.3.2 ^{1}H NMR study of [40]octaphyrin 45

II.3.3 Crystal structure and packing of [40]octaphyrin 48

II.3.4 Computational studies for stable conformation of [40]octaphyrin 50

II.3.5 Splitting of 40π octaphyrin into 20π isophlorin 52

II.3.6 Study of [38]octaphyrin dication 53

II.3.7 Electronic absorption and Cyclic Voltammogram studies 55

II.3.8 Spectro-electrochemistry (SEC) studies 56

II.3.9 Quantum mechanical calculations 57

II.4.1 Isolation and Characterisation of [50]decaphyrin 59

II.4.2 ^{1}H NMR study of [50] decaphyrin 60

II.4.3 Topoisomers of Decaphyrin 62

II.4.4 Electronic absorption and Cyclic Voltammogram studies 65

II.4.5 Synthesis and Characterisation of [48]decaphyrin dication 67

II.4.6 Molecular structure of [48]decaphyrin dication 68

II.4.7 Computational studies 70
II.5.1 Isolation and Characterisation of [60]dodecaphyrin 72
II.5.2 ^{1}H NMR study of [60]dodecaphyrin 72
II.5.3 Molecular structure of [60]dodecaphyrin 74
II.5.4 Electronic absorption and cyclic voltammogram studies 74
II.5.5 Computational studies 76
II.6.1 Isolation and Characterisation of [70]tetradecaphyrin 77
II.6.2 ^{1}H NMR study of [70]tetradecaphyrin 78
II.6.3 Molecular structure of [70]tetradecaphyrin 80
II.6.4 Electronic and redox studies 80
II.6.5 Computational studies 82
II.7 [80]hexadecaphyrin 82
II.8 Conclusions 84
II.9 General Experimental Methods 85
II.10 References 92

III. Synthesis and Characterisation of 24π and 26π Pentathia Sapphyrin and its higher analogues

III.1 Introduction 96
III.2 Synthesis of 24π and 26π Sapphyrins 98
III.3 Synthesis of 24π Sapphyrin and higher analogues 99
III.4.1 Isolation and Characterisation of [24]Sapphyrin 100
III.4.2 ^{1}H NMR study of [24]Sapphyrin 101
III.4.3 Molecular structure of [24]sapphyrin 103
III.4.4 Electronic absorption and Cyclic Voltammogram studies……...……..…….103
III.4.5 Synthesis and characterisation of [22]sapphyrin dication 105
III.4.6 Computational studies 108
III.5.1 Isolation and Characterisation of [48]decaphyrin 109
III.5.2 ^{1}H NMR study of [48]decaphyrin 109
III.5.3 Molecular structure of [48]decaphyrin 111
III.5.4 Electronic absorption and Cyclic Voltammogram studies 112
III.5.5 Computational studies 113
III.6.1 Isolation and Characterisation of [72]pentadecaphyrin 114
III.6.2 ^{1}H NMR study of [72]pentadecaphyrin 114
III.6.3 Electronic absorption studies 117
III.7 Synthesis of 26π Sapphyrin and higher analogues 118

III.8.1 Isolation and Characterisation of [26]Sapphyrin 119
III.8.2 ^{1}H NMR study of [26]sapphyrin 120
III.8.3 Electronic absorption and Cyclic Voltammogram studies 122
III.9.1 Isolation and Characterisation of [52]decaphyrin 124
III.9.2 ^{1}H NMR study of [52]decaphyrin 124
III.9.3 Electronic absorption studies 127
III.10 Conclusions 128
III.11 General Experimental Methods 129
III.12 References: 134

IV. Aromaticity in Thieno[3,2-*b*]thiophene incorporated Expanded Isophlorinoids

IV.1 Introduction 137
IV.2.1 Synthesis and Characterisation of Thieno[3,2-*b*]thiophene incorporated 22π Isophlorin 139
IV.2.2 ^{1}H NMR study of 22π Isophlorin 140
IV.2.3 Electronic absorption and Cyclic Voltammogram studies 142
IV.3.1 Synthesis and Characterisation of Thieno[3,2-*b*]thiophene incorporated 34π Hexaphyrin 144
IV.3.2 ^{1}H NMR study of 34π Hexaphyrin 145
IV.3.3 Molecular structure of [34]hexaphyrin 146
IV.3.4 Electronic absorption and Spectro-Electrochemical studies 147
IV.3.5 Computational studies 150
IV.4 Conclusions 151
IV.5 General Experimental Methods 152
IV.6 References 157

Summary of the Thesis 159

Synopsis

Porphyrins are commonly referred to "pigments of life" because of their presence in chlorophyll and haemoglobin as life molecule. β-substituted porphyrin was synthesised by R. B. Woodward during the synthesis of Chlorophyll, with simple precursors pyrrole and aldehyde. In acidic media it gives the unconjugated cyclic system called as porphyrinogen, and further undergoes four electron ring oxidation to yield the transient intermediate called as isophlorin. Isophlorin is a hypothetical and unstable 20π antiaromatic macrocyclic system. It further undergoes two-electron ring oxidation to yield the planar and stable aromatic 18π porphyrin. Both 18π porphyrin and 20π isophlorin represent two redox states of aromaticity and antiaromaticity inter-convertible through two π-electrons aided by Proton Coupled Electron Transfer (PCET) reaction. Aromaticity in expanded porphyrins varies with molecular flexibility and due to more degrees of freedom they majorly adapt to non-aromatic and non-planar geometry. Redox chemistry in expanded porphyrins is extensively studied because of its amine-imine interconversion through PCET reactions. Yet the chemistry of non-pyrrolic macrocycles is limited to eight or less number of heterocyclic units. The aromaticity, molecular conformation and its topological studies in expanded isophlorinoids are not much explored, and in this thesis it's an endeavour to synthesize the expanded non-pyrrolic macrocycles majorly from the thiophene units to study their (non)-aromaticity/antiaromaticity through redox chemistry. Therefore the thesis is entitled "***Synthesis, Conformational Dynamics and Spectro-electrochemical Characteristics of Core-Modified Expanded Isophlorinoids***". Towards this effort, both (4n+2)π and 4nπ electronic systems were synthesized and characterized by appropriate analytical techniques including ^{1}H NMR and single crystal X-ray crystallography. The spectroscopic and redox properties have been elucidated by electronic absorption spectroscopy and cyclic voltammetry studies respectively. In addition, spectro-electrochemistry studies were also performed to determine the redox active species in support of the reversible chemical redox reaction. In some cases both neutral and oxidised state are isolated and characterised through ^{1}H NMR spectroscopy to evaluate the aromatic characteristics of the species. All these results are further supported by suitable and appropriate quantum chemical calculations such as NICS and ACID values to substantiate the aromatic properties as inferred from experimental results.

First chapter is a historical short review on expanded porphyrinoids from sapphyrin to recent expanded macrocycles including both pyrrolic and non-pyrrolic systems. It also explains their

aromaticity along with redox chemistry by both PCET and ring oxidation reactions. In addition to these studies, their conformational changes along with inter conversion between aromatic and anti-aromatic states induced by altering pH and redox reactions is also described.

Second chapter describes a one-pot condensation of thiophene and pentafluorobenzaldehyde through modified Lindsey-Rothemund synthesis to yield a series of thia-isophlorinoids from four to sixteen membered heterocyclic units containing (4n+2), 4n, (4n+1), (4n+3) π electron systems. Open shell radicals bearing (4n+1) and (4n+3) π-electrons larger than pentathia-isophlorin systems were highly sensitive under ambient conditions and difficult to isolate for further characterisation. Macrocycles up to six members adopt a rigid framework to sustain a planar conformation. Twelve and fourteen membered macrocycles are also rigid, but adopts a non-planar conformation. In contrast, octaphyrin and decaphyrin macrocycles display conformational dynamics with respect to temperature and based on the solvent chosen for the crystallisation.

40π octaphyrin displayed temperature dependent conformational changes from planar to non-planar conformation in solution state. In the ^{1}H NMR, at room temperature macrocycle displayed the fluxional behaviour. At lower temperatures all signals are well resolved, but lacked paratropic ring current effect to reveal non-antiaromatic character of the macrocycle in solution state. But a planar conformation was confirmed in the solid state confirming the antiaromatic character of the macrocycle as supported by NICS and AICD calculations. Further, it displayed variations in crystal packing with different solvent systems. Computational calculation supports that figure-of-eight conformation is the most favourable

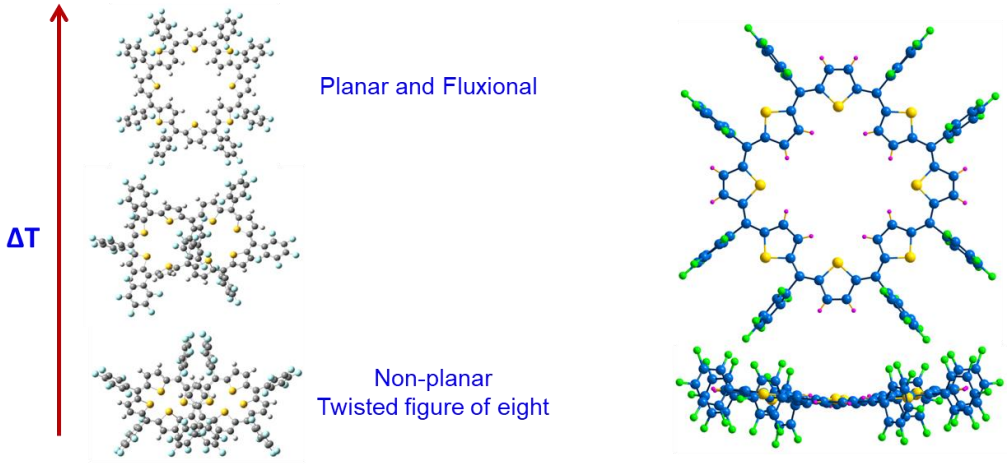

40π Octaphyrin in solution state

Solid State Structure

conformation in the solution state. 40π octaphyrin was also found to undergo mitotic division in the presence of C_{60} fullerene into two tetrathia 20π isophlorin units. Alternatively, macrocycle also undergoes facile two electron ring oxidation to yield 38π dicationic state through a 39π radical cation intermediate as confirmed by SEC studies.

50π decaphyrin displayed non-aromatic character in the solution state, as observed by the absence of diatropic ring current in its ^{1}H NMR spectrum. But in the solid state, macrocycle displayed two distinct topoisomers based on the solvent of crystallization. In acetonitrile macrocycle adopts an unequal [6+4] conformation evident for non-aromatic character and, in benzene macrocycle adopts to [5+5] near planar conformation with aromatic character. Upon crystallizing with a combination of both benzene and acetonitrile, the macrocycle was found to adopt [6+4] conformation exclusively. Because of its non-aromatic character in the solution state the macrocycle undergoes two-electron ring oxidation from 50π electronic state to the largest 48π antiaromatic dication. The dication displayed planar conformation in solid state and the estimated NICS value of +36.21 ppm confirmed the antiaromatic nature of the macrocycle. In the ^{1}H NMR spectrum, macrocycle displayed strong paratropic ring current where two protons strongly resonate in the downfield suggesting that macrocycle sustained [6+4] conformation in the solution state. The formation of the dication was supported by cyclic voltammetric studies and confirmed by SEC studies.

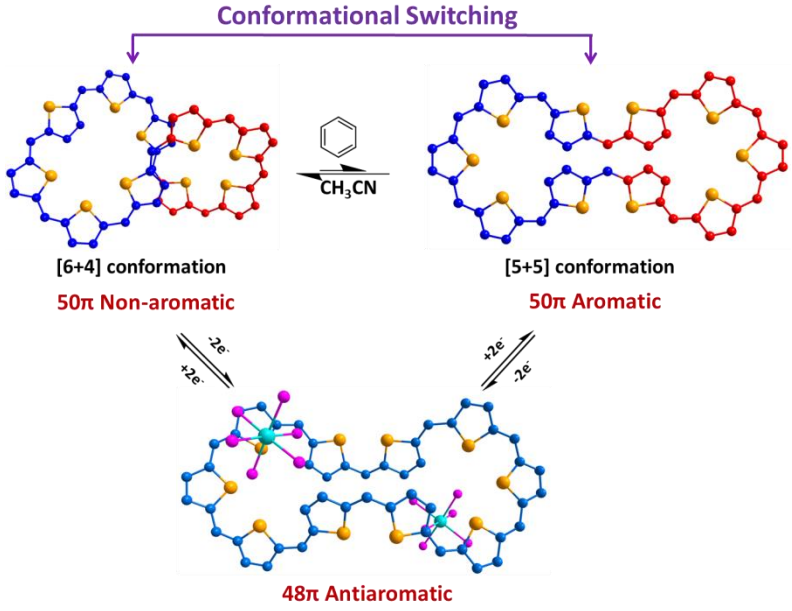

60π dodecaphyrin and 70π tetradecaphyrin represent the first example of the largest macrocycles in π-electron count with equal number of meso-carbons and heterocyclic units. Both the macrocycles were non-(anti)aromatic in nature because of non-planar, twisted

conformation in solid state and in solution state they didn't display any significant ring current effect in the ^{1}H NMR spectrum. The isolated 80π hexadecaphyrin is the largest macrocycle isolated from this one-pot synthesis.

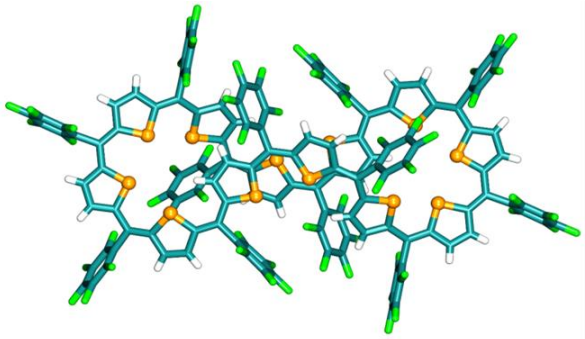

60π Non-antiaromatic Dodecaphyrin

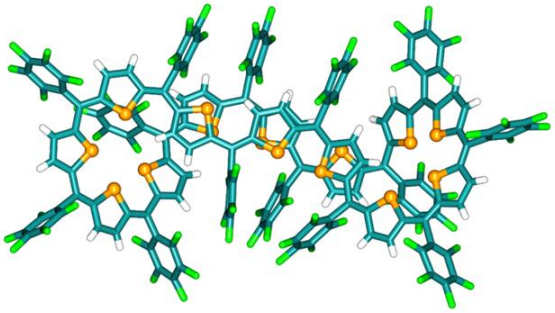

70π Non-aromatic Tetradecaphyrin

Third chapter is a detailed study of pentathia sapphyrin and its higher analogues, which is inspired by air and water stable open shell neutral radical (4n+1)π (25π) cyclopentathiophene macrocyclic system. The macrocycle undergoes one electron ring oxidation to antiaromatic 24π cation and also undergoes one electron ring reduction to the aromatic 26π anion state. Isoelectronic species of each state was synthesised by ring contracted 24π pentathia sapphyrin and ring expanded 26π ethyelene bridged pentathia sapphyrin. Both are antiaromatic and aromatic respectively. These macrocycles were synthesised through [3+2] type condensation of bithiophene or ethylene bridged bithiophene condensed with thiophene based tripyrromethane diol. In addition to sapphyrin macrocycles, higher analogues of this series were also formed in this reaction mixture.

24π sapphyrin is anti-aromatic in nature both in solution and solid state study. In the ^{1}H NMR spectrum, macrocycle displayed paratropic ring current with a C_2-axis of symmetry. Single crystal X-ray diffraction study revealed a planar conformation of the macrocycle in support for the anti-aromatic character in solid state. Because of its antiaromatic character the macrocycle undergoes two-electron ring oxidation from 24π electrons system to 22π aromatic dication, which displayed the diatropic ring current in the ^{1}H NMR. Both NICS and AICD values supports the (anti)aromatic character of the macrocycles. 26π sapphyrin was non-aromatic in solution state, as it did not exhibit significant diatropic ring current in the ^{1}H NMR. Since both 24π and 26π sapphyrin macrocycles are antiaromatic and non-aromatic in nature, they undergo two-electron ring oxidation by the formation of radical cation intermediate as confirmed from spectro-electro chemistry studies.

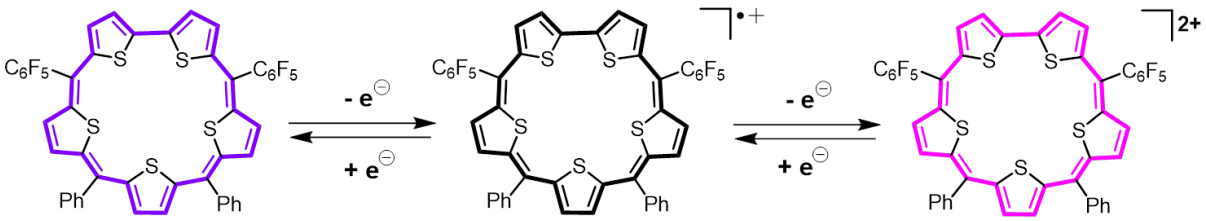

24π 23π 22π

Both 48π decaphyrin and ethylene bridged 52π decaphyrin displayed C_2-axis of symmetry in the ^{1}H NMR spectrum. They were non-antiaromatic and non-aromatic in solution state respectively because these macrocycles were devoid of any significant ring current. Single crystal X-ray diffraction studies revealed 48π decaphyrin with a non-planar and twisted 'figure-of-eight' conformation confirming the non-antiaromatic character in solid state. Both macrocycles undergoes two-electron ring oxidation to their respective dicationic state. The largest expanded macrocycle of this series 72π pentadecaphyrin suggests a C_3-axis of symmetry in the ^{1}H NMR spectrum. But it did not display any significant paratropic ring current confirming the non-antiaromatic character. Both the macrocycles undergo two-electron ring oxidation to yield dicationic species which displayed the strong red shifted absorption in the NIR region of the electromagnetic spectrum.

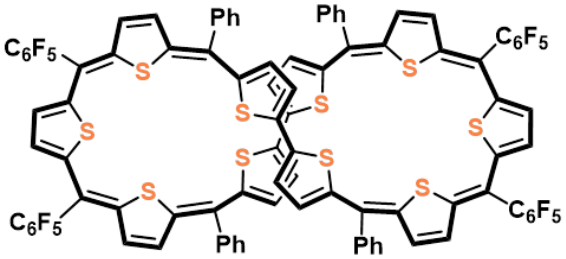

48π Decaphyrin

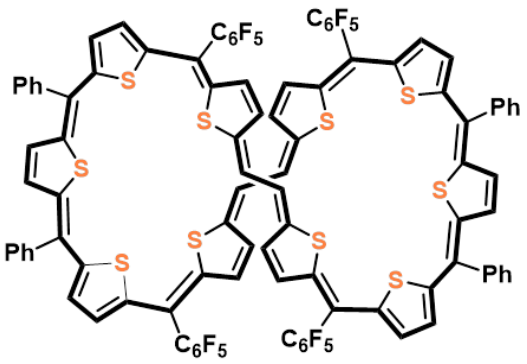

52π Decaphyrin

The final chapter of this thesis describes the change in aromaticity of isophlorin by the incorporation of thieno[3,2-*b*]thiophene hetrocyclic subunit in an isophlorin skeleton. 22π isophlorin and 34π hexaphyrin are (4n+2)π systems, along with extended the π-conjugation. 22π isophlorin in the ^{1}H NMR spectrum displayed C_2-axis of symmetry, but was found non-aromatic due to the absence of diatropic ring current. Because of non-aroamtic character 22π macrocycle undergoes two-electron ring oxidation through a radical cation intermediate as

confirmed by the SEC studies. 34π hexaphyrin displayed diatropic ring current in its ^{1}H NMR spectrum to confirm the Huckel's aromatic nature of the macrocycle. Single crystal X-ray diffractometer studies revealed a planar conformation in support of the aromatic nature of the macrocycle. Remarkably oxidising agents like TFA or $NOBF_4$ or Meerwein's salt oxidises the aromatic macrocycle by two electrons to antiaromatic dication; from 34π to 32π dication through the formation of 33π radical cation intermediate as witnessed in the SEC studies.

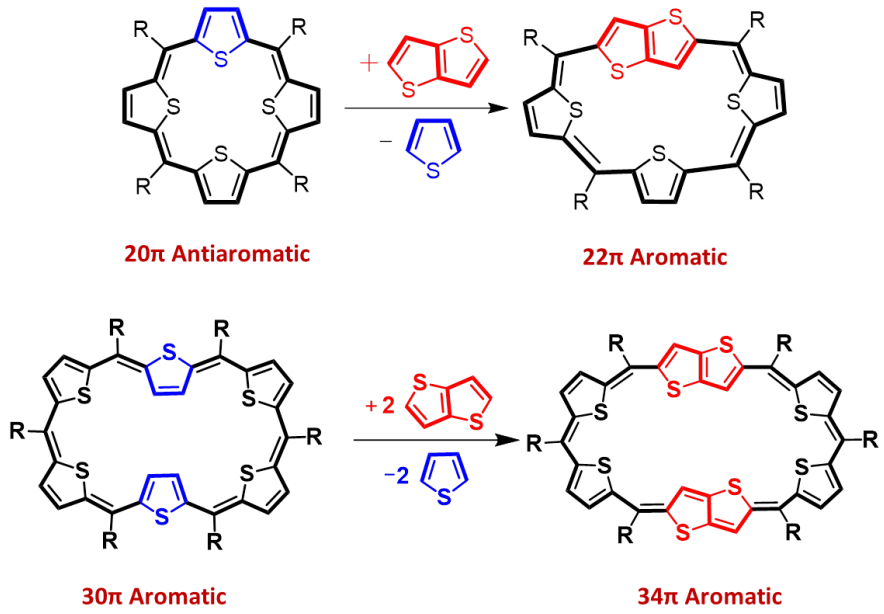

Overall, this thesis describes the role of thiophene as a building block for the synthesis of isophlorinoids. Based on the number of thiophene subunits, they can be tuned to either (4n+2) or 4n π-electrons macrocycles. However, their aromaticity is dependent on the conformation or topology as detected from analytical studies. Further, replacing the thiophene by a thienothiophene unit not only alters the π-conjugation but also the structure and aromatic features of the macrocycle. An important outcome of the study is the similarity of redox property for antiaromatic and non-aromatic species. This thesis reveals that both these species are susceptible to reversible two-electron ring oxidation. Hence, they appear to be much better redox active species in comparison to their aromatic counterparts.

Publication

- Hosahalli S. Udaya, Ashokkumar Basavarajappa, Tullimilli Y. Gopalakrishna and Venkataramanarao G. Anand, Topoisomers and aromaticity of a redox active 50π core-modified isophlorinoid, *Chem. Commun*., **2022**, *58*, 13931–13934.

Chapter I

Introduction

I.1 Porphyrin

Porphyrin is a *Life molecule*, because of its vital role in biological systems. It is mainly present in most of the enzymes as chelating agent for redox active metals that display significant and interesting physical and electronic properties (figure I.1). This molecule is widely studied in physiological processes as heme containing proteins or coenzymes (figure - I.1). It also binds Mg^{2+} and identified as chlorophyll, **I.1**, in the plant kingdom which is crucial to production of oxygen through photosynthesis. The produced oxygen is transported, stored and utilized by Fe^{2+} containing heme proteins, **I.2**. Therefore they are commonly known as "pigments of life". [1]

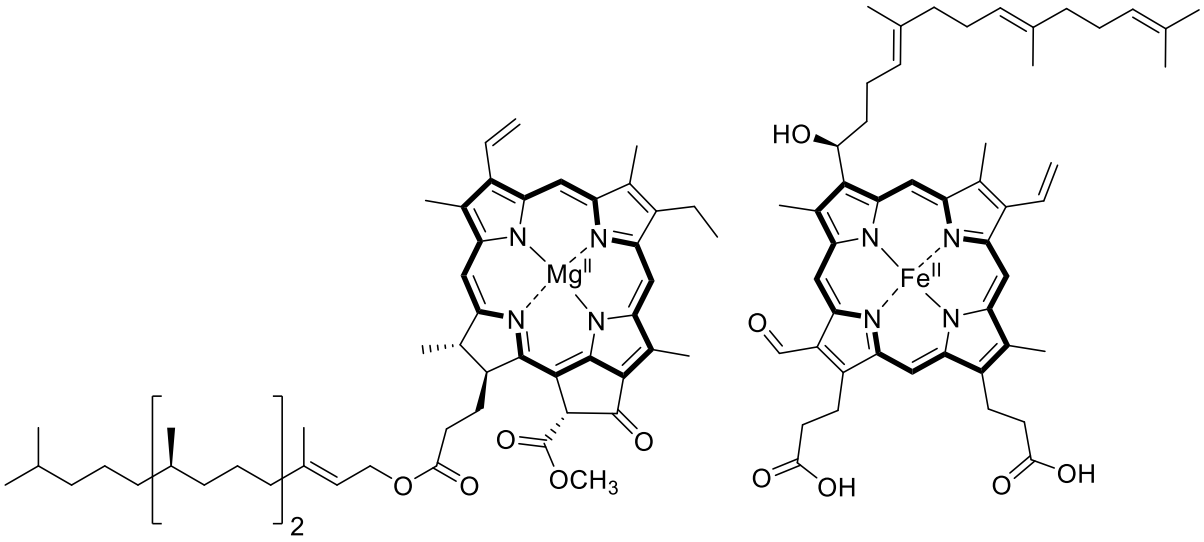

I.1 **I.2**

Figure I.1: *Structure of Chlorophyll a and Heme a.*

Now it is well understood that π-conjugation is responsible to induce colour in pigments. Many pigments like carotenoids, xanthophyll and lycopene derive their colour from extended *linear* π-conjugation. Whereas, in case of porphyrin pigment, the π-conjugation is *circular* and it creates a global ring current. Such property in porphyrin is chiefly attributed to its planar, 18π electrons in the global conjugation flows along the carbon and hetero atoms (**I.3**). It obeys Huckel's rule of aromaticity in accordance with the empirical (4n+2)π formula. Electronic absorption shows a Soret like band and four Q bands in the range of 400 to 600 nm. In ^{1}H NMR spectrum, the two inner –NH protons, resonate up field (shifts to negative region) and outer protons resonate in the down field due to strong diatropic ring current in the aromatic macrocycle (figure – I.2).

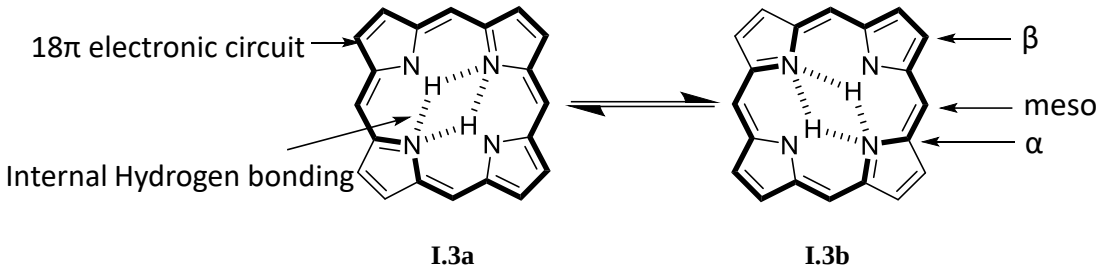

I.3a **I.3b**

Figure I.2: *Tautomeric form of Porphyrin.*

I.2 Isophlorin to Porphyrin

β-substituted porphyrin was first reported by R. B. Woodward in 1960 during the synthesis of Chlorophyll.[2] Condensation of pyrrole and aldehyde in acidic conditions is supposed to initiate the unconjugated sp^3 hybridized tetrapyrrolic porphyrinogen, **I.4**. Subsequently it undergoes four-electron oxidation to yield the 20π antiaromatic transient intermediate termed as Isophlorin, **I.5**. In the final step, **I.5** further undergoes two-electron oxidation to yield the stable, planar, sp^2 hybridised 18π aromatic porphyrin, **I.6**.

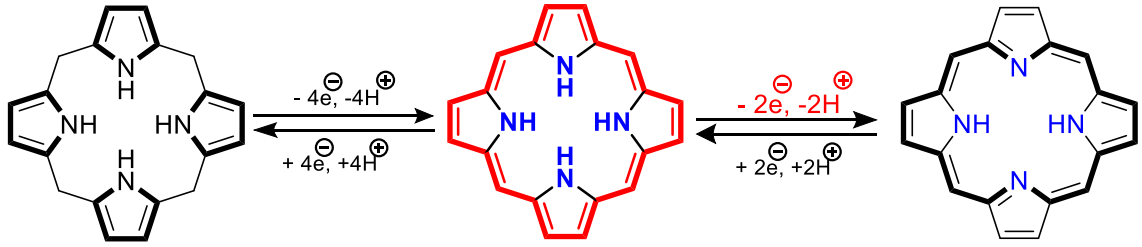

I.4 **I.5** **I.6**

Scheme I.1: *Stepwise oxidation of porphyrinogen to 18π porphyrin **I.6** through the transitory 20π isophlorin **I.5**.*

Isophlorin[3] is an unnatural macrocycle and is a hypothetical intermediate during the synthesis of porphyrin. Chemical structure of 20π isophlorin **I.5** differs from porphyrin **I.6** by two-electrons in the core of the macrocycle. In principle, addition of two hydrogens to porphyrin drastically changes the conjugation pathway to yield the 4nπ isophlorin. This difference enables isophlorin to adopt π-conjugation through sp^2 hybridised carbons along with the periphery of the macrocycle. In contrast, porphyrin's π-conjugation adopts the shortest pathway through the sp^2 carbons and sp^2 hybridised nitrogen of the pyrrole rings. Hence, it is also termed as N-doped [18]heteroannulene.[4] 20π isophlorin belongs to the class of Huckel's 4nπ systems and 18π porphyrin fits to Huckel's (4n+2)π system. However, the stable 20π

tetrapyrrolic antiaromatic isophlorin has remained elusive till date. This is partially attributed to the steric hindrance caused by internal four hydrogens of the macrocycle inducing a non-planar geometry.[5] Consequently, it results in a repulsive force towards a rapid two-electron oxidation to attain a stable and planar 18π aromatic porphyrin under ambient conditions. Additionally, the perceived unstable nature of antiaromaticity is also reasoned as a major reason for its unstable nature.

I.3 Different class of Expanded Porphyrins

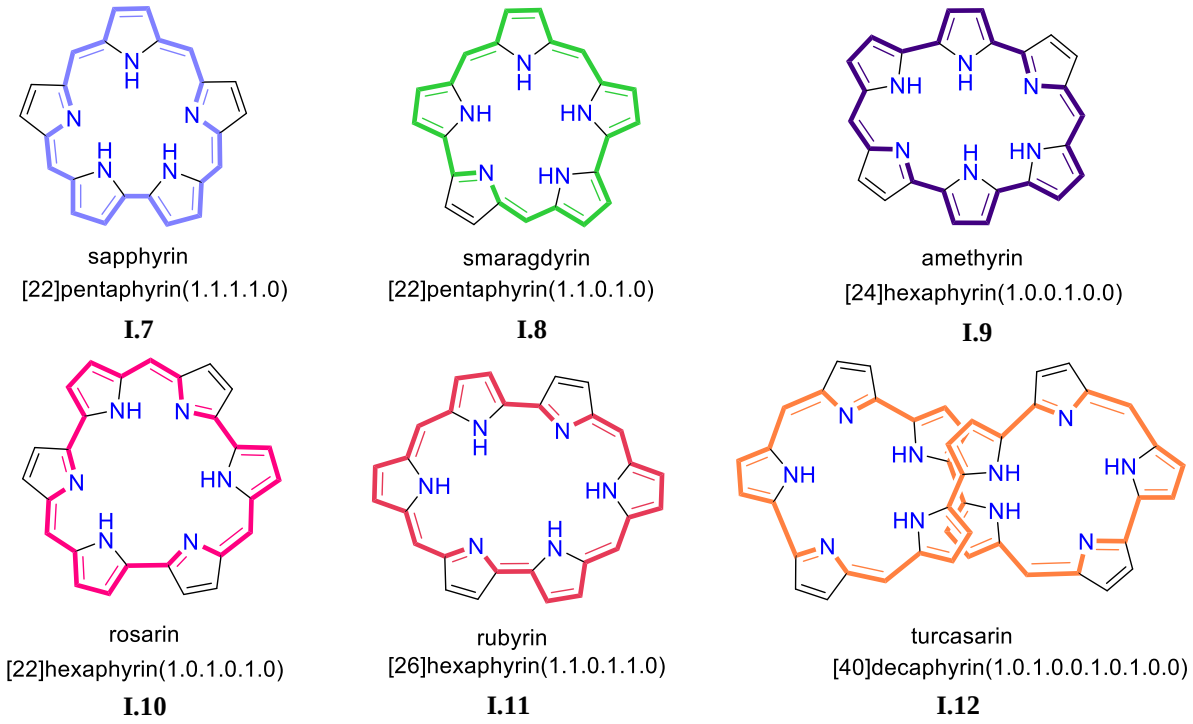

Figure I.3: *Structure and trivial name of expanded porphyrins.*

Over the decades, porphyrin chemistry has been studied extensively. Synthetic efforts from various research groups led to the identification of its synthetic structural isomers such as N-confused porphyrin[6] and porphycene.[7] Porphycene represents an example of spatial rearrangement of the porphyrin skeleton in which the four *meso* carbons are reoriented as two ethylene bridges connecting the two bipyrrole moieties. In N-confused porphyrin, β-carbon and nitrogen atom of a pyrrole ring interchanged their respective positions leading to a CH in the core of the macrocycle. Both the isomers follow Huckel's 4n+2π aromaticity, but exhibit different structural, physical and electronic properties and their reactivity differs from the parent porphyrin. Apart from these two structural isomers, structural variants of the parent porphyrins have also been explored. Among such variants include, core-modification of a porphyrin by replacing one or nitrogen by different chalcogens, ring contraction by removing one or two meso-carbons and peripheral modification by changing different substituents of the porphyrin ring.

Expansion of a porphyrin ring has been achieved by increasing the length of π-conjugation either by the addition of heterocycles or meso-carbons leading to a class of macrocycles known as expanded porphyrins. Different types of expanded porphyrins are displayed in figure – I.3. [8-10]

A simple definition of an expanded porphyrin could be "A porphyrinoid larger than a porphyrin". In 2003 Sessler defined this class of molecules as "*macrocycles that contain pyrrole, furan, thiophene, or other heterocyclic subunits linked together either directly or through one or more spacer atoms in such a manner that the internal ring pathway contains a minimum of 17 atoms*".[11] Based on this definition, expanded porphyrin chemistry can be traced back to the first report by R. B. Woodward. Sapphyrin **I.14** is the first expanded porphyrin and was serendipitously discovered during the synthesis of Vitamin B_{12} in 1966.[12] Sapphyrin was identified as a dark blue coloured solid and pentapyrrolic macrocycle with four bridging methine groups involving a bipyrrole link (figure – I.4). It accounts for 22π electrons in the conjugation and confirms to Huckel's rule of aromaticity with (4n+2)π system. In 1983, from the same group, they synthesised the decamethaylsapphyrin, with alkyl groups as peripheral substituents. By virtue of diatropic ring current, all the –NH protons are shielded and methyl groups are deshielded in its ^{1}H NMR spectrum. This macrocycle displayed porphyrin type electronic absorption with red shifted Soret and Q bands. From its molecular structure reported later in 1990, it was observed that all nitrogens were oriented towards the centre of the macrocycle. In the diprotonated state it is known to bind fluoride and other anions.[13]

.

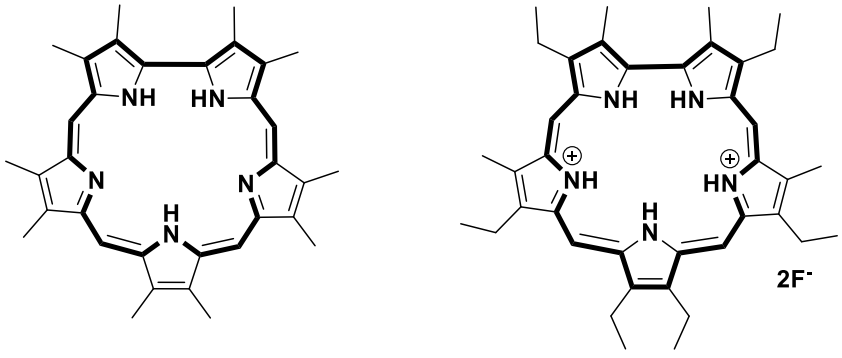

I.13 **I.14**

Figure I.4: *Freebase and the diprotonated forms of Sapphyrin.*

A high congener of sapphyrin identified as rubyrin, **I.15**, with six pyrrole units was reported by Sessler and co-workers in 1991.[14] This macrocycle accounts for 26π electrons along the conjugated pathway and obeys Huckel's (4n+2)π rule of aromaticity. Just similar to the parent porphyrin, its inner –NH protons were shielded and outer protons deshielded in its ^{1}H NMR spectrum. In the electronic absorption this macrocycle displayed red shifted Soret-like

band and Q bands in comparison to the parent porphyrin. The molecular structure displayed a planar topology with all the nitrogen oriented towards the centre of the macrocycle. Further it was also identified as a dicationic salt with characteristic anion binding properties for fluoride and phosphate.

In 1994, a structurally novel expanded porphyrin with ten pyrroleunits, i.e. 40π decaphyrin [0.0.1.0.1.0.0.1.0.1] **I.16** was reported by Sessler and co-workers. Due to its intense turquoise colour in organic solvents it was termed as turcasarin.[15] Turcasarin is a [40] aza-annulene, which exhibits strong red shifted absorption compared to porphyrin moiety. However, this macrocycle was identified as non-aromatic because, it did not exhibit significant paratropic ring current effect. Particularly, the pyrrolic protons were not found to exhibit any significant shift in resonance compared to pyrrole -NH in its ^{1}H NMR spectrum. From ^{13}C NMR, this macrocycle was identified to adopt a C_2 axis of symmetry. Interestingly, ^{1}H NMR suggested interconversion between two limiting right and left handed enantiomeric form with a pseudocircular intermediate. Its molecular structure obtained as tetraprotonic salt with four chloride anions, displayed a ribbon-like crossing geometry which was later coined as 'figure of eight' conformation. Turcasarin is the first example of an expanded porphyrin with a twisted 'figure eight' conformation.

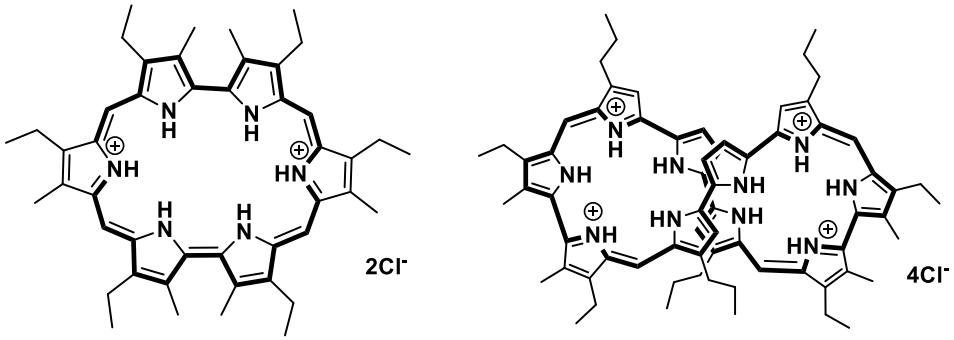

I.15 **I.16**

Figure I.5: *Diprotonated Rubyrin (left) and figure-of-eight tetraprotonated Turcasarin (right).*

Remarkably, Vogel's pioneering contributions to synthetic chemistry of porphyrin and its structural isomers have had a significant impact on the development its chemistry. Further, his contribution in the field of expanded porphyrin chemistry continued with a variety of non-planar octaphyrins during the attempted synthesis of porphyrin isomers. In 1995, attempts to isolate porphyrin isomers like hemiporphycene[2.1.1.0] and corrphycene[2.1.0.1] led to serendipitous discovery of octapyrrolic "figure eight" macrocycles (figure – I.6).[16] Later, Octaphyrin **I.17**, was prepared by McDonald condensation of bipyrrole dialdehyde and dipyrrylethane dicarboxylic acid in the presence of perchloric acid. The isolated violet

crystals of the macrocycle was not completely oxidised to yield the expected conjugation. Even further addition of oxidising agent DDQ could not completely oxidize the macrocycle. However, complete oxidation was achieved by thermal dehydrogenation in the presence of 10% palladium on carbon. This macrocycle accounts for 36π electrons in ^{1}H NMR spectrum. As it didn't show any significant paratropic ring current, the macrocycle was characterized as non-antiaromatic species. It was further confirmed by the molecular structure which displayed figure of eight geometry with C_2 axis of symmetry. Furthermore, this macrocycle was also enantiomeric in nature. Under similar reaction conditions, 34π and 32π systems, **I.18** and **I.19**, were isolated and they were characterized as non-aromatic and non-antiaromatic respectively with similar twisted figure-of-eight conformation.[17]

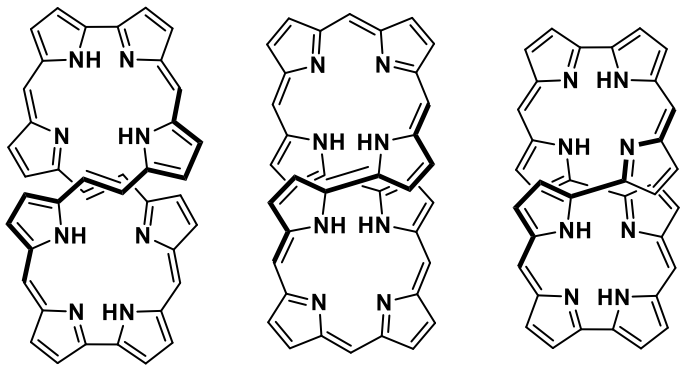

I.17 **I.18** **I.19**

Figure I.6: *Different enantiomeric form of 'figure eight' 36π, 34π and 32π octaphyrins.*

In 1992, Sessler and co-workers prepared a new class of hexapyrrolic expanded porphyrin named Rosarin,[18] **I.20**. In a protocol similar to Rothemund type condensation, beta alkylated bipyrrole and aldehyde were reacted in the presence of catalytic amount of TFA, followed by DDQ oxidation. The macrocyclic product was isolated in 70% yields as a red purple colour in the free base. Its molecular structure was obtained in the form of a triprotonated salt with three counter chloride anions. In the electronic absorption, the macrocycle displayed red shifted absorption than the formal porphyrin molecule. The shape of the molecule was non planar and triangle in shape. It accounts for 24π electrons, but no significant paratropic ring current effect was observed in its ^{1}H NMR spectrum and hence the macroycle was characterized as non-antiaromatic in nature.

Later, in 1999, Sestune and co-workers reported the higher homologues of Rosarian, by condensing the tetra β-ethyl bipyrrole with benzaldehyde (scheme I.2) in the presence of TFA followed by the oxidation of DDQ leading to the formation of [32]octaphyrin-(1.0.1.0.1.0.1.0), **I.21**, [48]dodecaphyrin-(1.0.1.0.1.0.1.0.1.0.1.0.1.0.1.0), **I.22**, and

[64]hexadecaphyrin-(1.0.1.0.1.0.1.0.1.0.1.0.1.0.1.0), **I.23.**[19] Octaphyrin adopted the thermodynamically favourable figure of eight confirmation. Its higher congener [48]dodecaphyrin **I.22**, with twelve pyrrole units, a much more larger macrocycle, adopted a circularly zigzag shape generating a larger internal cylindrical cavity with a diameter of 10 Å. In the subsequent year they reported the largest expanded porphyrin [64]hexadecaphyrin **I.23**, with sixteen pyrrole units. It displayed a square type molecular structure having a tetragonal cut end with 18.8 x 16.3Å, and height of the molecular pillar being 14.4 Å along the b-axis of the unit cell.[20] The macrocycle exhibited face to face packing arrangement very precisely with C_2 axis of symmetry. These expanded rosarin-type molecules are unique in their molecular folding to yield extended figure of eight shapes. These conformations were found to be highly stable because of internal hydrogen bonding observed in the twisted geometry.

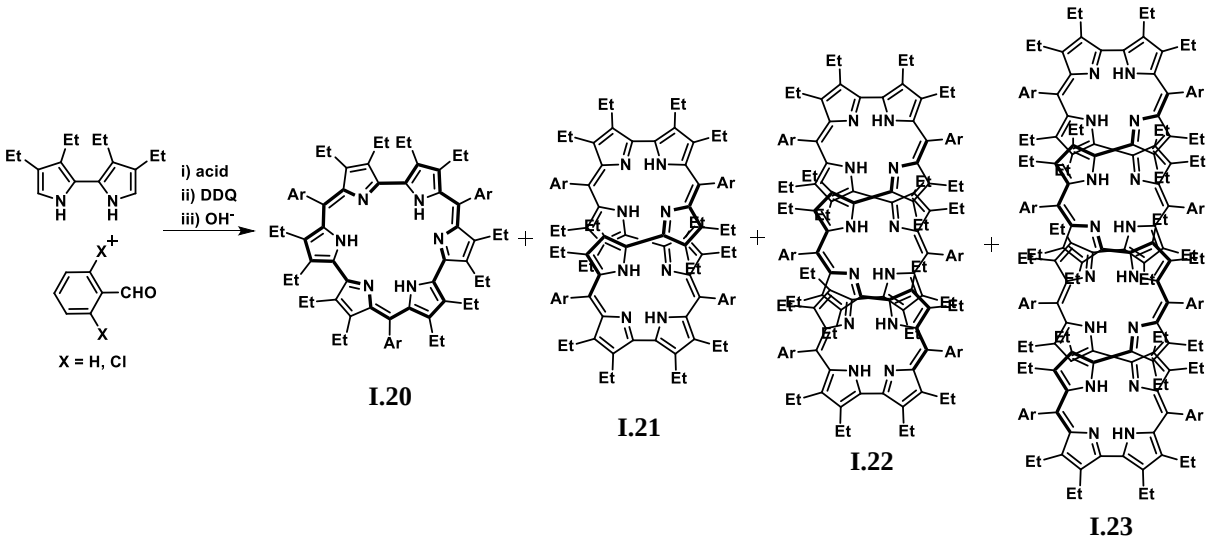

Scheme I.2: *One-pot synthesis of Rosarin and Giant porphyrins.*

I.4 Meso-Aryl substituted Expanded Porphyrins

The first synthesis of a tetraphenylporphyrin (TPP) was reported by Paul Rothemund in 1936[21] and later continued by Alder and Longo in 1967.[22] Lindsey and co-workers introduced an alternate and novel synthetic strategy for the synthesis of TPP and its higher homologues which was fundamentally different from the Rothemund and Alder and Longo.[23] Reaction of the pyrrole and desired benzaldehyde at room temperature in the presence of catalytic amount of acid either $BF_3{\cdot}OEt_2$ or TFA leads to the formation of tetraphenylporphyrinogen **I.24** and polypyrrylmethanes (scheme I.3). Addition of an oxidant such as *p*-chloronil or DDQ irreversibly oxidized the porphyrinogen into a stable 18π aromatic TPP **I.25**. Importantly yield of the macrocycle increased drastically up to 35-55% based on the reaction condition and substituents on the macrocycle.

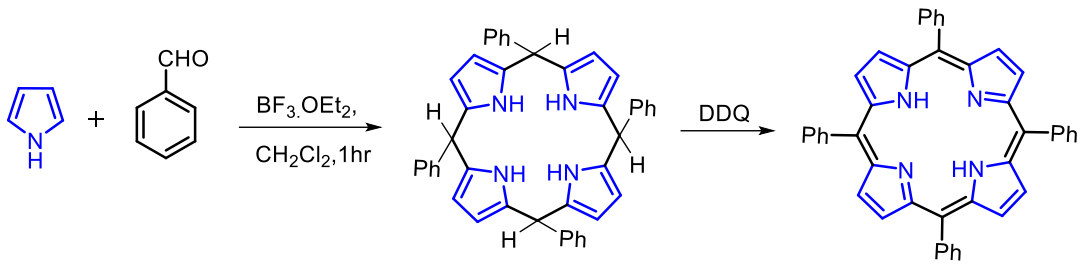

I.24 **I.25**

Scheme I.3: One-pot *synthesis of TPP from pyrrole and benzaldehyde.*

In 2001, Osuka and workers reported a series of meso-aryl substituted expanded porphyrins that were synthesized by employing Rothemund-Lindsey conditions.[23, 24] At higher concentrations of 67 mM, both pyrrole and pentafluorobenzaldehyde were condensed in the presence of $BF_3.OEt_2$ in dichloromethane followed by DDQ oxidation (scheme I.4). The macrocycles were separated by the repeated silica column chromatography to yield a series of macrocycles such as porphyrin, N-fused pentaphyrin **I.27**, hexaphyrin **I.28**, heptaphyrin **I.29**, octaphyrin **I.30**, nonaphyrin **I.31**, decaphyrin **I.32** and their higher homologues.

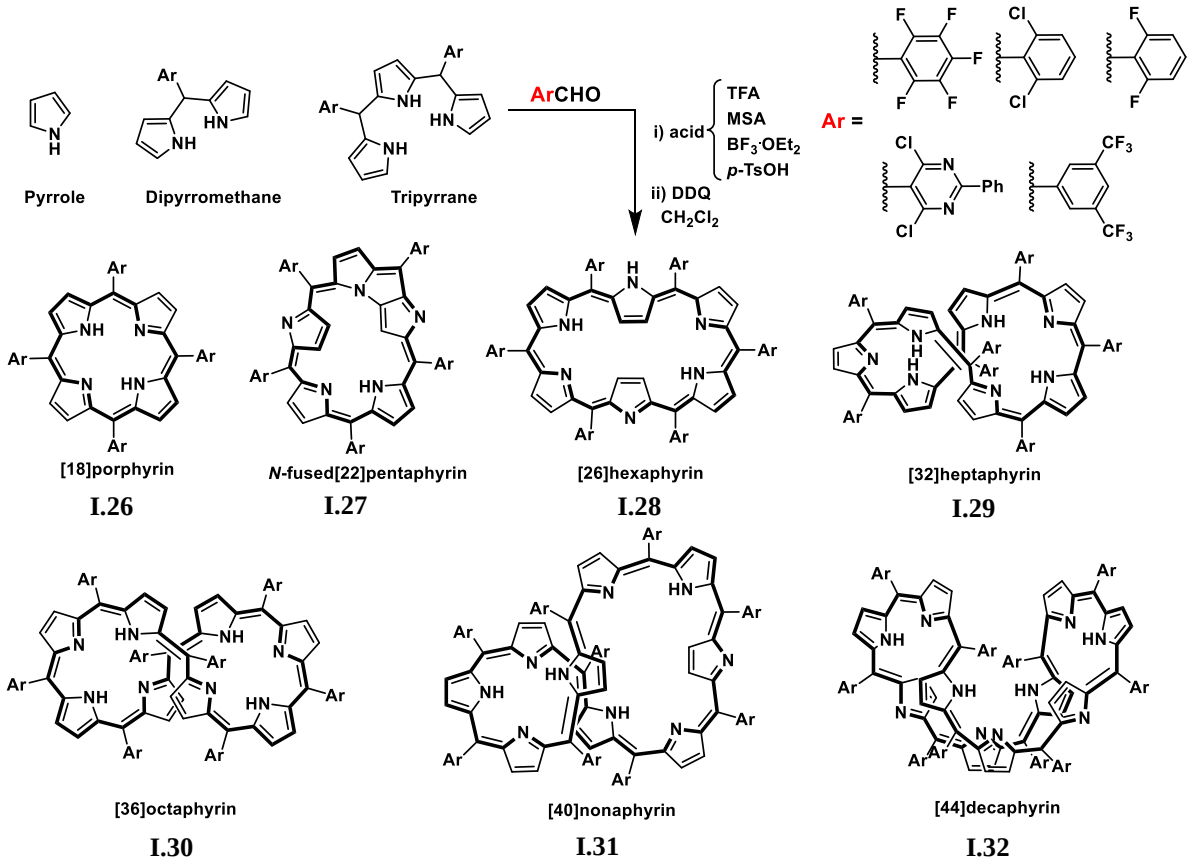

I.26 **I.27** **I.28** **I.29**

I.30 **I.31** **I.32**

Scheme I.4: *One-pot synthesis of meso-aryl substituted expanded porphyrins.*

The formation of a fused pentaphyrin, **I.27**, under this reaction condition is attributed to the steric congestion inside the macrocycle.[25] However, no non-fused pentaphyrins were

observed in this reaction suggesting the stability of fusion between N of a pyrrole ring and the *β*-carbon of an inverted pyrrole ring.

Meso-phenyl substituted hexaphyrin, was first reported by David Dolphin in 1997, through 3+3 type condensation of 5, 10-diphenyltripyrrane with benzaldehyde, followed by chloranil oxidation to yield a blue coloured [26]hexaphyrin(1.0.1.0.1.0).[26] Later in 1999, Cavaleiro's group isolated the meso-hexa (pentafluorophenyl), **I.28a - I.28b** porphyrin by the Rothemund type condensation.[27] Thin layer chromatography revealed two spots coloured blue and violet. However, mass spectrometry displayed the same *m/z* values despite they had two different absorption maxima in the electronic spectra. Blue and violet coloured solutions displayed absorptions at 591, 762 nm and 568, 712 nm respectively. Later it was confirmed experimentally that addition of DDQ turns the blue compound to violet. On the contrary, addition of TsNHNH2 turned violet to blue coloured compound (scheme – I.5). Based on these two experiments, it was confirmed that blue colour compound corresponded to [28]hexaphyrin and violet one to [26]hexaphyrin. ^{1}H NMR spectroscopy further confirmed the aromatic character of the violet compound which displayed strong diatropic ring current. Its protons inside the macrocyclic cavity were shielded and appeared in the up field. However, the blue compound differed from violet compound which did not display significant ring current effect and exhibited poor aromaticity. Molecular structure revealed a rectangular and non-planar topology attributed to the internal steric hindrance in the macrocycle.

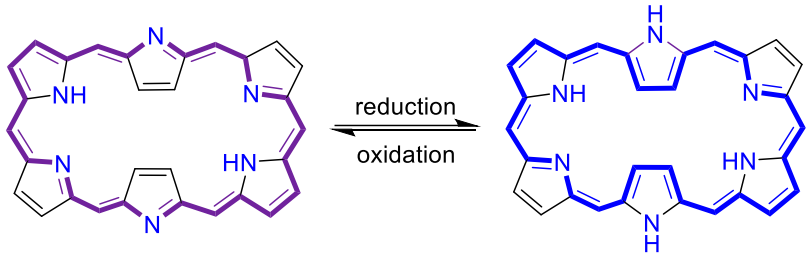

[26]hexaphyrin(1.1.1.1.1.1) [28]hexaphyrin(1.1.1.1.1.1)

I.28a **I.28b**

Scheme I.5: *Redox chemistry of Hexaphyrin*.

Products isolated from the reaction described in scheme – I.4, [32]heptaphyrin, **I.29**, was the smallest macrocycle, identified with 'figure of eight' molecular twist, having a C_2 axis of symmetry. Due to structure induced loss of planarity, the macrocycle was characterized as non-aromatic in nature. Macrocycle displayed different patterns of electronic absorption in polar and non-polar solvents.[28] Interestingly protonation of heptaphyrin triggers the

conformational changes to Mobius twist. Addition of TFA breaks the internal hydrogen bonding, and induces a macrocyclic rearrangement through the pyrrole ring causing a conformational change to Mobius aromatic form. [29]

The eight pyrrole octaphyrin, **I.30**, accounts for 36π electrons and adopted a figure eight conformation with C_2 axis of symmetry similar to the earlier octaphyrins reported by Vogel and co-workers. By virtue of complete twist, two tetrapyrrolic porphyrin pockets in each twist of the molecule forms the hemi macrocycles. Therefore this macrocycle is rendered non-aromatic in nature. Akin to heptaphyrin, **I.29**, protonation breaks the intra-molecular hydrogen bonding and encourages inter molecular hydrogen bonds. Upon protonation, the macrocycle is reduced by two electrons to [38]octaphyrin with a modified conformation to adopt Mobius aromaticity (scheme – I.6).[30]

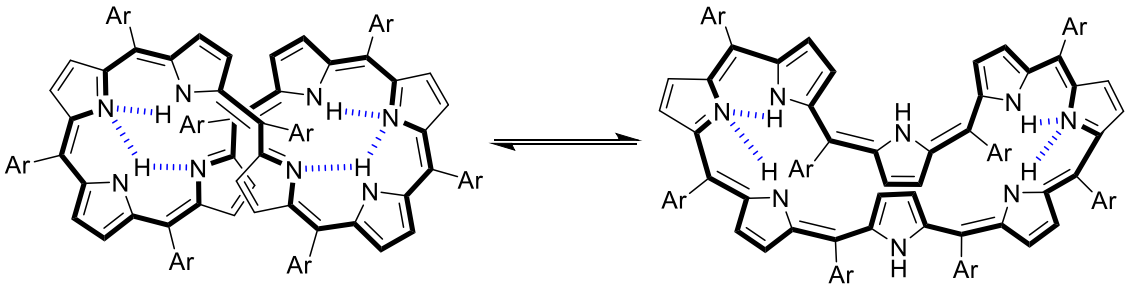

I.30a **I.30b**

Scheme I.6: *Protonation triggered conformational changes of octaphyrin, from Huckel non-aromatic to Mobius aromatic.*

Nonaphyrin, **I.31**, has 42π electrons in the global conjugation. Its molecular structure reported in the protonated form of TFA, is helically twisted along C_2 axis of symmetry and showing the near mirror plane from the centre of the molecule. Because of molecular twist and non-significant ring current effect in ^{1}H NMR, the molecule considered to be non-aromatic.[31]

Molecular structure of [44]Decaphyrin, **I.32**, shows a non-twisted crescent-like conformation and also C_2 axis of symmetry. This conformation is mainly achieved by the intra molecular hydrogen bonding. The macrocyclic non-planarity makes the molecule non-aromatic as supported by the ^{1}H NMR, where there is no significant diatropic ring current expected for (4n+2)π species. It is a dark yellow-green coloured compound with an electronic absorption displaying significant red shift up to 700 nm due to its extended conjugation.[32]

In 2006, Anand and co-workers replaced the pyrroles of a TPP by furan to yield furan porphyrinoids. Under similar reaction conditions as described in scheme – I.4, furan and

pentafluorobenzaldehyde were condensed in the presence of $BF_3.OEt_2$ followed by the addition of $FeCl_3$ to yield six membered cyclohexafuran, **I.33**, and eight membered cyclooctafurans, **I.34** (scheme – I.7). The six membered macrocycle accounts for 30π electrons, displaying two signals in ^1H NMR at δ 7.85 and 2.5 ppm suggesting a planar topology with furan units arranged alternatively in an inverted orientation. Inner protons experience strong diatropic ring currents and hence the molecule is aromatic in nature. Eight member macrocycle accounts for 40π electrons in the global conjugation and displayed two discrete signals in ^1H NMR at δ 9.4 and 5.85 ppm. Molecular structure revealed a square like shape with a near planar geometry wherein the furan units were arranged alternatively in and out fashion. Because of the paratropic ring current, the macrocycle is antiaromatic in nature and it was the first expanded eight membered antiaromatic macrocycle having planar geometry and also the largest planar antiaromatic isophlorin.[33]

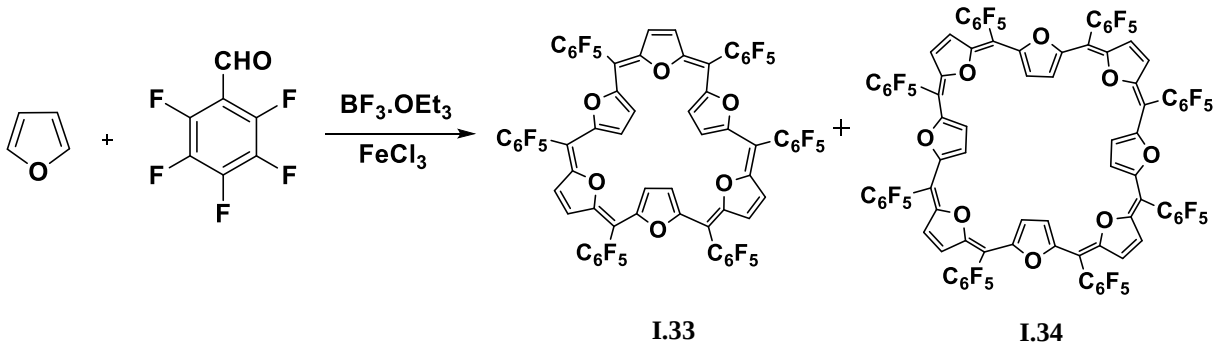

I.33 **I.34**

Scheme I.7: *One-pot Synthesis of cyclohexafuran I.33 and cyclooctafuran I.34.*

Osuka and co-workers, in 2006, reported another class of giant molecules by the replacing the aromatic groups with trifluoromethyl on the meso-positions of porphyrinoids. Trifluoromethane group is a electron withdrawing substituent and sterically less hindered to adopt flexible twist to accommodate a favourable geometry. 2-(2, 2, 2-Trifluoro-1-hydroxyethyl)pyrrole in dichloromethane was treated with an equivalent amount of 1 M HCl in diethyl ether (scheme – I.8). This reaction mixture was refluxed for twelve hours followed by DDQ oxidation and further stirred for six hours at room temperature to yield a series of macrocycles similar to those described in scheme – I.4. N-fused [24]pentaphyrin **I.36** structure was found similar to phenyl substituent. Interestingly, both [28]hexaphyrin and [26]hexaphyrin **I.37** were found to adopt a figure-of-eight structure. Molecular structure of [46]decaphyrin **I.39** attained a crescent conformation and [56]dodecaphyrin **I.40** displayed two-pitch helical conformation. In addition calix[5]phyrin analogues of -H/OH were also isolated and the molecules exhibited near planar geometry with an inverted pyrrole ring and sp^3 hybridised meso-carbon atom.[34]

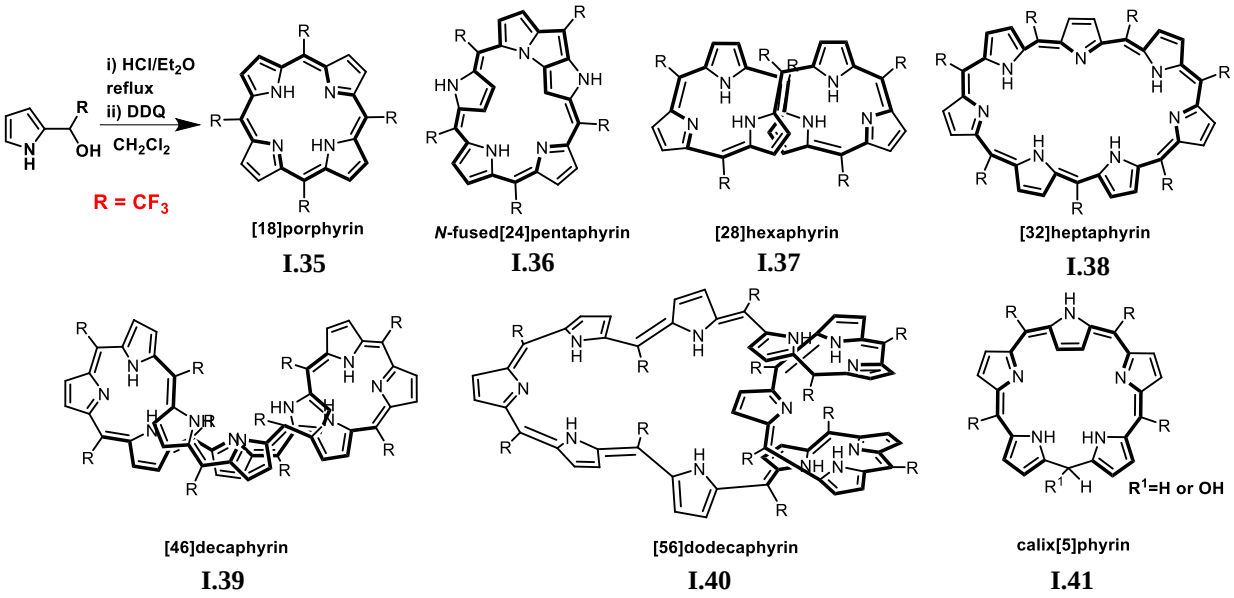

Scheme I.8: *One-pot synthesis of meso-trifluoromethyl substituted expanded porphyrins.*

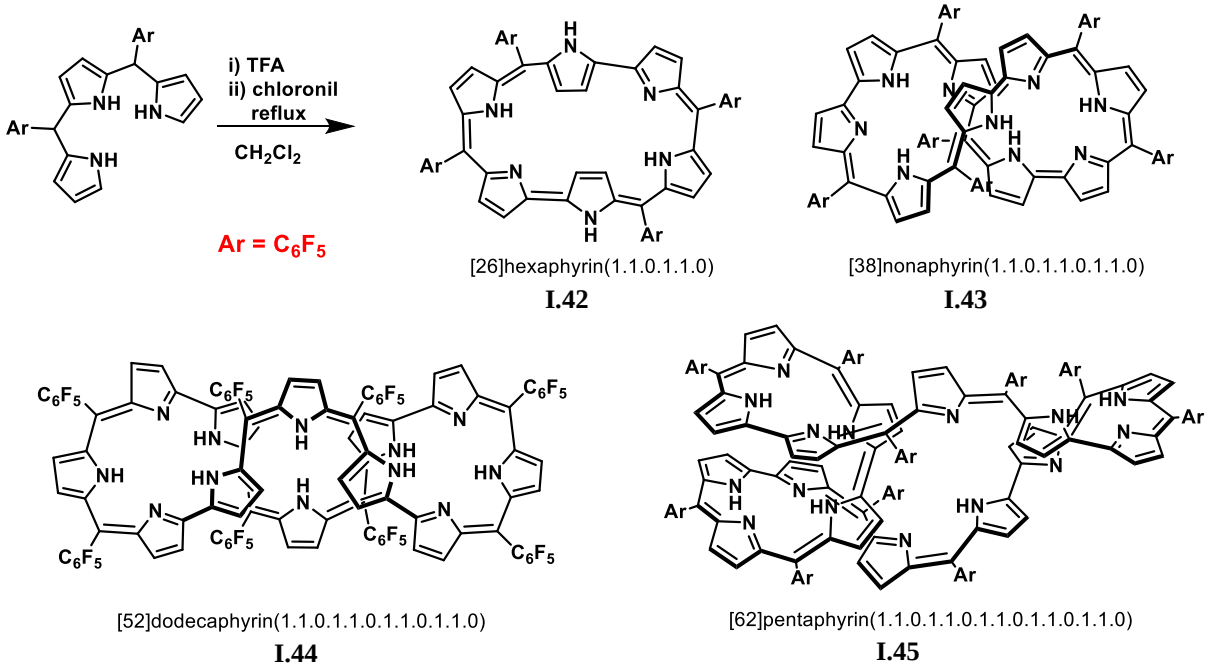

Scheme I.9: *Synthesis of higher homologue of rubyrin from tripyrrane.*

In 2007, Sessler and Osuka's groups continued the synthesis of meso-aryl rubyrin and higher porphyriniods. Oxidative coupling of tripyrrane (scheme – I.9) under acidic and reflux conditions followed by silica column chromatography gave a series of macrocycles [26]rubyrin(1.1.0.1.1.0) **I.42**, [38]nonaphyrin(1.1.0.1.1.0.1.1.0) **I.43**, [52]dodecaphyrin(1.1.0.1.1.0.1.1.0.1.1.0) **I.44** and [62]pentadecaphyrin(1.1.0.1.1.0.1.1.0.1.1.0.1.1.0) **I.45**. Molecular structure of dodecaphyrin and pentadecaphyrin were well studied. Single crystal studies of dodecaphyrin revealed the

macrocycle adopt a twisted geometry with two inward orienting tripyrrane units with near D_{2h} symmetry. However, the macrocycle was analysed as non-aromatic due to insignificant ring current effect in ^{1}H NMR spectrum. Pentadecaphyrin system was found to be non-symmetric, distorted with helically wounded moiety along with internal amine-imine hydrogen bond. This macrocycle was also non-aromatic in nature, because of loss of planarity and lack of diatropic ring current effect. [35]

Later in 2016, Osuka's group explored the redox chemistry of [52]dodecaphyrin through PCET reactions.[36] [52]dodecaphyrin is non-aromatic, blue coloured macrocycle with electronic absorptions at 379 and 598 nm. By the addition DDQ (10 equiv.) the blue colour turns to dark green colour signifying the oxidation to [50]dodecaphyrin. Its molecular absorption shows a strong B band at 845 nm and Q band at 1323 nm suggesting the aromatic nature of the macrocycle. Molecular structure of this macrocycle displayed a non-twisted, simple cyclic conformation having C_i molecular symmetry. ^{1}H NMR spectroscopy revealed its fluxional nature at room temperature. Upon reducing the temperature to -94 ℃ it could exhibit diatropic ring current effects and the molecule was analysed as aromatic in nature. Again, upon the addition of excess of MnO_2 the dark green colour turns to yellow green confirming oxidation by two electrons to yield [48]dodecaphyrin. Its molecular absorption exhibits bands at 360, 441 and 708 nm. In ^{1}H NMR, lack of significant ring current confirmed the molecule as non-aromatic in nature. The molecular structure the molecule shows doubly twisted figure of eight conformation with C_2 axis of symmetry. These redox states are reversible in nature by the addition of an equivalent amount of $NaBH_4$ to give back sequentially [48] $\rightarrow$ [50] $\rightarrow$ [52]dodecaphyrins. Expanded porphyrins adapt to twisted or coiled non planar geometry due to conformational flexibility and internal hydrogen bonding. It has been observed that protic acids such as MSA, [50]dodecaphyrin breaks the intramolecular hydrogen bonding and yields the tetraprotonated system (scheme – I.10). The electronic absorption of the tetra-protonated molecule shows a sharp and an intense Soret band at 906 nm followed by Q bands at 1346 and 1600 nm in support of the aromatic nature of the macrocycle. From molecular structure the macrocycle was found to have co-planarly arranged cyclic conformation with a C_{2h} axis of symmetry which was further supported from ^{1}H NMR. A significant influence of diatropic ring current in ^{1}H NMR and a NICS value of -12.67 ppm suggest strong aromatic nature of the molecule. Both [50]dodecaphyrin and its tetraprotonated states are identified among the largest Huckel aromatic molecules.

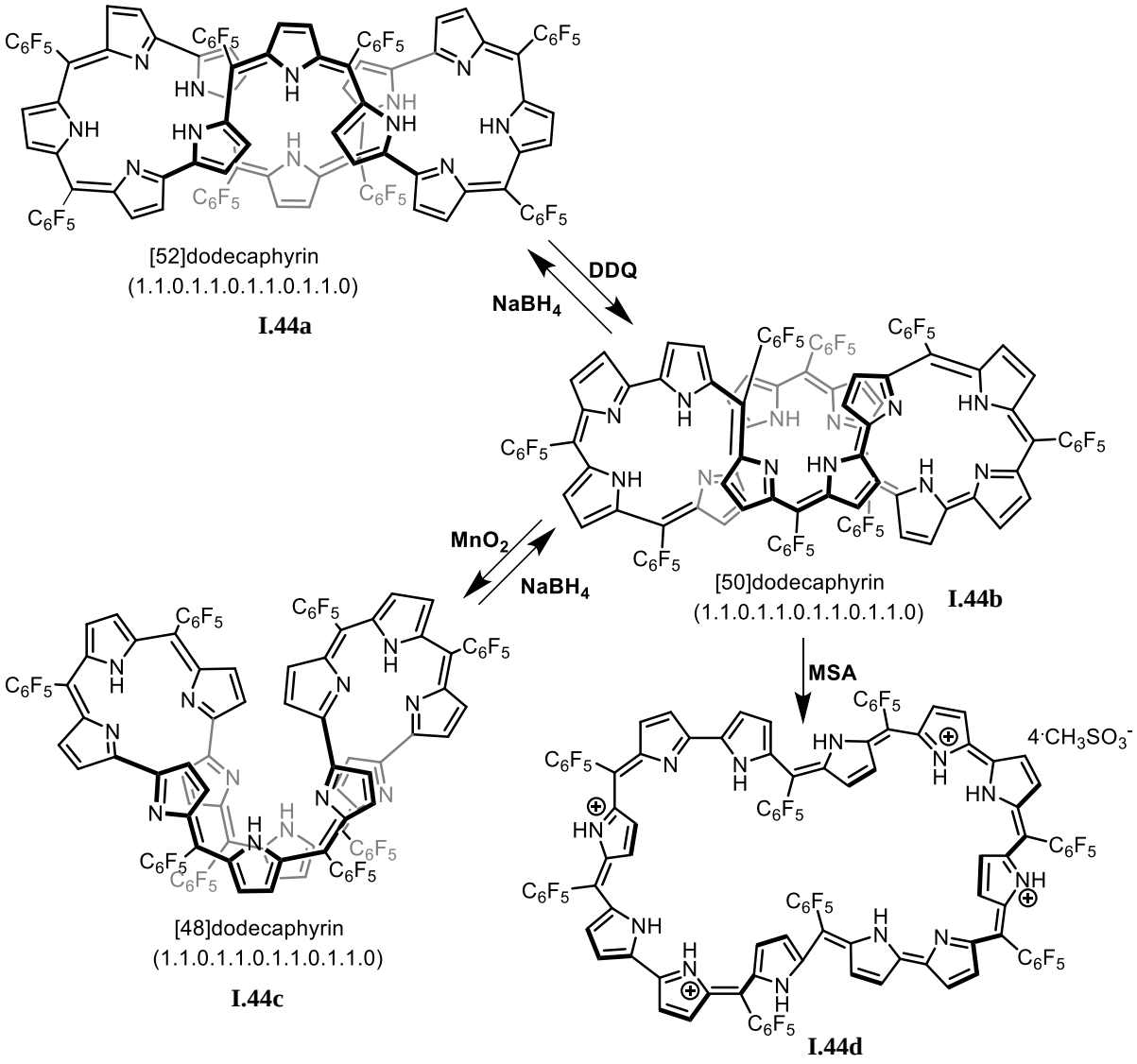

Scheme I.10: *Proton coupled electron transfer of [52], [50], [48] dodecaphyrins.*

[62]tetradecaphyrin **I.46** and its mono and bis Zn(II) metal complexes were further studied by Osuka and co-workers (figure – I.7). [62] Tetradecaphyrin was synthesised by the acid catalysed condensation of meso pentafluoro substituted dipyrromethane with pentafluorobenzaldehyde followed by oxidation. Tetradecaphyrin is green coloured compound and in solid state its structure has a C_1-symmetric conformation with complex hydrogen bonding. It shows broad electronic absorption at 899 nm and no Q band suggestive of non-aromatic character and further confirmed from ^{1}H NMR spectroscopy. Mono Zn(II) tetradecaphyrin **I.47** complex lost the conformation flexibility and adopted a twisted structure. Electronic absorption shows five peak maxima at 377, 482, 649, 1008 and 1530 nm unlike a typical porphyrinoid. Very importantly, cyclic voltammogram revealed eleven

reversible redox waves. Bis Zn (II) tetradecaphyrin **I.48**, electronic absorption shows Soret-like band at 1083 nm and Q-bands in the region of 1600-2000 nm and was found to exhibit significant diatropic ring current in its ^{1}H NMR spectrum in support of aromatic character. Molecular structure revealed two porphyrin pockets on both sides connected with an octaphyrin-like cavity in rectangular geometry.[37]

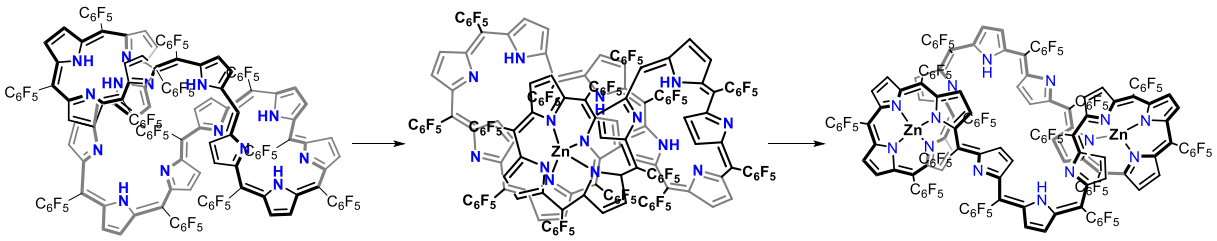

I.46 **I.47** **I.48**

Figure I.7: *Molecular structure of Tetradecaphyrin, mono Zn(II) and Bis Zn (II) tetradecaphyrin.*

I.5 Vinylogous Porphyrins

Vinylogous porphyrins are another class of aromatic aza-annulenes having Huckel's empirical formula of (4n+2)π electrons. Expansion of π-conjugation of porphyrin by increasing the number of carbon atoms in between the pyrrole rings gives a new family of co-planar vinylogous porphyrin. The platyrins (derived from the Greek word "platys" meaning "wide or broad" and the sufix "-pin" meaning of "porphyrin") are porphyrins with a general formula, [m,n,m,n]platyrins (m and n = odd numbers) (figure – I.8). This class of macrocycles are expected to be aromatic because of strong diatropic ring current. Vinylogous porphyrins are isoelectronic to π-expanded [n] annulene systems (figure I.8).

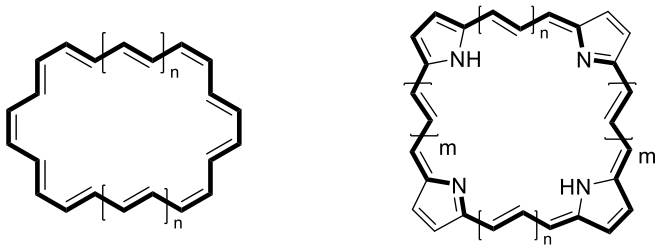

n = 0 [18]annulene	n,m = 0 [18]porphyrin
n = 1 [22]annulene	n=1, m = 0 [22]porphyrin (1.3.1.3)
n = 2 [26]annulene	n,m = 1 [26]porphyrin (3.3.3.3)
n = 4 [34]annulene	n,m = 2 [34]porphyrin (5.5.5.5)

Figure I.8: *Isoelectronic comparison of Annulene and Porphyrin.*

Vinylogous porphyrin was first synthesised by R. A. Berger and Eugene LeGoff in 1978.[38] They synthesised the 22π aromatic tetrapyrrolic, [1, 3, 1, 3] platyrin, and the aromaticity of the molecule was confirmed by the ^{1}H NMR, which showed strong diamagnetic ring current. Its extended conjugation was confirmed from electronic absorbance spectrum where it displayed Soret-like band at 477 nm with a higher ε value.

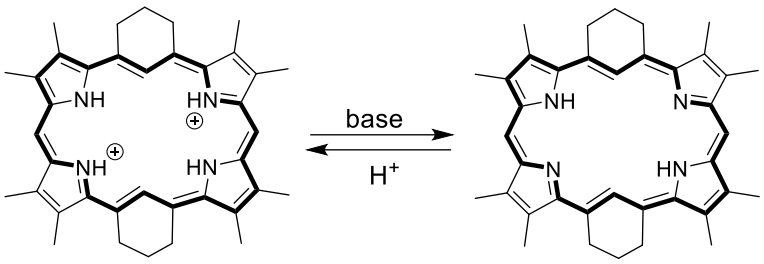

I.49a **I.49b**

Scheme I.11: *Structure of 22π aromatic tetrapyrrolic, [1, 3, 1, 3] platyrin.*

In 1986, Burchard Franck synthesised the fourfold enlarged porphyrin having strong diamagnetic ring current. The molecule was isolated as a deep red-violet coloured compound and isoelectronic to [26] annulene (figure I.9). A key motivation to study the molecule was N, N', N", N"'-tetramethylporphyrin's diatropic ring current even though molecule was non-planar due to steric hindrance from internal methyl groups.[39] In order to achieve planarity along with internal methyls, they extended the π-conjugation of bridged carbon three times (C_3) on all the four sides between the two pyrrole units. Finally the molecule was oxidised/dehydrogenated by Br_2 to obtain the fully conjugated bisquaternary [26] porphyrin-[3, 3, 3, 3] (m and n = 3). They isolated the dicationic salt with either Br^- or CF_3COO^-. Both the salts were planar, aromatic and displayed strong diatropic ring currents in ^{1}H NMR. In the electronic absorption it displayed a Soret-like band at 547 nm (909600) with molar extinction coefficient (ε) twice than the porphyrin (400000).[40]

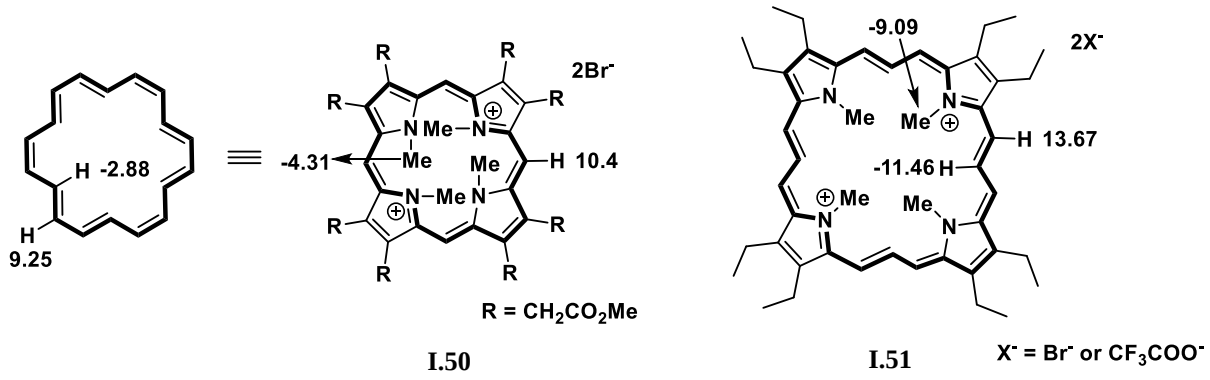

I.50 **I.51**

Figure I.9: *18π annulene and its isoelctronic structure of n-methyl porphyrin and fourfold larger bisquaternary [26] porphyrin-(3, 3, 3, 3).*

They extended the π-conjugation from fourfold to eight fold to yield octavinylogous porphyrin [34]annulene system with enhanced aromaticity (figure I.10). Isolation of a bisquaternary dibromide [34] porphyrin-[5, 5, 5, 5][41] as a deep blue coloured macrocycle displayed a λ_{max} at 664 nm in its absorption spectrum. Its ^{1}H NMR spectrum shows large diatropic ring current having maximum chemical shift difference Δδ of 31.5 ppm, wherein the inner and outer protons resonate at δ -14.27 and 17.19 ppm respectively. This diatropic ring current supports the aromaticity of 34π system with C_5 carbon chains in between the pyrrole rings with conformational stability greater than that of [18] annulene.[42]

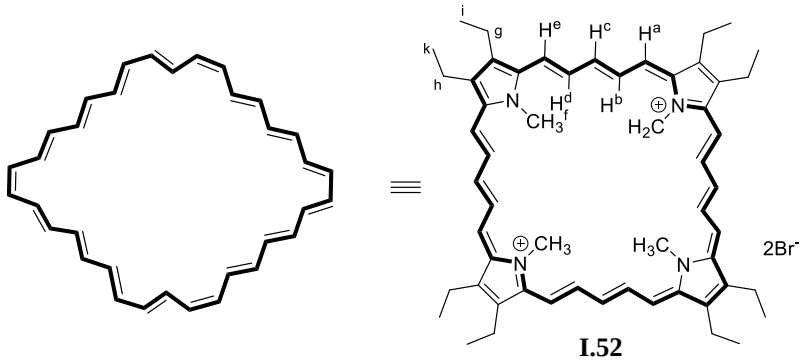

I.52

	δ (ppm)
H^a, H^e	16.18
H^b, H^d	-14.27
H^c	17.19
H^f	-11.44
H^g, H^h	6.04
H^i, H^k	2.83

Figure I.10: *Structure of Bisquaternary dibromide [34] porphyrin-(5, 5, 5, 5) isoelectronic to [34]annulene.*

Further, a bisvinylogous octaethylporphyrin [22]octaethylporphyrin (1, 3, 1, 3) **I.53** with 22π was synthesised in 1990 (figure I.11). Being a (4n+2)π system, it displayed diatropic ring current where inner and outer protons resonated at up field and downfield respectively with a large chemical shift difference of Δδ 20.2. Single crystal structure of dicationic species of this macrocycle was highly planar with two counter trifluoroacetate anions placed above and below the macrocycle. Later they extended the π-conjugation laterally and achieved the synthesis of [26]octaethylporphyrin (1, 5, 1, 5) **I.54**. As expected of a (4n+2)π electron species it displayed diatropic ring current effects in the ^{1}H NMR spectrum with an increased Δδ of 24.1, confirming enhanced aromaticity by increasing the length of the carbon chain. Molecular structure of the dicationic species shows a highly planar conformation with two counter ions placed above and below the plane of the macrocycle. A maximum extension of the π-conjugation reached up to 30π conjugation with [30]octaethylporphyrin (1, 7, 1, 7) **I.55** having a deep violet colour, with strong diatropic ring current and a Δδ value of 19.7.[43,44]

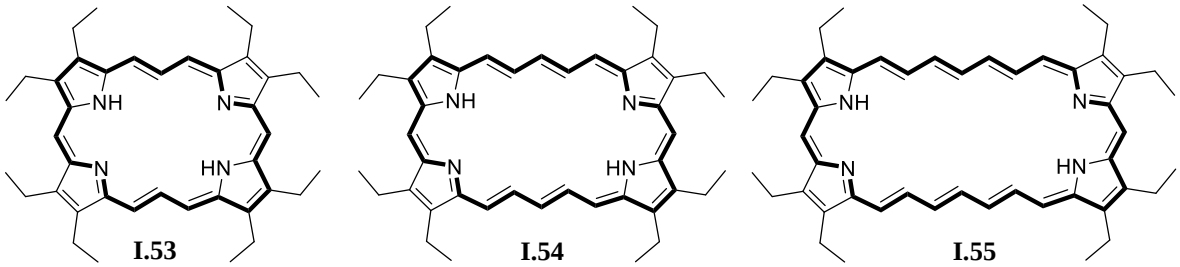

Figure I.11: *Structural representation of [22]octaethylporphyrin (1, 3, 1, 3), [26]octaethylporphyrin (1, 5, 1, 5) and [30]octaethylporphyrin (1, 7, 1, 7).*

I.6 Thiophene Incorporated Porphyrinoids

Core modification of porphyrin was pioneered by James A. Ibers in 1992, with the synthesis and characterisation of a thiophene containing 26π macrocycle (figure I.12). An insertion of thiophene into bipyrrole system of porphycene was achieved by McMurry coupling of 2, 5-bis (5-formyl-4-propyl-2-pyrrolyl)thiophene followed by the air oxidation. The isolated macrocycle **I.59** was planar with a D_{2h} symmetry and aromatic in nature as confirmed by diatropic ring current in its ^{1}H NMR spectrum. In the UV-visible spectrum it displayed a Soret like band at 460 and 501 nm followed by Q bands at 745, 780, 790 and 859 nm.[45]

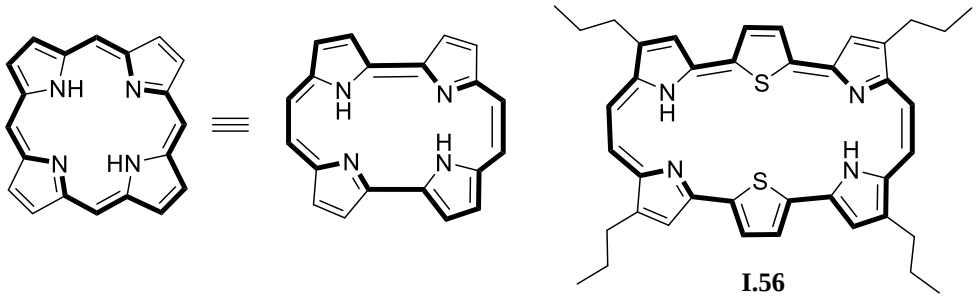

Figure I.12: *Structure of core modified, thiophene appended porphycene.*

In 1994, Michael P. Cava's group synthesised a new class of sulphur bridged annulenes through McMurry type of condensation (scheme I.12). They employed McMurry condensation of (a) 2, 5-thiophenedialdehyde in the presence of $TiCl_4$/Zinc reagent in pyridine and THF under reflux conditions.[46] The reaction was followed by the column chromatography to yield three and four membered macrocycles of [18]annulene trisulfide and [24]annulene tetrasulfide. Molecular structure of the three membered [18]annulene trisulfide determined from X-ray diffraction studies revealed a non-planar geometry. Employing McMurry condensation under similar conditions for (b) 2, 2'-bithiophene 5, 5'-dicarboxaldehyde yielded four membered thiophene containing 20π porphycene. It was expected to be antiaromatic (4nπ) system and UV/visible and NMR study suggested a non-

planar geometry. Tetrafuran porphycene and its dication were successfully studied by Vogel's group but the formation of dication to 20π system of tetrathiophene remained elusive. Six membered thiophene containing 30π conjugate system was also expected to display diatropic ring current. However from NMR spectroscopy this macrocycle was identified as non-aromatic in nature. MuMurry condensation was further employed to couple of 5, 5'-terthiophenedicarboxaldehyde to yield the 28π antiaromatic macrocycle.[46] Unexpectedly, a dark red coloured macrocycle was identified with moderate stablity under ambient conditions. ^{1}H NMR suggested a non-coplanar, centrosymmetric structure with all protons resonating in the range δ 6.94 to 6.26 ppm. Its UV/vis spectrum shows 431, 394, 381, 272 and 227 nm suggesting molecule could not attain complete conjugation and highlighting the non-antiaromatic nature of the macrocycle. Addition of H_2SO_4 to the dark red colour changes to purple colour indicating the oxidation to 26π system. This two-electron ring oxidation and aromatic character was confirmed by the strong diatropic ring current from ^{1}H NMR spectroscopy. In addition, (c) an aromatic tetrathia[22]annulene(2,1,2,1) was also synthesised, as confirmed by the diatropic ring current from ^{1}H NMR spectroscopy. Its aromatic characteristics was further supported by the observation of a Soret like absorption at 415 nm followed by Q-like bands at 503, 540, 579 and 771 nm in the UV/vis spectrum.[46]

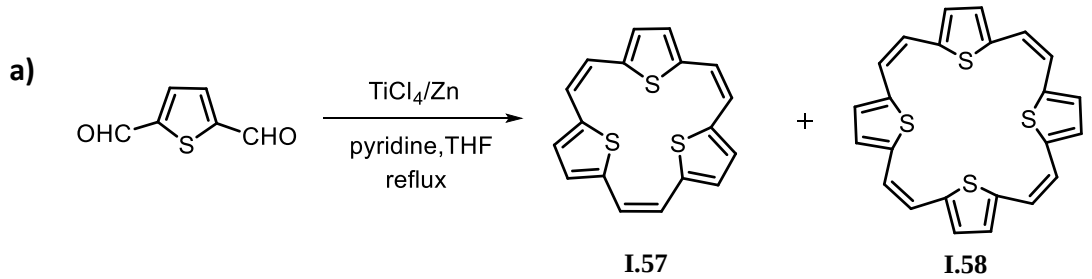

I.57 **I.58**

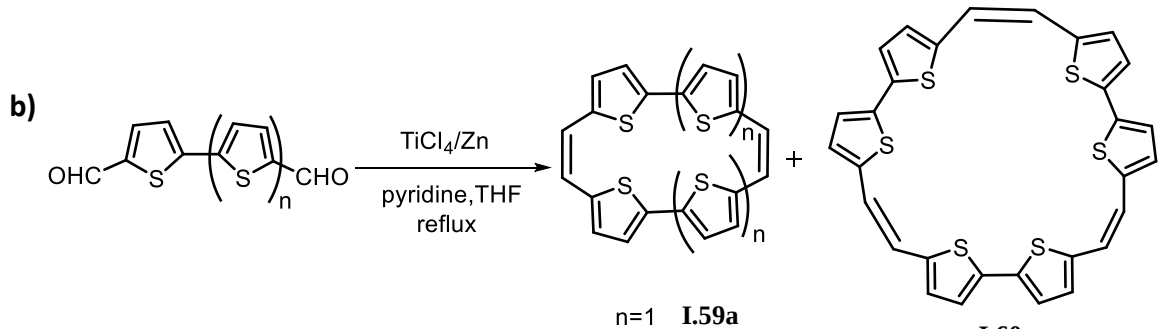

n=1 **I.59a**
n=2 **I.59b**

I.60

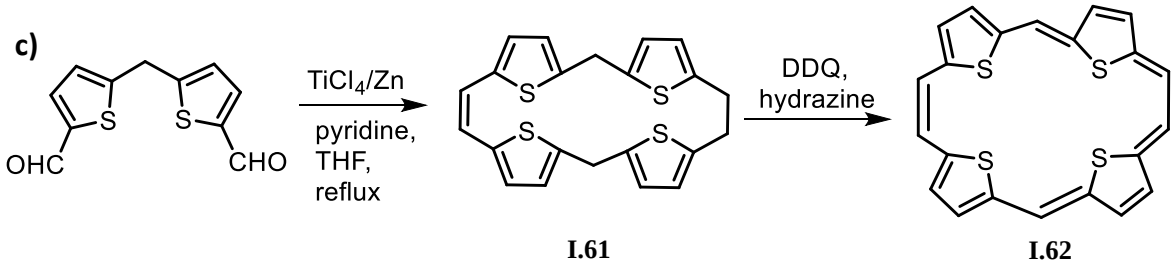

I.61 **I.62**

Scheme I.12: *Synthesis of ethylene bridged macrocycles from McMurry coupling of thiophene, bithiophene and terthiophene dialdehyde.*

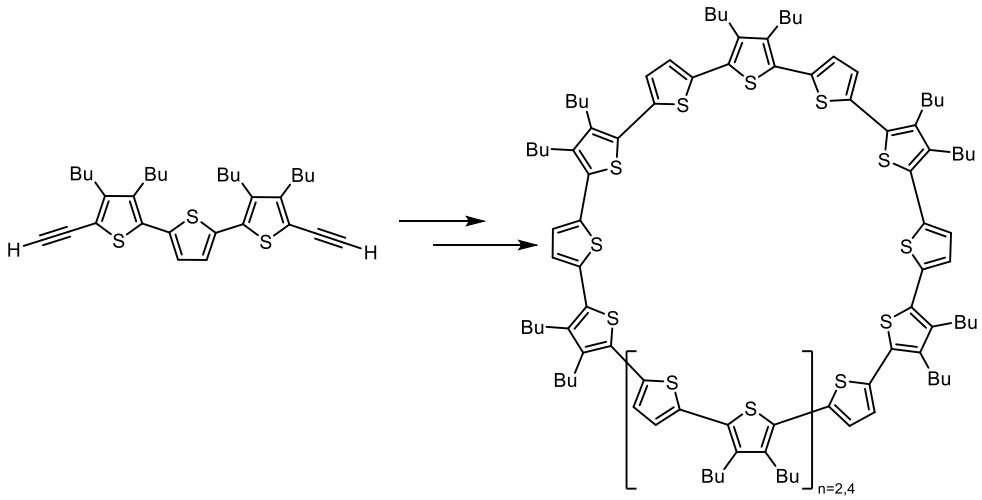

I.63a - I.63d

Scheme I.13: *Synthesis of α-conjugated Macrocyclic Oligothiophenes.*

In 2000, Peter Bauerle and co-workers synthesised a fully α-conjugated macrocyclic oligothiophenes with tuneable cavity size (scheme I.13). The synthetic strategy starts from β-butylated thiophenes 1-3 (in alternative thiophene) followed by the selective α-thiophene iodination by molecular iodine and mercury (II) acetate in chloroform. It was followed by the introduction of acetylenic groups at terminal position achieved by the Sonagashira-Hagihara coupling using Pd catalyst. Terminal TMS was deprotected under mild basic conditions to yield the thiophenediynes. A better yield for the formation of cyclooligothiophenediacetylenes, was obtained by the Eglinton-Glaser coupling (through oxidative coupling). This reaction was performed in pyridine by addition of oligothiophenes in the presence of anhydrous CuCl and $CuCl_2$ at room temperature for three days to yield stable, bright yellow to red microcrystalline solids. These compounds were soluble in common organic solvents due to the presence of β-butyl groups. The macrocycles formed with 39, 52, 57 and 76 chains were found to have cavities with internal diameter of 1.37,

1.99, 2.14 and 3.07 nm respectively. Addition of sodium sulfide to cyclooligothiophenediacetylenes gave fully α-conjugated cyclo[n]thiophenes. Scanning tunnelling microscopy (STM) offered excellent image structure for cyclo[12]thiophene as well ordered and very stable 2D crystalline monolayers packed hexagonally like a honeycomb pattern. The estimated diameter of the molecule shows 2.34 nm and diameter of the π-conjugated system is 1.83 nm with a height of 0.48 nm (from side view).[47]

In 2008, Masahiko Iyoda and co-workers synthesised the giant thienylene acetylene ethylene macrocycles with large two photon absorbance. Acetylene bridged hexathiophene with β-butyl substituted dialdehyde oligomers undergo McMurry coupling in the presence of $TiCl_4$/Zn reagent in pyridine/THF solvent system to yield a series of macrocycles of n-mers of 12, 18, 24 and 30 with 21- 60 Å of internal diameter along with moderate molecular rigidity (scheme I.14). These macrocycles (**I.67a - I.67d)** account for 72, 108, 144 and 180 π-electrons. An increase in the number of π-conjugation is expected to red shift the λ_{max} to a lower energy with a concomitant increase in the molar extension coefficient (ε). However, these macrocycles displayed saturation of absorption maxima after **I.67c** and **I.67d**. Hence it was concluded that the effective conjugation saturated beyond 18 thiophene units. Molecular structure shows nearly a circular shape structure with all thiophene in cisoid form. However, the two double bonds were in transiod form with thiophene of sulphur flipped outside and the overall molecule adopted a slightly bent chair like structure. The macrocycles from **I.67a - I.67d** have dissimilar molecular symmetry through D_2, D_3, D_4 and D_5 respectively. While going to higher ring size, the macrocycles were highly flexible with more degrees of freedom, and hence the molecules lose planarity.[48]

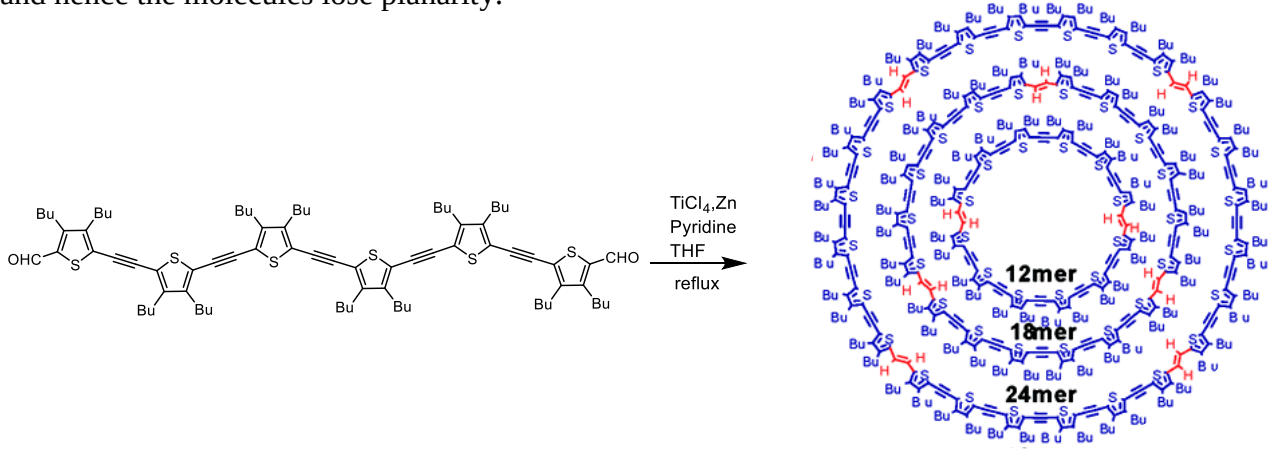

I.64a - I.64d

Scheme I.14: *Giant thienylene acetylene ethylene macrocycles from MuMurry coupling.*

I.7 Redox Chemistry

Except molecular rearrangement, most of the chemical reactions proceed through redox reactions. Among many, PCET and electron transfer (ET) reactions are highly dominant. Needless to say, oxidation of water in photosynthesis and reduction of oxygen in respiratory reaction proceeds through PCET and most of the metal mediated electron transfer reactions proceeds by ET. In porphyrin macrocycles the redox is driven by PCET reactions because of amine-imine interconversion and facile protonation of imine nitrogen. Accordingly, Huckel's aromatic (4n+2)π or antiaroamticity (4n)π species can undergo reversible redox through two electrons and protons as in case of [18] porphyrin and [20]isophlorin reversible redox switching happens via PCET.[49]

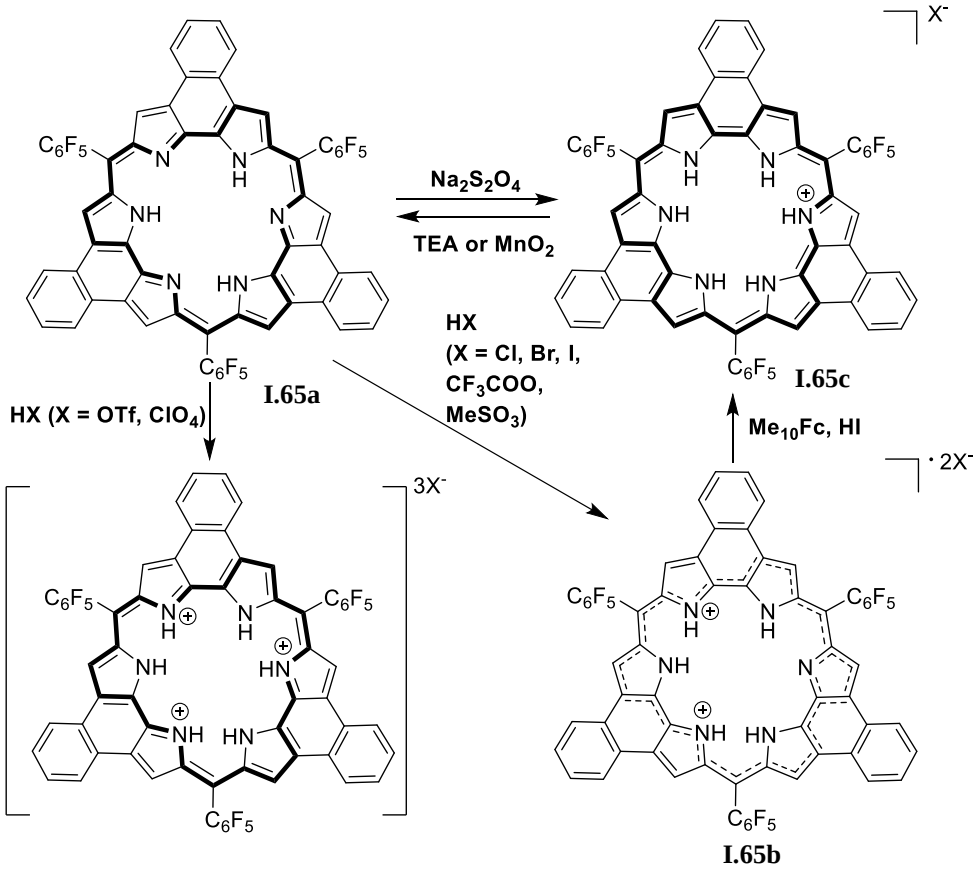

Scheme I.15: *Study of proton coupled electron transfer reaction in β, β′ -fused Rosarian.*

Among many examples, Sessler and co-workers reported a reversible PCET reaction in a β, β′-fused Rosarin (scheme I.15). Rosarin is a planar macrocycle and, accounts for 24π electrons as per Huckel's antiaromatic 4nπ systems, Its estimated NICS (0) value of +17.48 ppm and observation of paratropic ring current effects in ^{1}H NMR spectroscopy further confirmed its antiaromatic character. This macrocycle displayed redox active switch to 26π

aromatic system by the addition of sodium thiosulphate ($Na_2S_2O_4$) and can revert back to neutral state upon the addition of TEA or MnO_2. A stepwise study of the redox process was observed by the addition of hydrogen halides like HCl which yield the stable 25π radical dicationic intermediate. This was further confirmed by the ESR spectroscopy and the molecule was characterized as non-aromatic in nature based on the estimated NICS (0) value of +5.32 ppm. Addition of HI in the presence of decamethaneferrocene gave the 24π aromatic monocationic species, supported by the NICS (0) value of -14.39 ppm. In support of aromatic characteristics it displayed diatropic ring current effects in its ^{1}H NMR spectrum. Importantly the acid induced redox reactions and radical intermediate were not observed in the non-annulated rosarian.

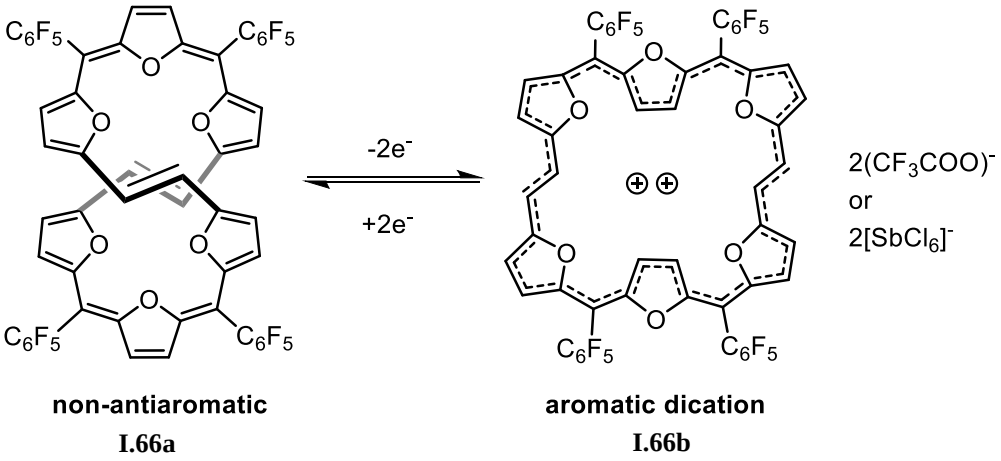

Scheme I.16: *Reversible two-electron oxidation of a 32π core-modified expanded Isophlorin.*

Other than PCET, ET processes have also been observed in metal complexes. Importantly, similar reactions have been observed due to ring oxidation of antiaromatic isophlorin, as observed by Vogel. Hence, isophlorin is also known as pseudometal.[50] The tetrapyrrolic [18] porphyrin is a stable aromatic system. However, core-modified porphyrins of tetra-furan/thiophene/selenophene/-N-methylpyrrole manifest as 20π antiaromatic isophlorin system and are widely known to adapt to the 18π dicationic state rather than neutral free base.[51] In contrast, Anand's group reported the first stable antiaromatic 20π tetrafuran isophlorin with electron withdrawing pentaflurophenyl meso substitutents.[57] Further, the same group reported a 32π antiaromatic system[52] which undergoes reversible two-electron ring oxidation to yield stable 30π aromatic dicationic species. Different core-modified 32π antiaromatic systems could be synthesized by varying the number of thiophene and furan heterocycles. Irrespective of heterocyclic units in these macrocycles, addition of TFA/$NOBF_4$/$[Et_3O]^+$ $[SbCl_6]^-$ induced two-electron oxidation to form 30π aromatic dicationic

system (scheme I.16). Addition of TEA/Zn/$FeCl_2$ reduces the dicationic speices by two electrons and reverts back to the neutral 32π antiaromatic state. Since these macrocycles exhibit reversible redox, it can be expected that they can be stabilized in different oxidation states with suitable redox reagent.

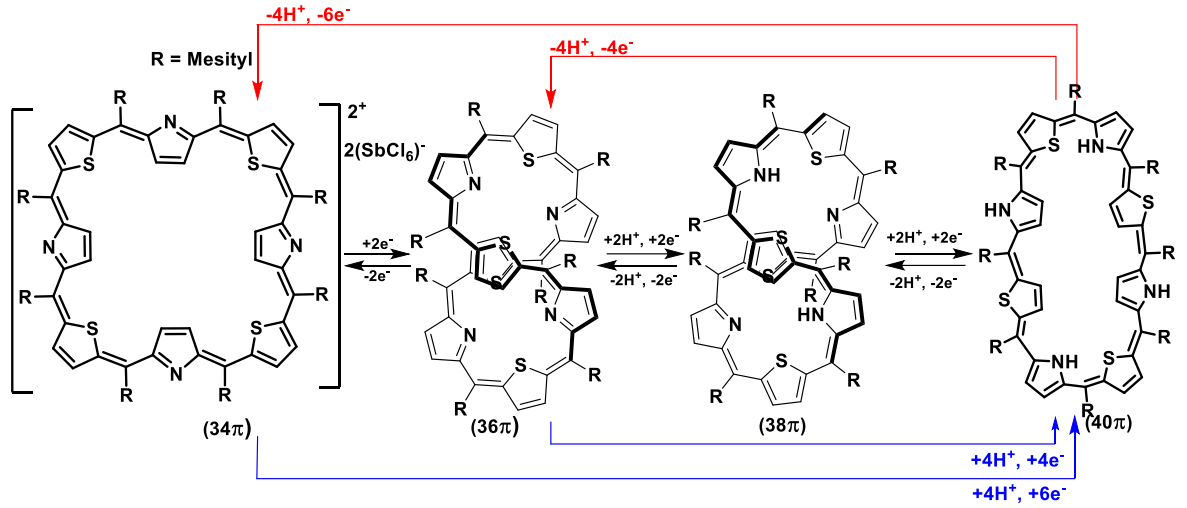

I.67a- I.67d

Scheme I.17: *Study of PCET and ET in core modified Octaphyrin.*

Studies from the same group revealed that PCET was more facile in partially core modified expanded porphyrinoids. Particularly, 30π hexaphyrin and 38π ocaphyrin shows multiple redox states and can be reversibly switched between stable aromatic / antiaromatic states which differ by two-electrons.[53] Core-modified dithia 28π hexaphyrin was characterized as antiaromatic and further supported by the estimated NICS value +19 ppm. It undergoes two-electron ring oxidation upon the addition of $[Et_3O]^+$ $[SbCl_6]^-$ to yield 26π aromatic species which undergoes facile two-electron reduction to revert back to its neutral state upon the addition of TEA. Addition of excess Zn metal along with NH_4Cl to 28π or 26π system readily reduces to 30π system through two or four electrons respectively. Partial oxidation to a neutral antiaromatic 28π is achieved by the addition of MnO_2. Addition of $[Et_3O]^+$ $[SbCl_6]^-$ to 30π system oxidizes the macrocycle by four electron oxidation to yield the aromatic and dicatioinc 26π system. Analogous to 28π hexaphyrin, a wide range of redox states has been observed in 38π octaphyrin (scheme – I.17). A non-planar 38π octaphyrin with meso-tolyl substituents was synthesised by the Latos and co-workers[49] and identified its two-electron reversible redox by the addition of MnO_2 to 36π system. It reverts back to 38π system by the addition $NaBH_4$. Further, Anand and co-workers identified two more redox states, i.e. 34π and 40π electrons of a similar octaphyrin obtained by the replacement of meso tolyl group by mesityl group. 36π system can be oxidized by two more electrons to its maximum oxidised

state with 34π electrons. In contrast to the figure-of-eight toplogy, the 34π dication was characterized as squarish macrocycle with thiophene and pyrrole facing in and out alternatively. The dicationic species was accompanied with two counter anions, $SbCl_6^-$, placed above and below the plane of macrocycle. Reduction of the 34π dication by Zn and NH_4Cl gives the most reduced species with 40π electrons and with a modified planar molecular structure. It changed to a rectangular geometry with alternative thiophene and pyrrole facing in and outward, and the macrocycle attained isophlorin-like conjugation.[54]

Unlike the reversible redox process described for the core-modified octaphyrins, Osuka and co-workers reported the deprotonation of non-aromatic [36] octaphyrin (1.1.1.1.1.1.1.1) to yield mono anionic and dianionic species by the stiochiometric addition of a strong base such as tetrabutylammonium fluoride (TBAF) (scheme I.18). By the addition of 40 equivalences of TBAF, a twisted figure of eight octaphyrin attains a monoanionic twisted Mobius aromatic state as confirmed from the estimated NICS value of -11.9 ppm and HOMA value of 0.77. Further addition of 7000 equivalence of TBAF yielded the dianionic 40π antiaromatic species, and transforms into squarish geometry with alternative pyrrole units facing in and out of the macrocycle akin to 40π cyclcoctafuran, **I.34**. A large positive NICS value of +22.6 ppm and HOMA value of 0.52 strongly supports the Huckel's antiaromatic nature of the macrocycle. Titration with TFA revived the monoanionic Mobius antiaromatic macrocycle and the diprotonated, neutral figure eight octaphyrin.[55]

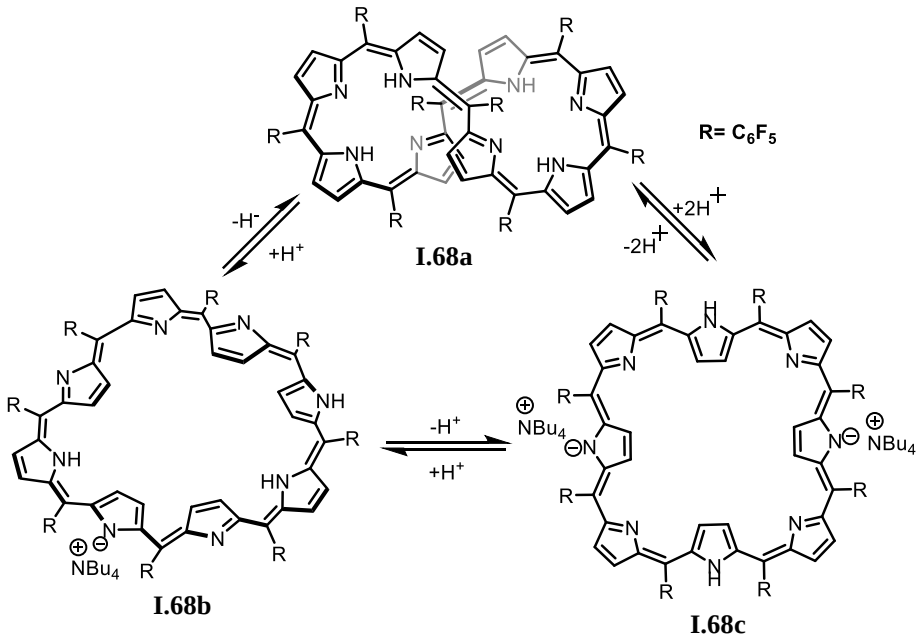

Scheme I.18: *Deprotonation of [36]octaphyrin to yield Mobius aromatic monoanionic and antiaromatic dianionic [36]octaphyrin.*

I.8 Aim of the thesis

Based on the above described chemistry of porphyrinoids, both ring oxidation and PCET mechanism are possible to access multiple oxidation states of redox active macrocycles even in the absence of metal. Moreover, as the circumference of a macrocycle tends to expand, they also induce flexible topology which can affect the aromatic characteristics of a given porphyrinoid. However, access to such large porphyrinoids has always been hindered by simple and efficient synthetic protocols. Even though pyrrole based giant porphyrinoids have been reported[56], non-pyrrolic porphyrinoids are limited only to eight or less heterocyclic units.[2] Since, non-pyrrolic porphyrnoids are known to adopt isophlorin like conjugation, they are expected to be highly susceptible to ring oxidation. Therefore, they have the potential to exhibit novel structural topologies and perhaps unexplored electronic properties. In this thesis, I have attempted to synthesize novel expanded isophlorinoids and elucidate their structural, electronic and redox properties. In order to study the role of ring oxidation, the macrocycles have been constructed mostly from thiophene subunits. The macrocyclic conjugation has been altered by incorporating subtle synthetic modifications to either increase or decrease the π-electron count in any given porphyrinoid. In this endeavour, both $(4n+2)\pi$ and $4n\pi$ electron macrocycles could be synthesized and characterized with all possible analytical techniques including single crystal X-ray crystallography. Their spectroscopic and redox properties have been elucidated by electronic absorption spectroscopy and cyclic voltammetry studies. In addition, spectro-electrochemistry studies were also conducted to substantiate the redox active species in support of the reversible chemical redox process. In some cases, both or more redox states of a given macrocycle could be isolated and characterized through NMR spectroscopy to evaluate the aromatic characteristics of the species. All these findings have been further supported by suitable and appropriate quantum chemical calculations such as NICS and ACID values to substantiate the aromatic properties as inferred from experimental results.

I.9 References:

1. a) The Porphyrin Handbook (Eds.: K. M. Kadish, K. M. Smith, R. Guilard), Academic Press, San Diego, 2000; b) Handbook of Porphyrin Science (Eds.: K. M. Kadish, K. M. Smith, R. Guilard) World Scientific Publishing, Singapore, 2010.
2. Reddy, B. K.; Basavarajappa, A.; Ambhore, M. D.; Anand, V. G., Isophlorinoids: The Antiaromatic Congeners of Porphyrinoids. *Chem. Rev.* **2017,** *117* (4), 3420-3443.
3. Woodward, R. B., Totalsynthese des Chlorophylls. *Angew. Chem.* **1960,** *72* (18), 651-662.
4. Vogel, E., The porphyrins from the 'annulene chemist's' perspective. In *Pure and Applied Chemistry*, 1993; Vol. 65,143-152.
5. Chao Liu, Dong-Mei Shen, and Qing-Yun Chen, Synthesis and Reactions of 20 π-Electron a-Tetrakis(trifluoromethyl)-meso-tetraphenylporphyrins, *J. Am. Chem. Soc.***2007**, *129*, 5814-5815.
6. Furuta, H.; Asano, T.; Ogawa, T., "N-Confused Porphyrin": A New Isomer of Tetraphenylporphyrin. *J. Am. Chem. Soc.* **1994,** *116* (2), 767-768.
7. Vogel, E.; Köcher, M.; Schmickler, H.; Lex, J., Porphycene—a Novel Porphin Isomer. *Angew. Chem., Int. Ed.***1986,** *25* (3), 257-259.
8. Saito, S.; Osuka, A., Expanded Porphyrins: Intriguing Structures, Electronic Properties, and Reactivities. *Angew. Chem., Int. Ed.* **2011,** *50* (19), 4342-4373.
9. Shivran, N.; Gadekar, S. C.; Anand, V. G., "To Twist or Not to Twist": Figure-of-Eight and Planar Structures of Octaphyrins. *Chem-Asian J.* **2017,** *12* (1), 6-20.
10. Tanaka, T.; Osuka, A., Chemistry of meso-Aryl-Substituted Expanded Porphyrins: Aromaticity and Molecular Twist. *Chem. Rev.* **2017,** *117* (4), 2584-2640.
11. Sessler, J. L.; Seidel, D., Synthetic expanded porphyrin chemistry. *Angew. Chem., Int. Ed.* **2003,** *42* (42), 5134-75.
12. Bauer, V. J.; Clive, D. L. J.; Dolphin, D.; Paine, J. B., III; Harris, F. L.; King, M. M.; Loder, J.; Wang, S. W. C.; Woodward, R. B., Sapphyrins: novel aromatic pentapyrrolic macrocycles. *J. Am. Chem. Soc.* **1983,** *105* (21), 6429-6436.
13. Sessler, J. L.; Cyr, M. J.; Lynch, V.; McGhee, E.; Ibers, J. A., Synthetic and structural studies of sapphyrin, a 22 π-electron pentapyrrolic "expanded porphyrin". *J. Am. Chem. Soc.* **1990,** *112* (7), 2810-2813.
14. Sessler, J. L.; Morishima, T.; Lynch, V., Rubyrin: A New Hexapyrrolic Expanded Porphyrin. *Angew. Chem., Int. Ed.*, **1991,** *30* (8), 977-980.
15. Sessler, J. L.; Weghorn, S. J.; Lynch, V.; Johnson, M. R., Turcasarin, the Largest Expanded Porphyrin to Date. *Angew. Chem., Int. Ed.* **1994,** *33* (14), 1509-1512.

16. Vogel, E.; Bröring, M.; Fink, J.; Rosen, D.; Schmickler, H.; Lex, J.; Chan, K. W. K.; Wu, Y.-D.; Plattner, D. A.; Nendel, M.; Houk, K. N., From Porphyrin Isomers to Octapyrrolic "Figure Eight" Macrocycles. *Angew. Chem., Int. Ed.* **1995,** *34* (22), 2511-2514.

17. Broring, M.; Jendrny, J.; Zander, L.; Schmickler, H.; Lex, J.; Wu, Y. D.; Nendel, M.; Chen, J. G.; Plattner, D. A.; Houk, K. N.; Vogel, E., Octaphyrin-(1.0.1.0.1.0.1.0). *Angew. Chem., Int. Ed.* **1995,** *34* (22), 2515-2517.

18. Sessler, J. L.; Weghorn, S. J.; Morishima, T.; Rosingana, M.; Lynch, V.; Lee, V., Rosarin: a new, easily prepared hexapyrrolic expanded porphyrin. *J. Am. Chem. Soc.* **1992,** *114* (21), 8306-8307.

19. Setsune, J.-i.; Katakami, Y.; Iizuna, N., [48]Dodecaphyrin-(1.0.1.0.1.0.1.0.1.0.1.0) and [64]Hexadecaphyrin-(1.0.1.0.1.0.1.0.1.0.1.0.1.0.1.0): The Largest Cyclopolypyrroles. *J. Am. Chem. Soc.* **1999,** *121* (38), 8957-8958.

20. Setsune, J.-i.; Maeda, S., Bis(azafulvene) as a Versatile Building Block for Giant Cyclopolypyrroles: X-ray Crystal Structure of [64]Hexadecaphyrin-(1.0.1.0.1.0.1.0.1.0.1.0.1.0.1.0). *J. Am. Chem. Soc.* **2000,** *122* (49), 12405-12406.

21. Rothemund, P., A New Porphyrin Synthesis. The Synthesis of Porphin1. *J. Am. Chem. Soc.* **1936,** *58* (4), 625-627.

22. Adler, A. D.; Longo, F. R.; Finarelli, J. D.; Goldmacher, J.; Assour, J.; Korsakoff, L., A simplified synthesis for meso-tetraphenylporphine. *J. Org. Chem.* **1967,** *32* (2), 476-476.

23. Lindsey, J. S.; Schreiman, I. C.; Hsu, H. C.; Kearney, P. C.; Marguerettaz, A. M., Rothemund and Adler-Longo reactions revisited: synthesis of tetraphenylporphyrins under equilibrium conditions. *J. Org. Chem.* **1987,** *52* (5), 827-836.

24. Shin, J.-Y.; Furuta, H.; Yoza, K.; Igarashi, S.; Osuka, A., meso-Aryl-Substituted Expanded Porphyrins. *J. Am. Chem. Soc.* **2001,** *123* (29), 7190-7191.

25. Shin, J.-Y.; Furuta, H.; Osuka, A., N-Fused Pentaphyrin. *Angew. Chem., Int. Ed.* **2001,** *40* (3), 619-621.

26. Brückner, C.; D. Sternberg, E.; W. Boyle, R.; Dolphin, D., 5,10-Diphenyltripyrrane, a useful building block for the synthesis of meso-phenyl substituted expanded macrocycles. *Chem. Comm.* **1997,** (17), 1689-1890.

27. G. P. M. S. Neves, M.; M. Martins, R.; C. Tomé, A.; J. D. Silvestre, A.; M. S. Silva, A.; Félix, V.; A. S. Cavaleiro, J.; G. B. Drew, M., meso-Substituted expanded porphyrins: new and stable hexaphyrins. *Chem. Comm.* **1999,** (4), 385-386.

28. Yoon, M.-C.; Shin, J.-Y.; Lim, J. M.; Saito, S.; Yoneda, T.; Osuka, A.; Kim, D., Solvent-Dependent Aromatic versus Antiaromatic Conformational Switching in meso-(Heptakis)pentafluorophenyl [32]Heptaphyrin. *Chem. Eur. J.* **2011,** *17* (24), 6707-6715.
29. Saito, S.; Shin, J.-Y.; Lim, J. M.; Kim, K. S.; Kim, D.; Osuka, A., Protonation-Triggered Conformational Changes to Möbius Aromatic [32]Heptaphyrins(1.1.1.1.1.1.1). *Angew. Chem., Int. Ed.* **2008,** *47* (50), 9657-9660.
30. Lim, J. M.; Shin, J.-Y.; Tanaka, Y.; Saito, S.; Osuka, A.; Kim, D., Protonated [4n]π and [4n+2]π Octaphyrins Choose Their Möbius/Hückel Aromatic Topology. *J. Am. Chem. Soc.* **2010,** *132* (9), 3105-3114.
31. Kamimura, Y.; Shimizu, S.; Osuka, A., [40]Nonaphyrin(1.1.1.1.1.1.1.1.1) and Its Heterometallic Complexes with Palladium–Carbon Bonds. *Chem. Eur. J.* **2007,** *13* (5), 1620-1628.
32. Tanaka, Y.; Shin, J.-Y.; Osuka, A., Facile Synthesis of Large meso-Pentafluorophenyl-Substituted Expanded Porphyrins. *Eur. J. Org. Chem.*, **2008**, 1341–1349.
33. Reddy, J. S.; Mandal, S.; Anand, V. G., Cyclic Oligofurans: One-Pot Synthesis of 30π and 40π Expanded Porphyrinoids. *Org. Lett.* **2006,** *8* (24), 5541-5543.
34. Shimizu, S.; Aratani, N.; Osuka, A., meso-Trifluoromethyl-Substituted Expanded Porphyrins. *Chem. Eur. J.***2006,** *12* (18), 4909-4918.
35. Shimizu, S.; Cho, W.-S.; Sessler, J. L.; Shinokubo, H.; Osuka, A., meso-Aryl Substituted Rubyrin and Its Higher Homologues: Structural Characterization and Chemical Properties. *Chem. Eur. J.* **2008,** *14* (9), 2668-2678.
36. Soya, T.; Kim, W.; Kim, D.; Osuka, A., Stable [48]-, [50]-, and [52]Dodecaphyrins(1.1.0.1.1.0.1.1.0.1.1.0): The Largest Hückel Aromatic Molecules. *Chem. Eur. J.* **2015,** *21* (23), 8341-8346.
37. Yoneda, T.; Soya, T.; Neya, S.; Osuka, A., [62]Tetradecaphyrin and Its Mono- and Bis-ZnII Complexes. *Chem. Eur. J.* **2016,** *22* (41), 14518-14522.
38. Berger, R. A.; LeGoff, E., The synthesis of a 22π-electron tetrapyrrolic macrocycle, [1,3,1,3] platyrin. *Tetrahedron. Lett.* **1978,** *19* (44), 4225-4228.
39. Franck, B.; Wegner, C., A N,N′,N″,N‴—Tetramethylporphyrinogen. *Angew. Chem., Int. Ed.* **1975,** *14* (6), 424-424.
40. Gosmann, M.; Franck, B., Synthesis of a Fourfold Enlarged Porphyrin with an Extremely Large, Diamagnetic Ring-Current Effect. *Angew. Chem., Int. Ed.* **1986,** *25* (12), 1100-1101.
41. Knübel, G.; Franck, B., Biomimetic Synthesis of an Octavinylogous Porphyrin with an Aromatic [34]Annulene System. *Angew. Chem., Int. Ed.* **1988,** *27* (9), 1170-1172.

42. König, H.; Eickmeier, C.; Möller, M.; Rodewald, U.; Franck, B., Synthesis of a Bisvinylogous Octaethylporphyrin. *Angew. Chem., Int. Ed .*, **1990,** *29* (12), 1393-1395.

43. LeGoff, E.; Weaver, O. G., Synthesis of a [1,5,1,5]platyrin, a 26.pi.-electron tetrapyrrolic annulene. *J. Org. Chem.* **1987,** *52* (4), 710-711.

44. Eickmeier, C.; Franck, B., Hexavinylogous Porphyrins with Aromatic 30 π-Electron Systems. *Angew. Chem., Int. Ed.* **1997,** *36* (20), 2213-2215.

45. Johnson, M. R.; Miller, D. C.; Bush, K.; Becker, J. J.; Ibers, J. A., Synthesis and characterization of a new 26.pi.-aromatic thiophene-containing macrocyclic ligand. *J. Org. Chem.* **1992,** *57* (16), 4414-4417.

46. Hu, Z. Y.; Atwood, J. L.; Cava, M. P., A Simple Route to Sulfur-Bridged Annulenes. *J. Org. Chem.* **1994,** *59* (26), 8071-8075.

47. Krömer, J.; Rios-Carreras, I.; Fuhrmann, G.; Musch, C.; Wunderlin, M.; Debaerdemaeker, T.; Mena-Osteritz, E.; Bäuerle, P., Synthesis of the First Fullyα-Conjugated Macrocyclic Oligothiophenes: Cyclo[n]thiophenes with Tunable Cavities in the Nanometer Regime. *Angew. Chem.* **2000,** *39* (19), 3481-3486.

48. Williams-Harry, M.; Bhaskar, A.; Ramakrishna, G.; Goodson, T., 3rd; Imamura, M.; Mawatari, A.; Nakao, K.; Enozawa, H.; Nishinaga, T.; Iyoda, M., Giant thienylene-acetylene-ethylene macrocycles with large two-photon absorption cross section and semishape-persistence. *J. Am. Chem. Soc.* **2008,** *130* (11), 3252-3.

49. Ishida, M.; Kim, S.-J.; Preihs, C.; Ohkubo, K.; Lim, J. M.; Lee, B. S.; Park, J. S.; Lynch, V. M.; Roznyatovskiy, V. V.; Sarma, T.; Panda, P. K.; Lee, C.-H.; Fukuzumi, S.; Kim, D.; Sessler, J. L., Protonation-coupled redox reactions in planar antiaromatic meso-pentafluorophenyl-substituted o-phenylene-bridged annulated rosarins. *Nat. Chem.* **2013,** *5* (1), 15-20.

50. Vogel, E., The porphyrins from the 'annulene chemist's' perspective. In *Pure and Applied Chemistry*, 1993; Vol. 65, p 143.

51. Emanuel Vogel, Peter Rohrig, Martin Sicken, Bernd Knipp, Adalbert Herrmann, Michael Pohl, Hans Schmickler and Johann Lex, The Thiophene Analogue of Porphyrin: Tetrathiaporphyrin Dication, *Angew. Chrm. Int. Ed. Engi.* **1989,** *28*, 12.

52. Gopalakrishna, T. Y.; Anand, V. G., Reversible Redox Reaction Between Antiaromatic and Aromatic States of 32π-Expanded Isophlorins. *Angew. Chem., Int. Ed.* **2014,** *53* (26), 6678-6682.

53. Sprutta, N.; Latos-Grażyński, L., Figure-Eight Tetrathiaoctaphyrin and Dihydrotetrathiaoctaphyrin. *Chem. Eur. J.* **2001,** *7* (23), 5099-5112.

54. Ambhore, M. D.; Basavarajappa, A.; Anand, V. G., A wide-range of redox states of core-modified expanded porphyrinoids. *Chem. Comm.* **2019,** *55* (47), 6763-6766.

55. Cha, W.-Y.; Soya, T.; Tanaka, T.; Mori, H.; Hong, Y.; Lee, S.; Park, K. H.; Osuka, A.; Kim, D., Multifaceted [36]octaphyrin(1.1.1.1.1.1.1.1): deprotonation-induced switching among nonaromatic, Mobius aromatic, and Huckel antiaromatic species. *Chem. Comm.* **2016,** *52* (36), 6076-6078.
56. Bartosz Szyszko, Michal J. Bialek, Ewa Pacholska-Dudziak, and Lechoslaw Latos-Grazynski, Flexible Porphyrinoids, *Chem. Rev.* **2017**, *117*, 2839−2909.
57. J. Sreedhar Reddy and Venkataramanarao G. Anand, Planar Meso Pentafluorophenyl Core Modified Isophlorins, *J. Am. Chem. Soc.*, **2008**, *130*, 3718-3719.

Chapter II

Redox Active π-Expanded Core-Modified Isophlorinoids at Crossroads of Topology and Antiaromaticity

II.1 Introduction

Aromatic and antiaromatic conjugated systems are governed by Huckel's empirical (4n+2) π and 4nπ electron rule.[1-4] In principle, inter-conversion between aromatic and antiaromatic systems can be perceived as reversible redox chemistry of two π-electrons as evinced by Woodward for, [18]porphyrin and [20]isophlorin.[5] Till date, aromatic porphyrin has been identified as more stable than the antiaromatic isophlorin and hence stabilizing [20]isophlorin under ambient conditions has remained a significant challenge. Invariably, anti-aromatic core modified porphyrins are found to stabilize as aromatic dications upon undergoing two-electron ring oxidation.[6, 7] Later, synthetic advances led to the understanding that expanded antiaromatic isophlorinoids undergo facile and reversible two-electron ring oxidation, as displayed by 32π antiaromatic expanded isophlorinoid[8] and 20π core modified porphyrin.[9] Proton coupled electron transfer (PCET) reactions are common in expanded porphyrinoids, because of amine-imine interconversion in pyrrole units. It has been established that [26]hexaphyrin(1.1.1.1.1.1) undergoes reversible two-electron of oxidation to [28]hexaphyrin(1.1.1.1.1.1) with concomitant oxidation of amine to imine bond.[10] PCET has been well studied in annulene based β, β′ -fused Rosarin, which exhibits one electron oxidation and stabilizes a radical dication. Further, it established that rosrain undergoes redox chemistry to yield a stable antiaromatic 24π and aromatic 26π system.[11] Similarly, isolated stable radical systems undergo one-electron oxidation and reduction to switch between aromatic and antiaromatic states respectively.[12] The chemistry and structural features are known to vary significantly with increase in the number of heterocycles for a given porphyrinoid. For pyrrole porphyrinoids with more than eight units, the macrocycle gains more degrees of freedom leading to non-planar structures. It is observed that most of these large porphyrinoids display either twisted figure-of-eight or non-planar conformation.[13] Due to loss of planarity, study of the aromaticity in expanded porphyrin systems is very limited. Therefore, redox properties in pyrrolic/non-pyrrolic porphyrinoids bearing eight or more heterocyclic rings rarely reflects aromatic/antiaromatic states because, the macrocycles generally tend to adopt a twisted conformation. Evident to that, octaphyrins reported by Vogel's group not only displayed figure of eight conformation but also were found to exist in enantiomeric form.[14] Prior to these enantiomeric octaphyrins, Sessler and co-workers reported a deca pyrrole turcasarin with a figure-eight conformation.[15]

Meso-aryl substituted expanded porphyrins, from Osuka's group reported planar tetrapyrrolic porphyrin along with a range of structurally diverse expanded porphyrins bearing up to

fourteen pyrrole rings.[16] Characterization of these macrocycles revealed that expanded porphyrinoids beyond hexaphyrins lose planarity to adopt the twisted or figure-of- eight structure, because of its molecular flexibility and internal hydrogen bonding.[16] In order to achieve synthetic control over twisted to non-twisted conformation and switching to (anti)aromaticity, various synthetic methods such as contraction, core modification, neo-confusion approach, *p*-phenylene bridging, dianionic have been employed so far.[17] However, altering the molecular topology and switching to (anti)aromaticity without incorporating any modifications has remained a synthetic challenge task. Very few examples are known in which either thermodynamic control or protonation induced aromaticity cum topology switching has been observed in solution state. Particularly [36] and [38] octaphyrin displayed protonation triggered conformational changes between Huckel and Mobius aromaticity.[18] Recently, Sessler and co-workers reported an antiaromatic cobalt (II) bimetallated [64]hexadecaphyrin (1.0.0.0.1.1.0.1.1.0.0.0.1.1.0.1) showing thermal conformational equilibrium between two stable conformations.[19] Moreover, the exclusive synthesis of size and shape specific expanded porphyrinoids itself has remained a challenging task till date. In an earlier study, synthesis of a planar and an antiaromatic 40π expanded isophlorin with eight furan units was achieved, when pyrrole was replaced by furan in the reaction with pentaflurobenzaldehyde.[20]

II.2 One-pot synthesis of Cyclooligothiophenes

Pyrrole and thiophene have similar structural, electronic and aromatic properties but pyrrole exhibits a significant difference when accommodated in the cyclic conjugated systems. This is attributed to the amine N-H, due to which pyrrole can be oxidized to an imine like nitrogen. Hence in case of porphyrins or expanded porphyrins, pyrrole shows continuous global conjugation along with the sp^2 carbon as well as nitrogen, either in the amine or imine forms, even with odd number of pyrroles. In contrast, when pyrrole was replaced by the furan or thiophene the global conjugation flows only through the sp^2 hybridised carbon frame work. Unlike pyrrolic porphyrinoids, only even numbered heterocyclic units were observed with furan based expanded porphyrinoids.[20] In principle, under these conditions, along with (4n+2) π and 4nπ systems it can be expected that neutral radical species having (4n+1) π and (4n+3) π electrons can be identified if macrocycles incorporate odd number of heterocyclic units.

Under modified Rothemund conditions, in a one-pot synthesis, an equimolar concentration of thiophene and pentaflurobenzaldehyde were condensed in dichloromethane with a catalytic amount of $BF_3.OEt_2$ in dark and inert conditions. The reaction mixture was stirred for an hour followed by oxidation with five equivalents of anhydrous $FeCl_3$ open to air and stirring continued for an additional one hour. Then, the reaction mixture was passed through a short bed of basic alumina (scheme – II.1). As confirmed from MALDI-TOF/TOF mass spectrum, the reaction (figure – II.1) yielded a series of isophlorinoids from four to sixteen thiophene rings bearing 4n, (4n+1), (4n+2) and (4n+3) π-electrons. Macrocycles with an odd number of thiophene units are expected to be neutral radical (open shell) species, while even numbered thiophene units correspond to diamagnetic (closed shell) species. Isolation and characterization of closed shell macrocycles (4nπ & (4n+2) π) were relatively easier compared to the radical species ((4n+1)π & (4n+3)π).

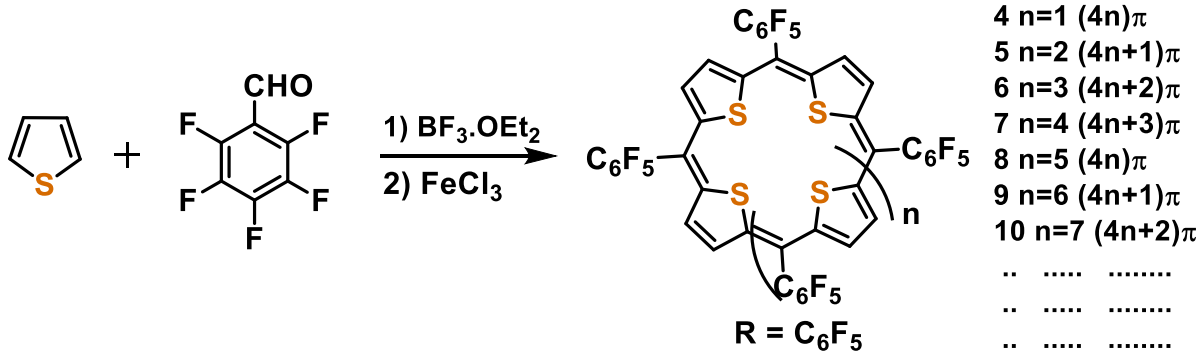

Scheme II.1: *One-pot synthesis of Cyclooligothiophenes.*

From the reaction mixture, air and water stable 25π cyclopentathiophene **(5)** macrocyclic radical was isolated which undergoes facile reversible one-electron redox chemistry to yield the 26π aromatic anion and 24π antiaromatic cationic species.[21] Along with this radical species, the anti-aromatic 20π tetrathiophene (**4**) was found to undergo reversible twoelectron oxidation to yield the 18π aromatic dicationic species.[22] Its next higher congener, 30π hexathiophene (**6**) was found to be aromatic in nature.[23] Particularly, the comprehensive characterization of the novel (4n+3)π 35π heptathiophene (**7**) and (4n+1)π 45π nonathiophene (**9**) remained elusive due to their unstable nature under ambient conditions. However, [40]octathiophene (**8**), [50]decathiophene (**10**), [60]dodecathiophene (**12**) and [70]tetradecathiophene (**14**) were isolated by repeated silica-gel column chromatography and size exclusion chromatography in 6%, 2%, 0.9% and 0.2% yields respectively.

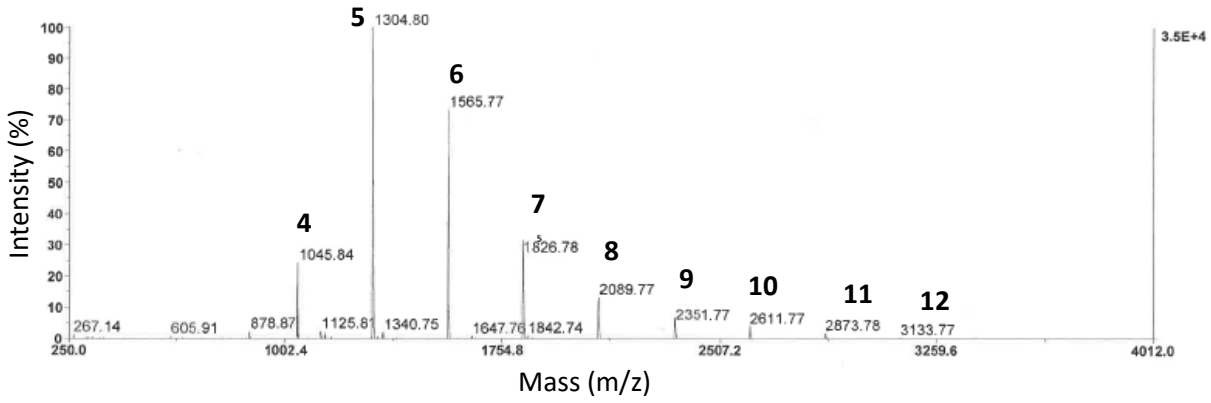

Figure II.1: *MALDI-TOF/TOF mass spectrum of reaction mixture as described in scheme -1.*

II.3.1 Isolation and Characterisation of [40]octaphyrin

Cyclooctathiophene, **8**, was identified as a pink coloured band isolated from repeated silica column chromatography and size exclusion chromatography. This macrocycle accounts for 40π electrons in the global conjugation and the composition of **8** was confirmed by High Resolution Mass Spectrometry (HR-MS), in which it displayed *m*/*z* value of 2087.7395 corresponding to $C_{88}H_{16}F_{40}S_8$ (figure – II.2).

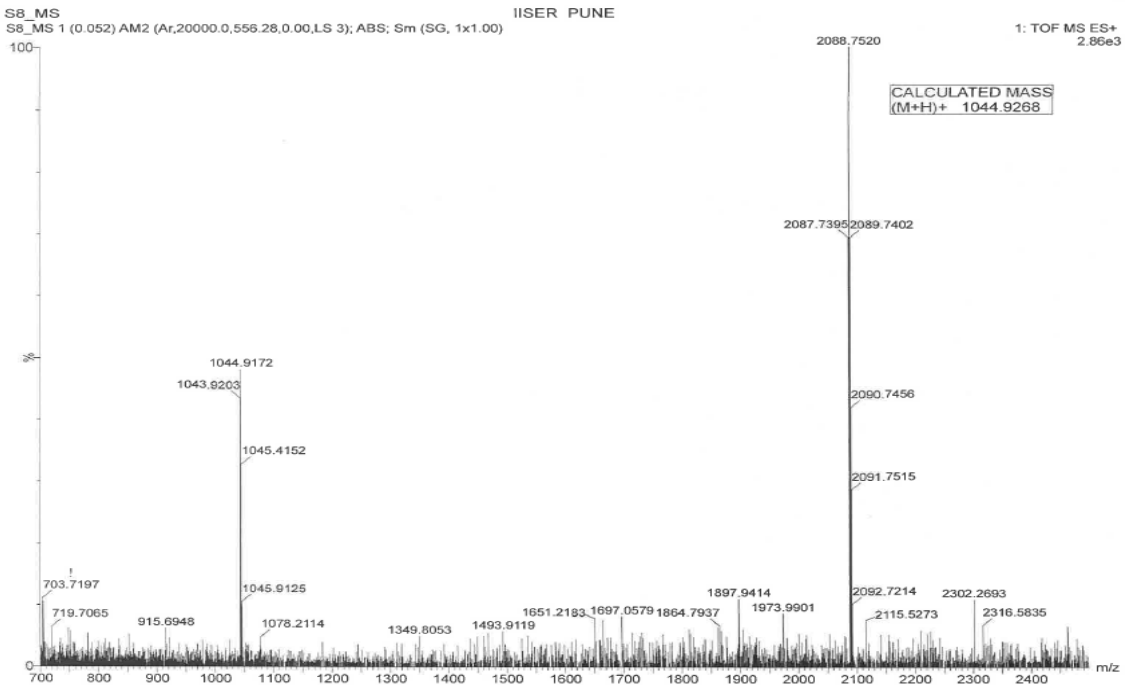

Figure II.2: *HR-ESI-TOF mass spectrum of Octaphyrin **8**.*

II.3.2 ^{1}H NMR study of [40]octaphyrin

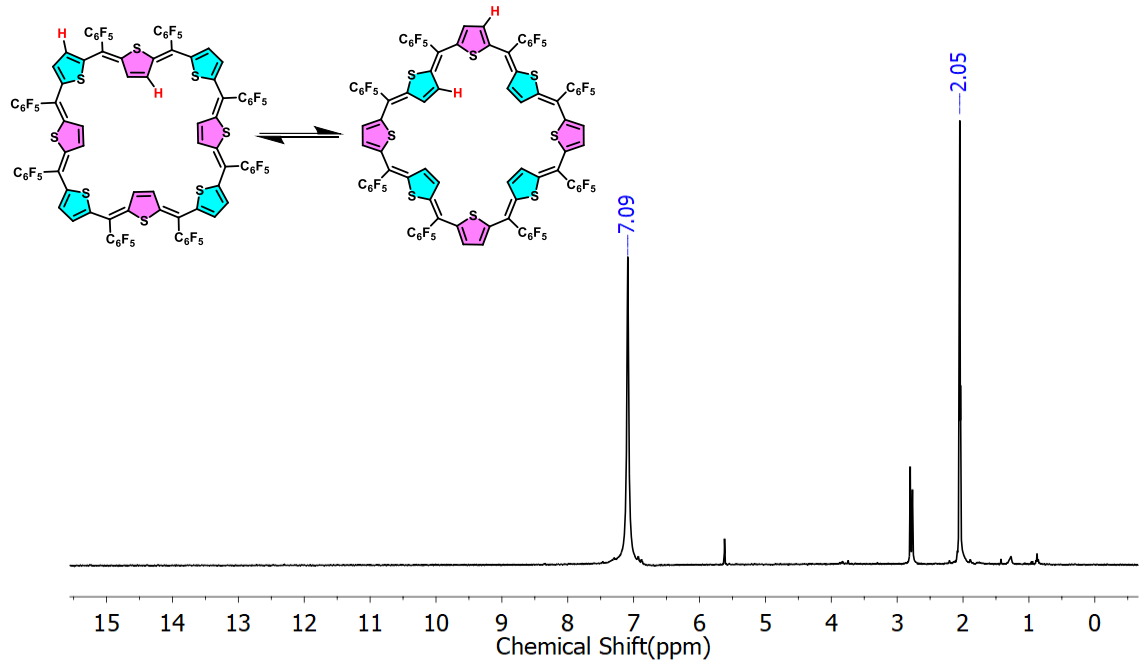

Figure II.3: *^{1}H NMR spectrum of **8** in Acetone-d_6 at 298 K.*

In the ^{1}H NMR spectrum, **8** displayed only a broad singlet at δ 7.09 ppm at room temperature. It is pertinent to note that [40]octafuran **I.35** and [40]octathiophene, **8**, are isoelectronic species. The [40]octafuran was characterized as a squarish and near-planar conformation in the solid state. Further, the octafuran macrocycle displayed two discrete signals in the ^{1}H NMR spectrum at δ 9.4 and 5.85 ppm for the inner and outer protons respectively at room temperature. In contrast, a broad signal signified octathiophene's, **8**, fluxional behaviour at room temperature (figure – II.3). This was further confirmed by the variable temperature ^{1}H NMR spectra recorded between 333 K and 175 K (figure –II.4). A broad singlet observed at δ 7.09 ppm in room temperature transformed into a sharp signal at 333 K, further supporting the fluxional behaviour of **8**. However, on reducing the temperature, the broad singlet transforms to two broad singlets at 252 K, and on further reducing the temperature to 175 K, the spectrum displayed multiple signals in the region between δ 9.5 to 6.0 ppm (figure – II.5) suggestive of a non-planar symmetry and lack of any significant ring current effects for the macrocycle. ^{1}H-^{1}H COSY NMR spectrum at 175 K (figure – II.6) revealed three correlations. The first correlation corresponds to two down field discrete singlets at δ 9.31 and 8.31 ppm while the second correlation was observed for signals at δ 6.86 and 6.56 ppm. The third correlation was identified for the signals at δ 6.46 and 6.35 ppm. Unlike the 40π octa furan macrocycle, these observations suggested a dynamic change in the structure of the **8** upon varying the temperature. Therefore, one can envisage more than

on one conformation or topology at different temperature for the octaphyrin, **8**. Since NMR spectra could not deduce the exact molecular structure, attempts were made to determine the absolute structure of **8** from single crystal X-ray diffraction.

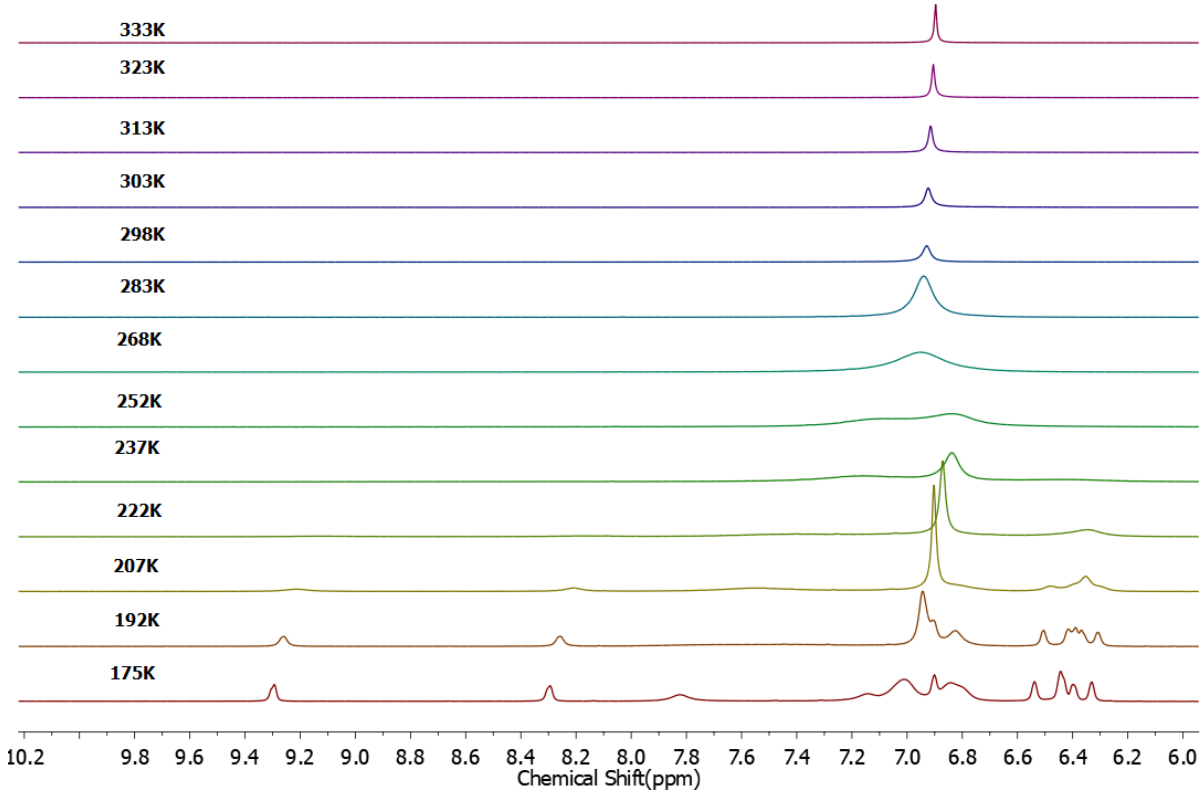

Figure II.4: *Variable temperature ^{1}H NMR spectra of **8** in Tetrahydrofuran-d_8 from 175 K to 333 K.*

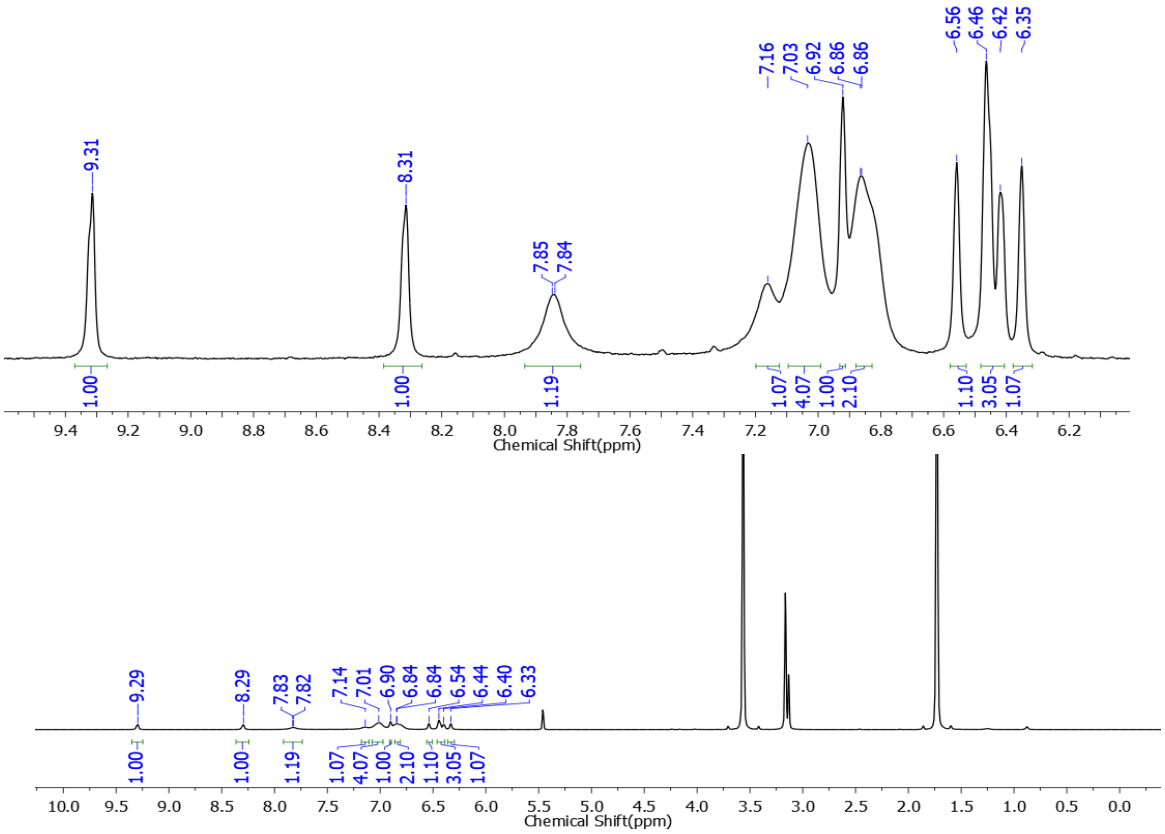

Figure II.5: *^{1}H NMR spectrum of **8** in Tetrahydrofuran-d_8 at 175 K.*

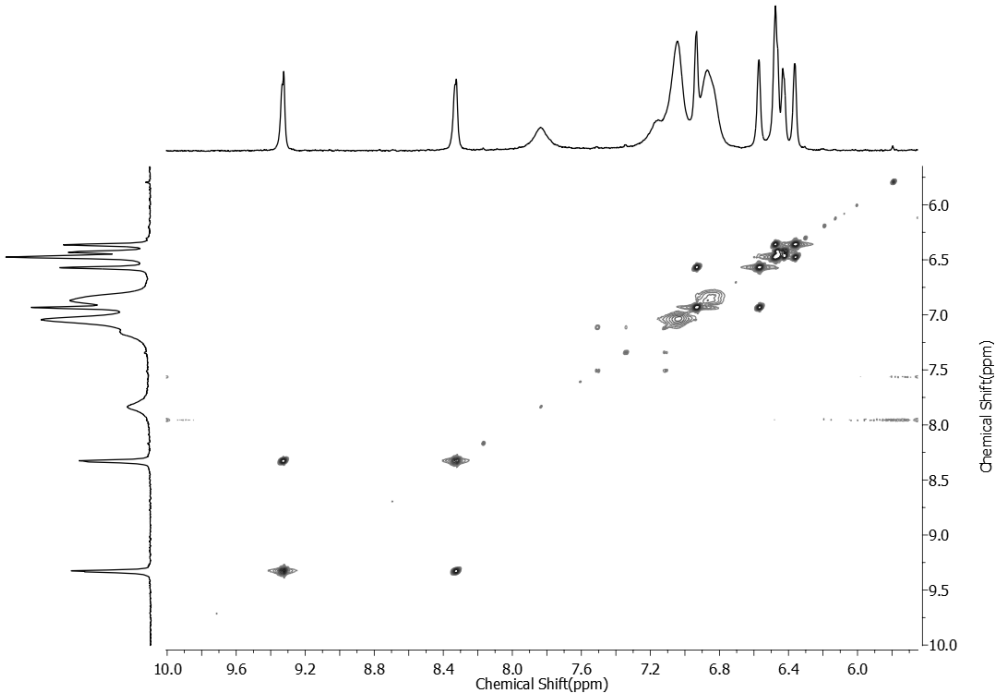

Figure II.6: *^{1}H-^{1}H COSY spectrum of **8** in Tetrahydrofuran-d_8 at 175 K.*

II.3.3 Crystal structure and packing of [40]octaphyrin

After many efforts, single crystals were grown by vapour diffusion of *n*-hexane into a solution of **8** either in dimethyl sulfoxide (DMSO) or 1, 2-dichloroethane (DCE). Molecular structure determined by single crystal X-ray diffraction confirmed planar macrocyclic geometry similar to cyclooctafuran when crystals were grown either in DMSO or DCE (figures – II.7 & II.8). It was observed that four of the eight thiophene rings, in an alternative fashion, adapted to an inverted orientation. In DMSO, **8** crystalized in tetragonal symmetry with I-4 space group and displayed non-covalent S···F (3.125 Å) interactions in its crystal packing. Each macrocycle is surrounded by eight similar neighbours such that there are four each above and below the macrocyclic plane. An inter-planar distance of 3.87 Å was measured between the central molecular plane and those surrounded above and below the central macrocycle.

8 also adopted a planar topology when crystalized in DCE, with triclinic crystal system and in P-1 space group but were devoid of any inter molecular non-covalent interactions. However, solvent molecules were observed in the crystal packing. DCE was found sandwiched between two planar macrocycles. DMSO was found to encourage intermolecular S···F bonding as observed by the S···F distance of 3.125Å, whilst DCE disrupts S···F bonding and interacts with macrocycle. Therefore, these two crystals represent crystal solvates of **8**. Yet, these two molecular structures confirmed the arresting of highly fluxional behaviour upon crystallization.

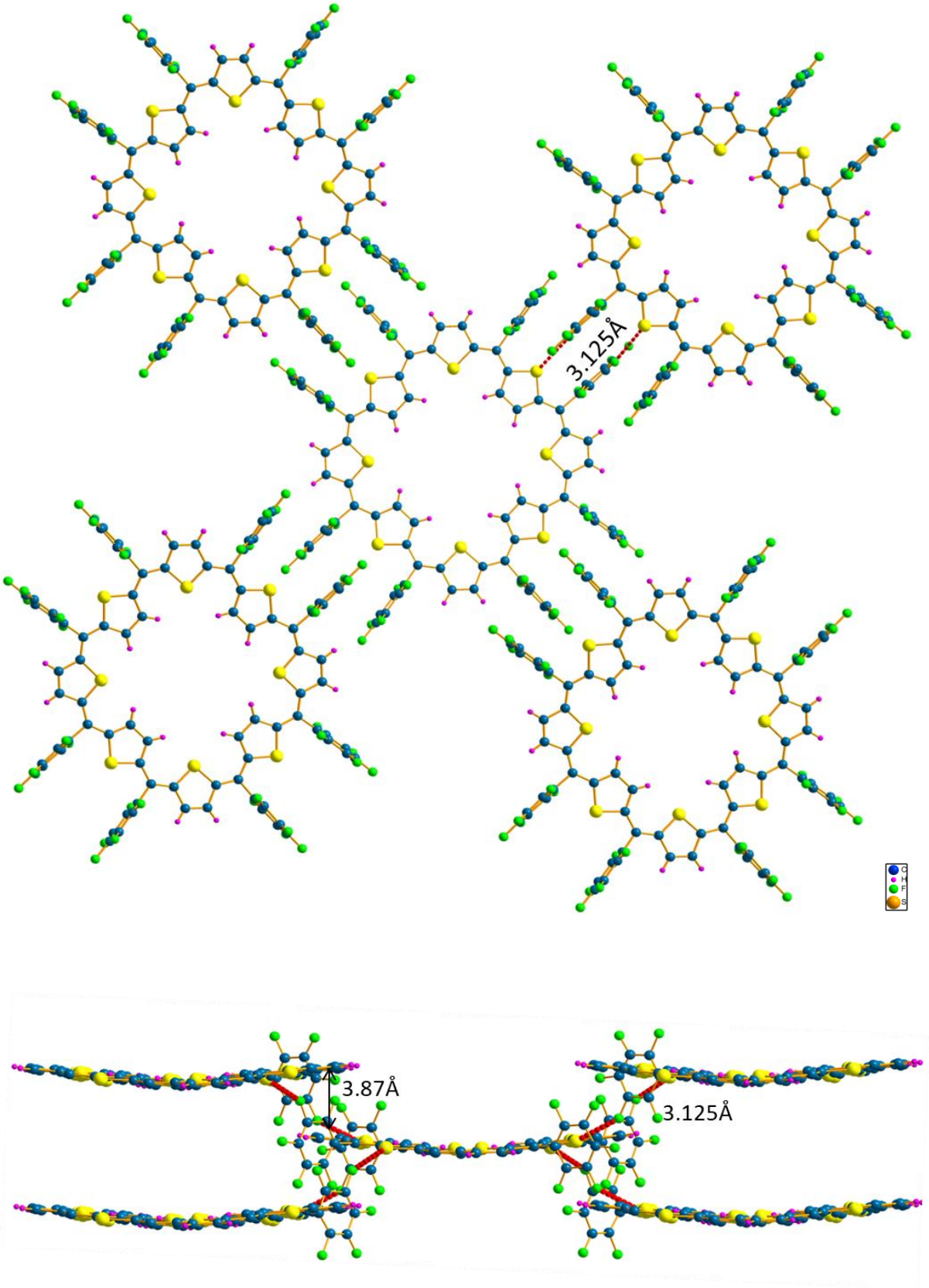

Figure II.7: *Inter molecular S⋯⋯F interactions in the crystal packing of Octaphyrin **8**, top view (top), side view pentafluorobenzyl rings are omitted for clarity(bottom). (Crystal grown in DMSO)*

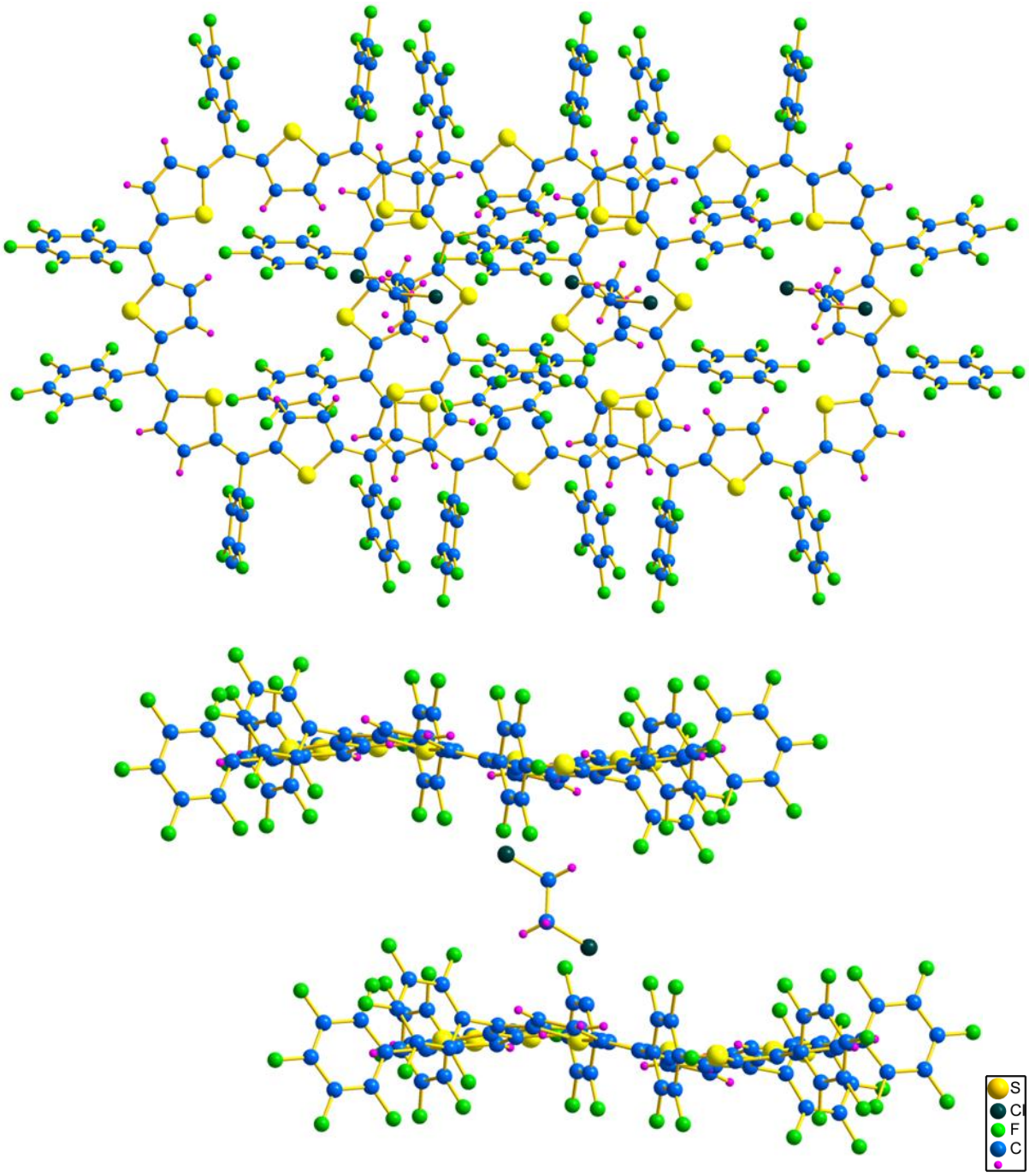

Figure II.8: *Crystal packing of (at the top) Top view (at the bottom) Side view of **8** showing sandwich kind of packing between the dichloroethane solvent. (Crystal grown in Dichloroethane)*

II.3.4 Computational studies for stable conformation of [40]octaphyrin

From the analysis described above, it is apparent that X-ray diffraction and ^{1}H NMR spectroscopy studies contradict the structural feature of octathiophene **8** in solution and solid states. Variable temperature ^{1}H NMR studies suggest both the high energy fluxional state and a low-energy non-planar topology. Therefore, it can be presumed that a figure of eight

structure as the most predominant topology that is well established for octaphyrins. Unfortunately, these multiple conformations are not easy to be accessed in the solid state. However, quantum chemical calculations support the temperature dependent structural transformation as observed in the solution state (figure – II.9). As described below, the estimated lowest energy structure was found to be for a non-planar figure-of-eight conformation, **8F**. In support of the observed ^{1}H NMR date, the fluxional topology attributed to the fast flipping of the thiophene rings has much higher energy in the solution state. The estimated change in free energy ($\Delta G^{\#}$= 12.84 kcal/mol) at coalescence temperature 268 K, suggested an equilibrium between a highly fluxional and a rigid, but a non-planar, conformation. The calculated energy for the planar **8P** with all sulphur atoms facing the centre of the macrocycle was found to be the highest energy state. Hence, the ^{1}H NMR spectrum at lower temperatures can be attributed to the figure-of-eight conformation.

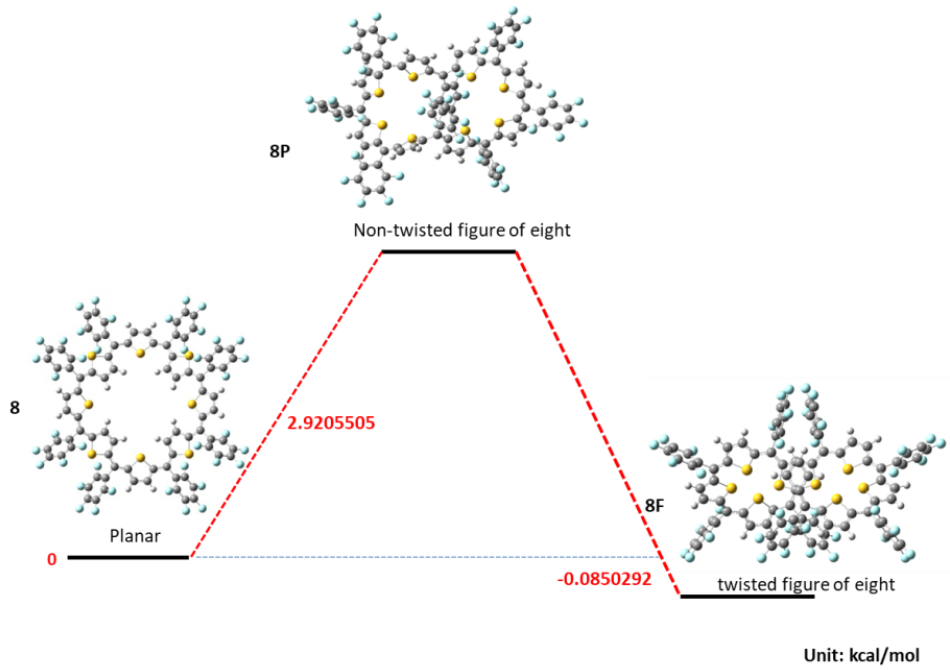

with respect to Planar Conformation (8)			
Conformation Name	8F	8P	8
Point group (S_4/C_2/C_1)	C_2	C_1	S_4
Energy (Hartree)	-10541.56537	-10541.56058	-10541.56524
Difference energy (Hartree)	-0.0001355000004	0.004654099999	0
Energy (eV)	-0.003687144711	0.1266445767	0
Energy (kcal/mol)	-0.08502924418	2.920550584	0

Figure II.9: *Optimized molecular structures of **8**, **8P** and **8F** and calculated total energies and their energy-differences at the B3LYP/6-31G(d,p) level.*

II.3.5 Splitting of 40π octaphyrin into 20π isophlorin

In order to arrest the fluxional behaviour of **8**, it was envisaged that addition of C_{60} fullerene can induce a stable conformation, as observed in porphyrin and fullerene interaction.[37] To confirm the possibility of fullerene-octaphyrin interaction, an attempt was made to co-crystallize them in a 1:1 mixture of toluene and acetone solvent system. Approximately after four weeks, brownish shiny crystals were obtained from this solution. Surprisingly single crystal X-ray diffraction analysis revealed a 20π tetrathia isophlorin structure instead of the expected co-crystal. Similar splitting of Bis-Cu(II) octaphyrin into two Cu(II) porphyrins under the influence of thermal energy was reported by the Osuka's group.[24] Encouraged by this observation, octaphyrin and fullerene were stirred in toluene. Even though it did not reveal immediate splitting of the macrocycle, but continued stirring for more than two weeks revealed the formation of 20π isophlorin. This was confirmed by MALDI TOF/TOF and ^{1}H NMR spectroscopy (figure – II.10).

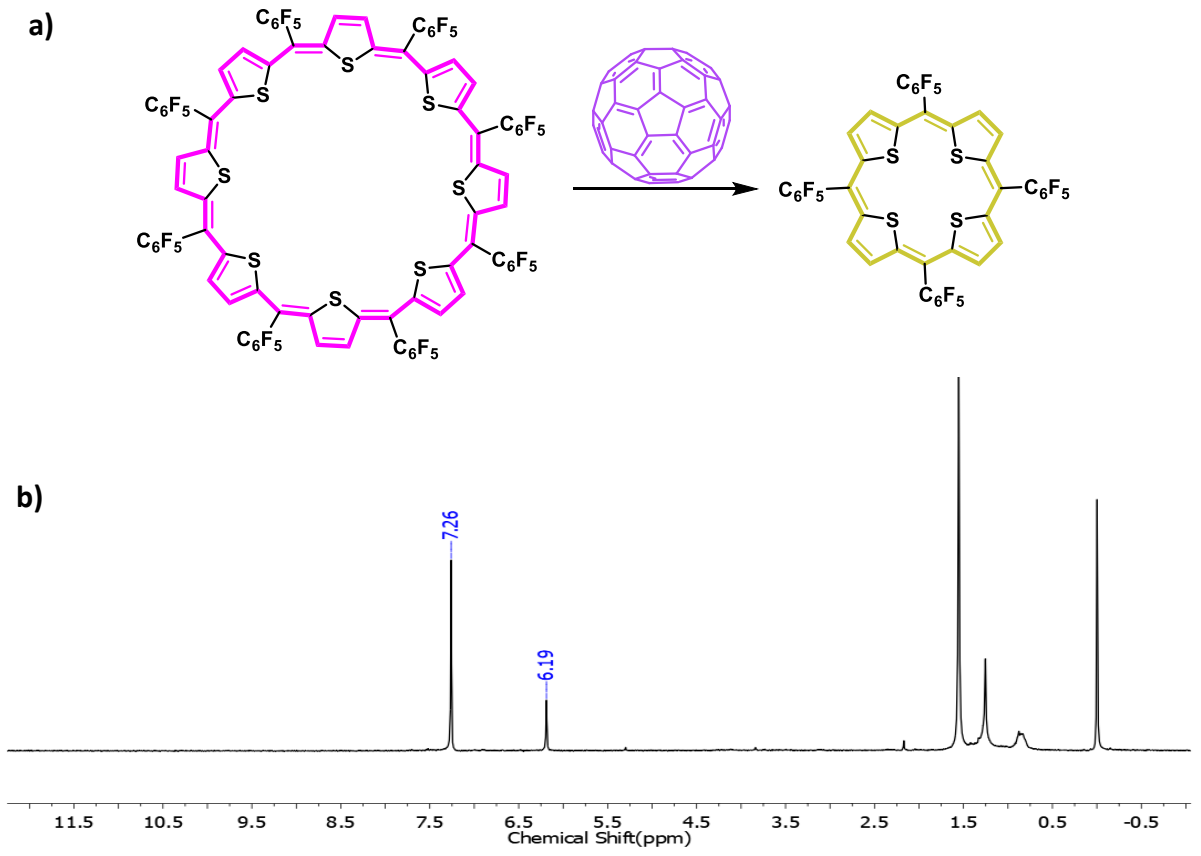

Figure II.10: *(a) Mitotic division of octaphyrin,* ***8****, under the influence of fullerene* C_{60}*. (b)* ^{1}*H NMR spectrum of 20π cyclotetrathiophene obtained from reaction described in 10a.*

II.3.6 Study of [38]octaphyrin dication

Antiaromatic macrocycles are known to undergo facile two-electron oxidation and can be stabilized in aromatic dicationic state. High resolution mass spectrum for neutral macrocycle shows both free base and dicationic *m/2* ion peak, supporting [40]octaphyrin's susceptibility to undergo two-electron oxidation. This was further confirmed by the chemical oxidation upon addition of $[Et_3O]^+[SbCl_6]^-$ or $NOBF_4$ or TFA to [40]octaphyrin, **8**. High resolution mass spectrum displayed an *m/2* value of 1043.9170 (Calcd. for 1043.9189), confirming the two-electron ring oxidation to yield the 38π dication $[\mathbf{8}]^{2+}$ quantitatively.

However, the ^{1}H NMR spectrum of the 38π aromatic dication obtained from TFA at room temperature displayed only a broad signal at δ 6.8 ppm (figure – II.12) implying the fluxional nature of the macrocycle. Therefore an attempt was made to record the spectrum at lower temperatures (figure – II.13). Upon lowering the temperature to 203 K, it exhibited broad resonances in the region between δ 6.00 to 8.5 ppm (figure – II.14) suggestive of a non-aromatic state. Unfortunately, the absolute structure of this dication could not be determined in the solid state due to the poor stability of the dication in solution state over long periods of time. It was observed that the dication $[\mathbf{8}]^{2+}$ could be spontaneously reduced back to the neutral 40π state either by addition of triethyl amine or zinc metal.

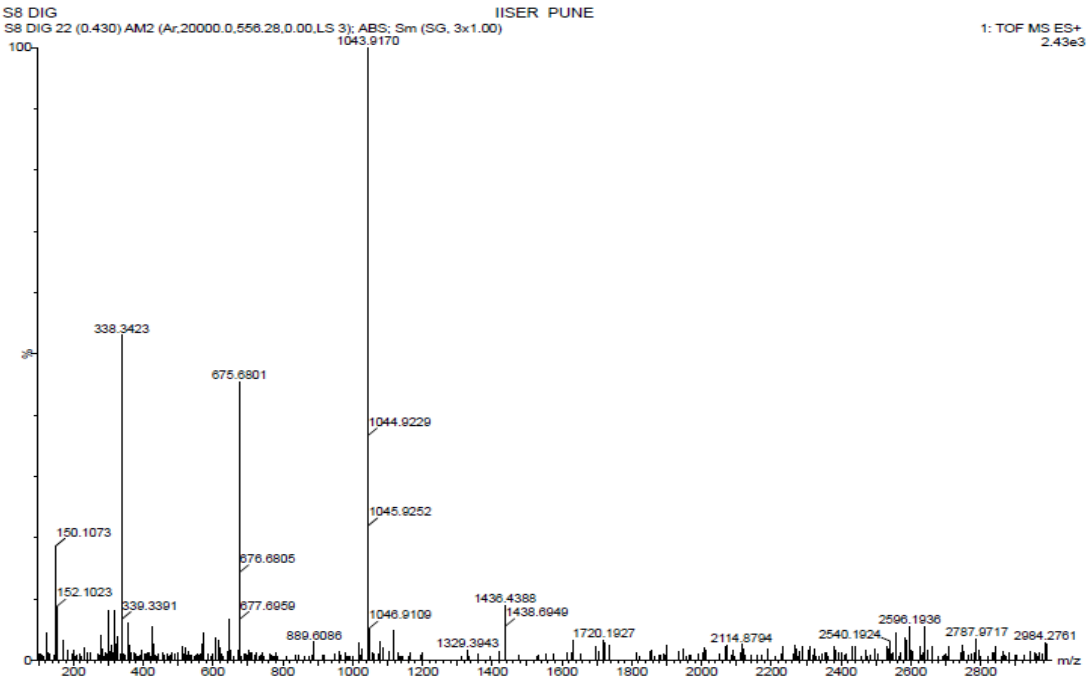

Figure II.11: *HR-ESI-TOF mass spectrum of Octaphyrin dication* ***[8]***$^{2+}$.

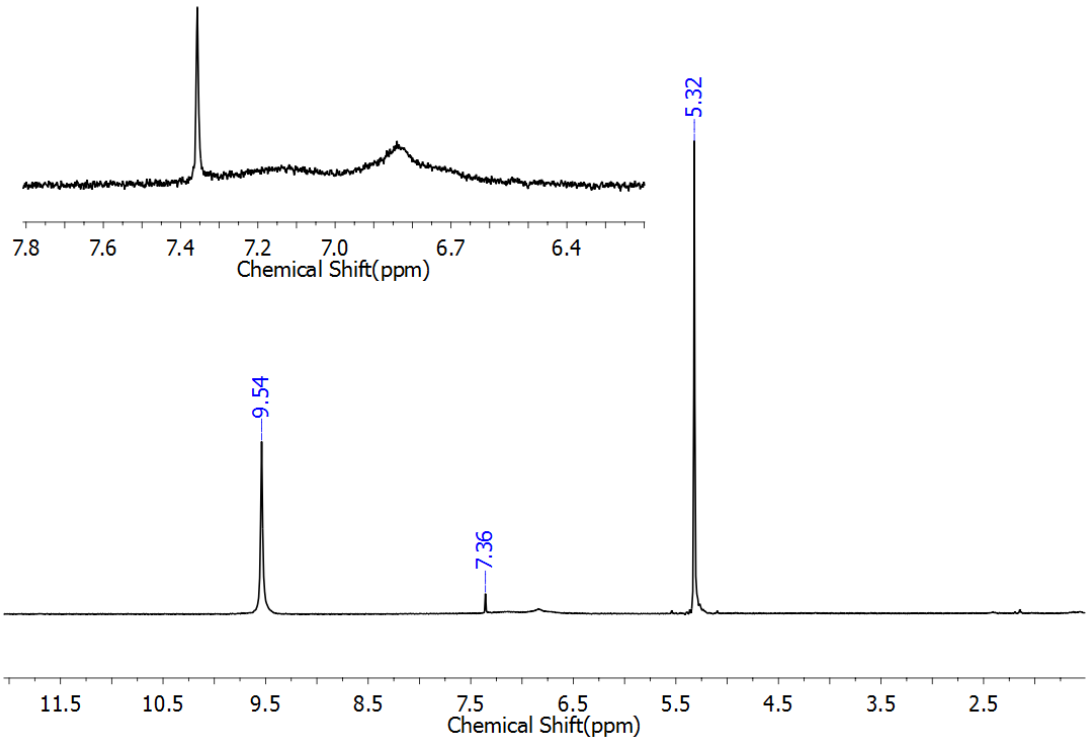

Figure II.12: *^{1}H NMR spectrum of **[8]**$^{2+}$ in Dichloromethane-d_2 at 298 K.*

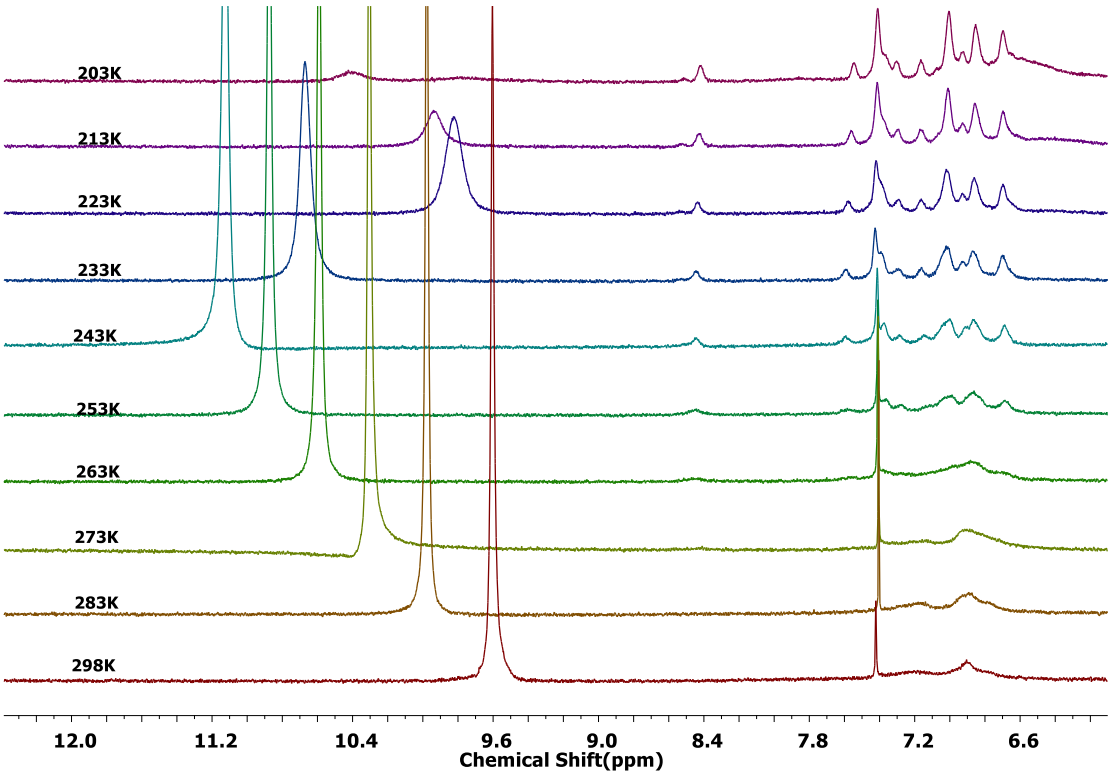

Figure II.13: *Variable temperature ^{1}H NMR spectrum of **[8]**$^{2+}$ in Dichloromethane-d_2.*

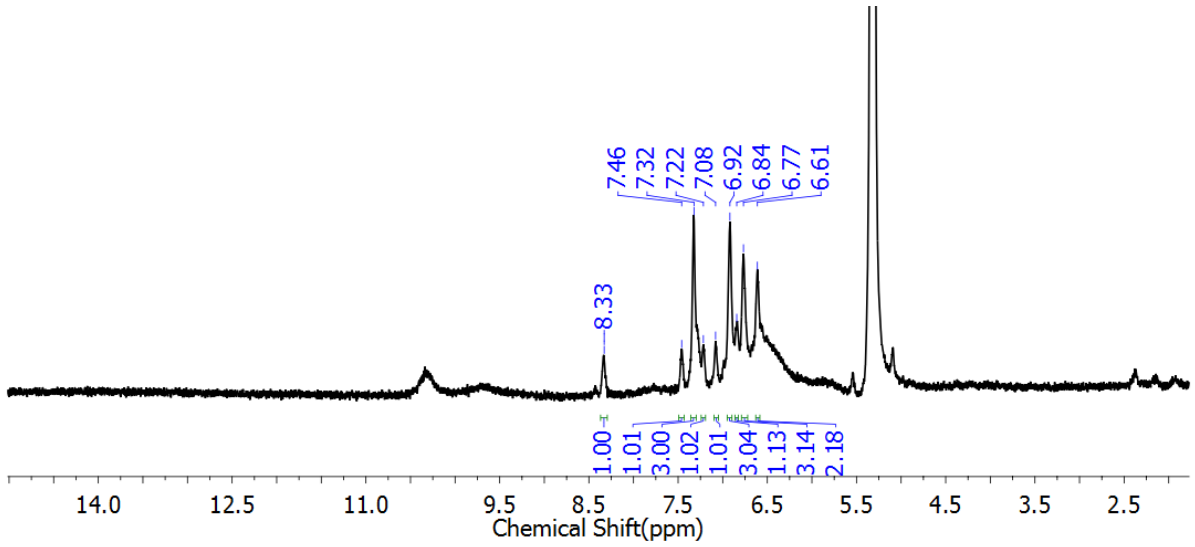

Figure II.14: *^{1}H NMR spectrum of **[8]**$^{2+}$ in Dichloromethane-d_2 at 203 K.*

II.3.7 Electronic absorption and Cyclic Voltammogram studies

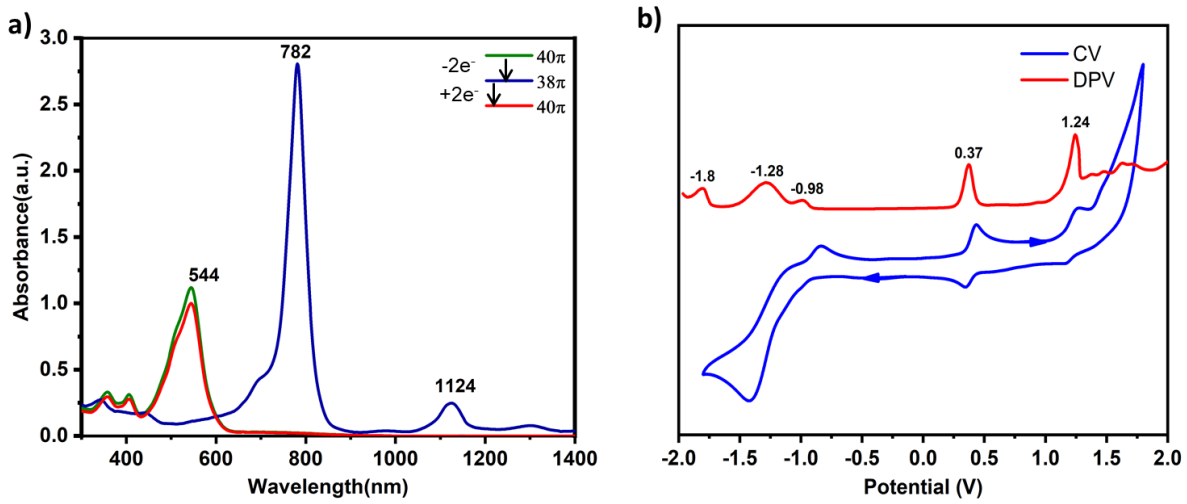

Figure II.15: *(a) UV/vis/NIR absorption spectrum of a 10^{-5}M solution of **8** and its two-electron oxidised species **[8]**$^{2+}$ recorded in CH_2Cl_2. (b) Cyclic voltammogram (CV, blue) and differential pulse voltammogram (DPV, red) in CH_2Cl_2 (with 0.1 M $(Bu)_4NPF_6$ as the supporting electrolyte.*

Even though ^{1}H NMR characterization revealed non-(anti)aromatic features, [40]octaphyrin, **8**, exhibits vibrant and vivid colour in solution and solid states. By virtue of extended conjugation, it is expected that **8** can be susceptible to reversible oxidation. Therefore its opto-electronic properties were explored through chemical redox and electrochemical techniques such as cyclic voltammetry (CV) and spectro-electrochemistry (SEC). It displayed an intense absorption at 544 nm (ε = 129300) in dichloromethane at room temperature (figure – II.15a). Preliminary CV studies (figure – II.15b), revealed that octathiophene **8** displayed two oxidation potentials at +0.37 V and +1.24 V along with three reduction potentials at -

0.98 V, -1.28 V and -1.8 V. Chemical oxidation of **8** with oxidizing agents such as $[Et_3O]^+[SbCl_6]^-$ or $NOBF_4$ or TFA induced an instantaneous colour change from pink to green in dichloromethane. In tune with this observation, the green coloured solution displayed an intense absorption at 782 nm (312800), with a red shift more than 200 nm in comparison to the parent 40π species and low energy bands at 1125 (27800), 1302 (10300) signifying the formation of the 38π dicationic species (figure – II.15a).

II.3.8 Spectro-electrochemistry (SEC) studies

The facile reversibility of the two-electron oxidation was confirmed by reducing the two-electron oxidized species which was further substantiated by SEC studies. Based on the potential values obtained from CV, the electronic spectrum of the 40π macrocycle, **8**, was recorded at first oxidation potential (+0.4 V) and second oxidation potential (+1.3 V) to identify the two-electron oxidized species. Its absorption at an applied potential of +0.4 V displayed a broad signal at 640 nm followed by an intense signal at 780 nm suggesting the admixture of radical cation and the two-electron oxidized species (figure – II.16a). However, at a higher potential value of + 1.3 V, it displayed only the intense band at 782 nm (figure – II.16b) in support of the two-electron ring oxidation as observed from electronic absorption spectroscopy and mass spectrometry.

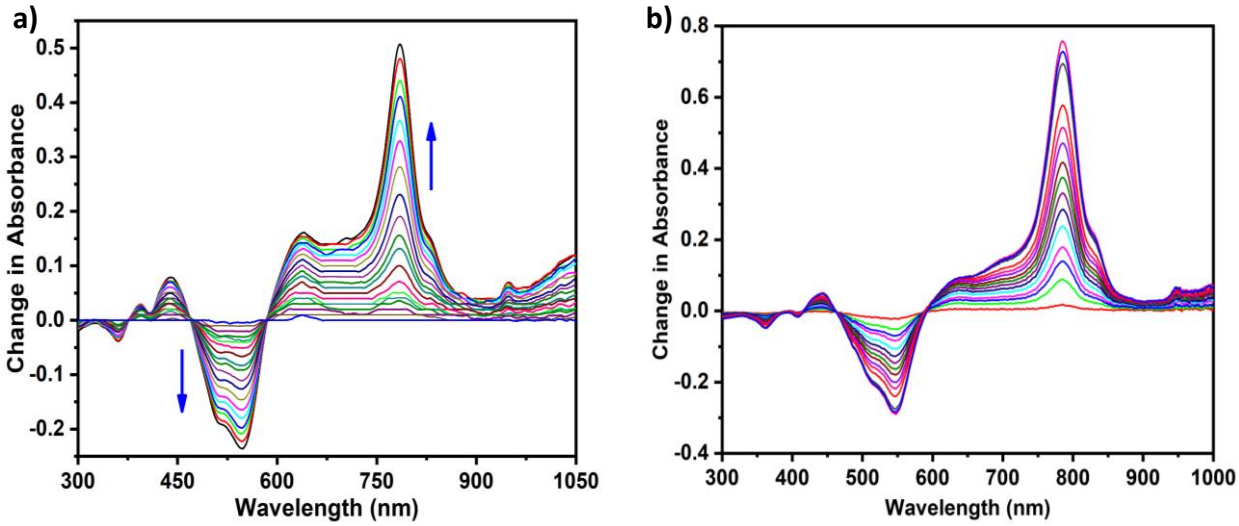

Figure II.16: *Spectroelectrochemistry studies shows, (a and b) Change in absorption spectrum of **8** at an applied potential of + 0.4 V and + 1.3 V, respectively with respect to time.*

II.3.9 Quantum mechanical calculations

Apart from the experimental characterisation, computational calculations were performed to correlate with the obtained the experimental data. These calculations were aimed to estimate the strength of Non-(anti)aromaticity through estimation of Nucleus Independent Chemical Shift (NICS), Anisotropy Induced Current Density (ACID), and Harmonic Oscillation Model for Aromaticity (HOMA) values. In addition to these calculations, TD-DFT calculations were also performed to support electronic absorption and the corresponding HOMO-LUMO energy gap for these species. Quantum mechanical calculations were performed with the Gaussian09 program. All calculations were performed by Density Functional Theory (DFT) with Becke's three-parameter hybrid exchange functional and the Lee-Yang-Parr correlation functional (B3LYP) and 6-31G(d,p) basis set, in the calculations all the atoms were employed. The molecular structure obtained by the single crystal X-ray diffraction analysis was directly taken for the geometry optimisation.

Based on the strength of the magnetic field, π-conjugated macrocycles show either paratropic or diatropic ring current effects. Theoretically it can be estimated by NICS calculationas proposed by Paul von Rague Schleyer.[25, 26] If the estimated NICS value is negative at the interior positions of the rings, then it signifies magnetically shielded or induced by diatropic ring current or termed as 'aromatic'. In contrast, a positive NICS value signifies magnetically deshielded or induced by paratropic ring current or 'antiaromatic' feature of the macrocycle. NICS values has no upper and lower limit and doesn't require reference standards, and is mainly estimated on energy, geometry, and magnetic criteria. The calculation consists of two parts, i) optimization of the molecular structure and ii) fixing the position of *Bq* (*Bq* = Banquo means ghost atom, here the smallest ionic metal used, that is Li^+) atom, where NICS is computed and iii) finally request the NMR type calculation. IGLO and GIAO are the two methods employed in calculations. Between the two, GIAO (gauge independent atomic orbital) is commonly used along with optimised basis set. Based on these computational calculations, the estimated Nucleus Independent Chemical Shift (NICS (0)) value for planar structure of [40]octaphyrin (figure – III.7) is δ +8.08 ppm, which emphasized a moderate anti-aromatic characteristics of this macrocycle in the solid state.

Anisotropy of the Induced Current Density (ACID) is a general method to quantify and visualize the density and direction of delocalized electrons.[27] ACID obtained by applying the Continuous Set of Gauge Transformations (CSGT) method to estimate the current density

and the results was plotted in POVRAY 3.7 for windows. Usually the standard isosurface value used for calculation is 0.05. If the delocalization of the π-electrons cloud shows clockwise current density the molecule is aromatic and if it's anti-clockwise current density, molecule is antiaromatic. [40]octathiophene displayed anti-clockwise delocalization of current density (figure – II.17) in support of macrocycle's anti-aromatic character.

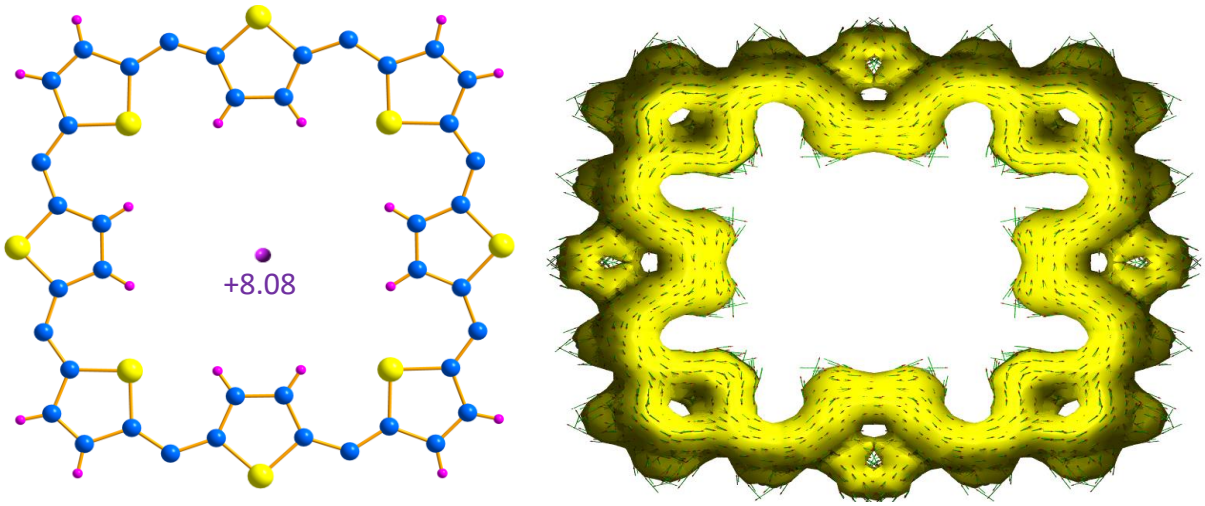

Figure II.17: *The calculated NICS (0) value of **8** mentioned at the centre of the macrocycle (left side), and AICD plot of **8** at an isosurface value 0.06 the external magnetic field is applied orthogonal to the macrocycle plane.*

HOMA (Harmonic Oscillator Model of Aromaticity) is another widely employed geometrical aromaticity index.[28] It basically depends on the bond length contribution for aromaticity, and if the HOMA value is 1 or near to one, then it is expected to be aromatic. On the contrary if the value is near to zero then the molecule is classified as non-aromatic, while a negative value renders the molecule as antiaromatic. These calculations were carried out through Density functional theory (DFT) with B3LYP/6-31G (d, p) basis set for all the atoms employed in the calculations. The geometry optimization was performed from the X-ray crystallographic structures. The harmonic oscillator model of aromaticity (HOMA) value 0.7154 was calculated along for the all-carbon of π-conjugation pathway in the macrocycle.

Time-dependent TD-DFT calculations were also performed on the optimized structures through DFT with B3LYP/6-31G (d, p) basis set and correlated with the experimental electronic absorption (figure – II.18). From the same basis set the estimated value of HOMO-LUMO energy gap was found to be 1.26 eV.

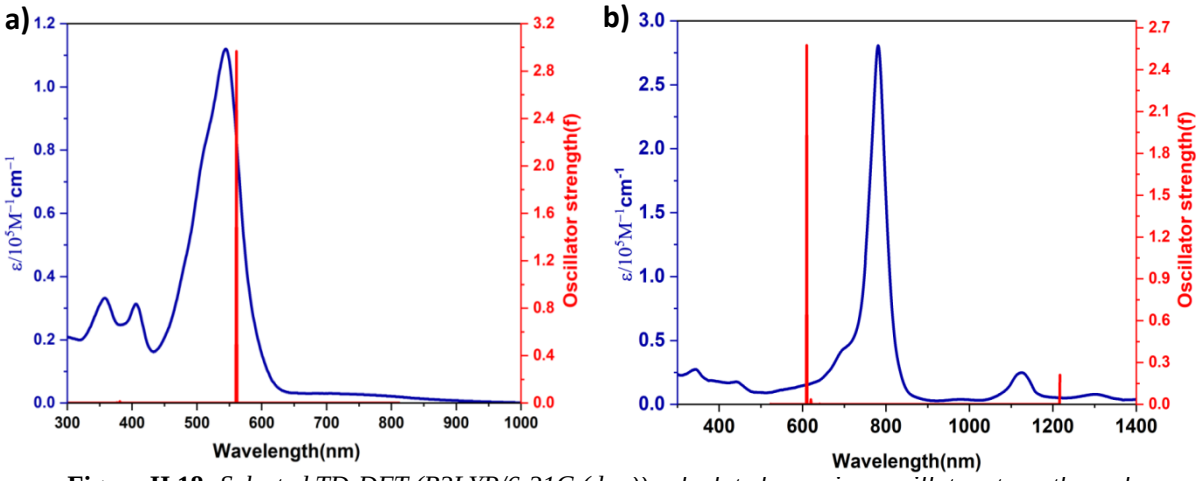

Figure II.18: *Selected TD-DFT (B3LYP/6-31G (d, p)) calculated energies, oscillator strengths and compositions of the major electronic transitions of* ***8*** *and* ***[8]***$^{2+}$.

All the above described computational calculations strongly supported the antiaromatic character for the isolated [40]octaphyrin in the solid state. Further studies and details of the other isolated macrocycles, i.e. **10**, **12** and **14** are described below.

II.4.1 Isolation and Characterisation of [50]decaphyrin

Decaphyrin (1.1.1.1.1.1.1.1.1.1), **10**, accounts for 50π electrons in the global conjugation, and is expected to follow Huckel's 4n+2π electron rule for aromaticity. This macrocycle was isolated as a green coloured band by repeated silica gel column chromatography and size exclusion chromatography in 2% yields. The composition of **10** was confirmed by HR-MS, in which it displayed *m/z* value of 2609.4253 corresponding to $C_{110}H_{20}F_{50}S_{10}$ (2609.7974) along with its *m/2* mass (figure – II.19).

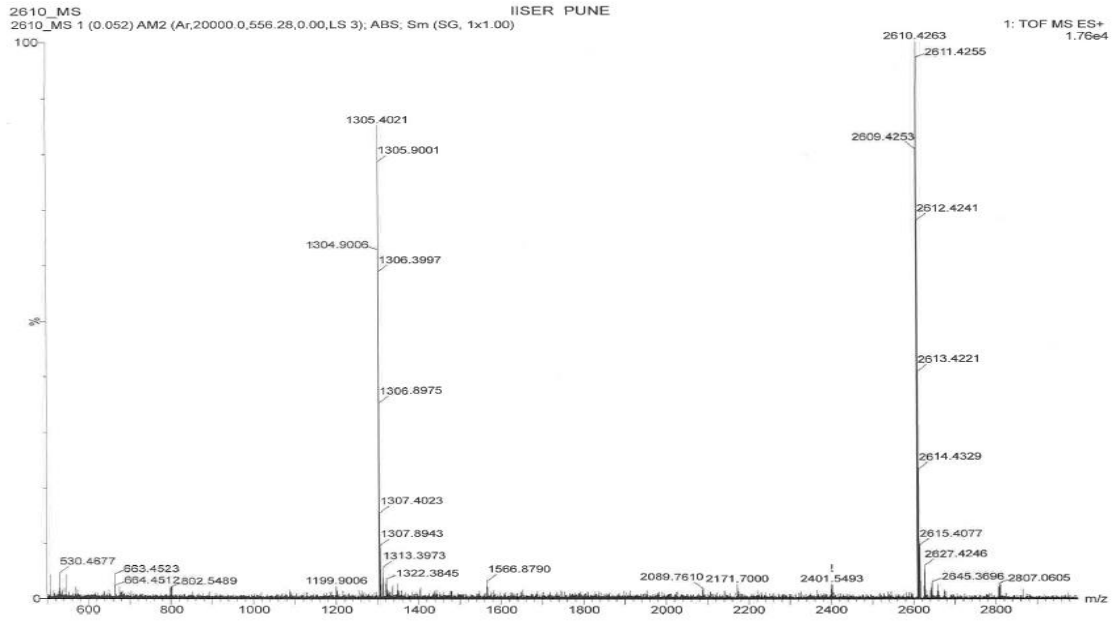

Figure II.19: *HR-ESI-TOF mass spectrum of Decaphyrin* ***10****.*

II.4.2 ^{1}H NMR study of [50] decaphyrin

In ^{1}H NMR spectrum, **10** displayed an uncharacteristic broad signal at δ 7.00 ppm at room temperature suggestive of a solution state dynamics expected for such large macrocycles. Therefore, variable temperature NMR spectroscopy was employed to arrest the suspected fluxional characteristics (figure – II.20). As expected, the spectrum resolved upon reducing the temperature to 198 K in acetone-d_6. More than ten signals were observed in the region between δ 8.50 and 5.75 ppm (figure – II.21). The spectra displayed eight distinct doublets along with few multiplets accounting for twenty protons and corresponding to an unsymmetrical structure of decaphyrin **10**. ^{1}H-^{1}H COSY NMR spectra shows seven sets of correlations (figure – II.22). However, these spectral details were not sufficient enough to determine its absolute molecular structure. Further, as these signals do not reflect significant diatropic ring current effect, it strongly suggested non-aromatic characteristics of the (4n+2) π macrocycle. Attempts to elucidate the macrocycle's absolute structure were attempted by single crystal X-ray diffraction studies.

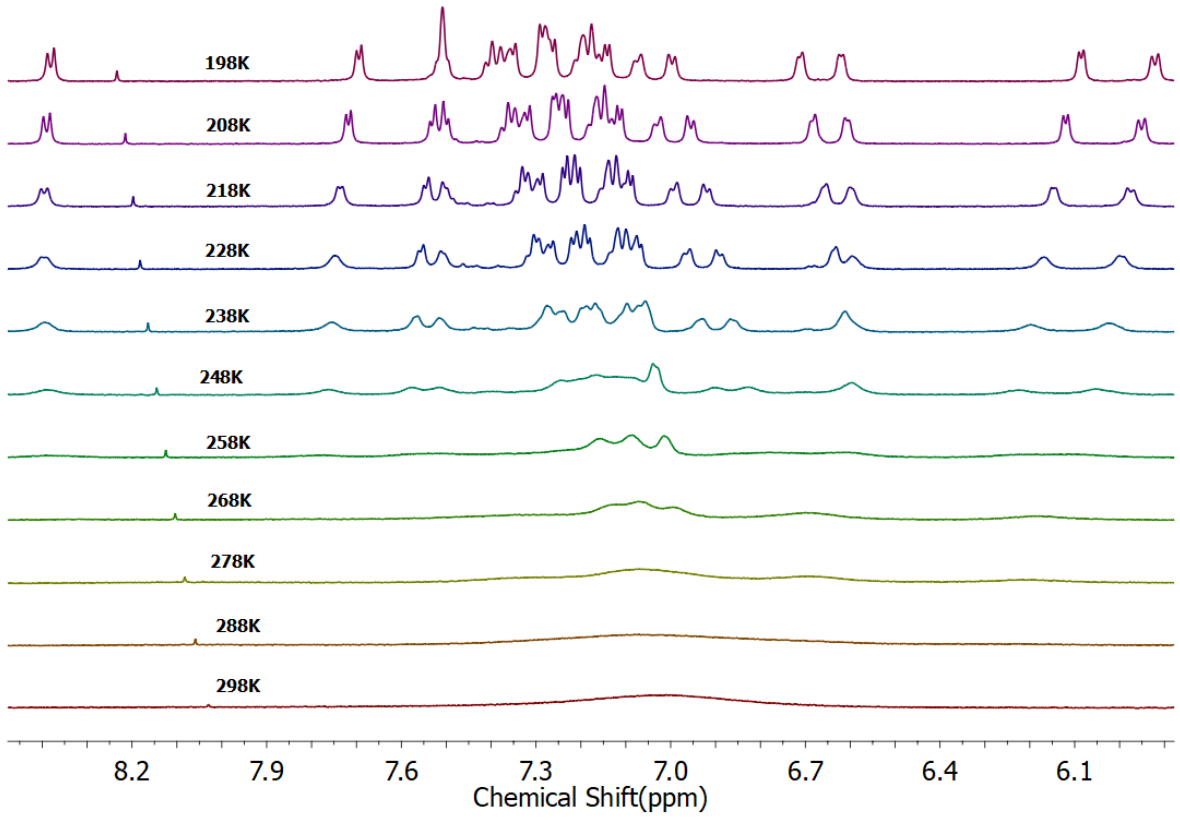

Figure II.20: *Variable ^{1}H NMR spectrum of **10** in Acetone-d_6.*

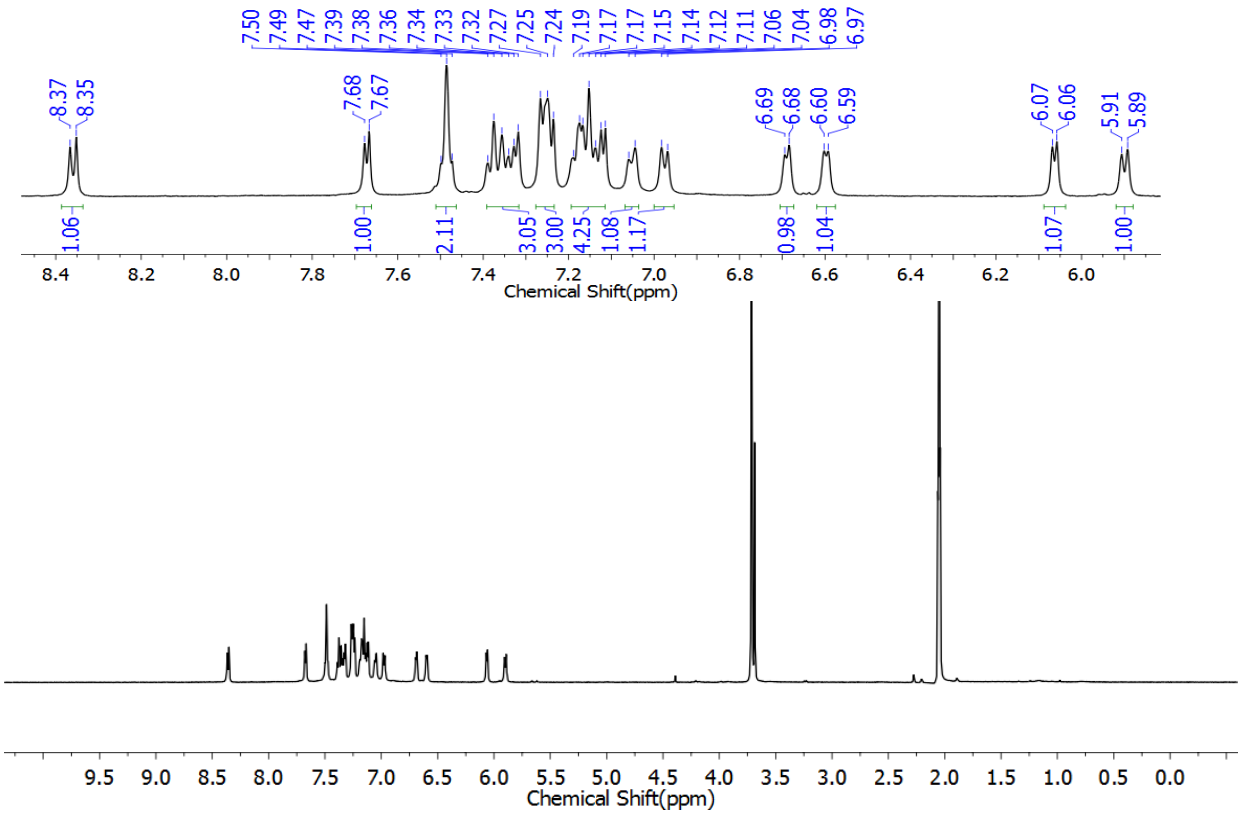

Figure II.21: *^{1}H NMR spectrum of **10** in Acetone-d_6 at 198 K.*

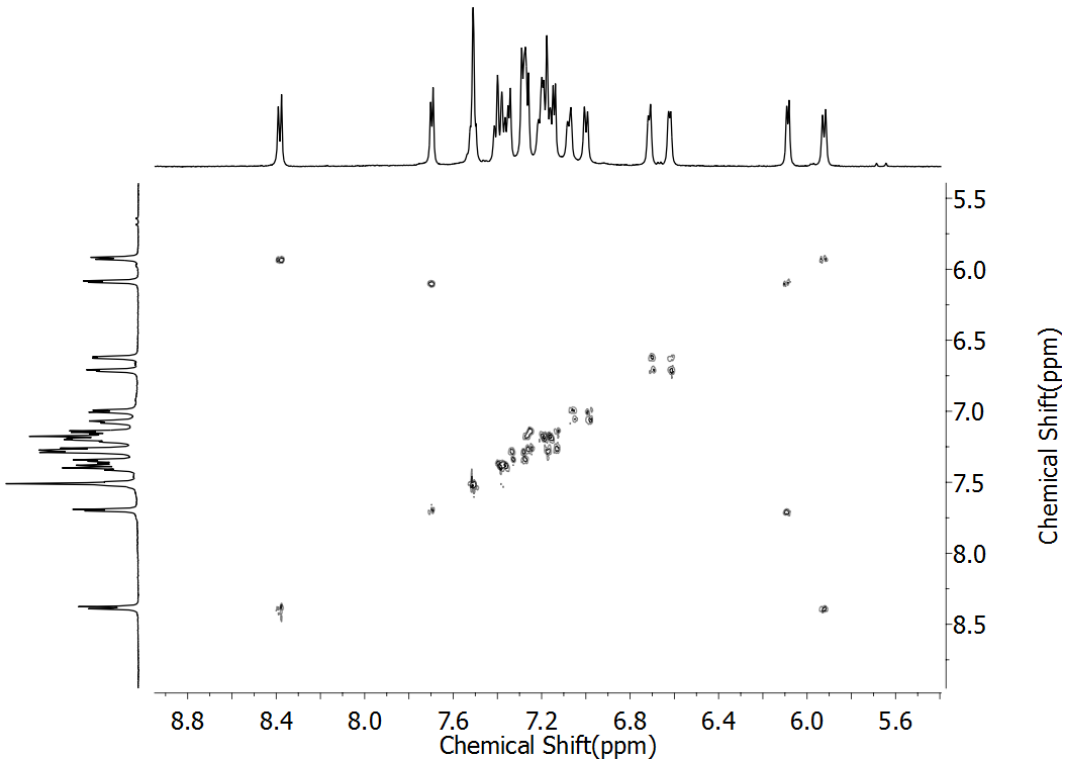

Figure II.22: *^{1}H-^{1}H COSY spectrum of **10** in Acetone-d_6 at 198 K.*

II.4.3 Topoisomers of Decaphyrin

Good quality single crystals of **10** were grown in acetonitrile by slow evaporation method. The structure, revealed a non-planar geometry in complete support of its non-aromatic character as observed from ^{1}H NMR spectrum at 198 K. In stark contrast to earlier reports of a symmetrical figure-of-eight conformation for Vogel's [36]Octaphyrin[14] and Sessler's Turcasain[15], the decaphyrin **10** displayed a unique [6 + 4] unsymmetrical twist (figure – II.23). It resembled a combination of a tetrathia iospholrin-like and hexathia hexaphyrin-like pockets than the generally observed pentaphyrin-like (5 + 5) pockets. It was also noted that the absence of acetonitrile in the crystal packing could have the encouraged the macrocycle to adopt the [6 + 4] unsymmetrical twisted conformation. The estimated NICS values of δ -0.62 and -1.66 ppm at the centre of hexaphyrin and isophlorin pockets respectively, provided sufficient support for the non-aromatic character of 50π macrocycle.

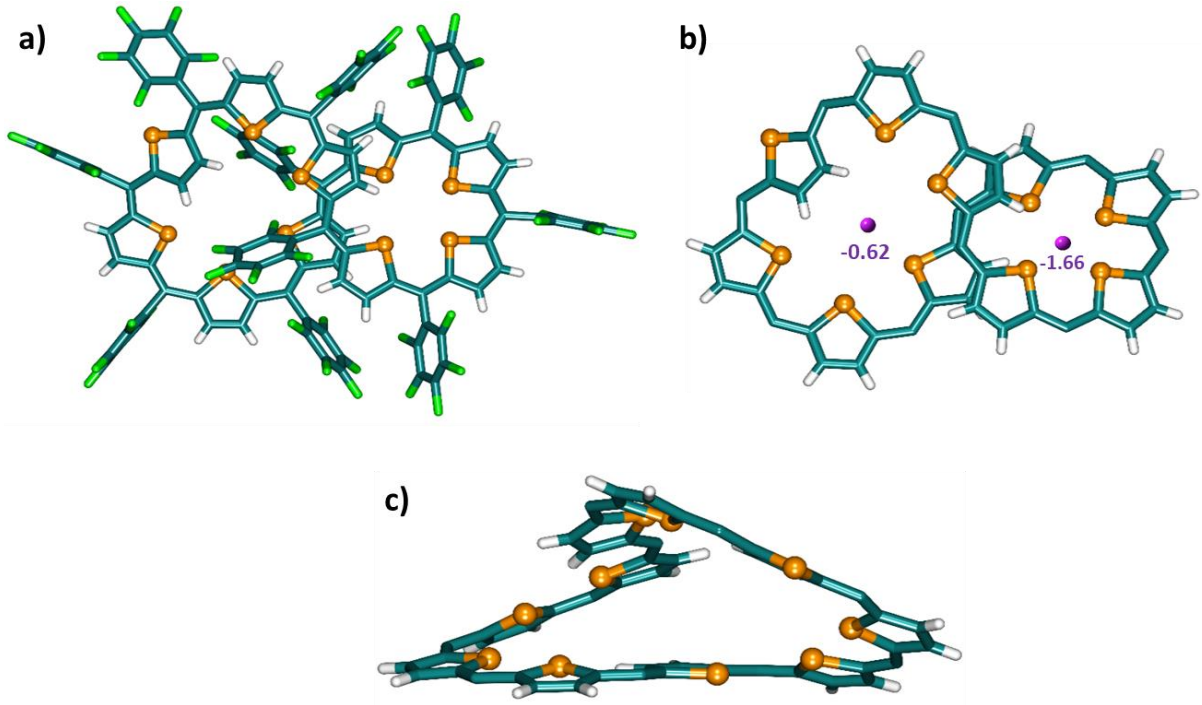

Figure II.23: *Molecular structure of **10** in acetonitrile, determined from single crystal X-ray diffraction, Pentafluorophenyl rings are omitted of clarity in the (b) (top view) and (c) (side view) rows. The estimated NICS values at two different positions are mentioned in the respective positions of the macrocycle.*

Based on the observed different crystal packing for the 40π octathiophene **8**, it was envisaged that even **10** can also exhibit solvent dependent packing in the crystal. Accordingly attempts were made to crystallize **10** in different organic solvents. Crystallizing **10** in benzene by vapour diffusion of hexane yielded an unprecedented near-planar topology (figure – II.24). In

contrast to the absence of acetonitrile in the crystal packing for [6+4] conformation of **10**, benzene was involved as a solvate in the crystal packing for the macrocycle to adopt the [5+5] planar conformation. This crystal structure can also be identified as a solvate or pseudopolymorph or a topological isomer[29, 30] of **10**. From the structure, it was evident that a pair of diagonally opposite dithia dipyrrane units was ring inverted and flanked by a trithiophene unit on either side resembling a pair of spectacles resulting from two pentathiophene units. The inverted dithiadipyrrane units are indeed at the centre of the macrocycle which folds along its longest axis. From the crystal data, an inter-planar distance of more than 4 Å was observed between these two dipyrrane units. In support of the (4n+2)π macrocycle, the estimated NICS (0) value of δ -6.75 ppm in the pockets of pentaphyrin unveiled an enhanced but moderate aromaticity for the 50π macrocycle.

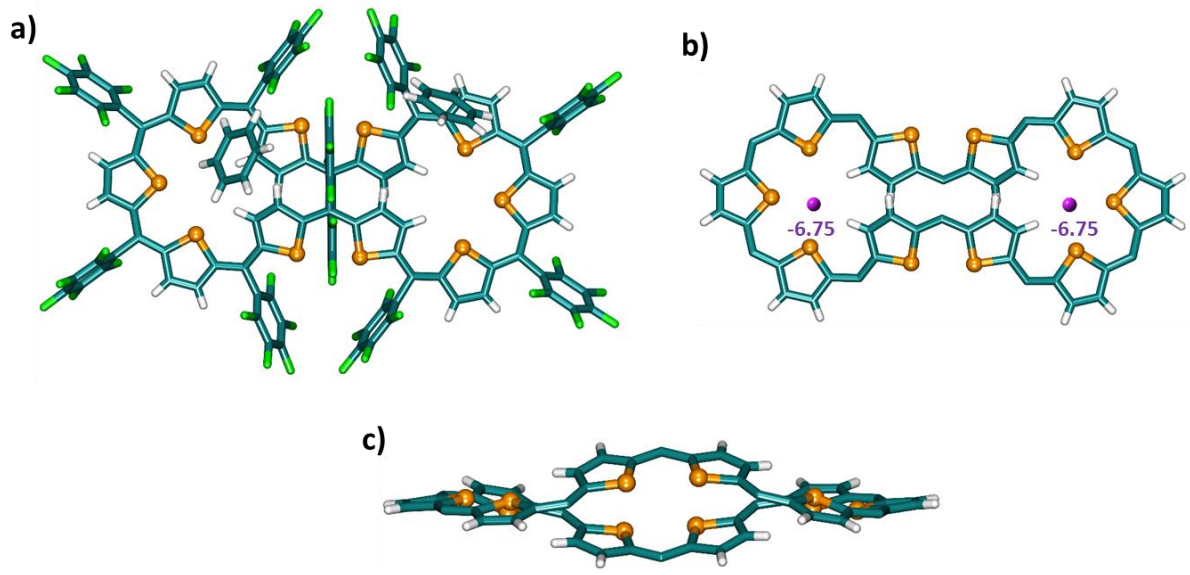

Figure II.24: *Molecular structure of **10** in benzene, Pentafluorophenyl rings and solvent molecules are omitted of clarity in the (b) (top view) and (c) (side view) rows. The calculated NICS (0) values are mentioned in the centre of the macrocycles.*

To identify the predominant conformation between benzene (planar) and acetonitrile (6+4 twist), crystallization was attempted with a combination of acetonitrile and benzene in different ratios. In this process a greenish needle shaped crystals of **10** were obtained, after many trails, through vapour diffusion method. In spite of two different solvents, **10** displayed predominantly [6+4] conformation. This observation implied acetonitrile was more preferred during the crystallization process even in the presence of benzene. Secondly, vapours of methanol employed for diffusion induce nucleophilic substitution reaction with para fluorine

of the pentafluorobenzene. Hence the obtained crystal displayed (-OCH_3) groups in the para position of ten pentafluoro phenyl substituents (figure – II.25).

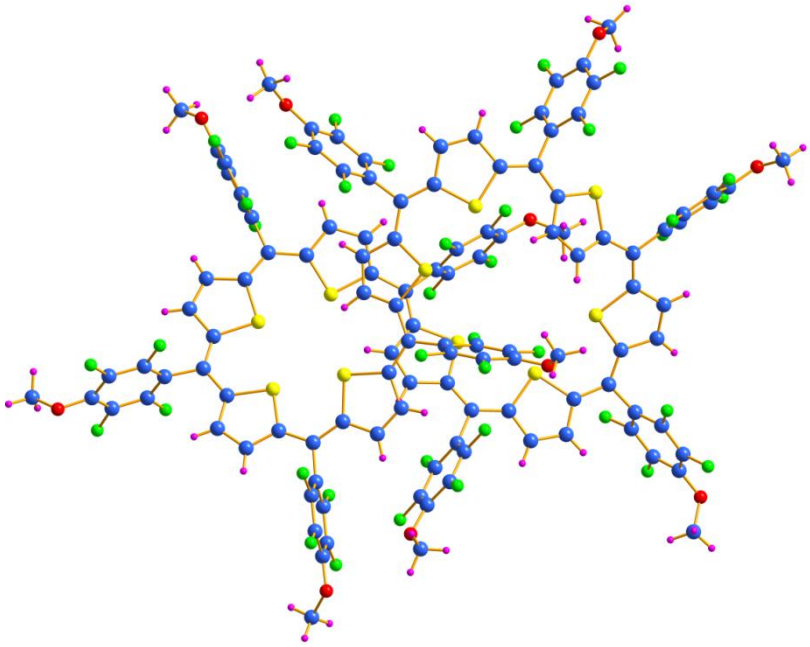

Figure II.25: *Molecular structure of **10**, obtained from the mixture the solvents (benzene and acetonitrile).*

In an attempt, a similar topology was observed when **10** was crystallized by diffusing vapours of *n*-heptane into a solution of **10** in DMSO (figure – II.26). Crystal packing of **10** in DMSO, displayed a butterfly-like structure. Each oxygen atom of DMSO molecule was found interacting with β-H of a thiophene, through hydrogen-bonding having the bond length 2.226Å and bond angle 159.04^0. Even though decaphyrin **10** was characterized to have different conformations in solid state with different solvents, yet similar structural variation could not be detected in solution state. ^{1}H NMR spectrum of **10** recorded in benzene-d_6 was found to be very much similar to the spectrum of **10** in CH_3CN. Hence, irrespective of the solvent, decaphyrin adopts the same conformation and corresponds only to non-aromatic species in the solution state. A similar molecular structure of **10** in benzene was observed.

^{1}H NMR spectrum of the decaphyrin in chloroform / DMSO/ acetonitrile / benzene revealed the same pattern at room temperature. Its NMR spectrum recorded at 208 K in toluene also resembled the same as observed in acetone-d_6. Hence it implied an identical unsymmetrical twist for the 50π-decaphyrin in the solution state irrespective of the solvent in which it was dissolved.

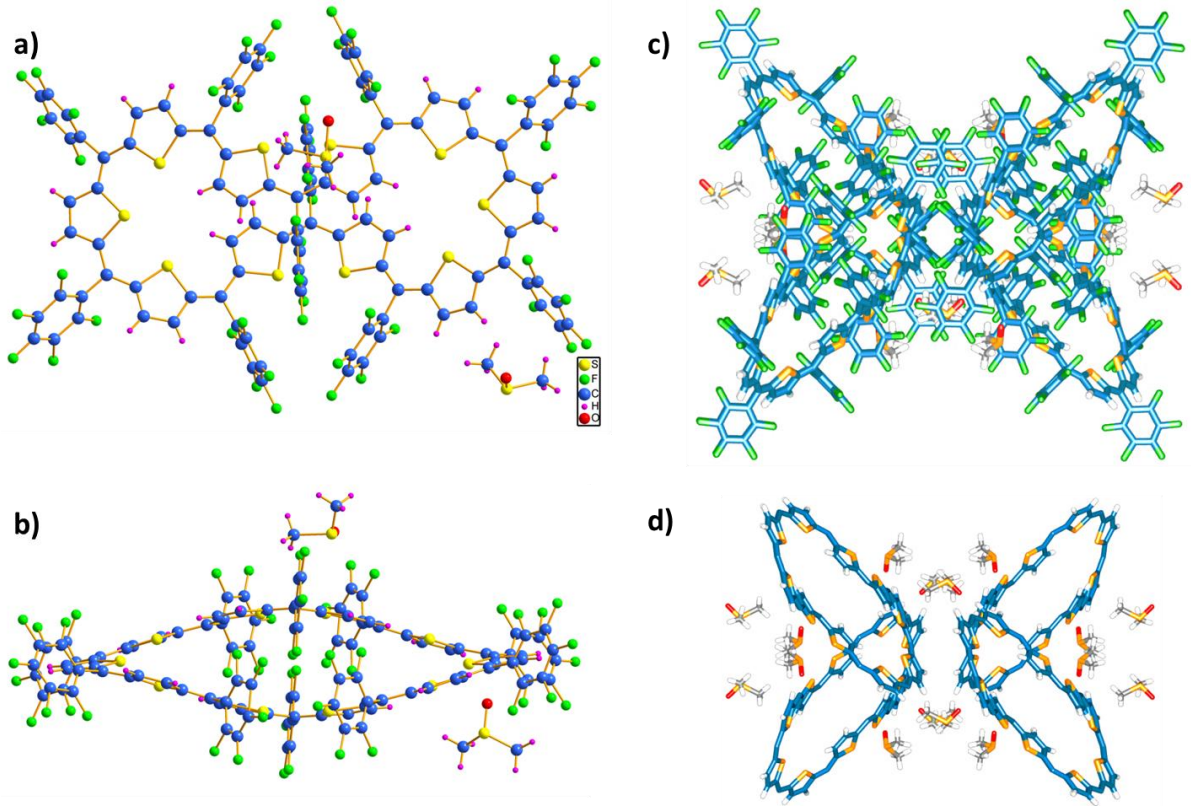

Figure II.26: *Crystal structure of **10** in DMSO, (b) (side view) and (c) crystal packing along with DMSO solvents (d) Pentafluorophenyl rings are omitted of clarity.*

II.4.4 Electronic absorption and Cyclic Voltammogram studies

[50]decaphyrin, **10**, has 50π electrons in the global conjugation and corresponds to (4n+2) number of π-electrons. However, from ^{1}H NMR analysis, it corresponds to a non-aromatic species in the solution state arising from non-planar topology. Yet, by virtue of its extended π-conjugation **10** displays an intense absorption at 456 nm (137500) followed by a low energy band at 650 nm (84200) in dichloromethane (figure – II.27a). Electronic spectrum in different solvents chloroform / DMSO/ acetonitrile / benzene also revealed a similar absorption spectrum. Despite its extended conjugation, **10** was found non-aromatic and hence it was suspected that decaphyrin can be susceptible to reversible oxidation. However, no such exclusive π oxidation has been observed for non-aromatic porphyrinoids till date. Addition of Meerwein's salt to a solution of decaphyrin **10** induced a subtle change from greenish to a red colour in dichloromethane. Accordingly, it exhibited intense red-shifted absorption maxima at 955 nm (144300); a shift by more than 300 nm compared to the parent 50π-macrocycle (figure - III.27a). Further, low energy bands were also observed at 1378 nm (13200) and

1624 nm (5900), which are expected for the two-electron oxidized species of [**10**]$^{2+}$. Ring oxidation of the macrocycle leads to loss of two π-electrons to eventually yield the 48π dicationic species. This oxidation was found to be reversible by obtaining the parent and neutral 50π decaphyrin upon the addition of triethyl amine. Further, its redox properties were studied through electrochemical techniques such as cyclic voltammetry (CV) and spectro-electrochemistry (SEC).

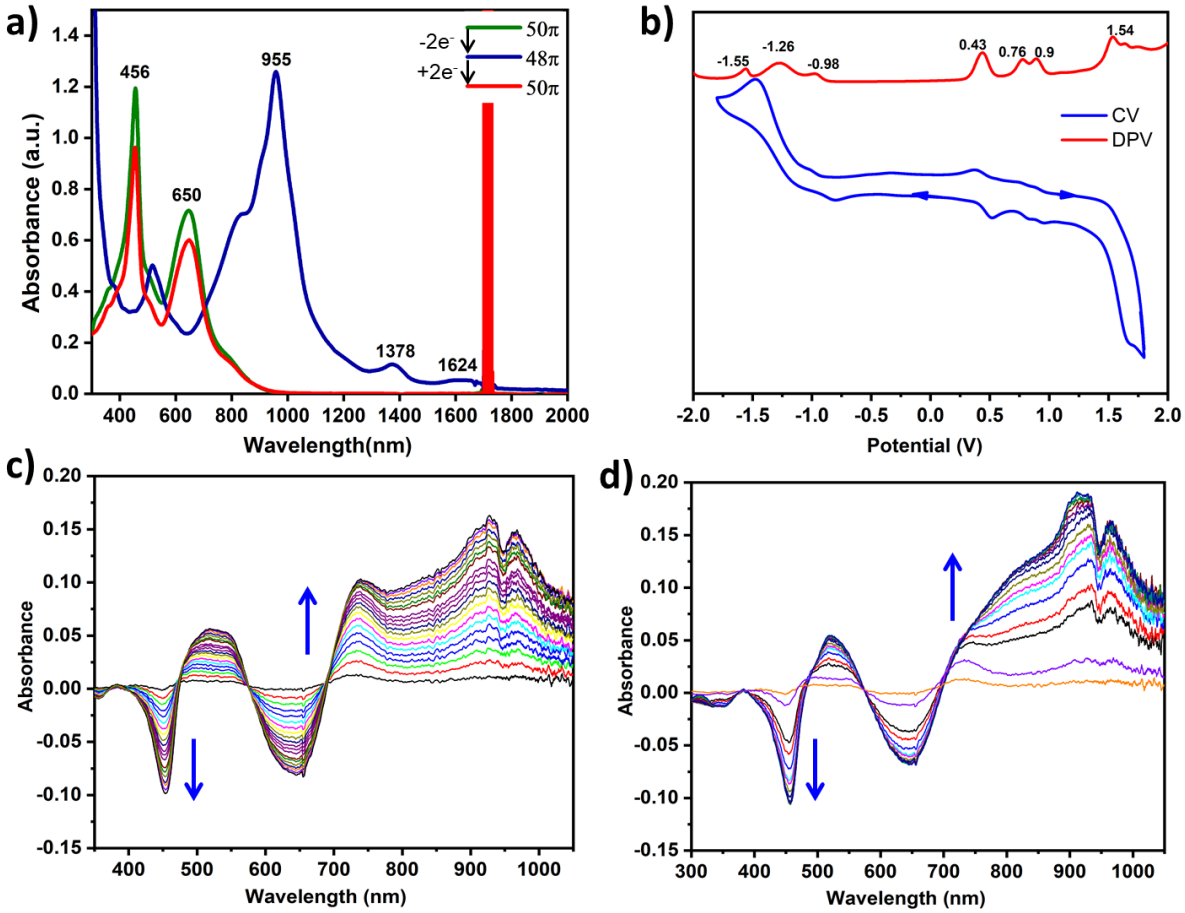

Figure II. 27: *(a) UV/vis/NIR absorption spectrum of 10^{-5} M solution of **10** (50π) and its oxidised species [**10**]$^{2+}$ (48π) recorded in CH_2Cl_2. (b) Cyclic voltammogram (CV, blue) and differential pulse voltammogram (DPV, red) of **10** in CH_2Cl_2 (with 0.1 M $(Bu)_4NPF_6$ as the supporting electrolyte). (c and d) Change in absorption spectra of **10** after applying a potential of + 0.5 V and + 0.85 V, respectively.*

Cyclic voltammogram and differential pulse voltammogram of 50π decaphyrin, **10**, revealed at least four oxidation potentials at +0.43, +0.76, +0.9 and +1.54 V along with three reduction potentials at -0.98, -1.26 and -1.55 V (figure – 27b). These values clearly establish 50π macrocycle as a redox active species capable of either reduction or oxidation. As per the observed chemical oxidation, the corresponding potentials determined from cyclic voltammogram were employed to record spectro-electrochemical (SEC) data. Based on the

oxidation potentials from CV studies, its absorption was recorded at an applied potential of + 0.5 V (figure – II.27c). It displayed a broad absorption band at 750 nm followed by another intense absorption at 950 nm suggestive of a cation radical species and two-electron oxidized species respectively. However, at a higher potential of + 0.85 V only the intense band at 955 nm was observed in support of the two-electron ring oxidation determined from electronic absorption spectroscopy (figure – II.27d). These absorptions unequivocally supported the two-electron ring oxidation of the 50π decaphyrin to 48π dication as a two-step one-electron process.

II.4.5 Synthesis and Characterisation of [48]decaphyrin dication

After confirming the two-electron oxidation of [50] decaphyrin by chemical and electrochemical measurements, further attempts were directed to isolate the dicationic species to determine its molecular structure. It was of particular interest since the same macrocycle displayed both aromatic and non-aromatic characteristic in solid state and non-aromatic characteristic nature in solution state. Addition of Meerwein's salt to a solution of 50π decaphyrin, induces subtle change from greenish to reddish colour. High resolution mass spectrum (HRMS) of the red-coloured solution displayed *m*/*z* value at 1305.4021 corresponding to *m*/*2* (figure – II.28) of the actual mass of two electron oxidised decaphyrin dication.

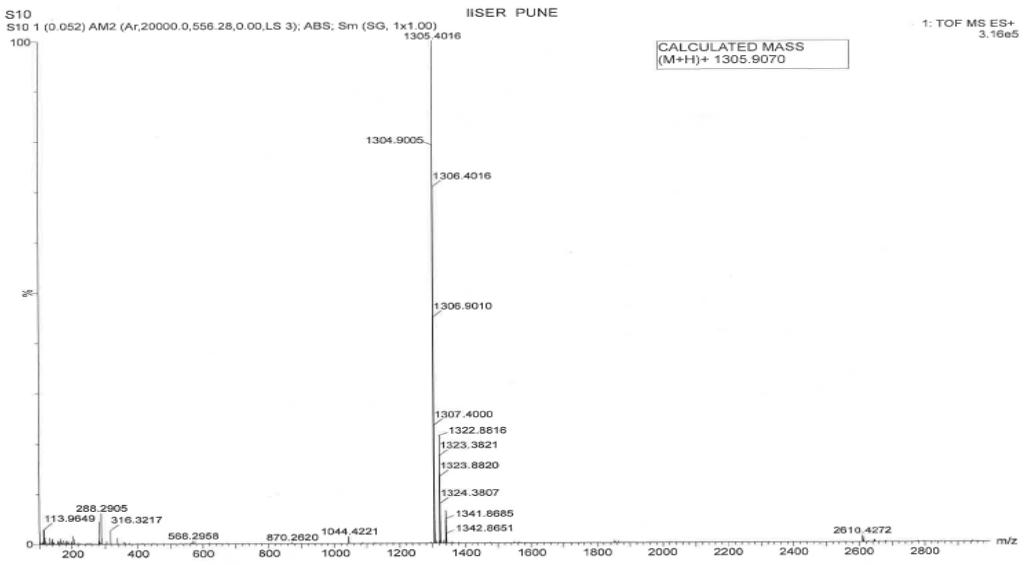

Figure II.28: *HR-ESI-TOF mass spectrum of decaphyrin dication,* ***[10]***$^{2+}$.

Further characterization of the 48π dicationic species was done by NMR spectroscopy and its absolute structure determined from single crystal X-ray diffraction studies. Being a 4nπ

system, it can be expected to display paratropic ring current effect if it could sustain a planar topology. In the ^{1}H NMR spectrum, the dicationic species [**10**]$^{2+}$ recorded at room temperature displayed only a broad signal in the region δ 8.0 – 9.0 ppm strongly suggestive of fluxional characteristics in the solution state. Therefore, the ^{1}H NMR spectrum was recorded by varying the temperature (figure – II.29) up to 193 K. Upon reducing the temperature to 193 K, well resolved multiple signals were observed between δ 6.0 and 23.0 ppm (figure – II.30). Even though it suggested a highly unsymmetrical structure in the solution state, but significantly differed from the possible planar free base conformation. The observation of large down field chemical shift values (δ 22.16 and 18.96 ppm) implies the dicatioinc species retained the same [6+4] conformation similar to the neutral state as crystallized in acetonitrile. By virtue of ring oxidation, the protons of the lone inverted thiophene ring in the hexaphyrin-like part of the macrocycle are suspected to resonate at a lower magnetic field strength.

II.4.6 Molecular structure of [48]decaphyrin dication

After many efforts, good quality single crystals of [**10**]$^{2+}$ could be grown in 1, 2-dichloroethane through vapour diffusion of *n*-hexane. The elucidated molecular structure was found very similar to the benzene solvate of the freebase macrocycle (figure – II.31). Two $[SbCl_6]^-$ counter anions were associated with macrocycle in support of the two-electron oxidized species. Remarkably, the estimated NICS (0) values at the centre of the pentaphyrin-like pockets was a staggering δ +36.21 ppm. This value is as high as the reported value of δ +37.5 ppm for the 24π pentathiophene cation and Ni(II)norcorrole.[31,32] Even though this conformation does not represent the conventional planar structure, yet due to the non-twisted topology, it does sustain antiaromaticity in the solid state. To the best of knowledge, 48π decaphyrin dication, is the largest anti-aromatic dication to be ever characterized in the solid state.

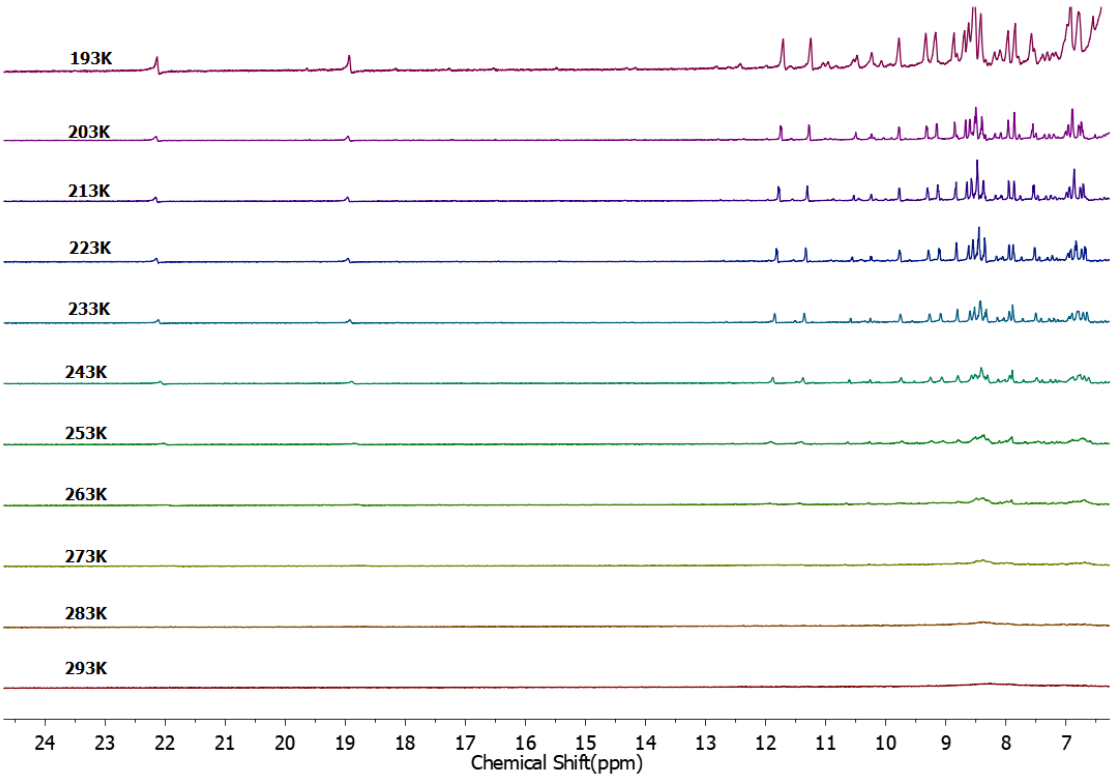

Figure II.29: *Variable temperature ^{1}H NMR spectra of* ***[10]***$^{2+}$ *in Acetone-*d_6.

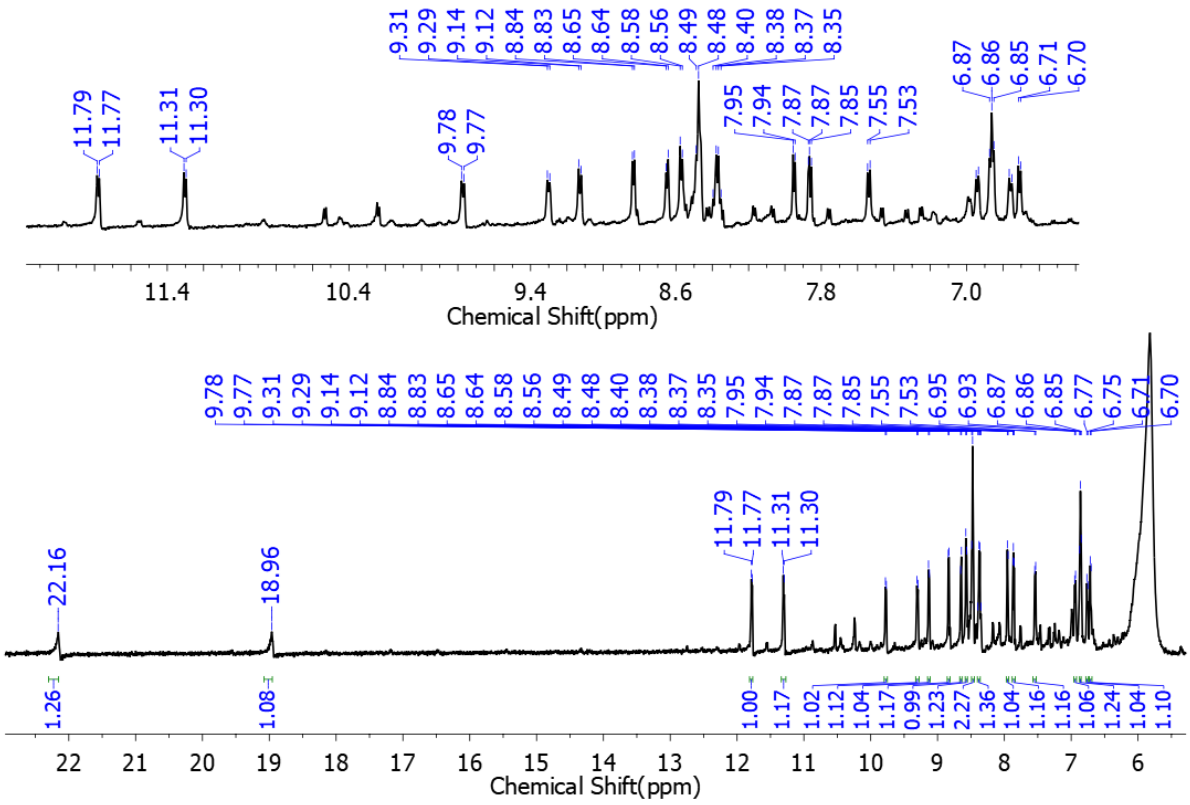

Figure II.30: ^{1}H *NMR spectrum of* ***[10]***$^{2+}$ *in Acetone-*d_6 *at 213 K.*

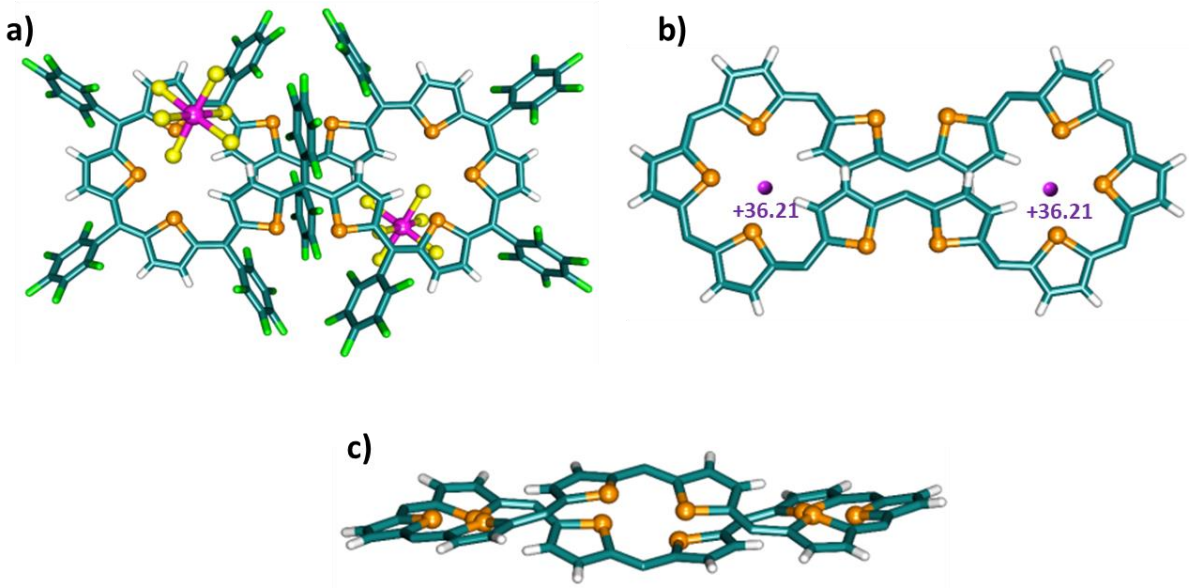

Figure II.31: *Molecular structure of decaphyrin dication* ***[10]***$^{++}$ *in benzene, Pentafluorophenyl rings and solvent molecules are omitted of clarity in the (b) (top view) and (c) (side view) rows. The calculated NICS (0) values are mentioned in the centre of the macrocycles.*

II.4.7 Computational studies

ACID can distinguish the three different aromatic states of [50]decaphyrin and its dication (figure – II.32). The molecular structure obtained in the [6+4] conformation displayed unidirectional ring current suggesting non-aromatic nature of the macrocycle. On the other hand, molecular structure obtained from benzene has planar topology and shows clockwise ring current in support of the aromatic nature. Correspondingly, 48π dicationic species displayed anti-clockwise ring current which represents the antiaromatic feature of the molecule in the solid state.

Further, the estimated HOMA value of 0.532337 for the (6+4) topology substantiates the non-aromatic feature, while a HOMO value of 0.924195 for the planar topology supports aromaticity in the solid state for the experimentally determined structures. However, a value of 0.797756 is in tune with the anticipated antiaromatic behaviour for the planar dication in the solid state.

Time-dependent TD-DFT calculations were found in agreement with the experimental electronic absorption (figure – II.33). The calculated oscillatory strength with the same basis set was very close and almost matched the nearest value with the experimentally obtained λ_{max} from electronic absorption (figure – II.32). HOMO-LUMO energy gap for both [6+4]

and planar conformations have the same values 1.41 and 1.40 eV respectively. For the two electrons oxidised dicationic species, it was observed there was a significant reduction in the HOMO-LUMO gap compared to the neutral molecule having the value of 0.73 eV. This value signifies a considerable decrease in the HOMO-LUMO energy gap, and concomitant with the red shift observed in the electronic absorption.

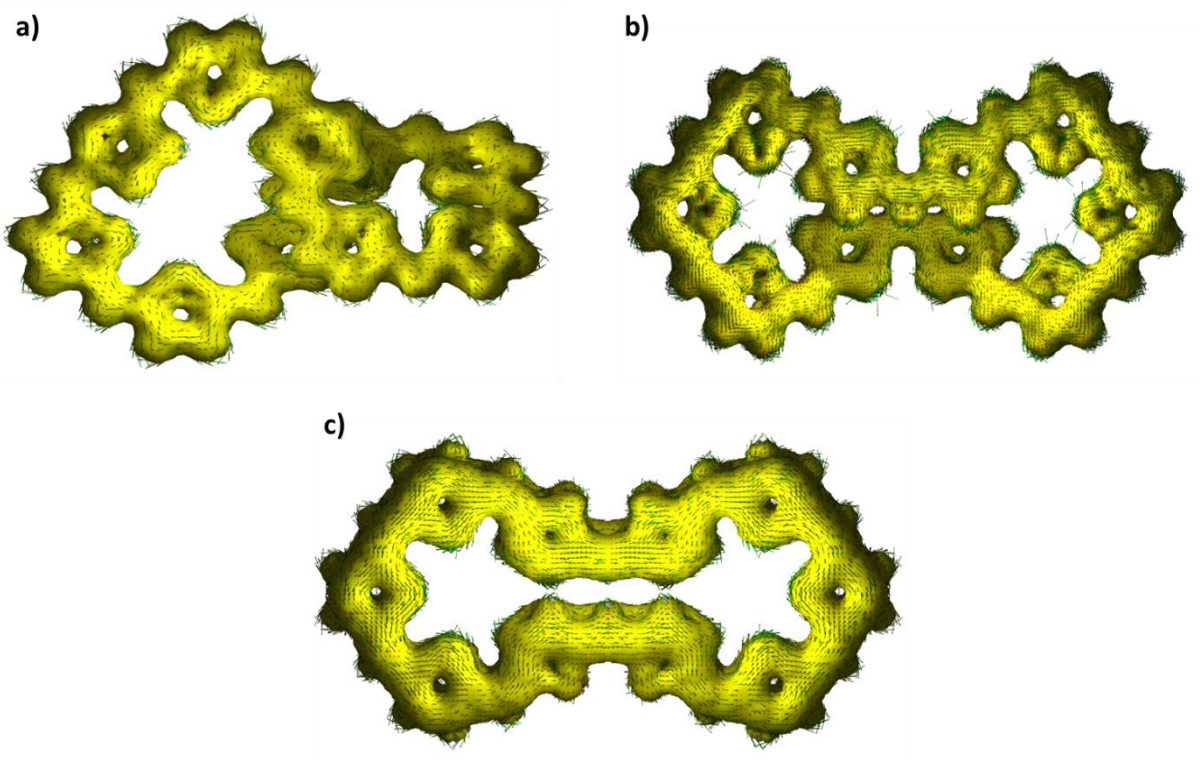

Figure II.32: *AICD plot of* ***10,*** *(a) in acetonitrile, (b) in benznene (c) dicationic species* ***[10]***$^{2+}$ *at the external magnetic field is applied orthogonal to the macrocyclic plane.*

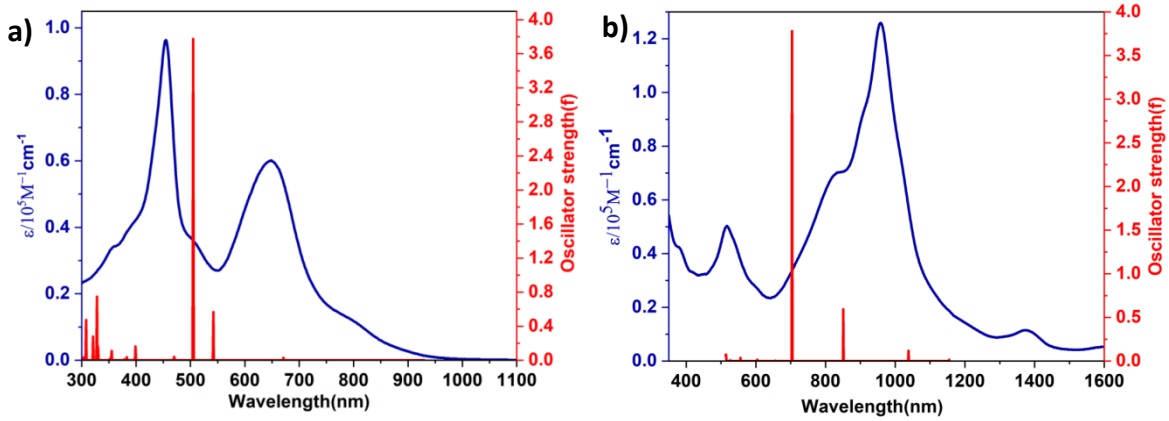

Figure II.33: *Selected TD-DFT (B3LYP/6-31G (d,p)) calculated energies, oscillator strengths and compositions of the major electronic transitions of* ***10*** *and* ***[10]***$^{2+}$.

II.5.1 Isolation and Characterisation of [60]dodecaphyrin

After the decaphyrin, the next higher congener identified in the reaction was [60]dodecaphyrin, **12**, bearing twelve thiophene units. It was isolated from a combination of column chromatography and repeated size exclusion chromatography as a cyan coloured solution is less than 1% yields. Its composition was confirmed by HR-MS (figure – II.34), in which it displayed an *m/z* value of 3131.7659 corresponding to $C_{132}H_{24}F_{60}S_{12}$ (3131.7568).

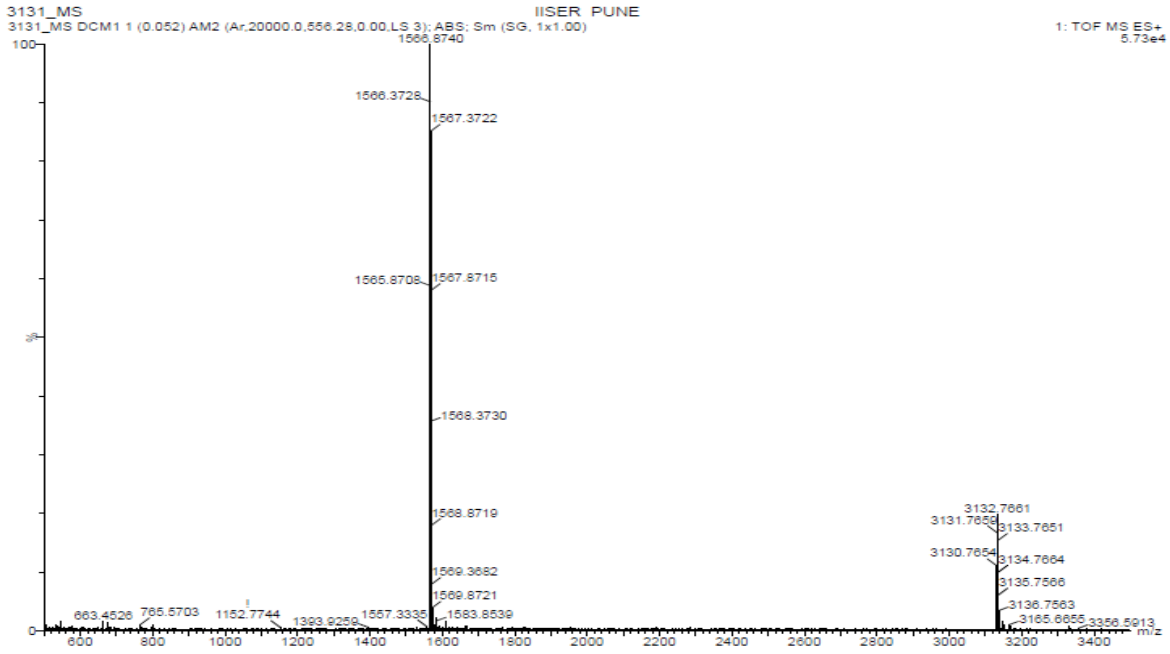

Figure II.34: *HR-ESI-TOF mass spectrum of Dodecaphyrin* ***12.***

II.5.2 ^{1}H NMR study of [60]dodecaphyrin

[60]dodecaphyrin, **12**, accounts for a formal count of 60 π-electrons along its global conjugation. Corresponding to a 4nπ count, it is supposed to exhibit anti-aromatic characteristics. However, its room temperature ^{1}H NMR spectrum displayed signals in the range of δ 7.2 to 6.7 ppm in acetone-d_6 signifying conformational dynamics as noted for its predecessors i.e. [40]octaphyrin, **8**, and [50]decaphyrin, **10**. Therefore, NMR spectra were recorded by varying the temperature (figure – II.35). Upon reducing the temperature from 298 K to 263 K, it transforms into a broad singlet at δ 6.94 ppm. Further decrease in the temperature to 188 K resolved the broad signal into multiple peaks between δ 8.5 to 5.5 ppm. Of the twenty-four thiophene protons, five distinct signals were observed as doublets at δ 8.3, 7.8, 7.6, 6.2 and 5.6 ppm (figure – II.36). The remaining protons corresponds to the overlapping signals in the region between δ 7.4 to 6.8 ppm and was hard to assign these

signals. Since these chemical shift values did not reflect any significant paratropic ring current effect, this spectrum suggests structure induced loss of anitaromaticity for the 60π macrocycle.

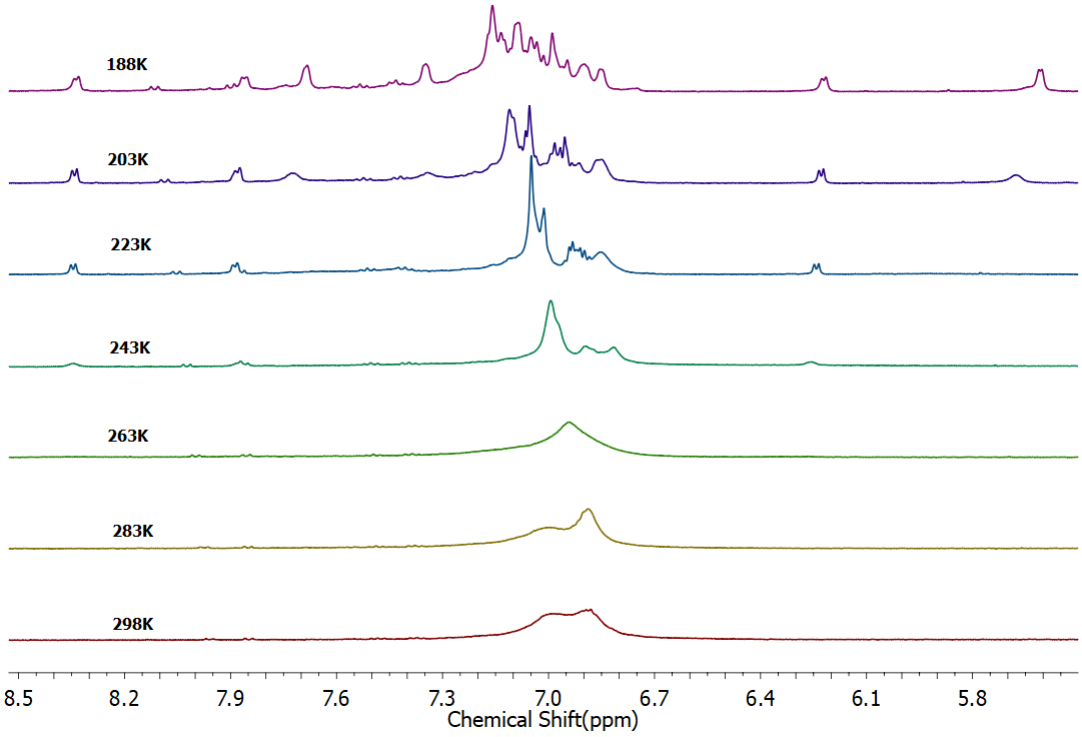

Figure II.35: *Variable temperature ^{1}H NMR spectrum of **12** in Acetone-d_6.*

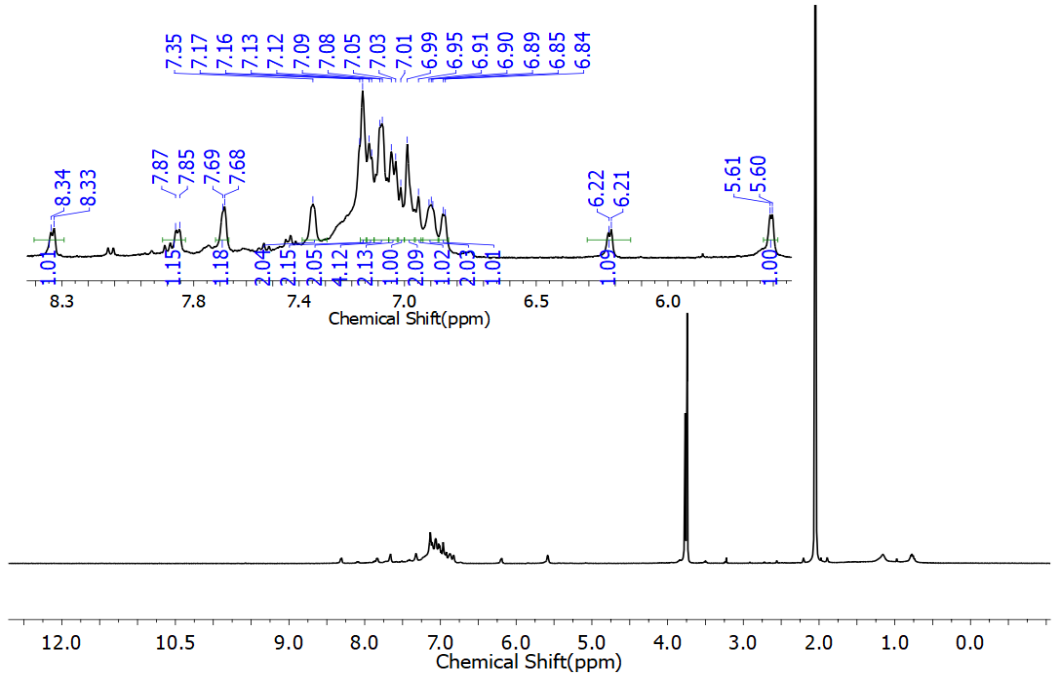

Figure II.36: *^{1}H NMR spectrum of **12** in Acetone-d_6 at 213 K.*

II.5.3 Molecular structure of [60]dodecaphyrin

Since ^{1}H NMR spectroscopy could not provide conclusive evidence for the molecular structure, efforts were directed to determine the same from single crystals. After many efforts with a variety of solvents, good quality crystals were finally grown by diffusing vapours of *n*-hexane into a solution of **12** in dichloromethane. Single crystals were bluish metallic and shiny in nature crystal. X-ray diffraction analysis of these crystals revealed a relatively symmetrical but coiled-like structure. Unlike the earlier known pyrrole based dodecaphyrins,[33] the twelve thiophene units macrocycle described here revealed twin pentathiophenes bridged by a dithiophene unit (figure – II.37). An interesting observation was the presence of ring inverted thiophenes from the dithiophene units. It is envisaged that the presence of meso aryl units might have inflicted a different topology in comparison to the meso trifluoromethyl substituents.[33] By far, this is the largest and the first structural characterization of a completely meso-aryl dodecaphyrin with 60π electrons in comparison to the earlier reported expanded rosarin macrocycle having different oxidation states of 48π, 50π and 52π-electrons with twelve pyrrole units.[34]

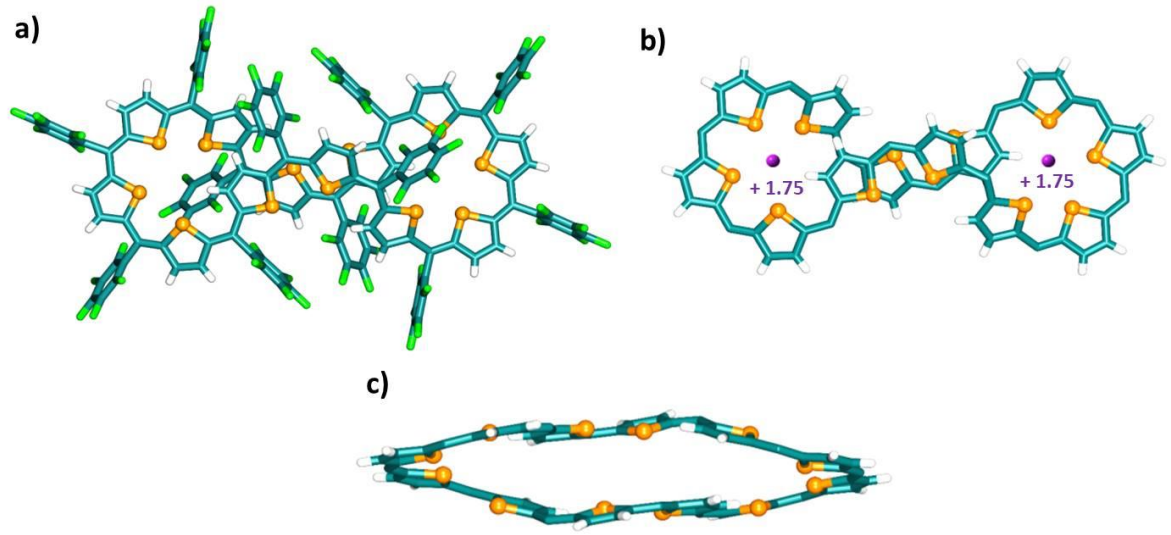

Figure II.37: *Molecular structure of cyclododecathiophene **12** as determined from single crystal X-ray diffraction. Pentafluorophenyl rings are omitted of clarity in the (b) (top view) and (b) (side view) rows. The calculated NICS values are mentioned in the centre of the macrocycle.*

II.5.4 Electronic absorption and cyclic voltammogram studies

As observed for [40[octaphyrin, **8**, and [50]decaphyrin, **10**, reversible two-electron ring oxidation was observed even for the 60π dodecaphyrin. In the electronic absorption spectrum, it displayed a low intense band at 404 nm (132400) and an intense absorption at 632 nm

(203300) (figure – II.38a). Addition of Meerwien's salt induced a subtle color change from cyan to blue along with a whopping red shift by more than 450 nm in dichloromethane. An intense band for the suspected dication was observed at 1104 nm (304400) followed by a weak band at 1560 nm (50800). The oxidized species could be reduced back to the freebase macrocycle by the addition of reducing agent triethyl amine, which immediately reverts to 60π neutral state. Cyclic voltammetry and differential pulse voltammetry of [70]dodecaphyrin displayed three oxidation potentials at +0.63, +1.09 and +1.61 V and four reduction potentials at -0.61, -1.1, -1.43 and -1.63 V respectively (figure – II.38b). During the spectro-electrochemistry scan, among three oxidation potentials, at an applied potential of +1.1 V, i.e. the second oxidation potential, this macrocrocycle displayed a broad peak at 1104 nm (figure II.38c) confirming the formation of dicationic species [**12**]$^{2+}$. The two-electron ring oxidation was further supported by an *m/z* value of 1565.8785 (Calcd. for 1565.8784) corresponding to *m/2* of the $(C_{132}H_{24}F_{60}S_{12})^{2+}$ in the HRMS spectra (figure – II.39). Owing to the poor solubility of dicationic species a well resolved ^{1}H NMR spectrum could not be obtained.

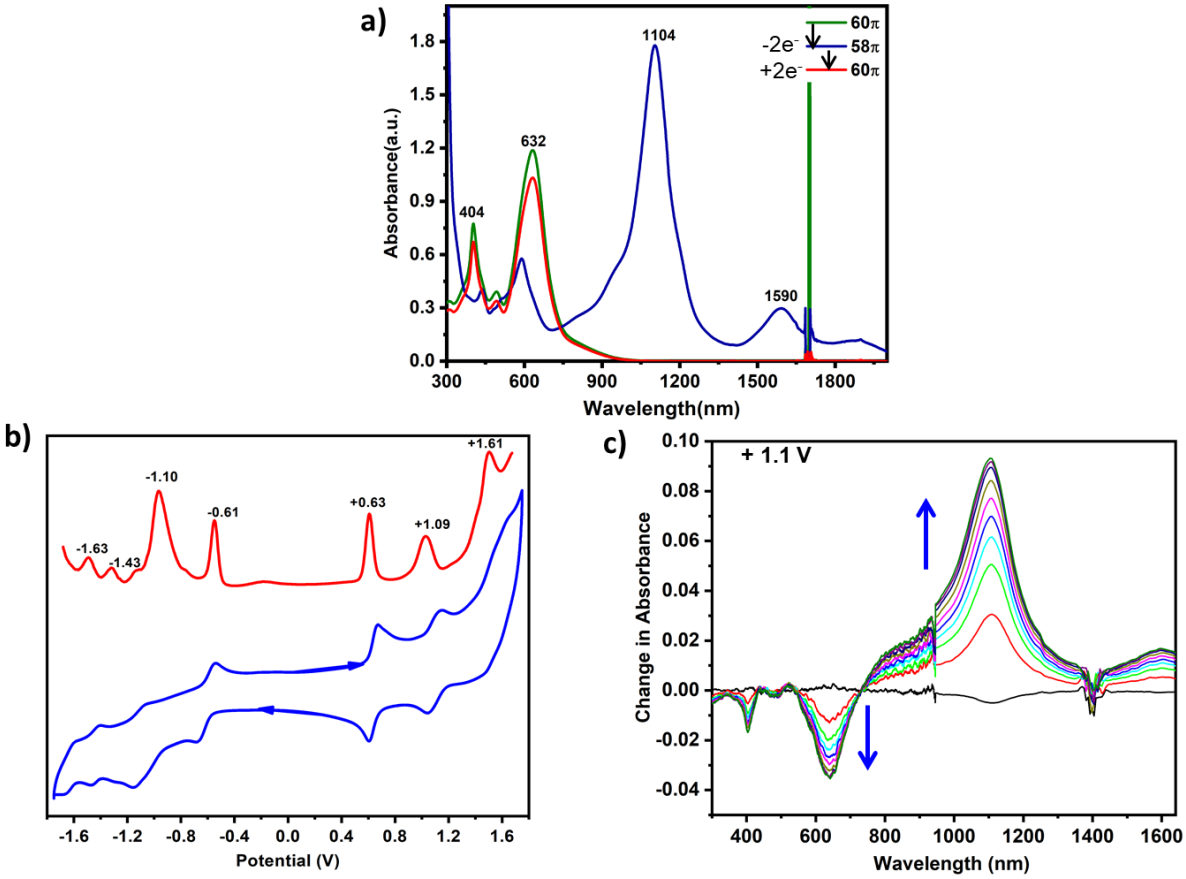

Figure II.38: *(a) and (d) UV/vis/NIR absorption spectrum of 10^{-5}M solution of **12** and its oxidised species [**12**]$^{2+}$ recorded in CH_2Cl_2. (b) Cyclic voltammogram (CV, blue) and differential pulse voltammogram (DPV, red) of **12** in CH_2Cl_2 (with 0.1 M $(Bu)_4NPF_6$ as the supporting electrolyte). (c) Change in absorption spectra of **12** after applying a potential of + 1.1 V.*

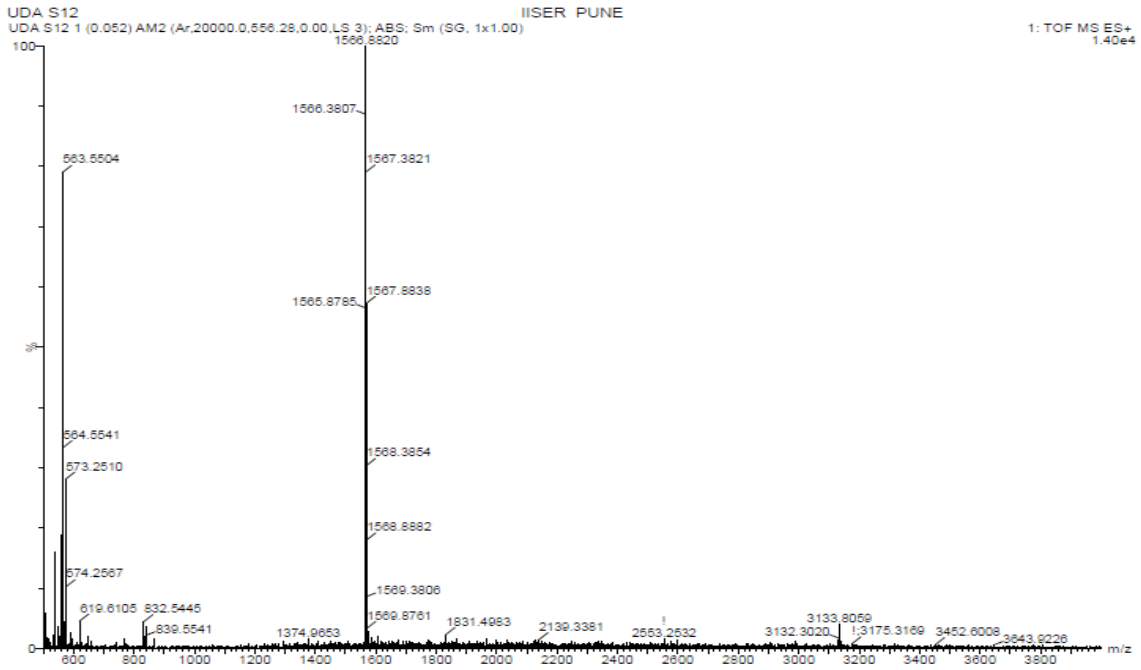

Figure II.39: *HR-ESI-TOF mass spectrum of* ***[12]*** $^{2+}$**.**

II.5.5 Computational studies

Quantum chemical calculations further supported the non-antiaromatic characteristics of [60]dodecaphyrin as observed from ^{1}H NMR spectroscopy. An estimated NICS(0) value of δ +1.75 ppm reflected weak antiaromatic characteristics for the 60π macrocycle and ACID plot displayed anti-clockwise ring current (figure – II.40), suggests the paratropic ring current at an isosurface value 0.09. TD-DFT plot was found to match the experimentally determined electronic absorption (figure – II.41). It was also observed that due to 70π electrons, the extended π-conjugation drastically decreased the HOMO-LUMO energy gap to 0.97 eV.

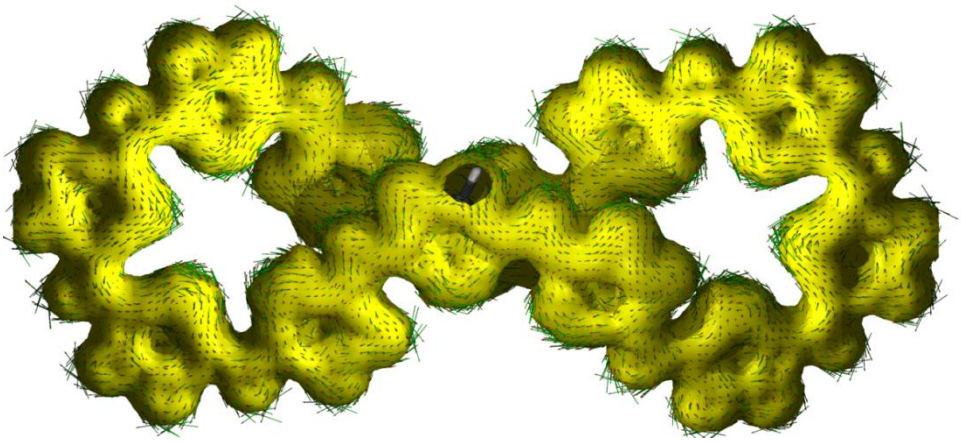

Figure II.40: *AICD plot of* ***12*** *at an isosurface value 0.09 the external magnetic field is applied orthogonal to the macrocycle plane.*

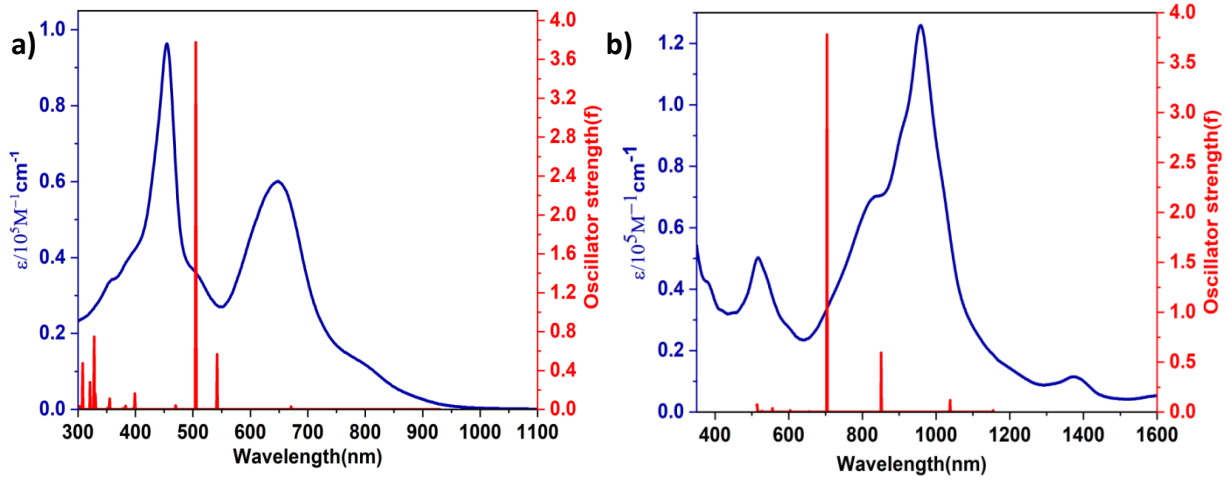

Figure II.41: *Selected TD-DFT (B3LYP/6-31G (d,p)) calculated energies, oscillator strengths and compositions of the major electronic transitions of* ***12*** *and* ***[12]***$^{2+}$.

II.6.1 Isolation and Characterisation of [70]tetradecaphyrin

The next higher analogue that was isolated was a macrocycle with fourteen thiophene units. It is the largest tetradecaphyrin to be characterized for 70π-electrons till date. [70]tetradecaphyrin, **14**, was isolated as a dark blue coloured solution in less than 1% yields. It was tedious to isolate, but was successfully isolated by repeated silica column chromatography and size exclusion chromatography. Its HR-MS spectrum displayed *m/z* value of 3654.0291 corresponding to $C_{154}H_{28}F_{70}S_{14}$ (3653.7163) along with *m/2* mass of its two electron oxidised dicationic species (figure – II.42).

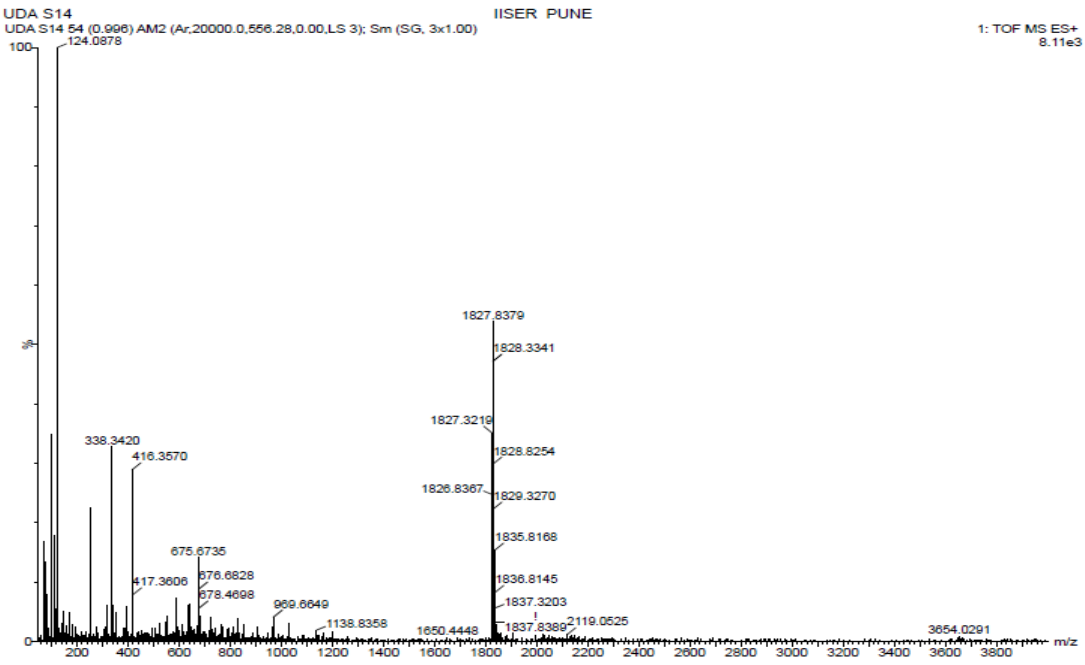

Figure II.42: *HR-ESI-TOF mass spectrum of Tetradecaphyrin* ***14***.

II.6.2 ^{1}H NMR study of [70]tetradecaphyrin

Even though macrocycle 70π-electrons accounts for (4n+2)π-electrons, its ^{1}H NMR spectrum revealed only a broad signal under ambient conditions suggestive of highly fluxional behavior in the solution state. Therefore, an attempt was made to record the ^{1}H NMR at lower temperatures (figure – II.43). A relatively resolved spectrum was observed at 218 K (figure II.44). The most shielded signal resonated at δ 5.1 ppm and the deshielded signal was recorded at δ 7.7 ppm. An estimated Δδ of 2.6 ppm between these two signals does not signify diatropic ring current as expected of 70π macrocycle and hence the molecule is identified as non-aromatic in the solution state. Except for the upfield doublets at δ 5.4, 5.1 ppm and six downfield doublets between δ 7.0 to 7.7 ppm, all the other resonances were found to overlap in a very small region between δ 6.7 to 6.2 ppm. Even though the spectrum did account for all the twenty-eight protons, yet it could not yield any conclusive evidence to assign the specific resonance for each proton. Six correlations observed from ^{1}H-^{1}H COSY NMR spectrum (figure – II.45) was not sufficient enough to elucidate the conformation or structure of the macrocycle.

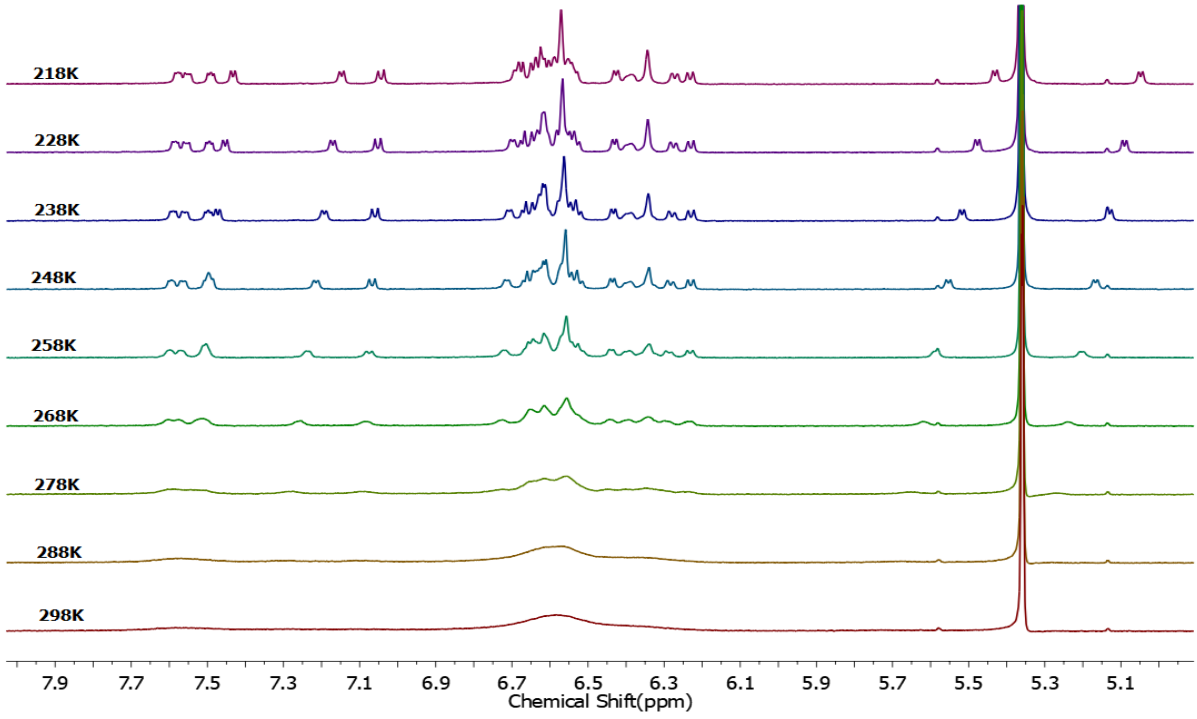

Figure II.43: *Variable temperature ^{1}H NMR spectrum of **14** in dichloromethane-d_2.*

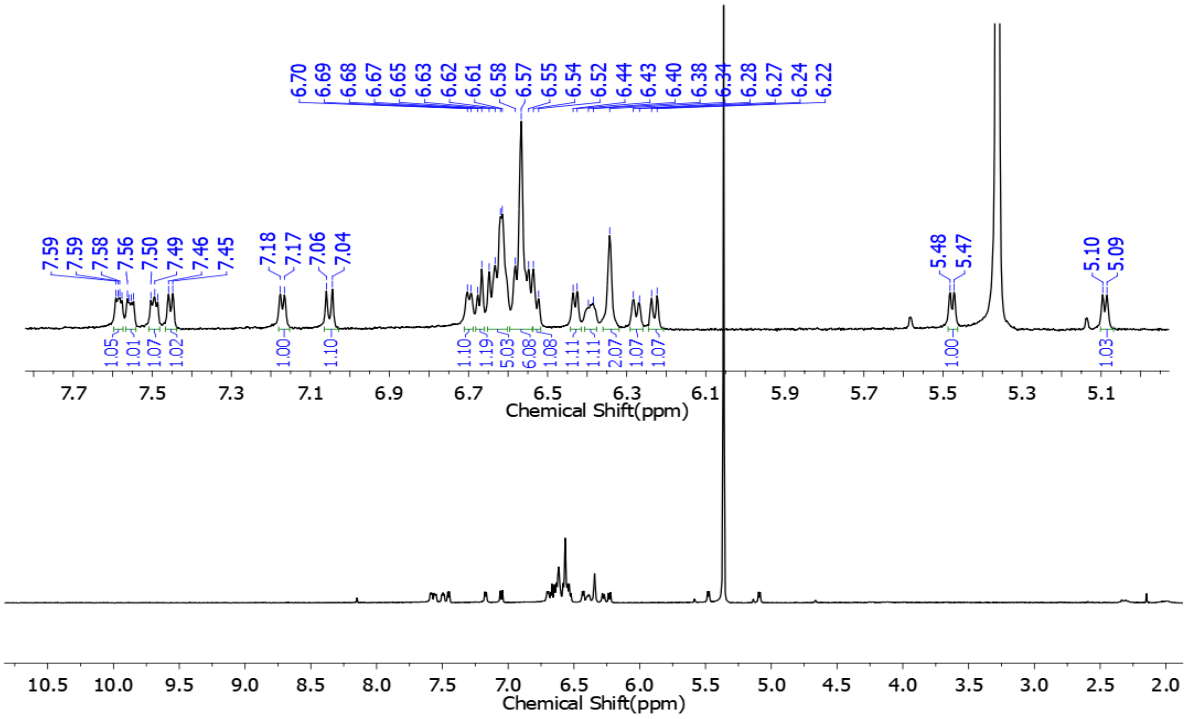

Figure II.44: *^{1}H NMR spectrum of **14** in Dichloromethane-d_2 at 228K.*

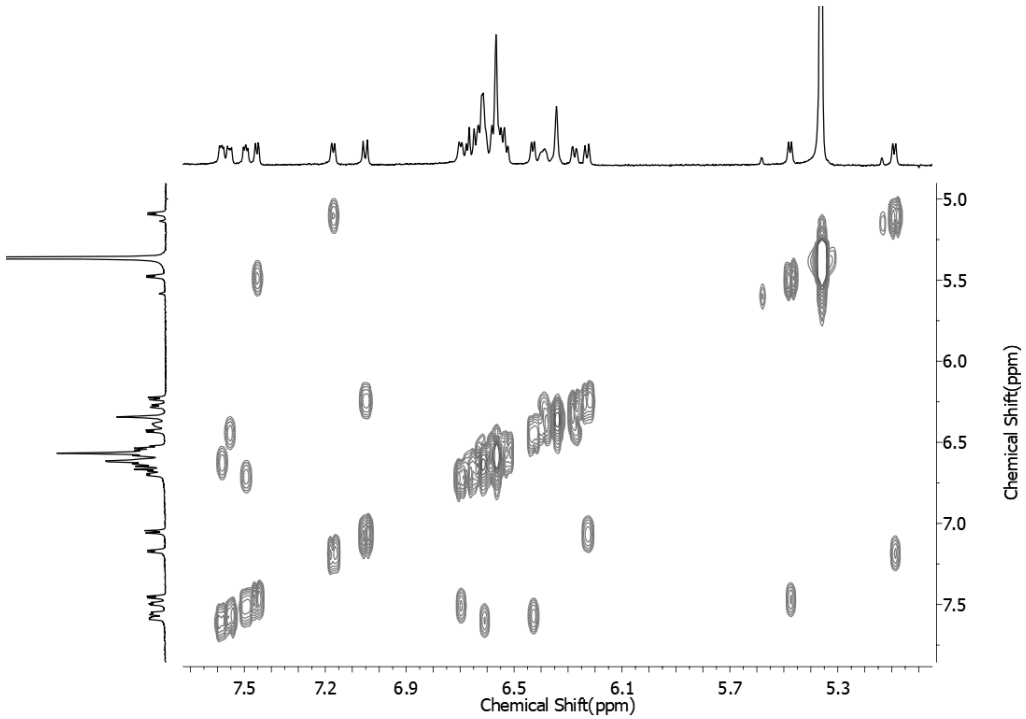

Figure II.45: *^{1}H-^{1}H COSY spectrum of **14** in Dichloromethane-d_2 at 198K.*

II.6.3 Molecular structure of [70]tetradecaphyrin

The absolute structure of **14** was elucidated from single crystal X-ray diffraction analysis. Crystals suitable for diffraction were grown by the vapor diffusion of *n*-hexane into a solution of [70]tetradecaphyrin in chloroform. Molecular structure of [70]tetradecaphyrin revealed a non-planar topology (figure – II.46) in support of the ^{1}H NMR spectrum. While, it did not adopt a twisted or coiled structure, found commonly in many such larger macrocycles,[35] it did display a unique conformation such that two pentaphyrin units were connected by a squeezed hexaphyrin-like bridge. One of the thiophene units in the pentaphyrin pocket appeared to be inverted such that a C-H was in the core of the pentaphyrin unit. From the side view, **14** shows boat shape conformation. This is in sharp contrast to the twisted conformation of pyrrole based tetradecaphyrins[35] which have been reported as a coiled structure.

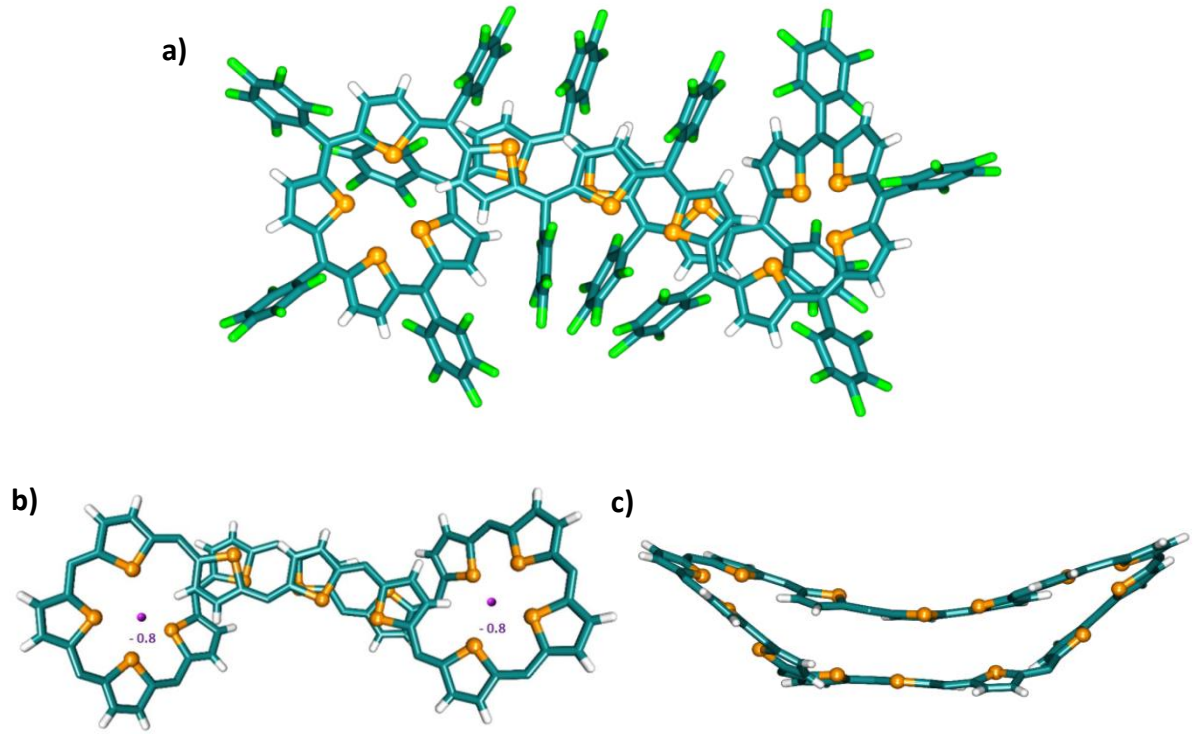

Figure II.46: *Molecular structure of cyclotetradecathiophene **14** as determined from single crystal X-ray diffraction. Pentafluorophenyl rings are omitted of clarity in the (b) (top view) and (c) (side view) rows. The calculated NICS values are mentioned in the center of the macrocycle.*

II.6.4 Electronic and redox studies

Electronic absorption of **14** displayed an intense broad band at 691 nm (196800) (figure – II.47a). Similar to its smaller congeners, 70π tetradecaphyrin also exhibited reversible two-electron ring oxidation. Addition of Meerwien's salt in dichloromethane induced facile

change in colour from dark blue to greenish solution. Further, this change is accompanied with a significant bathochromic shift of 480 nm for the most intense band suggesting the formation of the dicationic species [**14**]$^{2+}$. The oxidized species displayed a broad band at 1175 nm (548300) along with a lower intense band at 1757 nm (94300) (figure – II.47a). In support of this redox process, CV and DPV exhibited three oxidation potentials at +0.69 V, +0.99 V, and +1.24 V and two reduction potentials at -0.67 V and -0.97 V (figure – II.47b). From SEC studies (figure – II.47c) it was observed that a potential of +1.1 V, **14** displayed absorption similar to the oxidized species obtained upon the addition of Meerwein salt. Hence, it could be confirmed that Meewrwein's salt addition oxidized the macrocycle to yield the dicationic species of [**14**]$^{2+}$.

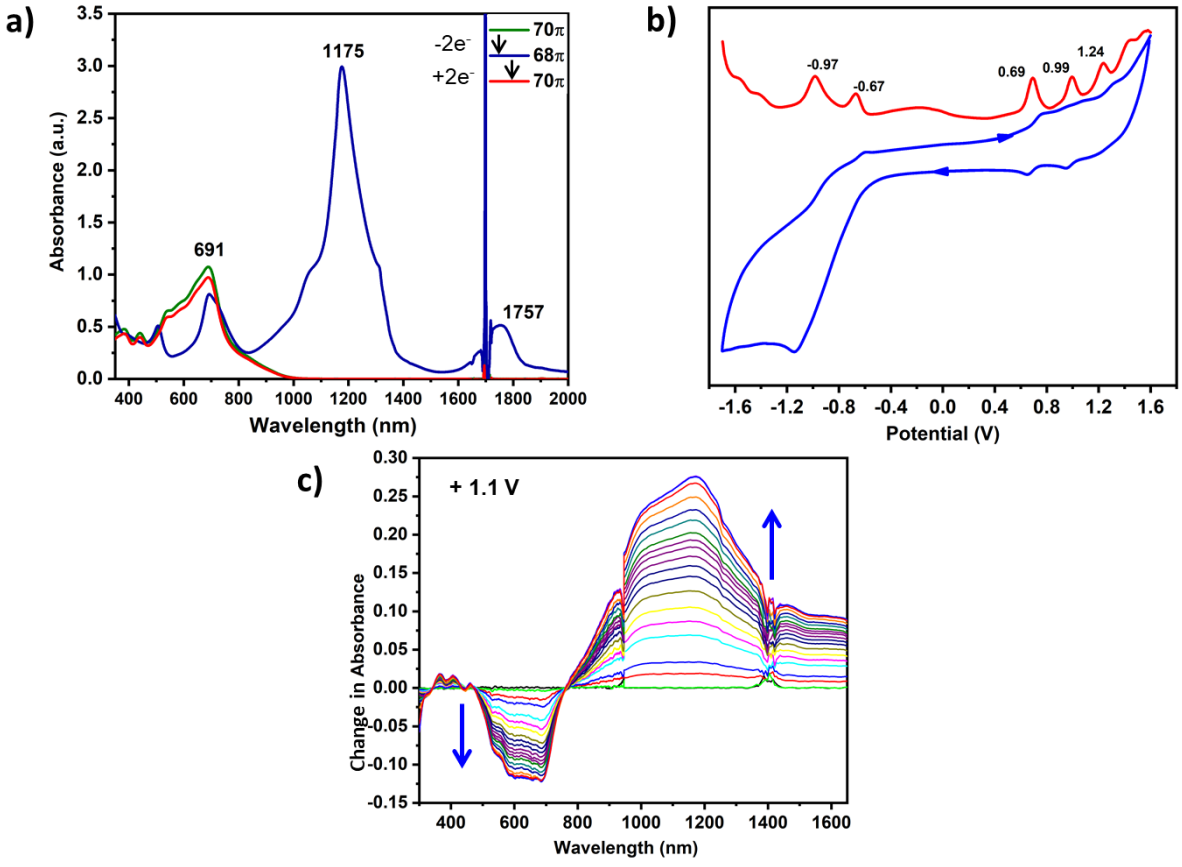

Figure II.47: *(a) and (d) UV/vis/NIR absorption spectrum of 10^{-5}M solution of **14** and its oxidised species [**14**]$^{2+}$ recorded in CH_2Cl_2. (b) Cyclic voltammogram (CV, blue) and differential pulse voltammogram (DPV, red) of **14** in CH_2Cl_2 (with 0.1 M $(Bu)_4NPF_6$ as the supporting electrolyte). (c) Change in absorption spectra of **14** after applying a potential of + 1.1 V.*

II.6.5 Computational studies

[70]tetradecaphyrin, **14**, accounts for 70π electrons and satisfies the (4n+2) π electrons count. However, being a non-planar structure it does not exhibit diatropic ring effect and hence non-aromatic in nature. In support of this understanding, the estimated NICS value on each penatphyrin pocket is δ -0.8 ppm underscoring the non-aromatic nature of the macrocycle as observed from its ^{1}H NMR spectrum. Time dependent TD-DFT calculations (figure – II.44) further supported the experimental data and the estimated HOMO-LUMO energy gap was 1.32 eV.

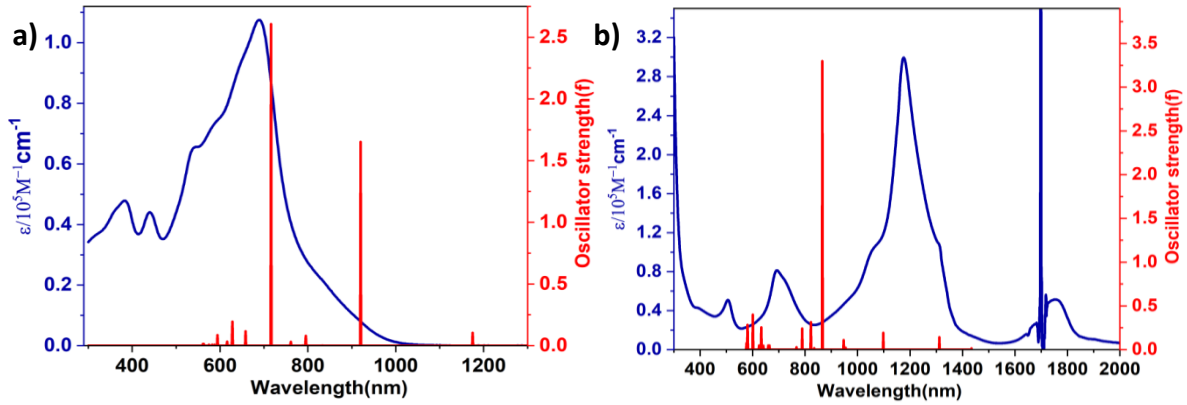

Figure II.44: *Selected TD-DFT (B3LYP/6-31G (d,p)) calculated energies, oscillator strengths and compositions of the major electronic transitions of* ***14*** *and* ***[14]***$^{2+}$.

Till date, [70]tetradecaphyrin, represents the first structure for a *meso* aryl macrocycle with the maximum possible π-electron with a 1:1 ratio of *meso* bridges and fourteen heterocyclic units.

II.7 [80]hexadecaphyrin

[80]hexaphyrin, **16**, is the least yielded macrocycle from this one-pot reaction and its isolation was most challenging from column chromatography. Only repeated size exclusion chromatography in addition to quick analysis by MALDI TOF/TOF spectrometry (figure – II.45) was crucial to identify this macrocycle. However, complete characterisation of the macrocycle was not successful due to very poor yields and tedious purification process.

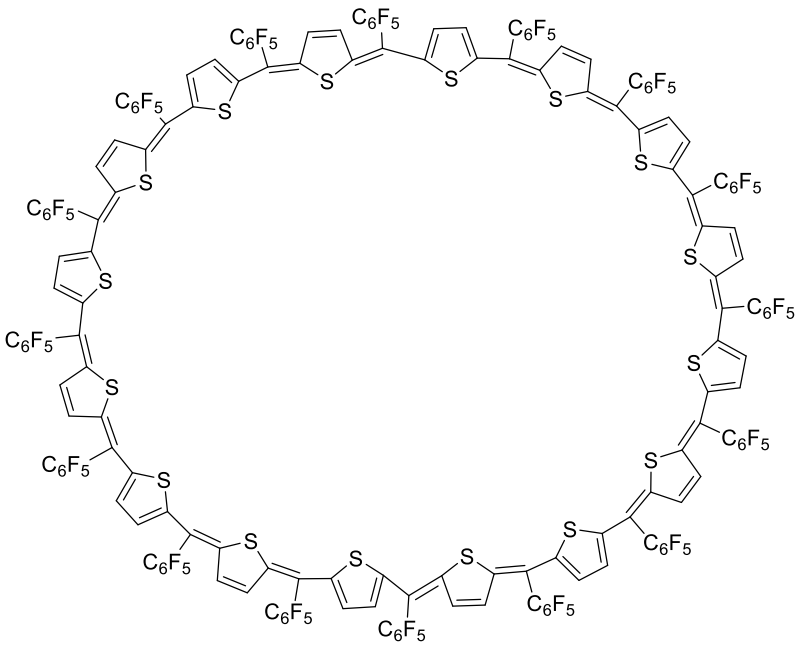

Chemical Formula: $C_{176}H_{32}F_{80}S_{16}$
Exact Mass: 4175.6758

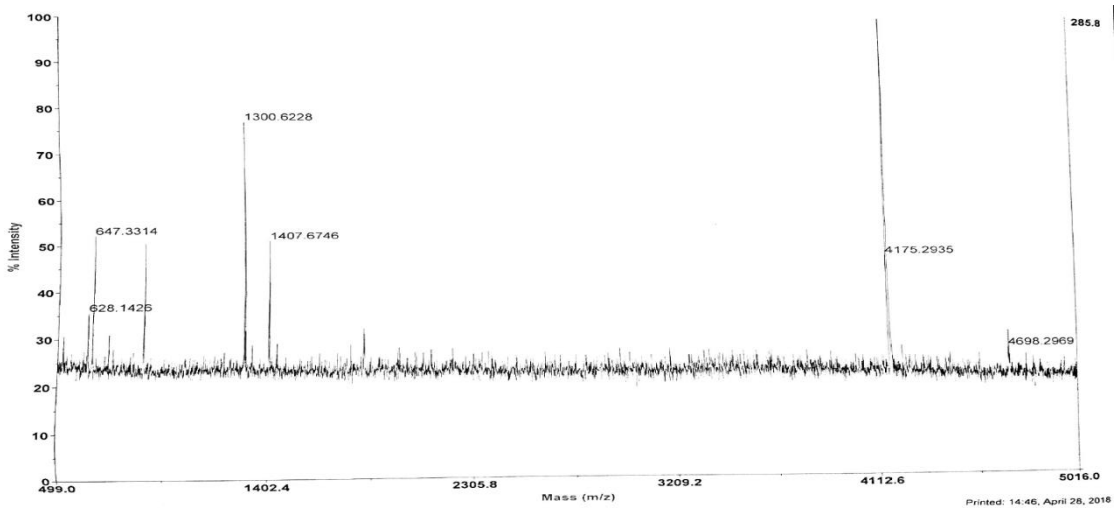

Figure II.45: *MALDI-TOF/TOF mass spectrum of [80]hexadecaphyrin* ***16****.*

II.8 Conclusions

In summary, a one-pot synthesis from commercially available simple starting materials of thiophene and pentafluorobenzaldehyde condensation yields a variety of plausible π-conjugated systems from four membered to sixteen membered macrocycles. These macrocycles exist between 4nπ and (4n+2)π electrons. Unfortunately, (4n+1) and (4n+3) π-electrons radical systems bearing more than five thiophene units were very sensitive at ambient atmosphere to evade comprehensive characterization. 40π octaphyrin, **8**, displays temperature dependent variation from planar to non-planar topology in the solution state, while sustains aplanar conformation in the solid state. Further this 40π macrocycle undergoes mitotic division in the presence of C_{60} fullerene to yield two 20π tetrathia isophlorins. The conformation of 50π decaphyrin in solid state was found to be dependent on the solvent of crystallization even though it displayed non-aromatic characteristics in the solution state. In the solid state, it displayed two distinct topoisomers based on the solvent of crystallisation. Between the two different conformations, one is non-aromatic [6+4] conformation in acetonitrile and another shows planar conformation with two pentaphyrin pockets in benzene solvent system. Moreover, a heterocycle ring inversion has been observed for the first time in a twisted conformation of an expanded porphyrinoid. It represents the first example two-electron oxidation of non-aromatic species in contrast to the typical one-electron oxidation quite prevalent among (4n+2)π systems. To the best of knowledge, 48π dication, $[\mathbf{10}]^{2+}$, is the largest and first ever antiaromatic dication to be ever characterized in the solid state. Its reversible two-electron oxidation has been unambiguously justified by spectro-electrochemical measurements for the first time. In addition to dicationic species, monoradical cation was also identified in the SEC measurement for both octaphyrin and decaphyrin. 60π dodecaphyrin and 70π tetradecaphyrin represents the first example of the largest macrocycles in π-electron count with equal number of meso carbons and heterocyclic units. 80π hexadecaphyrin is the largest macrocycle isolated in this one pot synthesis series, but could not be characterised comprehensively because of poor yield and tedious isolation. From these results, it can be concluded that reversible two-electron ring oxidations seem to be feasible in large isophlorinoid-like macrocycles. While, multiple redox states are very evident from electrochemical measurements, stabilization of these species remains a great challenge and further efforts to achieve them are in progress.

II.9 General Experimental Methods

Column chromatography was performed on silica gel (230-400) in glass columns. ^{1}H-NMR spectra were recorded either on a JEOL 400 MHz or Bruker 400 MHz or Bruker 500 MHz spectrometer. Chemical shifts were reported as the delta scale in ppm relative to $(CH_3)_2CO$ (δ = 2.05 ppm) or CD_2Cl_2 (δ = 5.51 ppm) or $CDCl_3$ (δ = 7.26 ppm) or Tetrahydrofuran-*d*$_8$ (δ = 3.58 and 1.73 ppm). Electronic spectra were recorded on a Shimadzu UV-3600 spectrophotometer and a quartz cuvette of path length 1 cm, over the range of 300-2000nm. High Resolution Mass spectra were obtained using WATERS G2 Synapt Mass Spectrometer. Single-crystal diffraction analysis data were collected at 100K with a BRUKER KAPPA APEX II CCD Duo diffractometer (operated at 1500 W power: 50 kV, 30 mA) using graphite-monochromated Mo Kα radiation (λ = 0.71073 Å). In case of disordered solvent molecules, the contributions to the scattering arising from the disordered solvents in the crystal were removed by use of the utility SQUEEZE [39] in the PLATON software package. More information on crystal structures can also be obtained from the Cambridge Crystallographic Data Centre, CCDC 2105348, 2105350, 2106320, 2105357, 2105359, 2105362, 2190179 and 2190180 for 8(DMSO), 8(DCE), 10(ACN), 10(benzene), 10(DMSO), $[10]^{2+}$, 12 and 14 respectively. Cyclic voltammetry (CV) and Differential pulse voltammetry (DPV) measurements were carried out on a BAS electrochemical system using a conventional three-electrode cell in dry CH_2Cl_2 containing 0.1 M tetrabutylammonium perchlorate (TBAP) as the supporting electrolyte. Measurements were carried out under an Ar atmosphere. A glassy carbon (working electrode), a platinum wire (counter electrode), and saturated Ag/Ag^+ (reference electrode) were used. The final results were calibrated with the ferrocene/ferrocenium couple.

Quantum mechanical calculations were performed with the Gaussian09 program suite using a High Performance Computing Cluster facility of IISER PUNE. All calculations were carried out by Density functional theory (DFT) with Becke's three-parameter hybrid exchange functional and the Lee-Yang-Parr correlation functional (B3LYP) and 6-31G(d,p) basis set for all the atoms were employed in the calculations. The molecular structures obtained from single crystal analysis were used for geometry optimization. To verify the optimized structures frequency calculations were performed where no imaginary frequency was found. To simulate the steady-state absorption spectra, the time-dependent TD-DFT calculations were employed on the optimized structures. Molecular orbital contributions were determined using GaussSum 2.2.Program package. The global ring centres for the NICS (0) values were

designated at the non-weighted mean centres of the macrocycles. The NICS (0) value was obtained with gauge independent atomic orbital (GIAO) method based on the optimized geometries. We calculated the Anisotropy of the current-induced density (ACID) to visualize delocalized π electrons. The AICD plots can directly display the magnitude and direction of the induced ring current when an external magnetic field is applied orthogonal to the macrocycle plane. Current density plots were obtained by employing the continuous set of gauge transformations (CSGT) method to calculate the current densities, and the results were plotted using POVRAY 3.7 for Windows. The molecular orbitals were visualized using Gauss View 4.1.

Materials: Dichloromethane (CH_2Cl_2) was dried by refluxing and distillation over P_2O_5. Thiophene and pentafluorobenzaldehyde were freshly distilled prior to use. Other reagents and solvents were of commercial reagent grade and were used without further purification.

General synthetic procedure for 8, 10, 12, 14 and their dications: An equimolar concentration of thiophene and pentafluorobenzaldehyde were taken in a flame-dried 250mL two neck round bottomed flask and dissolved in 100 ml dry dichloromethane and degassed with N_2 for ten minutes. Then, a catalytic amount of Boron trifluoride diethyl etherate ($BF_3{\cdot}OEt_2$) was added under dark using a syringe. After stirring for an hour, five equivalents of anhydrous $FeCl_3$ were added, opened to air and stirring continued for an additional one hour. Then few drops of triethyl amine were added and the resultant solution was passed through a short basic alumina column. This mixture was concentrated and further purified by silica gel column chromatography using CH_2Cl_2/Hexane as eluent and Size Exclusion Chromatography (SEC) using Toluene or THF. The dications were generated by the addition of TFA to a solution of the macrocycle in dichloromethane. Dicationic salt of hexachloroantimonate was prepared as per earlier report[36]

8: ^{1}H NMR (400 MHz, Acetone-d_6, 295K) δ ppm 7.09 (s, 16H). **UV/Vis/NIR** (CH_2Cl_2): λ_{max} nm (ε) $Lmol^{-1}cm^{-1}$ = 544 (129300). **HR-MS** (ESI-TOF): m/z = 2087.7395 (found, $[M]^+$), 2087.8379 (Calcd. For $C_{88}H_{16}F_{40}S_8$).

Selected Crystal data of 8 (in DMSO): $C_{88}H_{16}Cl_2F_{40}S_8$, ($M_r$ = 2089.49), tetragonal, space group *I-4*, a = 29.181(4), b = 29.181(4), c = 7.7421(11) Å, $\alpha = 90^0$, $\beta = 90^0$, $\gamma = 90^0$; V = 6593(2) $Å^3$, Z = 2, T = 100 K , D_{calcd} = 1.053 gcm^{-3}, R_1 = 0.0554 (I > 2sigma (I)), R_w (all data) = 0.1157, GOF = 0.941;

Selected Crystal data of 8 (in Dichloroethane): $C_{88}H_{16}F_{40}S_8,C_2H_4Cl_2$ (M_r = 2188.44), triclinic, space group *P-1*, *a* = 9.870(2), *b* = 12.440(3), *c* =18.194(4) Å, α = 80.045(5)^0, β = 79.628(5)^0, γ = 77.072(5)^0; *V* = 2121.1(8) Å^3, *Z* = 1, *T* = 100 K , D_{calcd} = 1.713g cm^{-3} , R_1 = 0.0748 (I > 2sigma (I)), R_w (all data) = 0.2209, GOF = 0.993;

[8]$^{2+}$: ^{1}H NMR (400 MHz, Dichloromethane-d_2, 298 K) δ ppm 7.36 (s, 16 H). **UV/vis/NIR** (CH_2Cl_2): λ_{max} nm (ε) Lmol^{-1}cm^{-1} = 782 (312800), 1125 (27800), 1302 (10300). **HR-MS** (ESI-TOF): m/z = 1043.9170 (found, [M]$^{2+}$), 1043.9189 Calcd. For $(C_{88}H_{16}F_{40}S_8)^{2+}$.

10: ^{1}H NMR (400 MHz, Acetone-d_6, 198 K) δ ppm 8.38 (d, *J* = 5.6 Hz, 1H), 7.70 (d, *J* = 4 Hz, 1H), 7.53 – 7.49 (m, 2H), 7.42 – 7.34 (m, 3H), 7.30 – 7.26 (m, 3H), 7.22 – 7.14 (m, 4H), 7.08 (d, *J* = 6 Hz, 1H), 7.00 (d, *J* = 6 Hz, 1H), 6.71 (d, *J* = 4.1 Hz, 1H), 6.62 (d, *J* = 3.9 Hz, 1H), 6.09 (d, *J* = 4 Hz, 1H), 5.92 (d, *J* = 5.6 Hz, 1H). **UV/vis/NIR** (CH_2Cl_2): λ_{max} nm (ε) Lmol^{-1} cm^{-1} = 456 (137500), 650 (84200). **HR-MS** (ESI-TOF): m/z = 2609.4253 (found, [M]$^+$), (2609.7974) (Calcd. For $C_{110}H_{20}F_{50}S_{10}$).

Selected Crystal data of 10 (in Acetonitrile): $C_{112}H_{23}F_{50}S_{10}N$, ($M_r$ = 2611.86), monoclinic, space group *P21/n*, *a* = 22.666 (3), *b* = 31.028(4), *c* = 33.689(4) Å, α = 90^0, β = 109.560 (2)^0, γ = 90^0; *V* = 22326(5) Å^3, *Z* = 8, *T* = 296 K , D_{calcd} = 1.925 gcm^{-3} , R_1 = 0.0975 (I > 2sigma (I)), R_w (all data) = 0.2758, GOF = 1.333;

Selected Crystal data of 10 (in Benzene): $C_{134}H_{44}F_{50}S_{10}$, ($M_r$ = 2924.29), triclinic, space group *P-1*, *a* = 10.7591 (5), *b* = 17.4880(9), *c* = 17.8046(7) Å, α = 63.540(1)^0, β = 83.089(2)^0, γ = 85.480(2)^0; *V* = 2976.1(2) Å^3, *Z* = 1, *T* = 296 K , D_{calcd} = 1.632 gcm^{-3} , R_1 = 0.0698 (I > 2sigma (I)), R_w (all data) = 0.0766, GOF = 1.286;

Selected Crystal data of 10 (in DMSO): $C_{118}H_{44}F_{50}O_4S_{14}$, ($M_r$ = 2924.37), monoclinic, space group *C2/c*, *a* = 32.114 (10), *b* = 17.231(4), *c* = 21.376(6) Å, α = 90, β = 96.380(13)^0, γ = 90; *V* = 11755(6) Å^3, *Z* = 4, *T* = 296 K , D_{calcd} = 1.652 gcm^{-3} , R_1 = 0.1615 (I > 2sigma (I)), R_w (all data) = 0.4782, GOF = 1.704;

[10]$^{2+}$: ^{1}H NMR (400 MHz, Acetone-d_6, 213K) δ ppm 22.16 (s, 1H), 18.96 (s, 1H), 11.78 (d, *J* = 4.7 Hz, 1H), 11.30 (d, *J* = 4.7 Hz, 1H), 9.77 (d, *J* = 5.5 Hz, 1H), 9.30 (d, *J* = 5.5 Hz, 1H), 9.13 (d, *J* = 5.5 Hz, 1H), 8.83 (d, *J* = 4.4 Hz, 1H), 8.65 (d, *J* = 4.7 Hz, 1H), 8.57 (d, *J* = 4.7 Hz, 1H), 8.49 (d, *J* = 15.0 Hz, 2H), 8.40 – 8.33 (m, 1H), 7.95 (d, *J* = 4.4 Hz, 1H), 7.86 (d, *J* = 4.5 Hz, 1H), 7.54 (d, *J* = 5.5 Hz, 1H), 6.94 (d, *J* = 5.1 Hz, 1H), 6.86 (t, *J* = 4.8 Hz, 1H), 6.76 (d, *J* = 5.9 Hz, 1H), 6.71 (d, *J* = 4.8 Hz, 1H). **UV/vis/NIR** (CH_2Cl_2): λ_{max} nm (ε) Lmol^{-1}cm^{-1} =

955 (144300), 1378 (13200), 1624 (5900). **HR-MS** (ESI-TOF): m/z = 1304.9005 (found, $[M]^{2+}$), 1304.8987 (Calcd. For $(C_{110}H_{20}F_{50}S_{10})^{2+}$).

Selected Crystal data of [10]$^{2+}$: $C_{59}H_{18}Cl_{10}F_{25}S_5Sb$ (M_r = 1838.28), triclinic, space group *P-1*, *a* = 13.852(4), *b* = 15.004(5), *c* = 18.787(8) Å, α = 81.290(8)^0, β = 69.677(8)^0, γ = 70.253(8)^0, *V* = 3443.7(19) Å^3, *Z* = 2, *T* = 100 K , D_{calcd} = 1.773 gcm^{-3} , R_1 = 0.0718 (I > 2sigma (I)), R_w (all data) = 0.1575, GOF = 1.038;

12: ^{1}H NMR (400 MHz, Acetone-d_6, 213K) δ 8.34 (d, *J* = 4.7 Hz, 1H), 7.86 (d, J = 6.4 Hz, 1H), 7.69 (d, J = 2.8 Hz, 1H), 7.35 (s, 2H), 7.16 (s, 2H), 7.13 (d, J = 4.0 Hz, 2H), 7.09 (d, J = 4.0 Hz, 4H), 7.04 (d, J = 6.7 Hz, 2H), 7.01 (s, 1H), 6.99 (s, 2H), 6.95 (s, 1H), 6.94 – 6.87 (m, 2H), 6.85 (d, J = 3.0 Hz, 1H), 6.22 (d, J = 3.7 Hz, 1H), 5.61 (d, J = 3.4 Hz, 1H). **^{1}H NMR** (500 MHz, Acetone-d_6, 213K) δ 8.31 (s, 1H), 7.85 (s, 1H), 7.68 (s, 1H), 7.32 (s, 1H), 7.18 – 6.78 (m, 18H), 6.20 (s, 1H), 5.61 (s, 1H). **UV/vis/NIR** (CH_2Cl_2): λ_{max} nm (ε) L mol^{-1} cm^{-1} =404 (132450), 632 (203307). **HR-MS** (ESI-TOF): m/z =3131.7659 (found, $[M]^+$), (3131.7568) (calcd. For $C_{132}H_{24}F_{60}S_{12}$).

Selected Crystal data of 12: $C_{132}H_{24}Cl_2F_{60}S_{12}$, (Mr =3134.23), triclinic, space group *P-1*, *a*=14.407(12), *b*=15.516(13), *c*=18.330(16) Å, α =66.002(13), β =89.870(13), γ =64.743(12); *V* = 3312(5) Å^3, *Z* = 1, *T* = 100(2) K , D_{calcd} = 1.571g cm^{-3} , R_1 = 0.0904 (I>2sigma (I)), *Rw* (all data) = 0.2290, GOF = 0.835;

[12]$^{++}$: UV/vis/NIR (CH_2Cl_2): λ_{max} nm (ε) L mol^{-1} cm^{-1} =1104 (304448), 1590 (50826). **HR-MS** (ESI-TOF): m/2 =1565.8785 (found, $[M]^+$), (1565.8784) calcd. For ($C_{132}H_{24}F_{60}S_{12})^{2+}$.

14: ^{1}H NMR (400 MHz, Dichloromethane-d_2, 228K) ^{1}H NMR (400 MHz) δ 7.53 (ddd, *J* = 11.8, 4.4, 2.2 Hz, 2H), 7.48 – 7.44 (m, 1H), 7.41 (d, *J* = 4.3 Hz, 1H), 7.13 (d, *J* = 4.1 Hz, 1H), 7.01 (d, *J* = 6.1 Hz, 1H), 6.68 – 6.47 (m, 14H), 6.39 (d, *J* = 4.0 Hz, 1H), 6.35 (d, *J* = 5.1 Hz, 1H), 6.30 (s, 2H), 6.24 (d, *J* = 6.2 Hz, 1H), 6.19 (d, *J* = 5.6 Hz, 1H), 5.44 (d, *J* = 4.1 Hz, 1H), 5.05 (d, *J* = 4.3 Hz, 1H). **UV/vis/NIR** (CH_2Cl_2): λ_{max} nm (ε) L mol^{-1} cm^{-1} =691 (196879). **HR-MS** (ESI-TOF): m/z =3653.7163 (found, $[M]^+$), (3654.0291) (calcd. For $C_{154}H_{28}F_{70}S_{14}$+H).

[14]$^{++}$: UV/vis/NIR (CH_2Cl_2): λ_{max} nm (ε) L mol^{-1} cm^{-1} =1175 (548333), 1757 (94319).

Selected Crystal data of 14: $C_{154}H_{28}F_{70}S_{14}$, (Mr =3656.61), monoclinic, space group *P 21/c*, *a*=25.696(13), *b*=29.223(14), *c*=27.012(13) Å, α =90, β =95.871(11), γ =90; *V* = 20177(17) $Å^3$, *Z* = 4, *T* = 150 K , D_{calcd} = 1.204g cm^{-3} , R_1 = 0.1777 (I>2sigma (I)), *Rw* (all data) = 0.4438, GOF = 1.746;

Macrocycle	NICS (0) ppm[a]	HOMA Values[b]	AICD[c]	Huckel Aromaticity
8	**+8.08**	**0.7154**	**Anti Clockwise**	**Antiaromatic**
10 in Acetonitrile	**-1.66 (on 4 membered ring)** **-0.62 (on 6 membered ring)**	**0.5323**	**-**	**Non-aromatic**
10 in Benzene	**-6.75 (on both rings)**	**0.9241**	**Clockwise**	**Aromatic**
$[10]^{2+}$	**+36.21 (on both rings)**	**0.7977**	**Anti Clockwise**	**Antiaromatic**
12	**+1.75 (on both rings)**	**0.4284**	**-**	**Non-antiaromatic**
14	**-0.8 (on both rings)**	**0.3914**	**-**	**Non-aromatic**

Table II.1: Experimental and computational parameters to classify ring current effects on expanded Isophlorins. [a]Determined from quantum chemical calculations.

[b]All calculations were carried out through Density functional theory (DFT) with B3LYP/6-31G(d,p) basis set for all the atoms employed in the calculations. HOMA values calculated using X-ray crystallographic structure. The harmonic oscillator model of aromaticity (HOMA) value calculated along the all-carbon of π-conjugation pathway.

[c]Direction of ring current obtained from ACID plots.

Crystal Parameters	**10 (in Acetonitrile)**	**10 (in Benzene)**	**10 (in DMSO)**	**10 (in Acetonitrile: Benzene)**	**$[10]^{2+}$**
empirical formula	$C_{112}H_{23}F_{50}S_{10}N$	$C_{134}H_{44}F_{50}S_{10}$	$C_{118}H_{44}F_{50}O_4S_{14}$	$C_{132}H_{62}F_{40}O_{10}S_{10}$	$C_{59}H_{18}Cl_{10}F_{25}S_5Sb$
Solvent syst	Acetonitrile	Benzene/heptane	DMSO/hexane	Acetonitrile: Benzene/MeOH	DCE/Hexane
Crystal syst	monoclinic	triclinic	monoclinic	triclinic	triclinic
Space group	*P21/n*	*P-1*	*C2/c*	*P-1*	*P-1*
Mr	2611.86	2924.29	2924.37	2886.0911	1838.28
a	22.666 (3)	10.7591 (5)	32.114 (10)	17.396 (5)	13.852(4)
b	31.028(4)	17.4880(9)	17.231(4)	18.828 (6)	15.004(5)
c	33.689(4)	17.8046(7)	21.376(6)	22.633 (6)	18.787(8)
α	90^0	$63.540(1)^0$	90	75.717(8)	$81.290(8)^0$
β	$109.560\ (2)^0$	$83.089(2)^0$	$96.380(13)^0$	74.228(7)	$69.677(8)^0$
γ	90^0	$85.480(2)^0$	90	64.505(7)	$70.253(8)^0$
V, Å^3	22326(5)	2976.1(2)	11755(6)	6367.05	3443.7(19)
T	296 K	296 K	296 K	150K	100 K
Z	8	1	4	1	2
D_{calcd} g cm^{-3}	1.925	1.632	1.652	1.741	1.773
Theta max	25.000	28.342	28.329	28.216	28.394
GOF	1.333	1.286	1.704	1.244	1.038
R1	0.0975	0.0698	0.1615	0.1154	0.0718
R2w	0.2758	0.0766	0.4782	0.374	0.1575

Table II.2: *Selected crystal data for **10** and **$[10]^{2+}$**.*

Crystal Parameters	**8 (in DMSO)**	**8 (in Dichloroethane)**	**12**	**14**
empirical formula	$C_{88}H_{16}Cl_2F_{40}S_8$	$C_{88}H_{16}F_{40}S_8$,$C_2H_4Cl_2$	$C_{132}H_{24}Cl_2F_{60}S_{12}$	$C_{154}H_{28}F_{70}S_{14}$
Solvent syst	DMSO/hexane	DCE/hexane	$CHCl_3$/hexane	$CHCl_3$/hexane
Crystal syst	tetragonal	triclinic	triclinic	monoclinic
Space group	*I-4*	*P-1*	*P-1*	*P 21/c*
Mr	2089.49	2188.44	3134.23	3656.61
a	29.181(4)	9.870(2)	14.407(12)	25.696(13)
b	29.181(4)	12.440(3)	15.516(13)	29.223(14)
c	7.7421(11)	18.194(4)	18.330(16)	27.012(13)
α	90^0	$80.045(5)^0$	$66.002(13)^0$	90^0
β	90^0	$79.628(5)^0$	$89.870(13)^0$	$95.871(11)^0$
γ	90^0	$77.072(5)^0$	$64.743(12)^0$	90^0
V, Å^3	6593(2)	2121.1(8)	3312(5)	20177(17)
T	100 K	100 K	100(2) K	150 K
Z	2	1	1	4
D_{calcd} g cm^{-3}	1.053	1.713	1.571	1.204
Theta max	28.285	25.500	25.499	23.275
GOF	0.941	0.993	0.835	1.746
R1	0.0554	0.0748	0.0904	0.1777
R2w	0.1157	0.2209	0.2290	0.4438

Table II.3: *Selected crystal data for **8**, **12** and **14**.*

II.10 References:

1. Allen, A. D.; Tidwell, T. T., Antiaromaticity in Open-Shell Cyclopropenyl to Cycloheptatrienyl Cations, Anions, Free Radicals, and Radical Ions. *Chem. Rev.* **2001,** *101* (5), 1333-1348.
2. Breslow, R., Antiaromaticity. *Acc. Chem. Res.* **1973,** *6* (12), 393-398.
3. Aromatic Character. *Chemical & Engineering News Archive* **1965,** *43* (26), 90-100.
4. Sondheimer, F., Annulenes. *Acc. Chem. Res.* **1972,** *5* (3), 81-91.
5. Reddy, B. K.; Basavarajappa, A.; Ambhore, M. D.; Anand, V. G., Isophlorinoids: The Antiaromatic Congeners of Porphyrinoids. *Chem. Rev.* **2017,** *117* (4), 3420-3443.
6. Vogel, E.; Haas, W.; Knipp, B.; Lex, J.; Schmickler, H., Tetraoxaporphyrin Dication. *Angew. Chem., Int. Ed.* **1988,** *27* (3), 406-409.
7. Vogel, E.; Rohrig, P.; Sicken, M.; Knipp, B.; Herrmann, A.; Pohl, M.; Schmickler, H.; Lex, J., The Thiophene Analog of Porphyrin - Tetrathiaporphyrin Dication. *Angew. Chem., Int. Ed.* **1989,** *28* (12), 1651-1655.
8. Gopalakrishna, T. Y.; Anand, V. G., Reversible Redox Reaction Between Antiaromatic and Aromatic States of 32π-Expanded Isophlorins. *Angew. Chem., Int. Ed.* **2014,** *53* (26), 6678-6682.
9. Panchal, S. P.; Gadekar, S. C.; Anand, V. G., Controlled Core-Modification of a Porphyrin into an Antiaromatic Isophlorin. *Angew. Chem., Int. Ed.* **2016**, n/a-n/a.
10. G. P. M. S. Neves, M.; M. Martins, R.; C. Tomé, A.; J. D. Silvestre, A.; M. S. Silva, A.; Félix, V.; A. S. Cavaleiro, J.; G. B. Drew, M., meso-Substituted expanded porphyrins: new and stable hexaphyrins. *Chem. Comm.* **1999,** (4), 385-386.
11. Ishida, M.; Kim, S.-J.; Preihs, C.; Ohkubo, K.; Lim, J. M.; Lee, B. S.; Park, J. S.; Lynch, V. M.; Roznyatovskiy, V. V.; Sarma, T.; Panda, P. K.; Lee, C.-H.; Fukuzumi, S.; Kim, D.; Sessler, J. L., Protonation-coupled redox reactions in planar antiaromatic meso-pentafluorophenyl-substituted o-phenylene-bridged annulated rosarins. *Nat. Chem.* **2013,** *5* (1), 15-20.
12. Gao, H.; Wu, F.; Zhao, Y.; Zhi, X.; Sun, Y.; Shen, Z., Highly Stable Neutral Corrole Radical: Amphoteric Aromatic–Antiaromatic Switching and Efficient Photothermal Conversion. *J. Am. Chem. Soc.* **2022,** *144* (8), 3458-3467.
13. Tanaka, T.; Osuka, A., Chemistry of meso-Aryl-Substituted Expanded Porphyrins: Aromaticity and Molecular Twist. *Chem. Rev.* **2017,** *117* (4), 2584-2640.
14. Vogel, E.; Bröring, M.; Fink, J.; Rosen, D.; Schmickler, H.; Lex, J.; Chan, K. W. K.; Wu, Y.-D.; Plattner, D. A.; Nendel, M.; Houk, K. N., From Porphyrin Isomers to Octapyrrolic"Figure Eight" Macrocycles. *Angew. Chem., Int. Ed.* **1995,** *34* (22), 2511-2514.
15. Sessler, J. L.; Weghorn, S. J.; Lynch, V.; Johnson, M. R., Turcasarin, the Largest Expanded Porphyrin to Date. *Angew. Chem., Int. Ed.* **1994,** *33* (14), 1509-1512.

16. Shin, J.-Y.; Furuta, H.; Yoza, K.; Igarashi, S.; Osuka, A., meso-Aryl-Substituted Expanded Porphyrins. *J. Am. Chem. Soc.* **2001,** *123* (29), 7190-7191.

17. Shivran, N.; Gadekar, S. C.; Anand, V. G., "To Twist or Not to Twist": Figure-of-Eight and Planar Structures of Octaphyrins. *Asian Journal of Organic Chemistry* **2017,** *12* (1), 6-20.

18. Lim, J. M.; Shin, J.-Y.; Tanaka, Y.; Saito, S.; Osuka, A.; Kim, D., Protonated [4n]π and [4n+2]π Octaphyrins Choose Their Möbius/Hückel Aromatic Topology. *J. Am. Chem. Soc.* **2010,** *132* (9), 3105-3114.

19. Anguera, G.; Cha, W.-Y.; Moore, M. D.; Lee, J.; Guo, S.; Lynch, V. M.; Kim, D.; Sessler, J. L., Hexadecaphyrin-(1.0.0.0.1.1.0.1.1.0.0.0.1.1.0.1): A Dual Site Ligand That Supports Thermal Conformational Changes. *J. Am. Chem. Soc.* **2018,** *140* (11), 4028-4034.

20. Reddy, J. S.; Mandal, S.; Anand, V. G., Cyclic Oligofurans: One-Pot Synthesis of 30π and 40π Expanded Porphyrinoids. *Org. Lett.* **2006,** *8* (24), 5541-5543.

21. Gopalakrishna, T. Y.; Reddy, J. S.; Anand, V. G., An Amphoteric Switch to Aromatic and Antiaromatic States of a Neutral Air-Stable 25π Radical. *Angew. Chem., Int. Ed.* **2014,** *53* (41), 10984-10987.

22. Kon-no, M.; Mack, J.; Kobayashi, N.; Suenaga, M.; Yoza, K.; Shinmyozu, T., Synthesis, Optical Properties, and Electronic Structures of Fully Core-Modified Porphyrin Dications and Isophlorins. *Chem. Eur. J.* **2012,** *18* (42), 13361-13371.

23. Reddy, J. S.; Anand, V. G., Aromatic Expanded Isophlorins: Stable 30π Annulene Analogues with Diverse Structural Features. *J. Am. Chem. Soc.* **2009,** *131* (42), 15433-15439.

24. Tanaka, Y.; Hoshino, W.; Shimizu, S.; Youfu, K.; Aratani, N.; Maruyama, N.; Fujita, S.; Osuka, A., Thermal Splitting of Bis-Cu(II) Octaphyrin(1.1.1.1.1.1.1.1) into Two Cu(II) Porphyrins. *J. Am. Chem. Soc.* **2004,** *126* (10), 3046-3047.

25. Schleyer, P. v. R.; Maerker, C.; Dransfeld, A.; Jiao, H.; van Eikema Hommes, N. J. R., Nucleus-Independent Chemical Shifts: A Simple and Efficient Aromaticity Probe. *J. Am. Chem. Soc.* **1996,** *118* (26), 6317-6318.

26. Chen, Z.; Wannere, C. S.; Corminboeuf, C.; Puchta, R.; Schleyer, P. v. R., Nucleus-Independent Chemical Shifts (NICS) as an Aromaticity Criterion. *Chem. Rev.* **2005,** *105* (10), 3842-3888.

27. Geuenich, D.; Hess, K.; Köhler, F.; Herges, R., Anisotropy of the Induced Current Density (ACID), a General Method To Quantify and Visualize Electronic Delocalization. *Chem. Rev.* **2005,** *105* (10), 3758-3772.

28. Krygowski, T. M.; Cyrański, M. K., Structural Aspects of Aromaticity. *Chem. Rev.* **2001,** *101* (5), 1385-1420.

29. Threlfall, T. L., Analysis of organic polymorphs. A review. *Analyst* **1995,** *120* (10), 2435-2460.

30. Nangia, A.; R. Desiraju, G., Pseudopolymorphism: occurrences of hydrogen bonding organic solvents in molecular crystals. *Chem. Comm.* **1999,** (7), 605-606.

31. Bröring, M.; Köhler, S.; Kleeberg, C., Norcorrole: Observation of the Smallest Porphyrin Variant with a N4 Core. *Angew. Chem., Int. Ed.* **2008,** *47* (30), 5658-5660.

32. Ito, T.; Hayashi, Y.; Shimizu, S.; Shin, J. Y.; Kobayashi, N.; Shinokubo, H., Gram-Scale Synthesis of Nickel(II) Norcorrole: The Smallest Antiaromatic Porphyrinoid. *Angew. Chem., Int. Ed.* **2012,** *51* (34), 8542-8545.

33. Shimizu, S.; Aratani, N.; Osuka, A., meso-Trifluoromethyl-Substituted Expanded Porphyrins. *Chem. Eur. J.* **2006,** *12* (18), 4909-4918.

34. Soya, T.; Kim, W.; Kim, D.; Osuka, A., Stable [48]-, [50]-, and [52]Dodecaphyrins(1.1.0.1.1.0.1.1.0.1.1.0): The Largest Huckel Aromatic Molecules. *Chem. Eur. J.* **2015,** *21* (23), 8341-8346.

35. Yoneda, T.; Soya, T.; Neya, S.; Osuka, A., [62]Tetradecaphyrin and Its Mono- and Bis-ZnII Complexes. *Chem. Eur. J.* **2016,** *22* (41), 14518-14522.

36. Rathore, R.; Kumar, A. S.; Lindeman, S. V.; Kochi, J. K., Preparation and Structures of Crystalline Aromatic Cation-Radical Salts. Triethyloxonium Hexachloroantimonate as a Novel (One-Electron) Oxidant. *J. Org. Chem.* **1998,** *63* (17), 5847-5856.

37. P. D. W. Boyd, M. C. Hodgson, C. E. F. Rickard, A. G. Oliver, L. Chaker, P. J. Brothers, R. D. Bolskar, F. S. Tham, C. A. Reed, Selective Supramolecular Porphyrin/Fullerene Interactions, *J. Am. Chem. Soc.* **1999**, *121*, 10487.

Chapter III

Synthesis and Characterisation of 24π and 26π Pentathia Sapphyrin and its higher analogues

III.1 Introduction

Porphyrin is 18π aromatic aza annulene and its simplest possible expanded porphyrin is 22π aromatic pentapyrrolic (1.1.1.1.0) compound called as Sapphyrin. It was identified serendipitously by R B Woodward and co-workers in 1960 during attempts to synthesize Vitamin B_{12}, but it was reported much later in 1983.[1] Woodward named the pentapyrrolic system as sapphyrin because of its dark blue coloured crystals. Sapphyrin has five pyrrolic units with four bridged carbons and two adjacent pyrroles connected directly through alpha carbon of the heterocyclic units. The macrocycle displays an intense Soret-like band at 450 nm along with Q-type transitions in the region 620 - 690 nm.

Later, Sessler and co-workers determined the molecular structure of 22π β-alkyl sapphyrin **III.3**. This macrocycle synthesised through [3+2] MacDonald type condensation (scheme - III.1) between bipyrrole dialdehyde **III.1** and dicarboxyl substituted tripyrrane **III.2** to yield the C_2-symmetric sapphyrin **III.3**. ^{1}H NMR spectrum of deprotonated sapphyrin dichloride salt displayed resonance for meso protons at δ 11.66 and 11.70 ppm and internal –NH of pyrrole molecules displayed at -4.31, -4.64 and -4.97 ppm with 2:1:2 ratios. These values confirmed the aromatic nature of the macrocycle because of strong diatropic ring current effect. Molecular structure of dicationic sapphyrin revealed a planar conformation with all nitrogens of pyrrole facing at the centre of the macrocycle.[2]

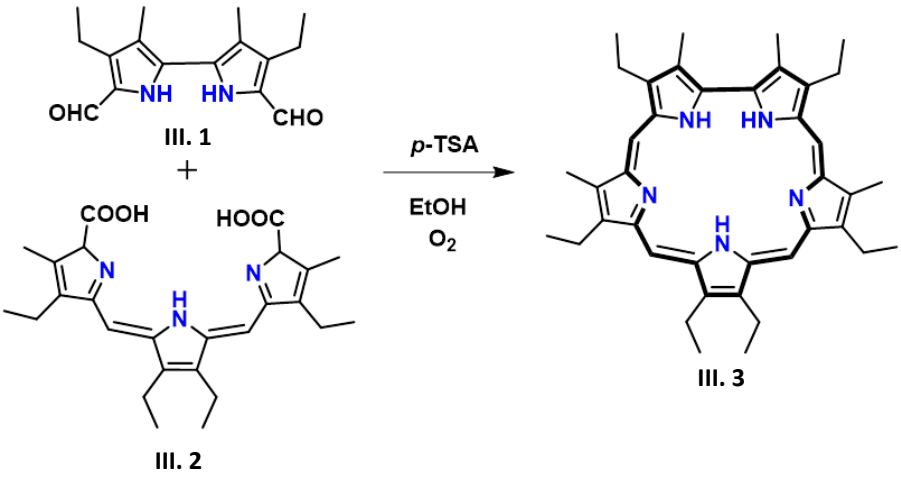

Scheme III.1: *Synthesis of β-alkyl Sapphyrin through [3+2] MacDonald type condensation.*

The first example of a meso-aryl substituted sapphyrin, **III.4a**, was reported by Latos-Grazynski and co-workers. Pyrrole and benzaldehyde were condensed in the presence of acid $BF_3.OEt_2$ followed by chloranil oxidation to yield the azasapphyrin, **III.4a**, in 1% yields

(scheme - III.2). [3] In its ^{1}H NMR spectrum the macrocycle showed one up field signal at δ -1.50 ppm corresponding to β-CH of pyrrole rings and one –NH resonated downfield at δ 12.24 ppm confirming ring inversion of a pyrrole unit. Protonation of the macrocycle, **III.4b**, induced flipping of the inverted pyrrole ring to orient all nitrogens towards the core of the macrocycle. Deprotonation of the macrocycle reverted back the freebase structure. Later, the yields of core-modified sapphyrins were improved by Chandrashekar and co-workers. In a generic process, dipyrromethane was treated with 1 equivalent of TFA followed by p-chloranil as an oxidant to obtain aza meso-aryl sapphyrin, **III.4a**, in 3-11% yields.[3]

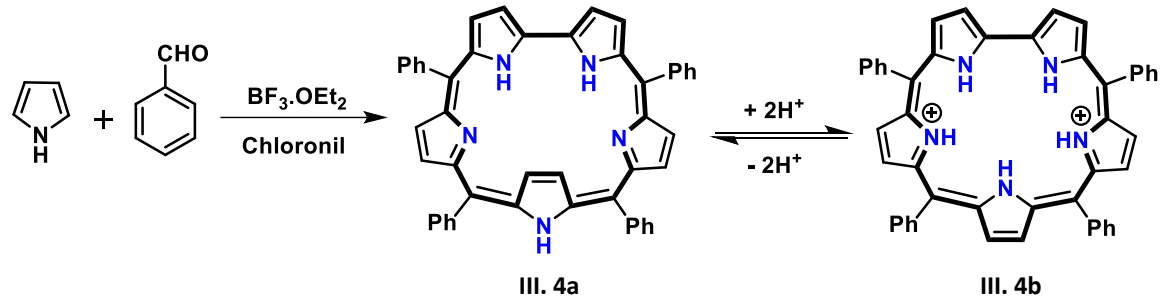

Scheme III.2: *One-pot synthesis of meso-aryl Sapphyrin.*

Core-modification of sapphyrin was achieved by replacing one or more pyrrole units by furan or thiophene or selenophene or tellurophene or N-methyl pyrrole. Core-modification alters the cavity size, electro-chemical properties, conformation and also redox chemistry of the macrocycle.[4] The first core-modified sapphyrin was reported by Johnson and co-workers. They synthesised the dioxasapphyrin, **III.5**, through a [3+2] MacDonald type condensation of tripyrromethane diacid and diformyl bifuran followed by an oxidation.[5] Later, Sessler and co-workers reported the monothia and monoselenasapphyrin, **III.6a-6b**, and further synthesised the mono, di and tri-oxasapphyrins.[6,7] Later, Chandrashekhar and co-workers synthesised a series of core- modified sapphyrins, **III.7a-7c** and **III.8a-8e**, by condensing either bithiophene diol or biselenophene diol with modified tripyrromethanes in the presence of TFA followed by chloranil as an oxidant to obtain the macrocycles up to 16-63% yields.[8] All core-modified sapphyrins with pyrrole units were stabilized as 22π aromatic macrocycles owing to the pyrrole's ability towards amine/imine interconversion. Due to the aromatic nature of sapphyrin, it doesn't undergo any redox reactions either by Proton Coupled Electron Transfer (PCET) or Electron Transfer (ET) reactions. But redox reaction can be possible only by complete core-modification of a sapphyrin by replacing all the pyrrole by thiophene or furan or selenophene or tellurophene or N-methyl pyrrole heterocyclic units. This leads to a drastic conversion from aromatic to antiaromatic state. It is well known that, antiaromatic

macrocycles undergo facile two-electron ring oxidation to yield stable aromatic dicationic species. [14]

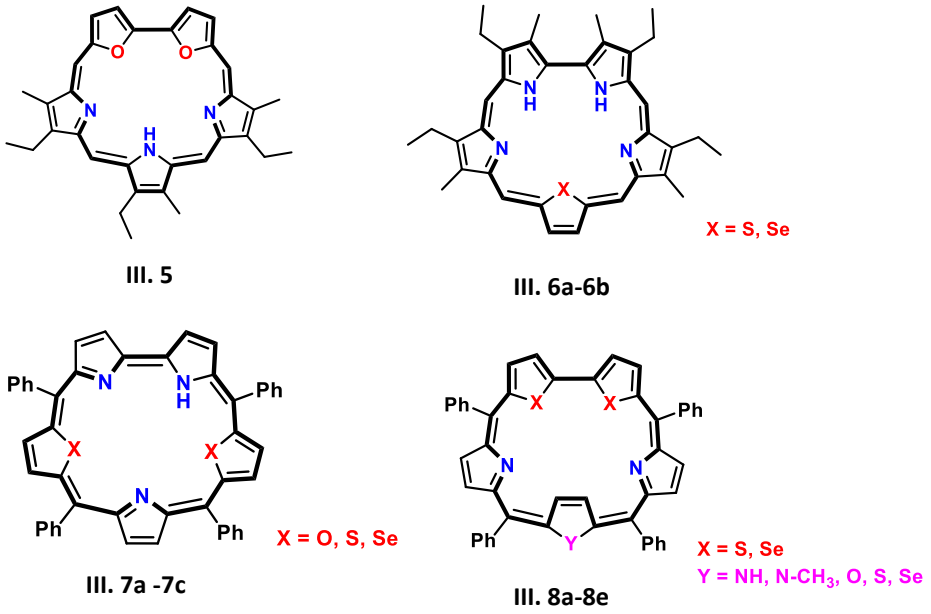

Figure III.1: *Different core-modified 22π aromatic Sapphyrin.*

III.2 Synthesis of 24π and 26π Sapphyrins

Since the serendipitous discovery of 22π sapphyrin by R B Woodward, the synthesis of sapphyrin and core modified sapphyrins has been achieved by the different research groups. Most of the sapphyrins are aromatic in nature and hence they do not undergo redox reactions, either by PCET or ET reactions. The motivation to synthesize a completely core-modified sapphyrin macrocycle was to understand and explore the redox chemistry of such antiaromatic macrocycles. It is expected that completely core-modified sapphyrins can undergo two-electron ring oxidation through ET reactions and also study the switching between aromatic and antiaromatic character of the macrocycle. A strategy to synthesis the 24π and 26π sapphyrin macrocycles stems from isoelectronic species obtained from redox states of a neutral 25π radical. Synthesis and characterisation of an air and water stable, neutral 25π open-shell cyclopentathiophene macrocyclic radical, **III.9**, exemplified one-electron reversible redox to yield antiaromatic 24π cation, **III.9b**, and aromatic 26π anion, **III.9a** (scheme III.3). Both the macrocycles as characterised by ^{1}H NMR spectroscopy, strongly support the paratropic ring current for 24π cationic system and diatropic ring current for the 26π anionic system. Further, the structure of macrocyclic ions were determined from

single-crystal X-ray diffraction studies revealed a planar conformation of the neutral radical, antiaromatic cation and aromatic anion.[9]

Ring contracted 24π sapphyrin macrocycle, **III.10**, and ring expanded sapphyrin, **III.11**, are expected to be isoelectronic with antiaromatic 24π cation and aromatic 26π anion respectively (Scheme - III.3). With this initiative, the synthesis of the first core-modified antiaromatic 24π sapphyrin, aromatic 26π sapphyrin and their higher analogues was explored to evaluate the aromatic and redox properties in comparison to the parent 22π sapphyrin.

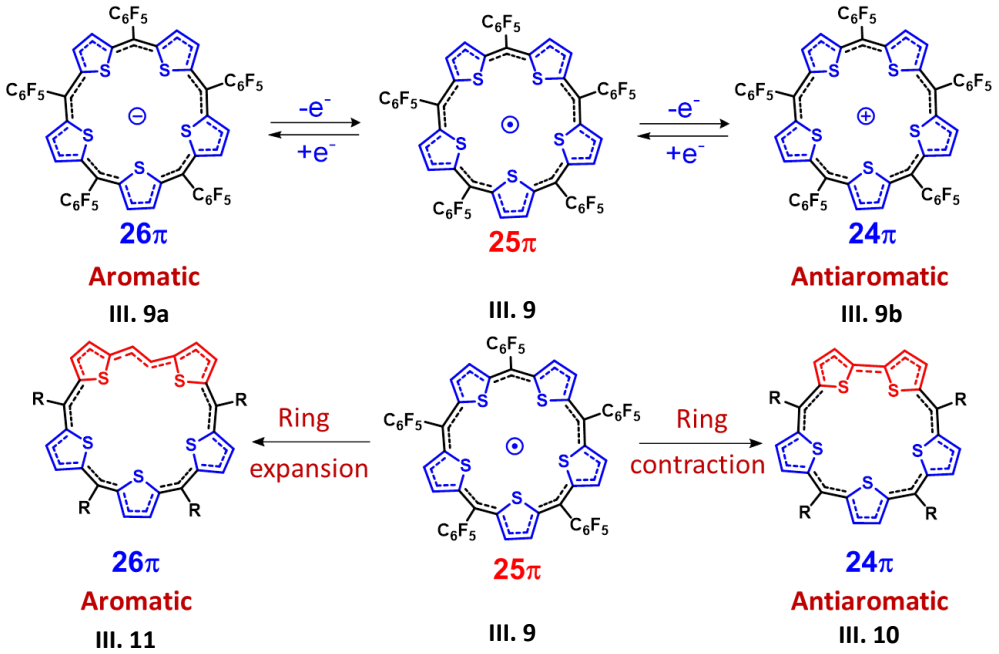

Scheme III.3: *Synthetic strategy for the complete core-modified 24π and 26π Sapphyrin.*

III.3 Synthesis of 24π Sapphyrin and higher analogues

The synthesis of antiaromatic 24π sapphyrin and its higher analogues was attempted through a [3+2] type condensation (Scheme - III.4). To an equimolar concentration of bithiophene, **III.12**, and tripyrromethane diol, **III.13**, in dichloromrthane, was added a catalytic amount of $BF_3.OEt_2$ and stirred in dark for two hours under inert conditions. It was followed by the addition of 2.5 equivalents of DDQ as the oxidising agent. Stirring was continued for another two hours in open atmosphere and the reaction mixture passed through short bed of basic alumina to yield three products as analysed by mass spectrometry. They were identified as 24π sapphyrin, **III.10**, 48π decaphyrin, **III.14**, and the largest one as 72π pentadecaphyrin, **III.15**. Progress of product formation from the reaction was monitored by thin layer chromatography (TLC) and also by the MALDI TOF/TOF spectrometry. Isolation/separation of each band was achieved through repeated basic alumina column chromatography and

further by size exclusion chromatography. These macrocycles were found to be unstable on silica-gel column as observed by the slow disappearance of colour, suggesting the degradation of macrocycles.

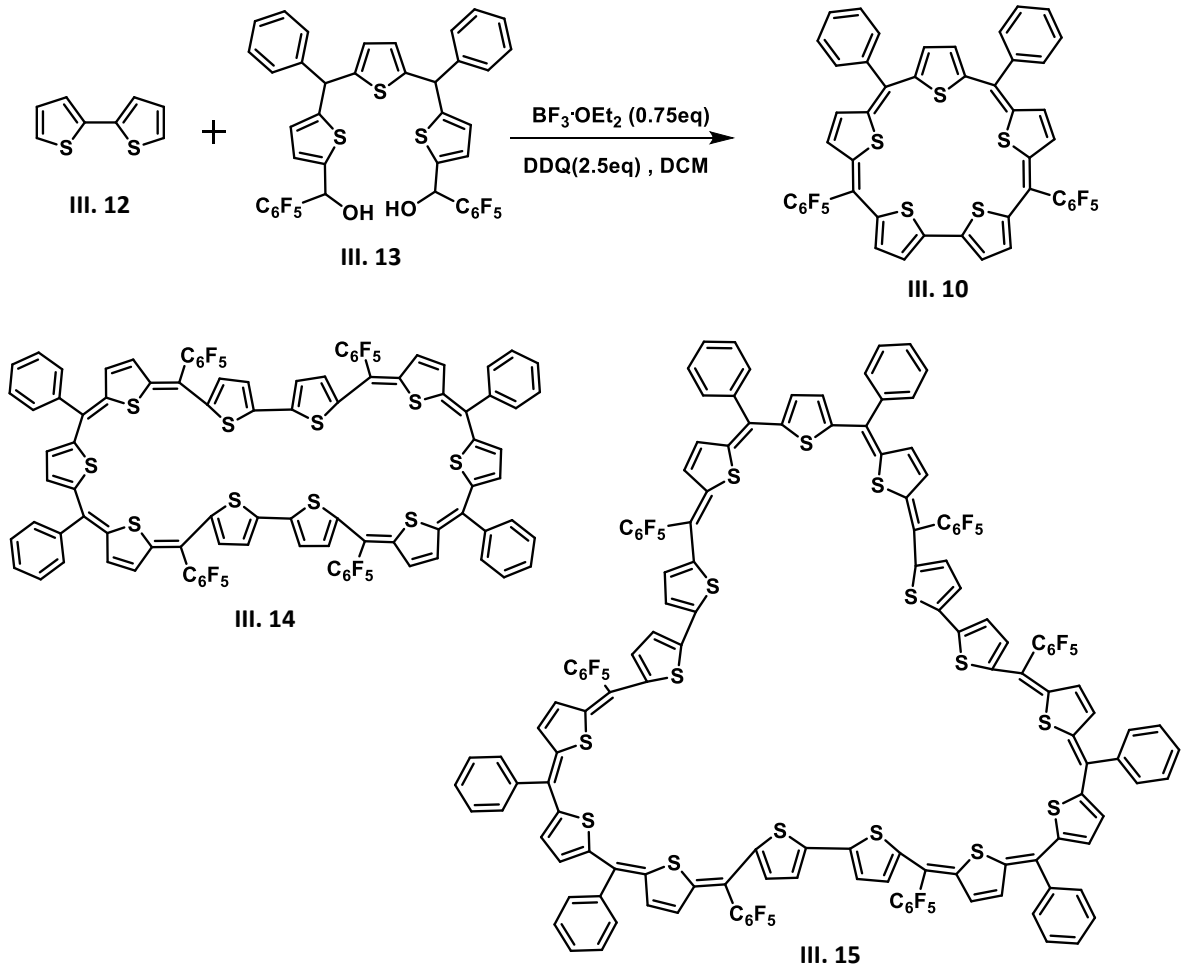

Scheme III.4: *Synthesis of core-modified 24π Sapphyrin and higher analogues.*

III.4.1 Isolation and Characterisation of [24]Sapphyrin

[24] Sapphyrin (1.1.1.1.0), **III.10**, is the first example with highest number of π-electrons along the conjugated path and the first neutral antiaromatic macrocycle in the sapphyrin family. It bears a close resemblance to antiaromatic isophlorin. This macrocycle was identified as a greenish yellow coloured band and the first band in this series to be isolated by column chromatography in 16% yields. Further, it was confirmed by High Resolution Mass Spectrometry (HR-MS) in which it displayed an *m*/*z* value of 946.0003 corresponding to $C_{48}H_{20}F_{10}S_5$ (946.0009) (figure – III.2).

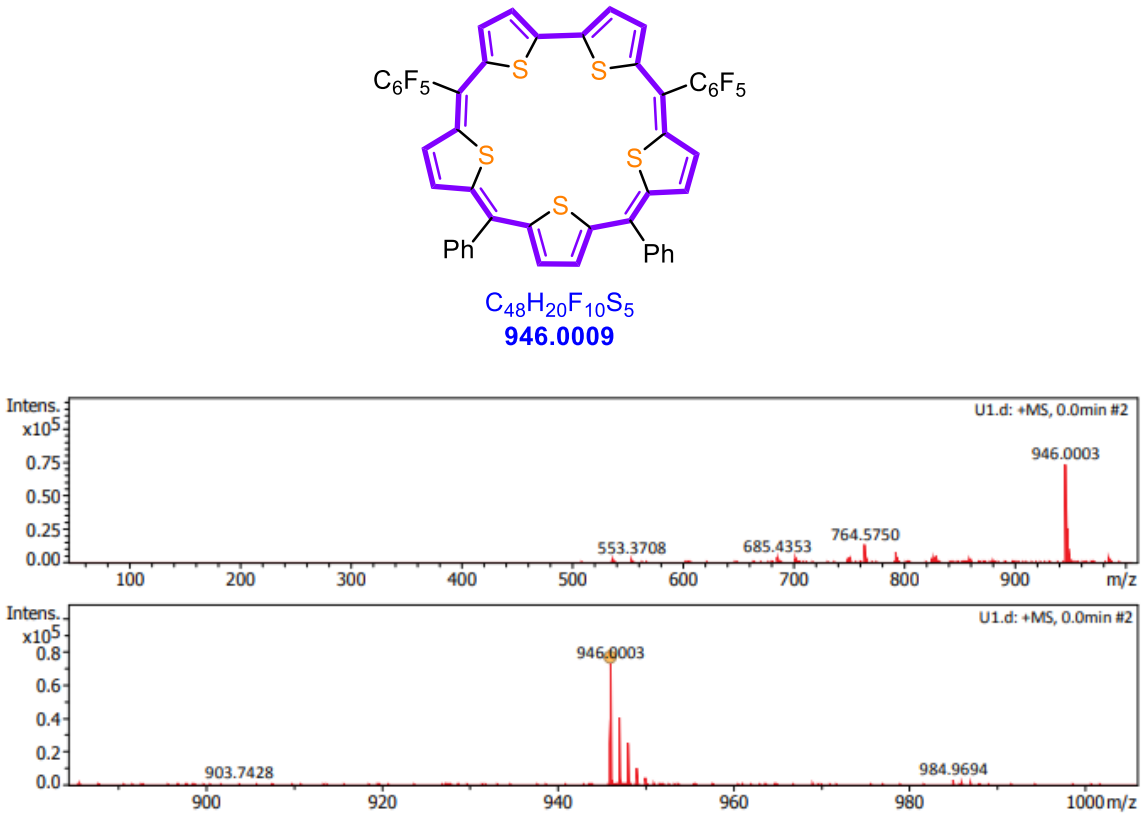

Figure III.2: *HR-ESI-TOF mass spectrum of* ***III.10***.

III.4.2 ^{1}H NMR study of [24]Sapphyrin

[24]Sapphyrin is pentathiophene system with four bridged carbons and two thiophenes are directly connected through α-carbon of the thiophene. This macrocycle accounts for 24π electrons in the global conjugation and satisfies Huckel's antiaromatic 4nπ electronic system. In its ^{1}H NMR spectrum, it displayed seven signals resonances in the region between δ 4.0 to 7.5 ppm (figure – III.3) in support of the expected C_2 axis of symmetry for the macrocycle. All β-protons of the thiophene resonate upfield, confirming the paratropic ring current antiaromatic nature, for (4n)π electron species. All the thiophene protons were found to resonate in the region between δ 4 ppm to 5.2 ppm confirming that all β-protons of the thiophene are oriented towards the periphery and sulphur of thiophenes are facing at the centre of the macrocycle. Hence, there is no ring flipping of any thiophene ring in the macrocycle. ^{1}H-^{1}H COSY spectrum (figure – III.4) shows the correlation for phenyl protons that resonate between δ 6.5 to 7.2 ppm. Two sets of correlations for β-protons of the thiophene; *b* is correlating with *c* and *d* correlating with *e* is attributed to the four thiophene rings, while a singlet resonating at δ 4.38 ppm is assigned to the central thiophene along the C_2 axis of a planar macrocycle. From these NMR data it can be expected that macrocycle adopts a planar conformation in the solution state.

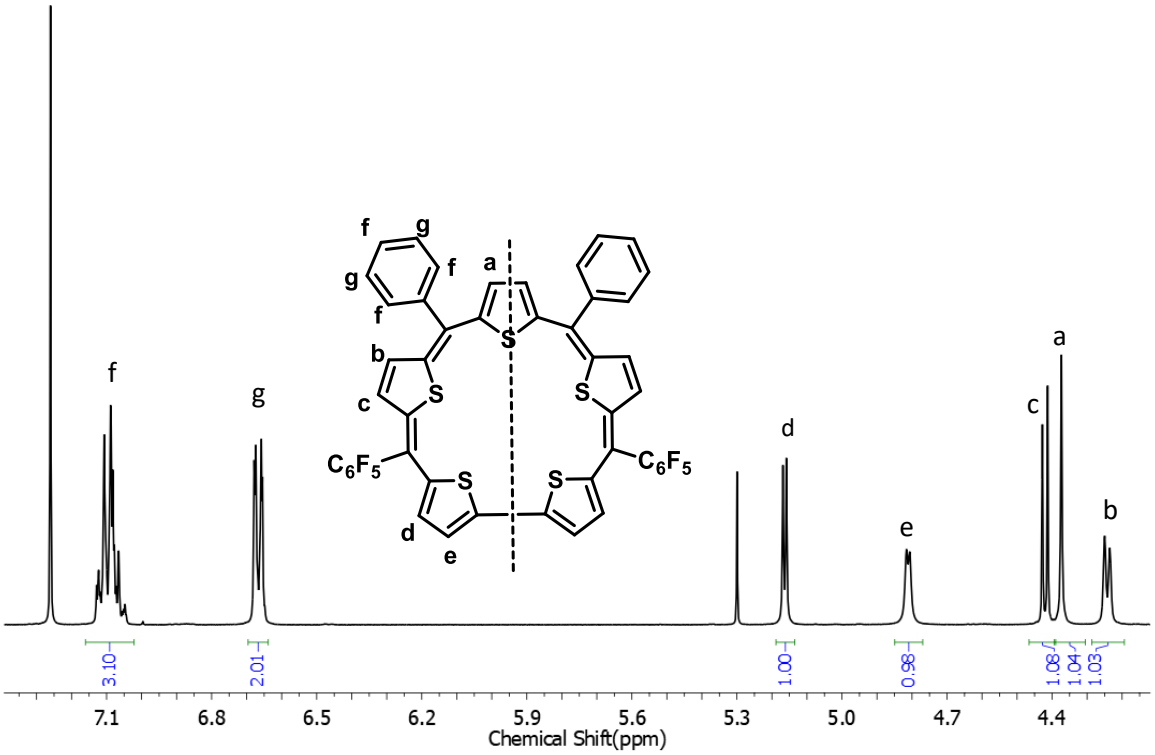

Figure III.3: *^{1}H NMR spectrum of **III.10** in Chloroform-d.*

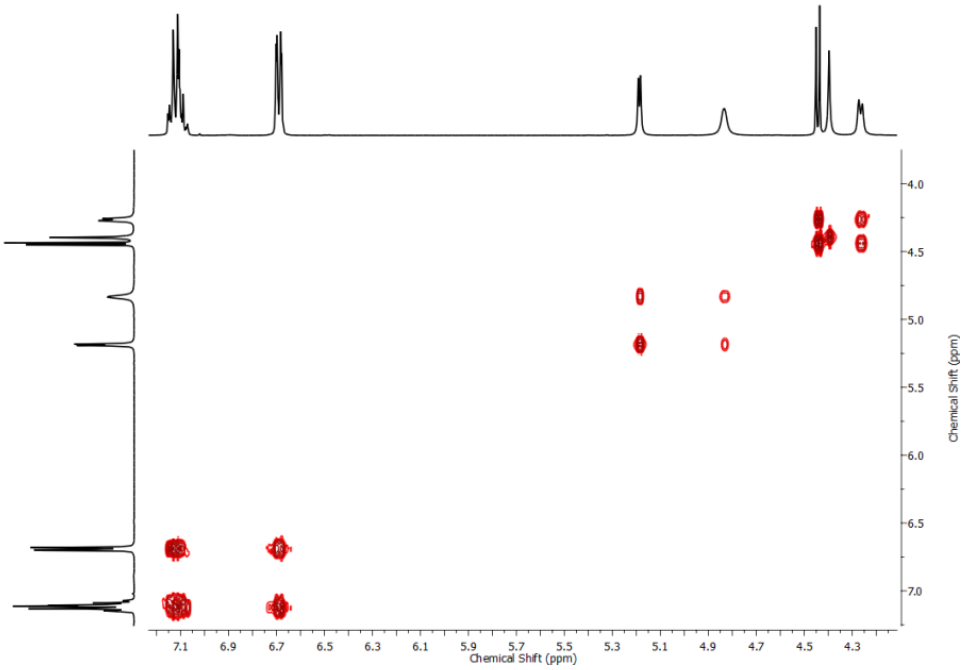

Figure III.4: *^{1}H-^{1}H COSY spectrum of **III.10** in Chloroform-d.*

III.4.3 Molecular structure of [24]sapphyrin

Characteristic shiny dark blue coloured crystals were obtained by recrystallization of sapphyrin inform a combination of dichloromethane and *n*-hexane. These crystals were rectangular in shape with sharp edges. Single crystal X-ray diffraction analysis revealed a planar conformation with sulphur atoms of all the thiophene units facing the core of macrocycle (figure – III.5). The bithiophene units were slightly bent out of the plane with one thiophene slightly above and another slightly below the macrocyclic plane defined by four meso carbons. Solid state studies support the ^{1}H NMR spectrum and confirmed that conformation of the macrocycle is same in both solid and solution states. A similar planar molecular structure was observed for a 25π cyclopentathiophene and its two different redox states. [9] In the crystal packing, sapphyrin molecules were found stacking one above the other with an inter planar distance of 4.127Å.

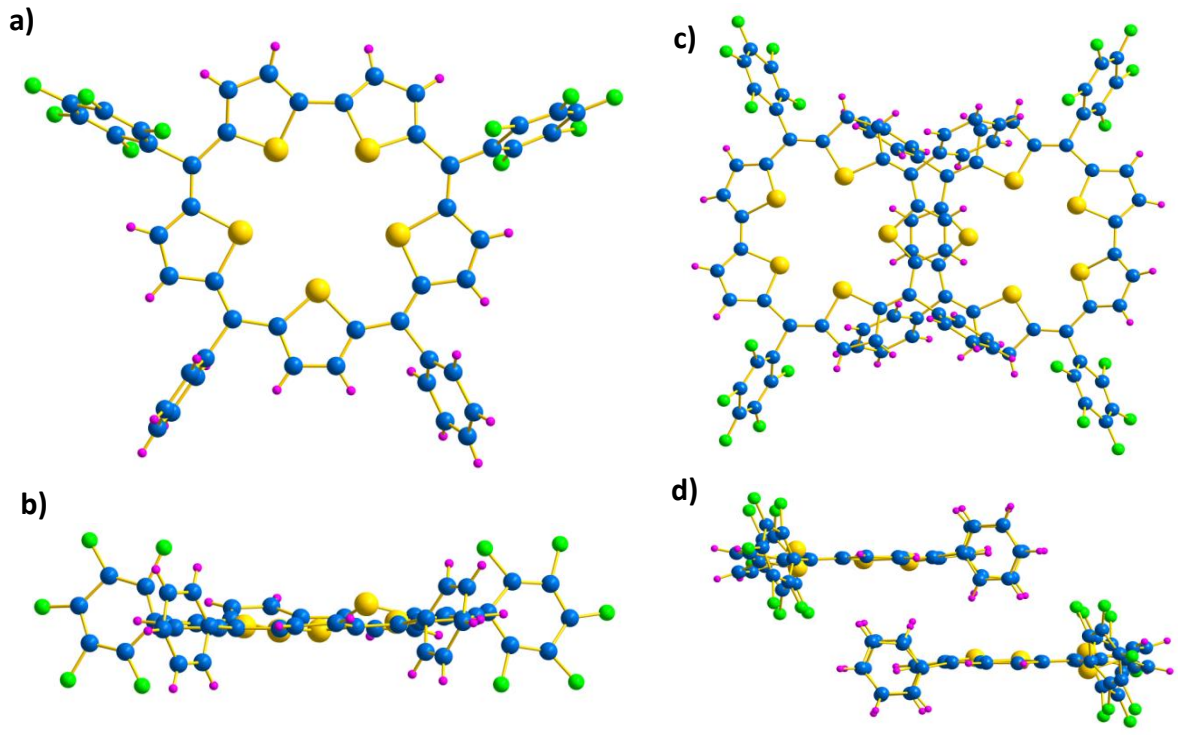

Figure III.5: *Molecular structure of **III.10** determined from single crystal X-ray diffraction. a) (top view), b) (side view) and crystal packing (c and d).*

III.4.4 Electronic absorption and Cyclic Voltammogram studies

Structurally, [24]sapphyrin with 24π electrons in the global conjugation confirmed to the Huckel's antiaromatic 4nπ electronic system, with a planar conformation in both solution and solid states. In the UV-visible spectrum, this macrocycle displayed absorption maxima at 430

nm (150780) along with a less intense shoulder band at 397 nm (99760) in dichloromethane. It did not display any lower energy bands in support of the antiaromatic nature for the macrocycle. It is well established that antiaromatic macrocycles undergo two-electron ring oxidation to yield aromatic dication.[14] Similarly, addition of Meerwein's salt to the greenish yellow coloured solution of antiaromatic sapphyrin, **III.10**, induced a subtle colour change to intense pink along with a red shift by more than 100 nm (figure – III.6). It displayed a sharp Soret like band at 534 nm with higher extinction co-efficient value (403400) along with two lower energy bands in the region between 720 nm (10890) and 805 nm (37900) supporting the aromatic nature of the 22π dicationic species (figure – III.6a). The stability of this dicationic salt was confirmed by its isolation and purification. Further, it was observed that this oxidation is reversible to yield the neutral 24π electronic state by the addition of suitable reducing agent like triethyl amine or Zinc dust as confirmed by electronic absorption spectroscopy. Its opto-electronic properties and chemical redox were further confirmed by electrochemical methods such as cyclic voltammetry (CV) and spectro-electrochemistry (SEC) studies.

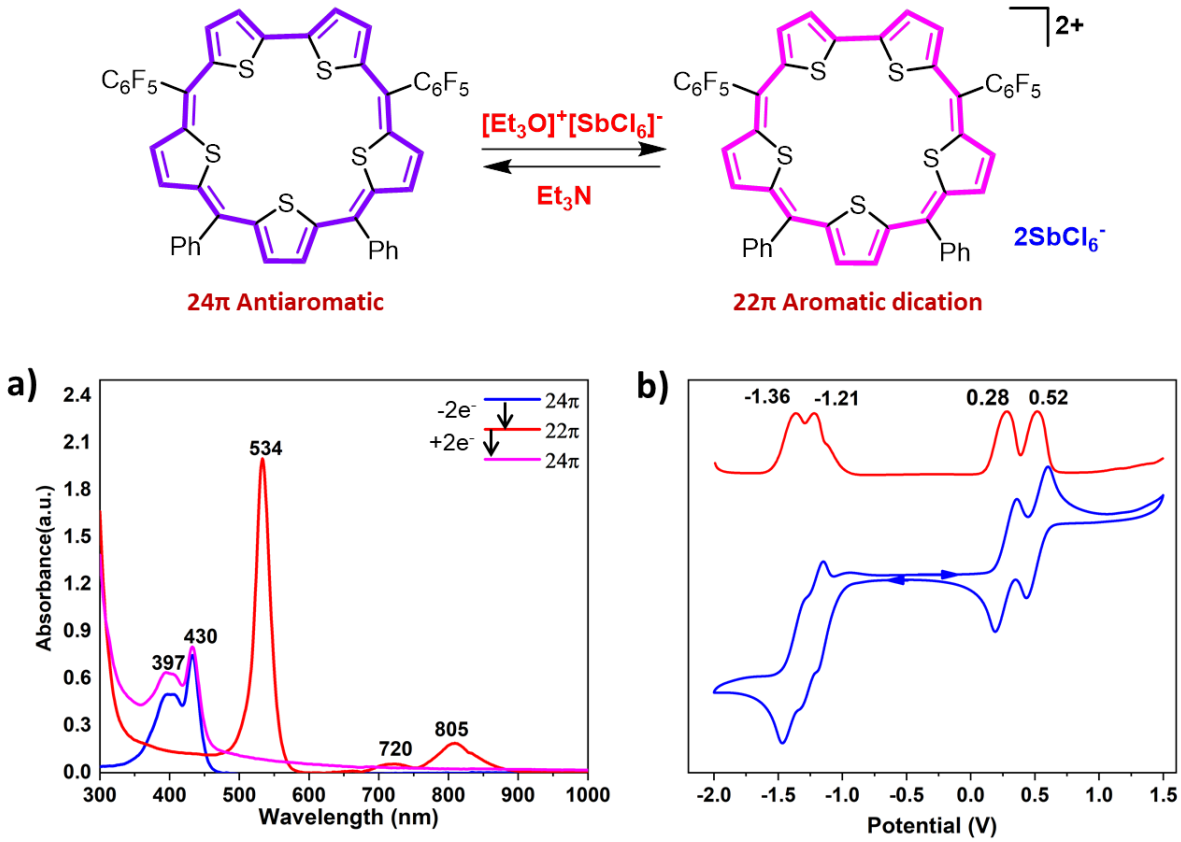

Figure III.6: *a) UV/vis/NIR absorption spectrum of 10^{-5} M solution of **III.10** (24π) and its oxidised species **[III.10]**$^{2+}$ (22π) recorded in CH_2Cl_2. b) Cyclic voltammogram (CV, blue) and differential pulse voltammogram (DPV, red) of **III.10** in CH_2Cl_2 (with 0.1 M $(Bu)_4NPF_6$ as the supporting electrolyte).*

Cyclic voltammogram (CV) and differential pulse voltammogram (DPV) studies (figure – III.6b) for [24]sapphyrin showed the characteristic redox potentials. Two oxidation potentials at +0.28 V, +0.52 V and two reduction potentials at -1.21 V and -1.36 V were revealed in the cyclic voltammogram. Based on these values, spectro-electrochemistry studies were conducted by recording the change in absorption at different oxidation potentials (figure – III.7). Upon applying the first oxidative potential at + 0.37 V, it displayed a broad band with λ_{max} at 486 nm corresponding to one-electron oxidation, leading to a radical cation intermediate with 23π electrons (figure – III.7a). Upon applying a higher potential at + 0.65 V, the radical cation was completely oxidized to 22π dication and displayed an absorption at 534 nm along with two low energy bands at 720 nm and 805 nm (figure – III.7b) as observed in the chemical oxidation (figure – III.6a).

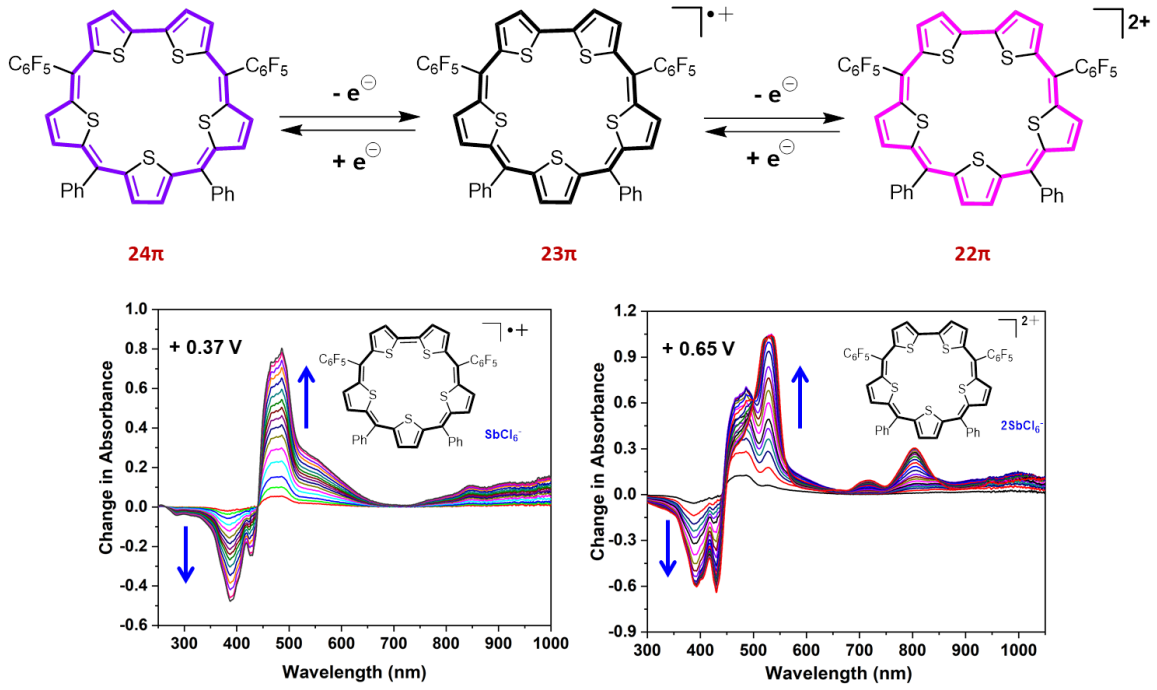

Figure III.7: *Spectro-electro chemistry studies of **III.10**. Change in absorption spectra of **III.10** after applying a potential of + 0.37 V (a) and + 0.65 V (b), respectively.*

III.4.5 Synthesis and characterisation of [22]sapphyrin dication

[24]sapphyrin is antiaroamatic in both solid and solution state and undergoes a facile two-electron ring oxidation as confirmed by spectro-electrochemical studies. Addition of Meerwein's salt to a solution of sapphyrin in dichloromethane induced a subtle colour change from greenish yellow to pinkish colour (Scheme - III.5). High resolution mass spectrum (HRMS) of the pink-coloured dicationic macrocycle, displayed *m/z* value at 472.9995 corresponding to *m/2* of the actual mass of two-electron oxidised [22]sapphyrin dication (figure – III.8).

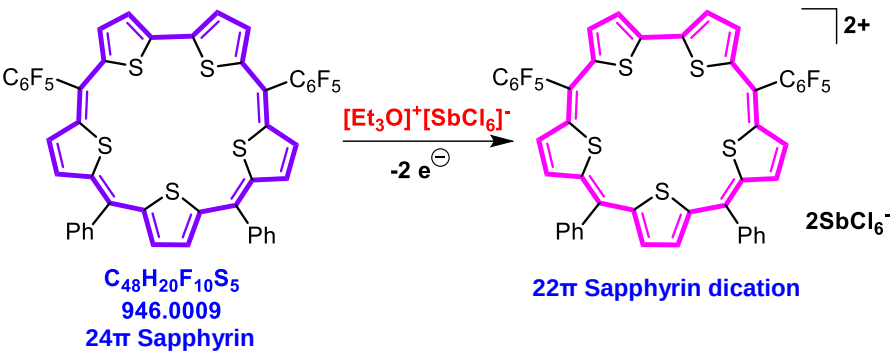

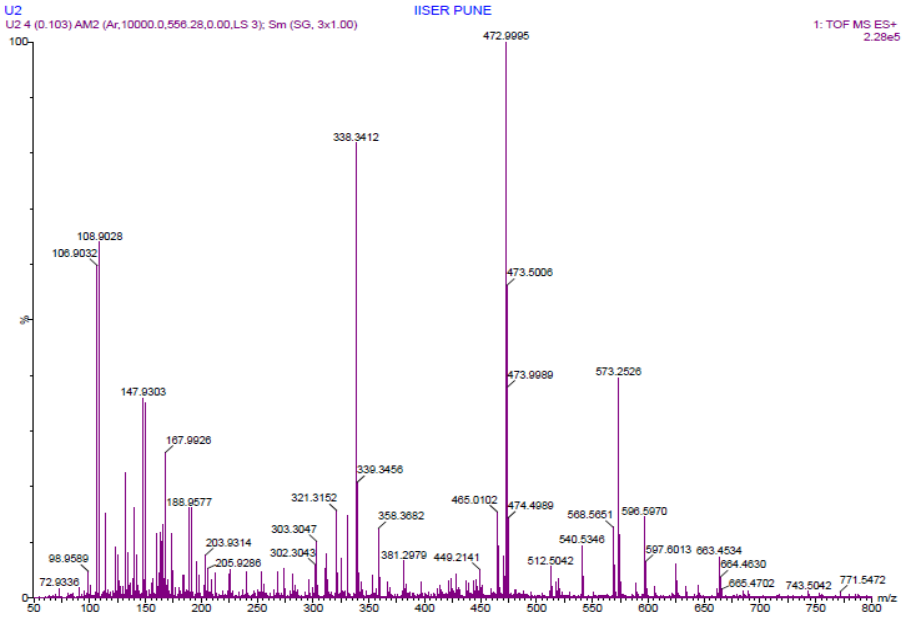

Figure III.8: *HR-ESI-TOF mass spectrum of sapphyrin dication,* ***[III.10]***$^{2+}$.

Further evidence for the aromatic character of [22]sapphyrin dication was obtained from ^{1}H NMR spectrum (figure – III.9). It displayed chemical shift values exactly opposite to the neutral 24π species (figure – III.10). For [24] sapphyrin all β-protons of the thiophenes were found to resonate upfield between δ 4 to 5.2 ppm. However, in the case of [22]sapphyrin dicationic species, [**III.10**]$^{2+}$, β-protons of the all the five thiophene rings resonated in downfield between δ 11.00 to 12.00 ppm. Such downfield chemical shift values confirm the diatropic ring current for the dicationic species, [**III.10**]$^{2+}$. The phenyl protons were not affected by ring current and were found resonating at δ 8.00 ppm to 9.00 ppm. Based on spectroscopic, electrochemical and structural analysis, 24π sapphyrin has been characterized as an antiaromatic macrocycle which readily undergoes reversible two-electron ring oxidation. Unfortunately, good quality crystals of [**III.10**]$^{2+}$ could not be obtained to determine its structure in the solid state.

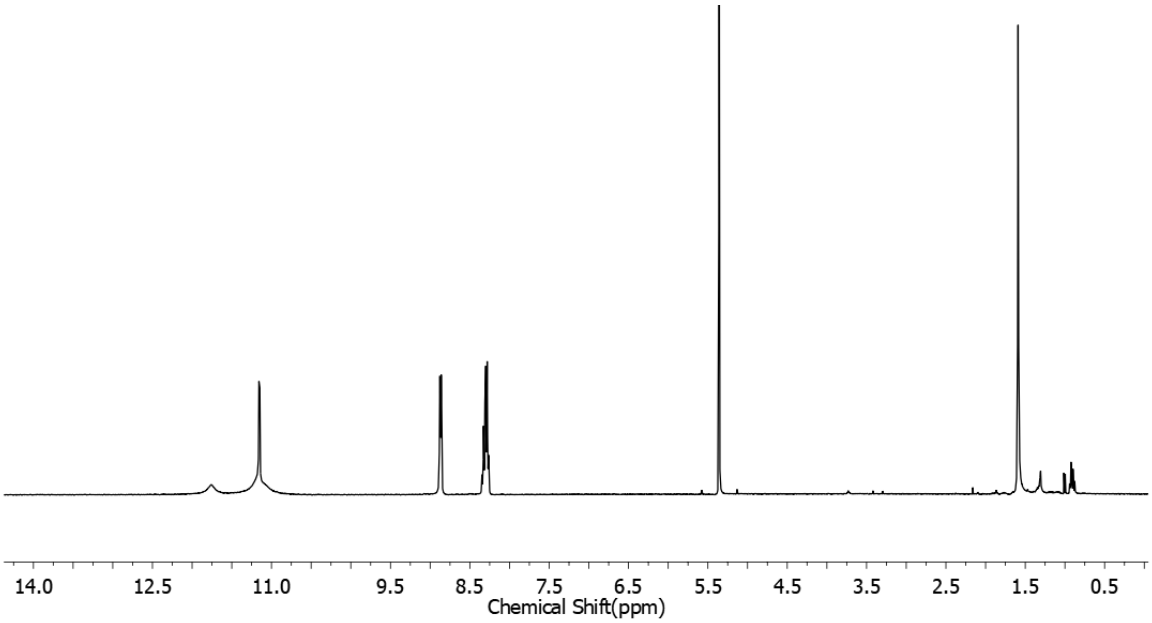

Figure III.9: *^{1}H NMR spectrum of **[III.10]**$^{2+}$ in Dichloromethane-d_2.*

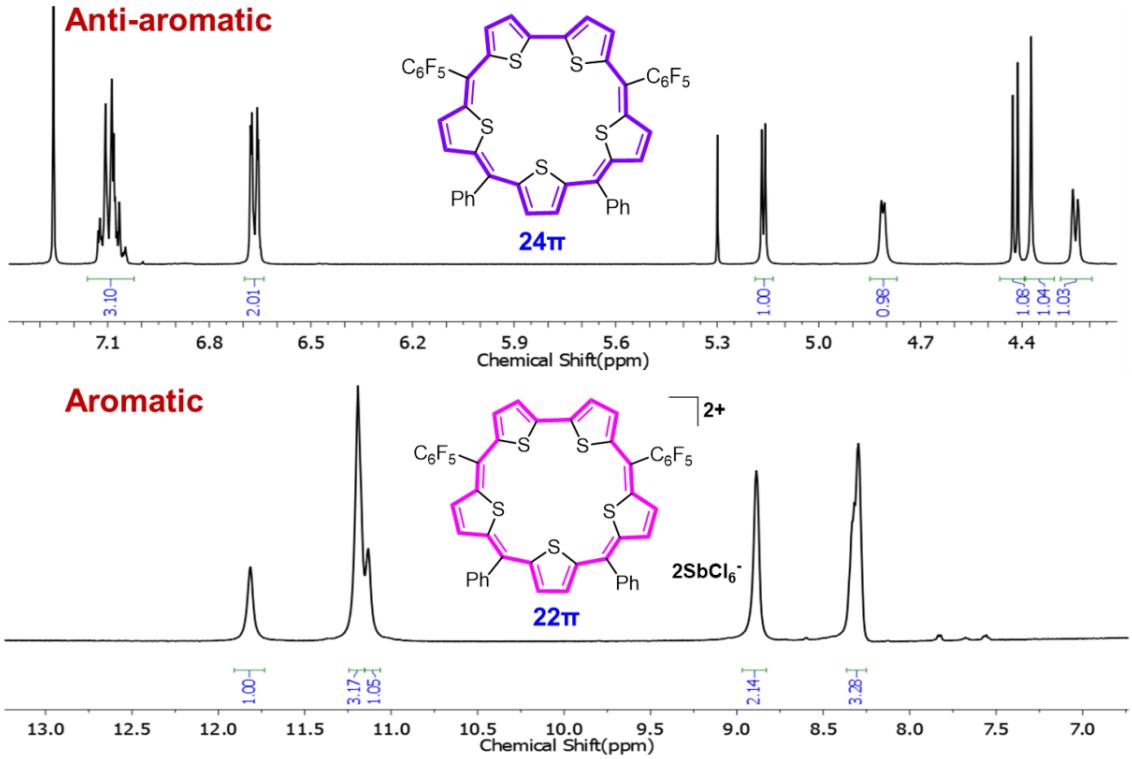

Figure III.10: *Comparative study of ^{1}H NMR spectrum between **III.10** and **[III.10]**$^{2+}$.*

III.4.6 Computational studies

DFT calculations supported the experimental results, as observed in the ^{1}H NMR and single crystal X-ray diffraction studies. The strength of (anti)aromaticity estimated through NICS (0) and AICD calculations. 24π antiaromatic sapphyrin displayed paratropic ring current effect in the ^{1}H NMR spectrum and an estimated NICS (0) value of +10.9 ppm substantiated the antiaromatic nature of the macrocycle. In the AICD plot, it displayed anti-clockwise electron density confirming the paratropic ring current of the macrocycle. In contrast, its dicationic species showed the estimated NICS (0) value -11.73 in support of the aromatic character of the macrocycle and in AICD plot displayed the clockwise electron density confirmed diatropic ring current of the macrocycle. Also the HOMO-LUMO energy gap was calculated for both neutral and dicationic sapphyrin macrocycle. For neutral species showed the energy gap 1.64 eV and dicationic species 1.66 eV.

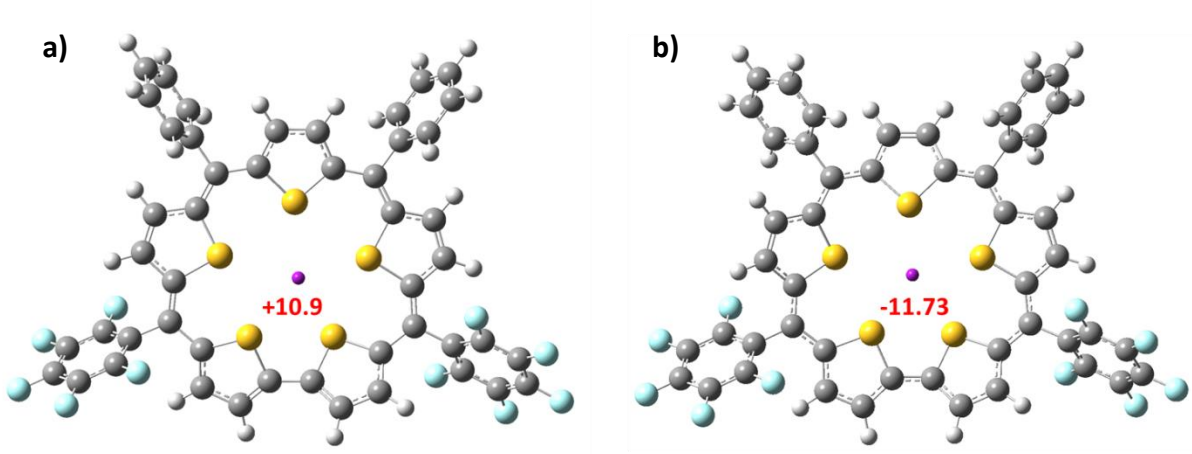

Figure III.11: *The estimated NICS (0) values mentioned at the centre of the macrocycles (a) neutral 24π sapphyrin* ***III.10*** *and (b) 22π sapphyrin dication* ***[III.10]***$^{2+}$.

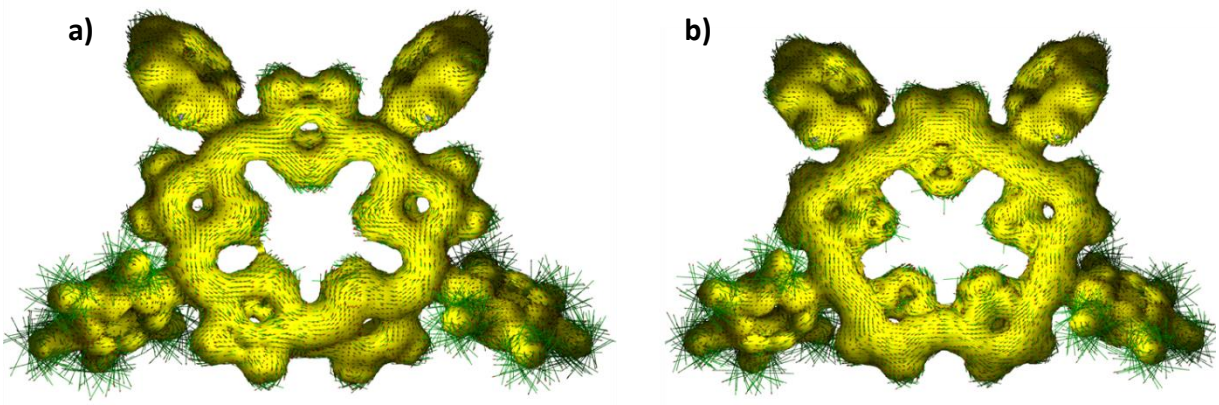

Figure III.12: *AICD plot of (a)* ***III.10*** *and (b)* ***[III.10]***$^{2+}$ *at an isosurface value 0.07 the external magnetic field is applied orthogonal to the macrocyclic plane.*

III.5.1 Isolation and Characterisation of [48]decaphyrin

[48]decaphyrin(1.1.1.1.0.1.1.1.1.0), **III.14**, identified as a violet-pink coloured band was isolated next to sapphyrin, **III.10**, by the repeated basic alumina column chromatography and also by size exclusion chromatography in 9% yields. The composition of this decaphyrin was confirmed by High Resolution Mass Spectrometry (HR-MS), in which it displayed *m*/*z* value of 1892.0186 corresponding to $C_{96}H_{40}F_{20}S_{10}$ (1892.0018) (figure – III.13).

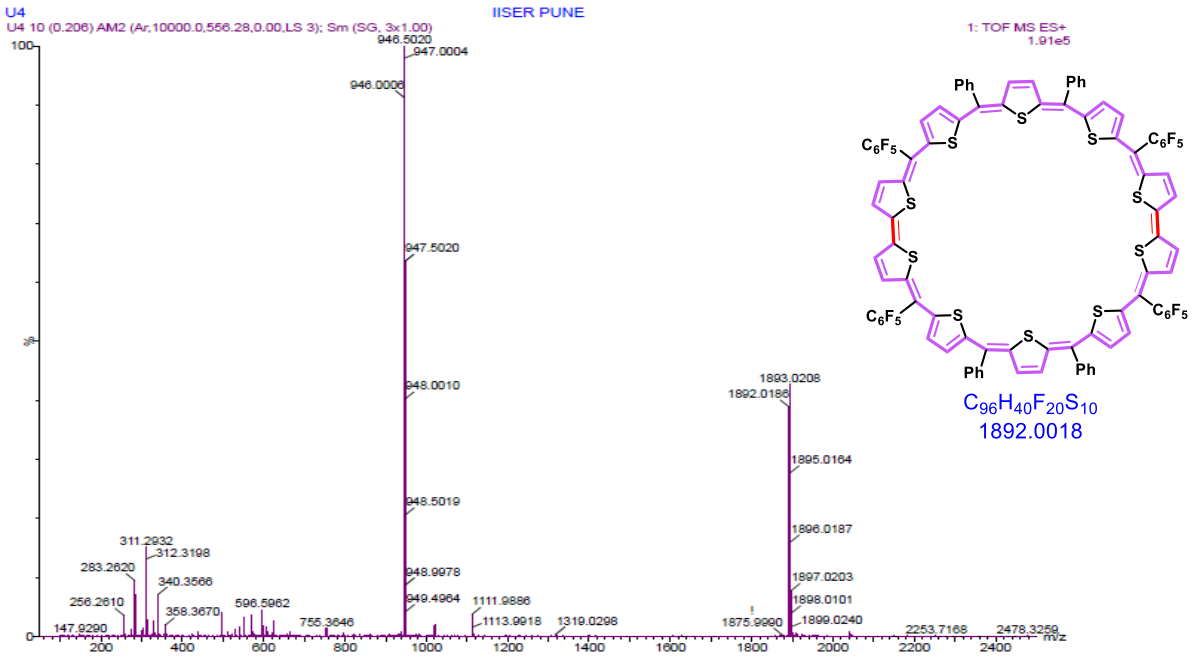

Figure III.13: *HR-ESI-TOF mass spectrum of **III.14**.*

III.5.2 ^{1}H NMR study of [48]decaphyrin

Ring contracted [48]decaphyrin, **III.14**, accounts for 48π electrons in the global conjugation and belongs to Huckel's 4nπ electronic system. Hence it is expected to show antiaromatic character and paratropic ring current effects in the ^{1}H NMR spectrum. However, its well resolved ^{1}H NMR at room temperature displayed resonances only in the region between δ 6.3 to 7.6 ppm (figure – III.14). Therefore it suggested the absence of paratropic ring current effects and macrocycle identified as non-antiaromatic in the solution state. There are five signals for β-protons of the thiophene rings which resonate in the region δ 6.3 to 7.1 ppm. Among them, were four doublets at δ 6.39, 6.48, 6.61 and 7.03 ppm and a singlet at δ 6.45 ppm. The phenyl protons resonated in the region δ 7.3 to 7.5 ppm corresponds to a doublet for eight protons and another multiplet for twelve protons. Based on the less number of signals and also due to the absence of paratropic ring current, it's possible to predict the

macrocycle with a C_2 axis and non-planar confirmation. Since it displayed less number of signals in the ^{1}H NMR and also to understand the fluxional nature of the macrocycle, ^{1}H NMR spectra were recorded at low temperatures. Even upon decreasing the temperature up to 193 K, no significant change in the chemical shifts of all the protons was observed (figure – III.15) confirming that macrocycle was devoid of fluxionality in the solution state.

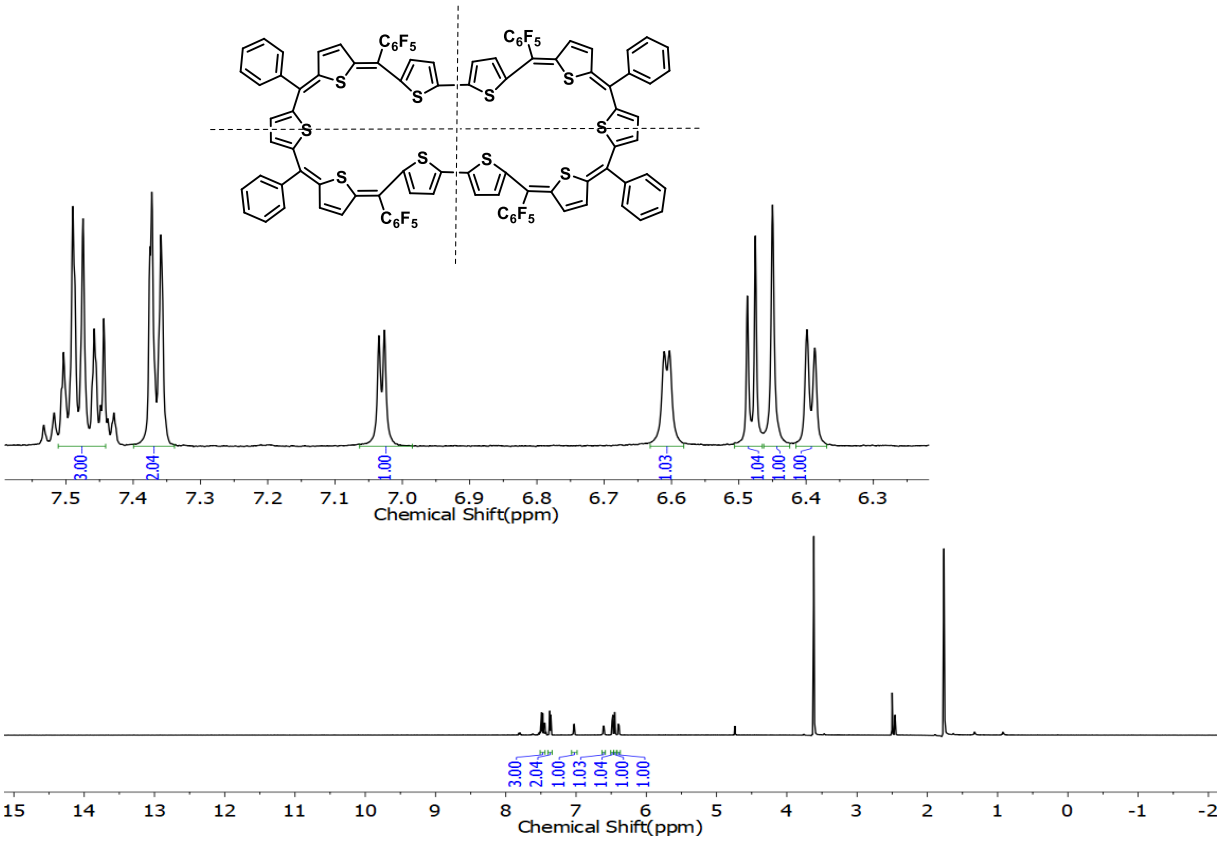

Figure III.14: *^{1}H NMR spectrum of **III.14** in Tetrahydrofuran-d_8 at 298 K.*

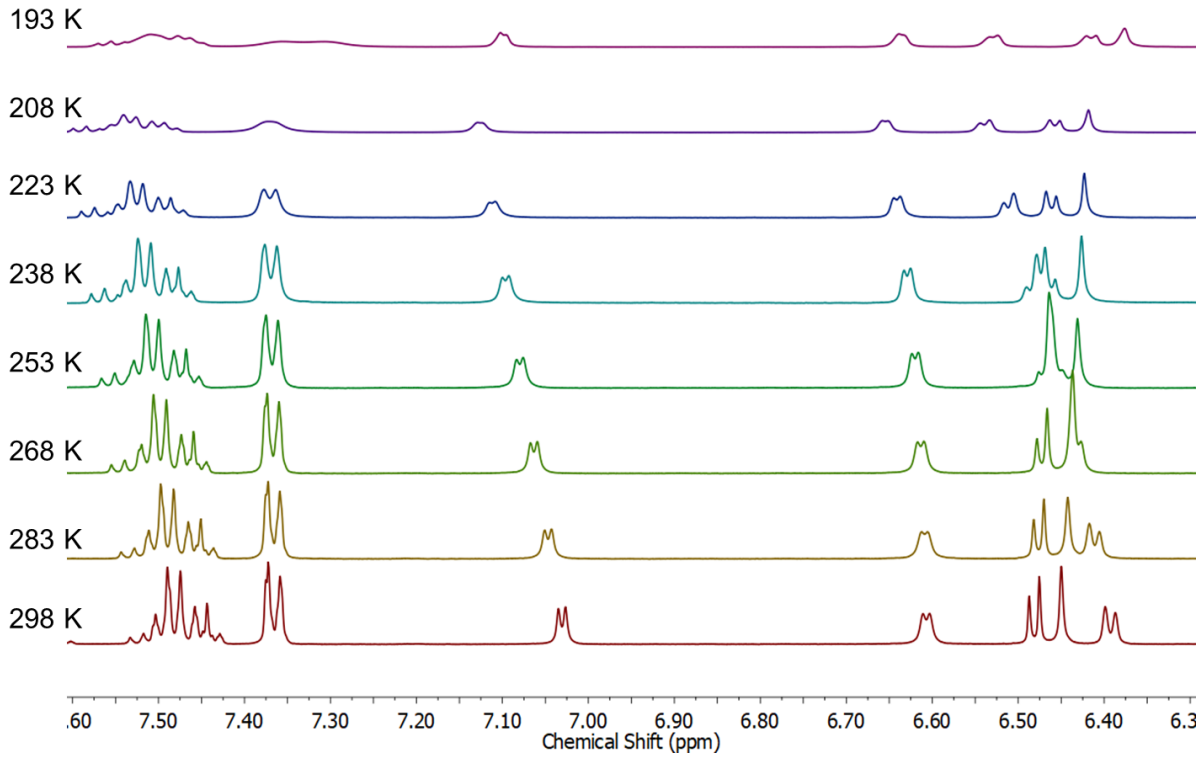

Figure III.15: *Variable temperature ^{1}H NMR spectra of **III.14** in Tetrahydrofuran-d_8 from 298 K to 193 K.*

III.5.3 Molecular structure of [48]decaphyrin

As described in the previous chapter, [50]decaphyrin (1.1.1.1.1.1.1.1.1.1) displayed topoisomerism in solid state with respect to the choice of the solvent used for crystallization. In acetonitrile, macrocycle displayed [6+4] unsymmetrical twisted figure of eight conformation with non-aromatic character. In contrast it displayed a symmetrical [5+5] untwisted near-planar conformation in benzene and characterized as aromatic in nature. Crystallization of ring contracted [48]decaphyrin was achieved after many efforts to obtain rectangular plate like shaped, dark pink coloured crystals though vapour diffusion of *n*-heptane into a chloroform solution of the macrocycle. Single crystal X-ray diffraction studies revealed a twisted 'figure of eight' conformation, with a symmetrical twist leading to two 24π saphhyrin like pockets (figure - III.16). It was observed that bithiophene units with an inverted orientation were exactly located at the centre of the macrocycle adhering to figure eight conformation. In each sapphyrin-like pocket, sulphur of all the thiophene units are oriented towards the centre of the macrocyclic core akin to the parent 24π sapphyrin. The

macrocycle can be identified as non-antiaromatic macrocycle due to the 'figure eight' conformation in the solid state.

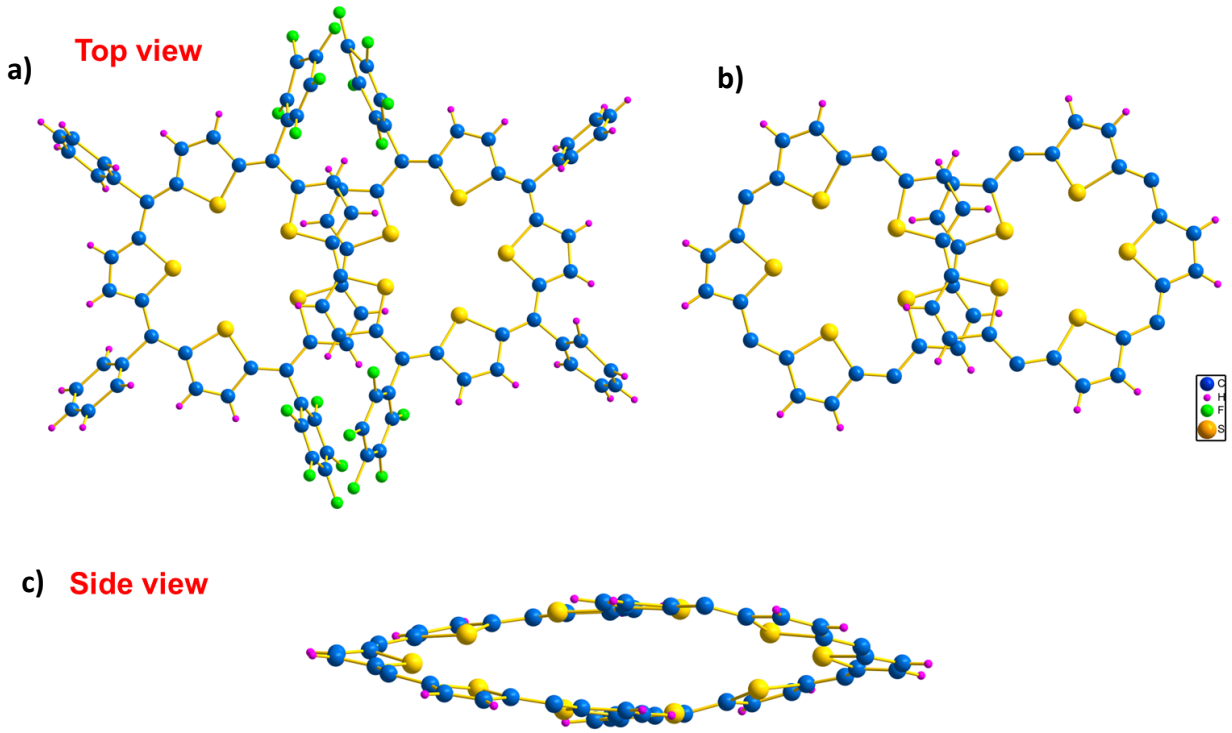

Figure III.16: *Molecular structure of [48]decaphyrin (**III.14**) as determined from single crystal X-ray diffraction. Pentafluorophenyl and phenyl rings are omitted of clarity in the (b) (top view) and (b) (side view) rows.*

III.5.4 Electronic absorption and Cyclic Voltammogram studies

Ring contracted [48]decaphyrin accounts for 48π electrons in the global conjugation, fits to Huckel's 4nπ electronic system, but molecule showed non-antiaromatic character both in solution and solid state. By virtue of its extended conjugation, **III.14** displayed a λ_{max} at 581 (167300) nm along with a less intense band at 395 nm (132100) in dichloromethane (figure – III.17a). Being a 4nπ system, **III.14** is expected undergo two-electron ring oxidation to yield the 46π dicationic species. Addition of TFA or $NOBF_4$ or Meerwein's salt, induced a subtle colour change from violet-pink colour to light-green and displayed a huge red shift by more than 250 nm. The oxidized species displayed an absorption maxima with a broad band at 865 nm (353300) and a less intense sharp band at 487 nm (297500) along with two lower energy bands at 1133 (37890) and 1287 nm (60200) suggesting the formation of 46π decaphyrin dicationic species [**III.14**]$^{2+}$ (figure – III.17a). Addition of a reducing agent like triethyl amine or zinc powder reduced the 46π dicationic species back to the neutral 48π decaphyrin state as confirmed by electronic absorption spectroscopy. In cyclic voltammogram (CV) and

differential pulse voltammetry (DPV) studies, macrocycle displayed at least four oxidation potentials at + 0.14 V, + 0.96 V, + 1.28 V and + 1.36 V and three reduction potentials at - 0.97 V, - 1.20 V and - 1.71 V (figure – III.17b). These studies confirmed the reversible redox property of the 48π decaphyrin, which can be oxidized to 46π dicationic species.

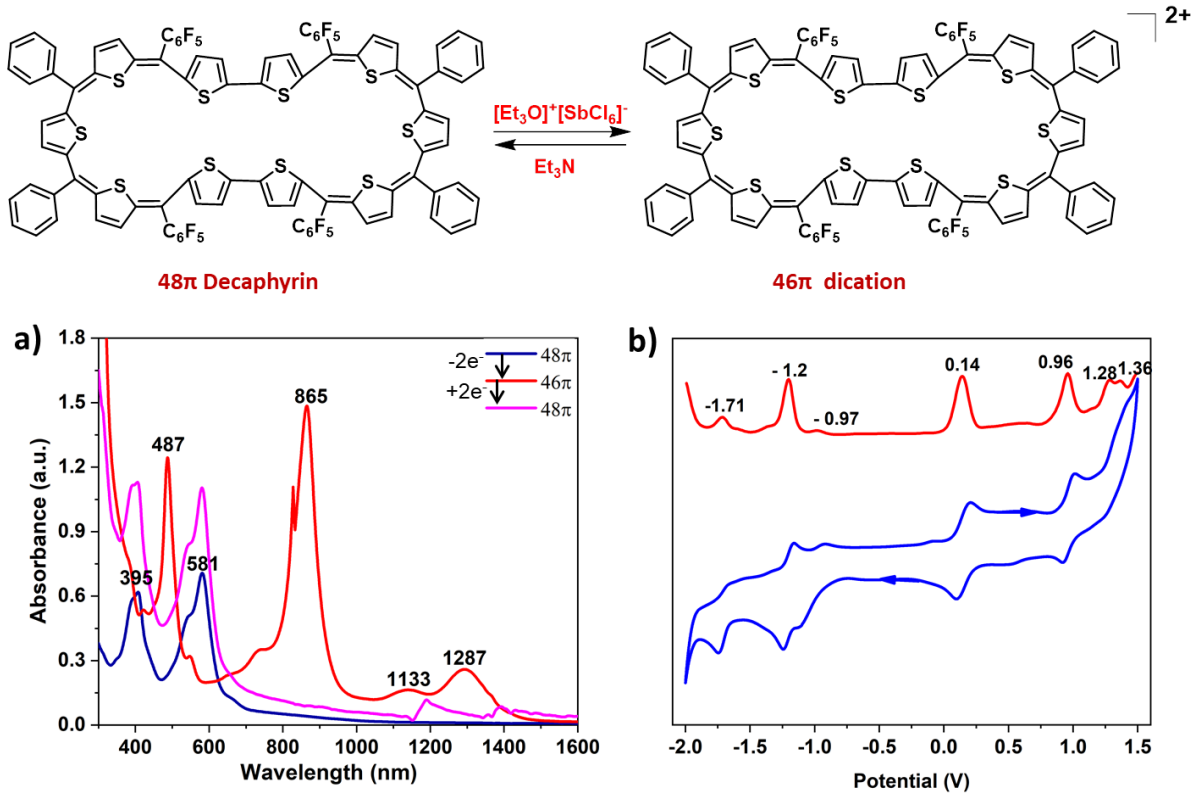

Figure III.17: *a) UV/vis/NIR absorption spectrum of 10^{-5} M solution of **III.14** (48π) and its oxidised species [**III.14**]$^{2+}$ (46π) recorded in CH_2Cl_2. b) Cyclic voltammogram (CV, blue) and differential pulse voltammogram (DPV, red) of **III.14** in CH_2Cl_2 (with 0.1 M $(Bu)_4NPF_6$ as the supporting electrolyte).*

III.5.5 Computational studies

The estimated NICS (0) value for decaphyrin on both pentaphyrin pockets is + 3.37 ppm, supporting to the non- antiaromatic characteristics of the macrocycle. Because of its extended π-conjugation the macrocycle showed the HOMO-LUMO energy gap is 1.24 eV.

III.6.1 Isolation and Characterisation of [72]pentadecaphyrin

[72]pentadecaphyrin, **III.15**, is the largest macrocycle identified in this reaction (scheme - III.4). This macrocycle was isolated in poor yields as a dark green coloured band after [48]decaphyrin by the repeated basic alumina column chromatography followed by size exclusion chromatography. Its yield was masked by the formation of sapphyrin and decaphyrin. Therefore this macrocycle was obtained in 1.2% yields. Its composition was confirmed by the High Resolution Mass Spectrometry (HR-MS), in which macrocycle displayed a *m/z* value of 2838.0103 corresponding to $C_{144}H_{60}F_{30}S_{15}$ (2838.0027) along with the *m/2* value of 1420.0075 (Cald. Mass 1419.0013) (figure – III.18).

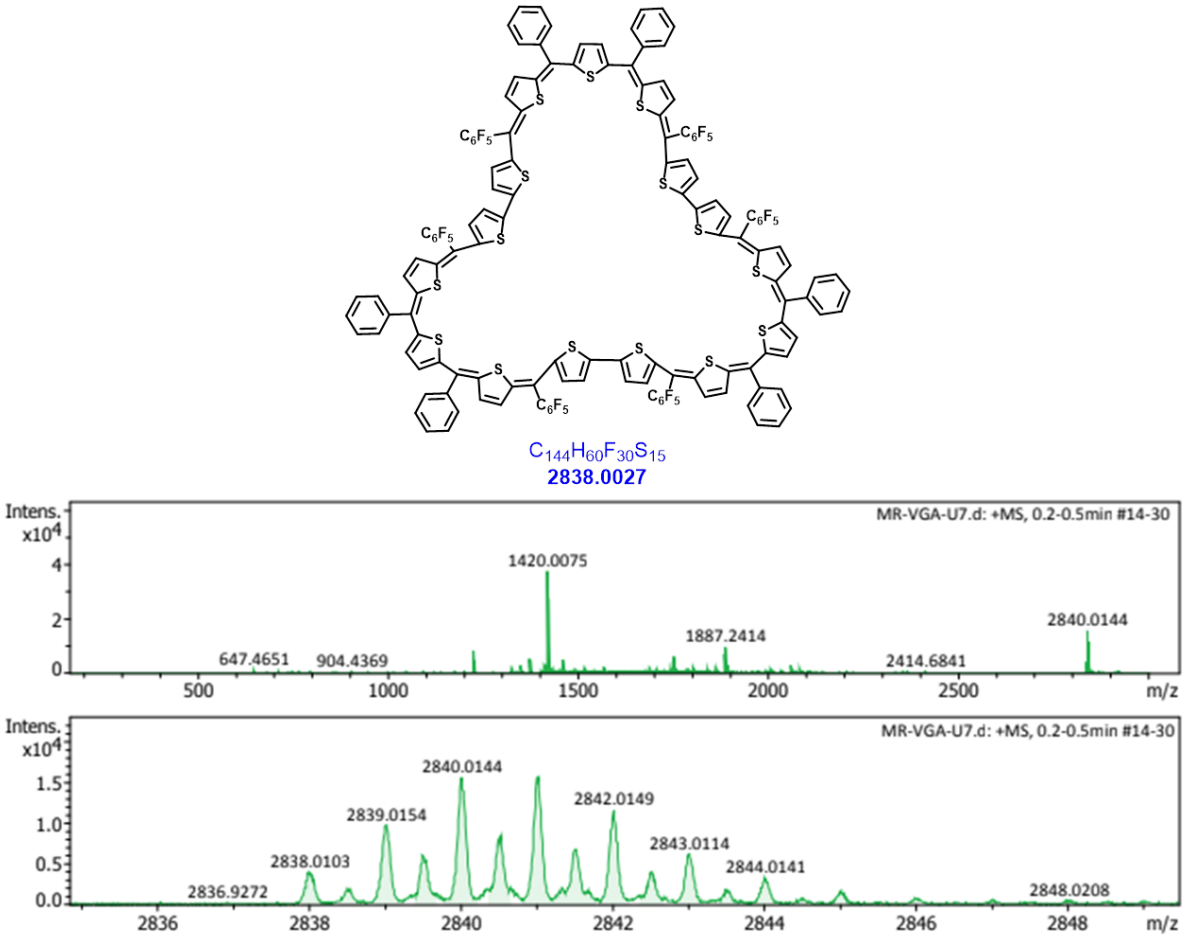

Figure III.18: *HR-ESI-TOF mass spectrum of* ***III.15****.*

III.6.2 ^{1}H NMR study of [72]pentadecaphyrin

[72]pentadecaphyrin obeys Huckel's antiaromatic 4nπ electronic system, by virtue of 72π electrons in the global π-conjugation. In ^{1}H NMR spectrum, all its protons were found to resonate in the region between δ 6.00 ppm to 8.20 ppm clearly signifying the absence of paratropic ring current effects. Therefore, the macrocycle is expected to be non-antiaromatic

in the solution state. Since the signals were not well resolved at the room temperature, it suggested the possibility of solution state dynamics. Hence, variable and low temperature ^{1}H NMR studies were employed to arrest the envisaged fluxional behaviour. Spectra were recorded up to 188 K (figure – III.19). But it was observed that a well-resolved spectrum could be obtained at 238 K (figure – III.20) and further decrease in temperature led to overlap of signals. In the ^{1}H NMR spectrum at 238 K, many signals were observed in the region between δ 6.0 to 8.5 ppm. Based on the integration values, these resonances accounted for twenty protons. From these chemical shift values, it could be concluded that the macrocycle was devoid of ring current effects possibly due to structure induced loss of planarity as observed for the decaphyrin, **III.14**. ^{1}H-^{1}H COSY NMR spectrum recorded at the same temperature displayed seven correlations (figure – III.21). Hence it could be deduced that among the twenty protons, five protons correspond to phenyl rings and the rest fifteen protons correspond to the β-protons of fifteen thiophene rings. Hence, one of the possibilities could be that the macrocycle adopts a C_3-axis of symmetry, and the macrocycle may have repeated three fold twists in the molecular conformation. Unfortunately, good quality crystals could not be obtained to determine its structure from X-ray diffraction studies.

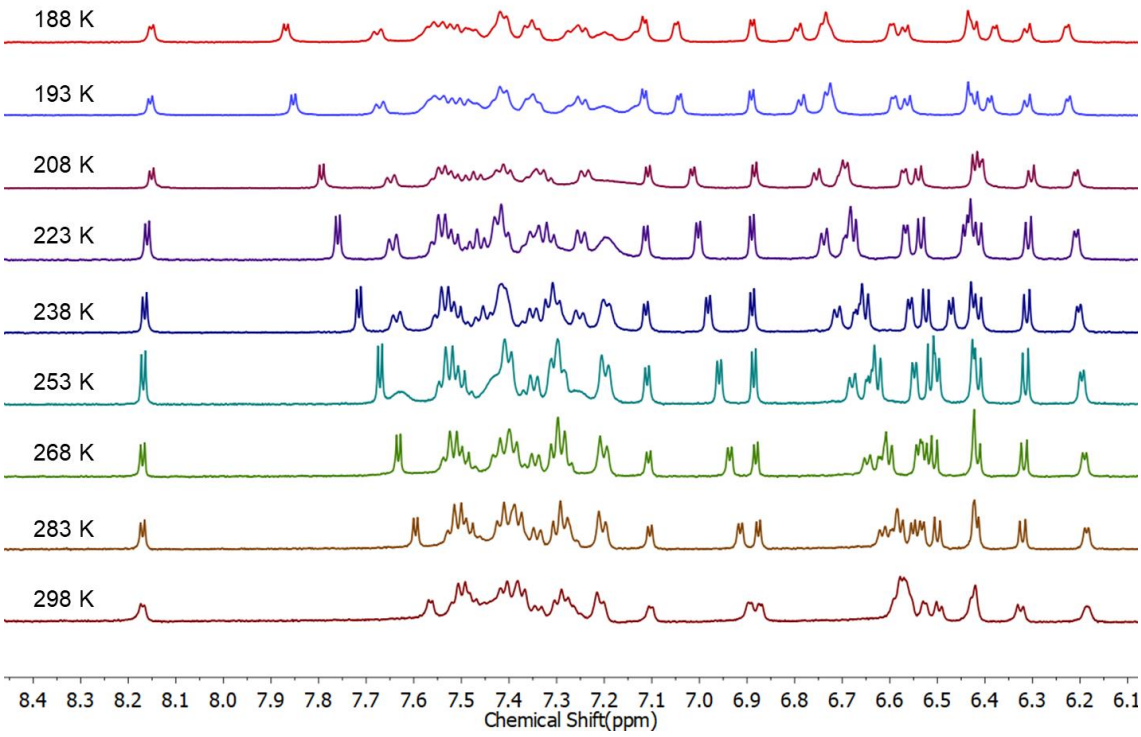

Figure III.19: *Variable temperature ^{1}H NMR spectra of **III.15** in Acetone-d_6.*

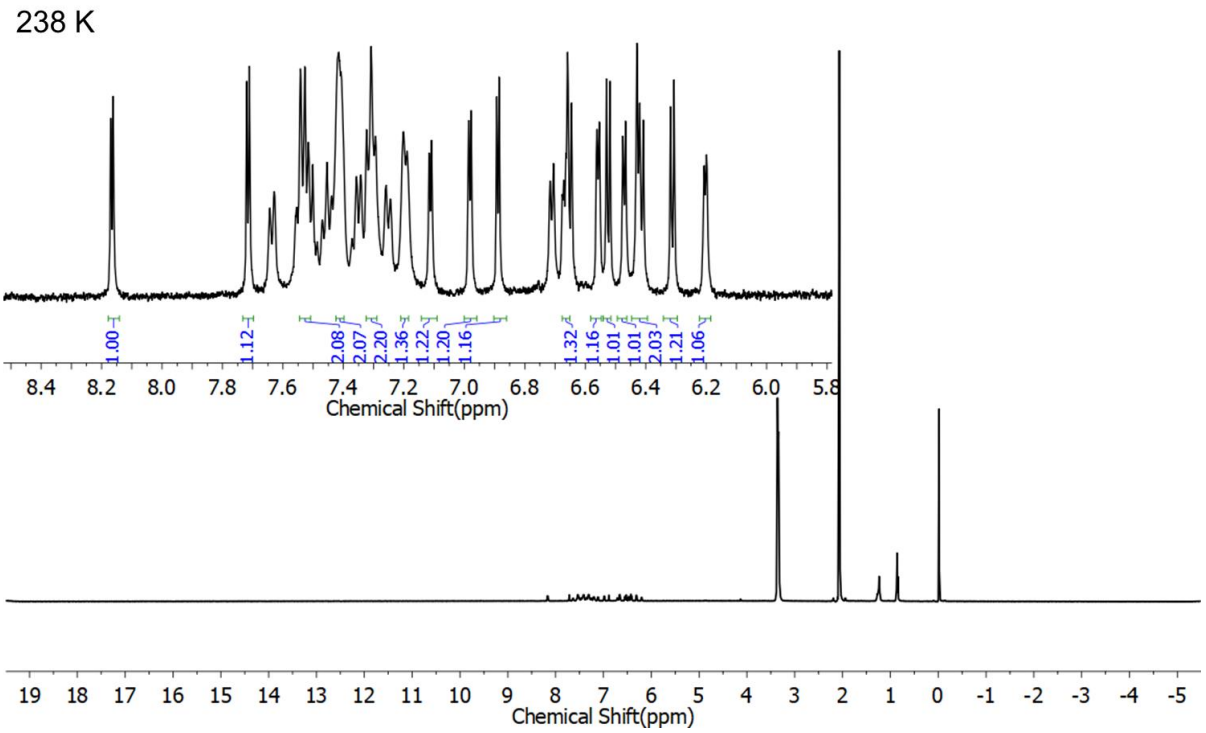

Figure III.20: *^{1}H NMR spectrum of **III.15** in Acetone-d_6 at 238 K.*

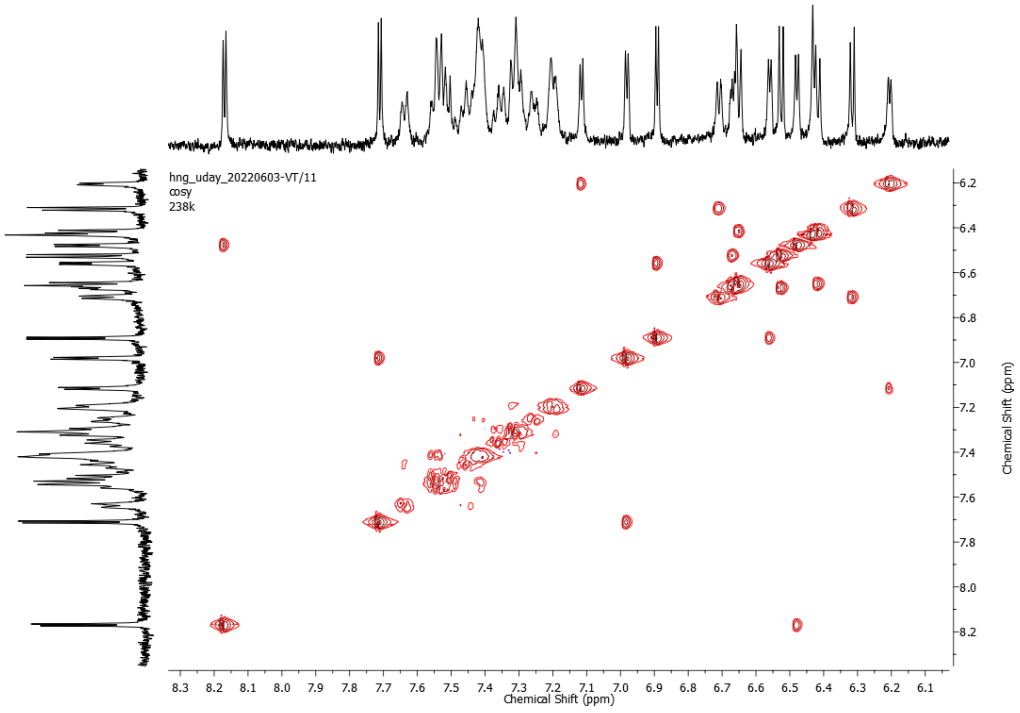

Figure III.21: *^{1}H-^{1}H COSY spectrum of **III.15** in Acetone-d_6.*

III.6.3 Electronic absorption studies

With [72]pentadecaphyrin having 72 π-electrons in the global conjugation it is expected to be Huckel's antiaromatic 4nπ electronic system. However due to a non-planar geometry it is identified as non-antiaromatic in solution state. Electronic absorption of the macrocycle displayed the λ_{max} at 438 nm (374300) along with a less intense band at 664 nm (341100). Being a 4nπ system, similar to **III.10** and **III.14**, it is expected to undergo two-electron oxidation to yield the 70π dication species. Addition of TFA or Meerwein's salt or $NOBF_4$ to **III.15** induced a subtle colour change from green to light brownish-yellow colour suggesting the formation of a 70π dicationic species, [**III.15**]$^{2+}$ (figure III.22). It shows a bathochromic shift and its absorption maxima displayed a broad band at 1237 nm (450200) in the NIR region along with a less intense band at 732 nm (323200). Compared to all the expanded isophlorinoids, this macrocyclic dication displayed the highest bathochromic shift in the lower energy region. This dicationic species could be reduced back to its neutral state (72π system) by the addition of a suitable reducing agent like triethyl amine or zinc powder.

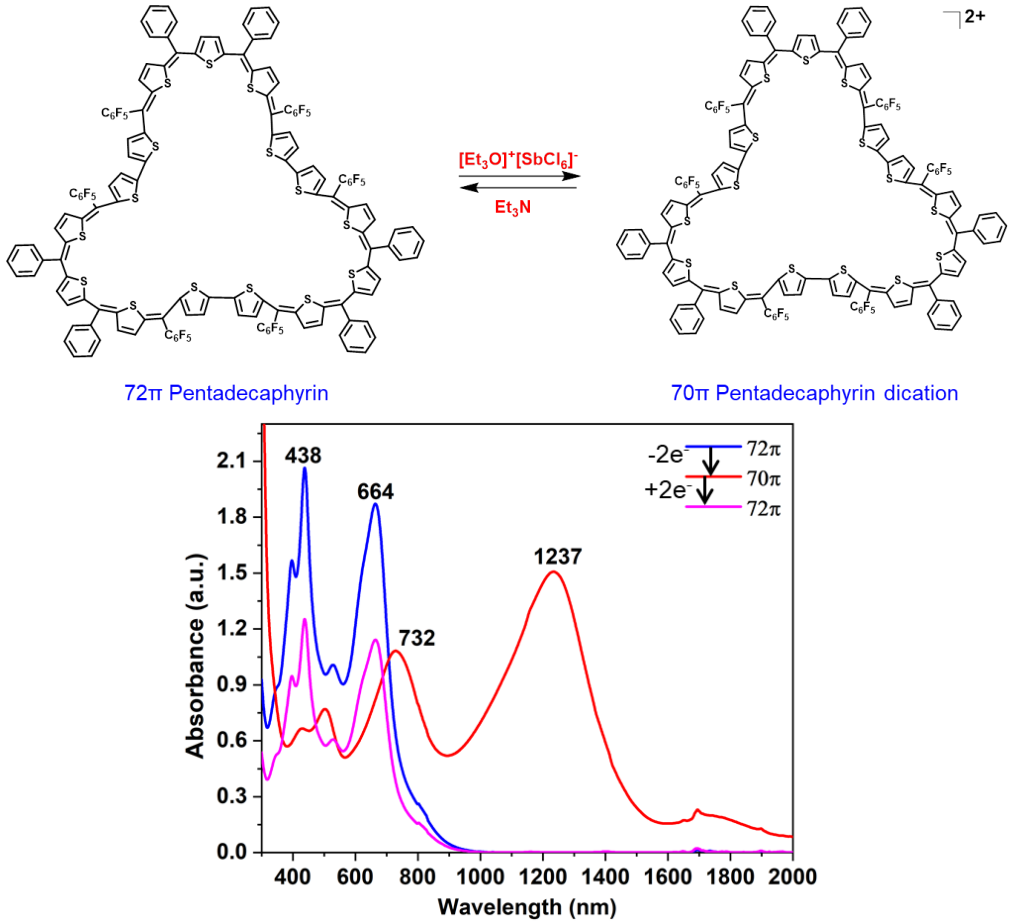

Figure III.22: *a) UV/vis/NIR absorption spectrum of 10^{-5} M solution of **III.15** (72π) and its oxidised species [**III.15**]$^{2+}$ (70π) recorded in CH_2Cl_2.*

In conclusion, three different macrocycles, **III.10**, **III.14** and **III.15** were isolated from a single reaction. Particularly, the 24π antiaromatic sapphyrin **III.10** could be characterized comprehensively and displayed the expected 22π dicationic species upon oxidation by two electrons. In continuation with these studies, an expanded sapphyrin with 26π electrons was attempted by modifying the synthesis described in scheme – III.4.

III.7 Synthesis of 26π Sapphyrin and higher analogues

In a strategy parallel to the synthesis of [24]sapphyrin , a similar synthetic approach was adopted to synthesize the [26]sapphyrin. A bithiophene was replaced by ethylene bridged bithiophene, **III.16**, and condensed with thiophene based tripyrromethane diol in the presence of a Lewis acid (scheme - III.5). $BF_3.OEt_2$ was added in dark and stirred for two hours, followed by addition of 2.5 equivalents of DDQ as the oxidising agent. Stirring was continued for another two hours in open atmosphere. This reaction mixture was then passed through a short bed of basic alumina. Two major products i.e., ethylene bridged [26]sapphyrin, **III.17**, and [52]decaphyrin, **III.18**, were detected from the reaction mixture. The progress of product formation in the reaction was monitored by the thin layer chromatography (TLC) and MALDI TOF/TOF mass spectrometry. Both the macrocycles were purified by repeated basic alumina column chromatography and size exclusion chromatography.

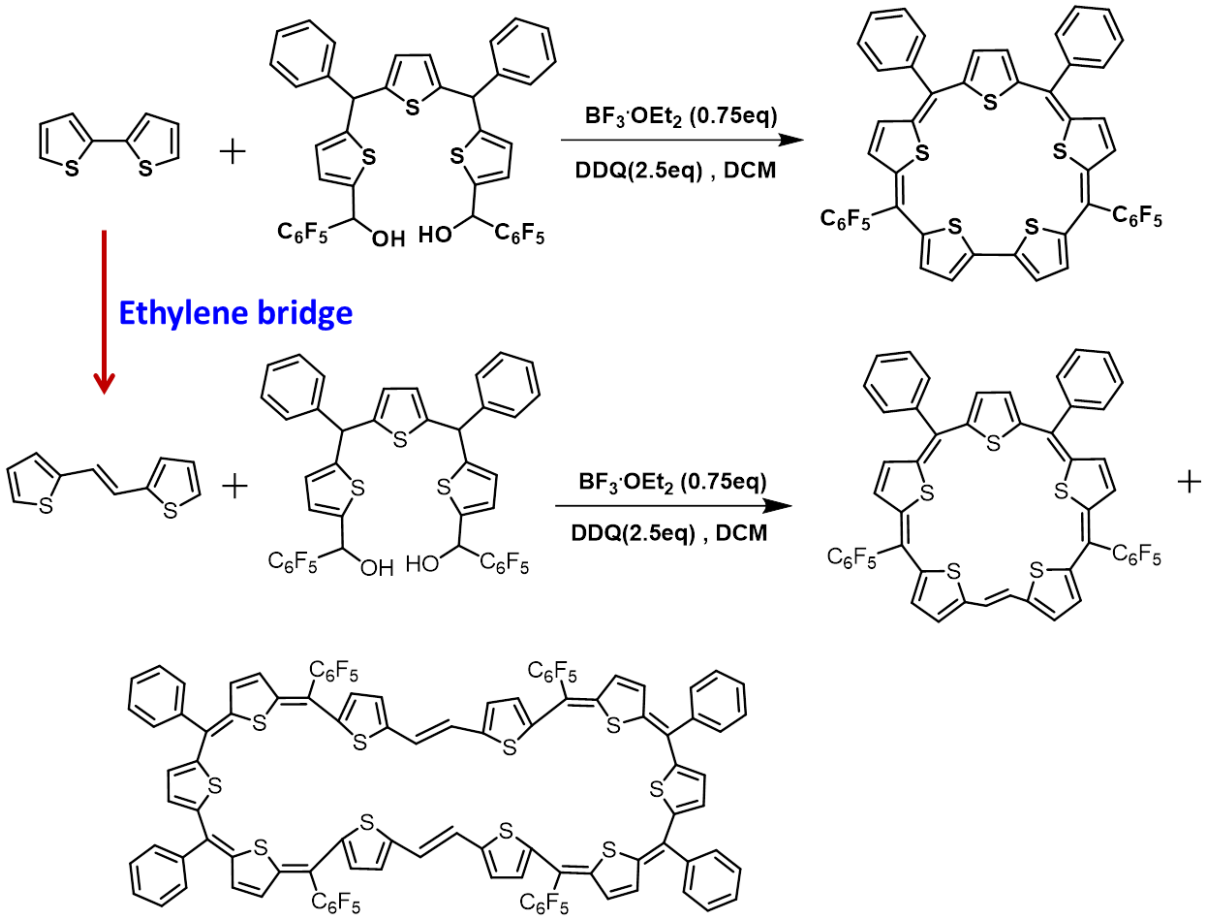

Scheme III.5: *Synthesis of core-modified 26π sapphyrin and its higher analogues.*

III.8.1 Isolation and Characterisation of [26]Sapphyrin

Ethylene bridged [26]sapphyrin (2.1.1.1.1) is the ring expanded macrocycle of 25π cyclopentathiophene radical macrocycle and isoelectronic to 26π aromatic cyclopentathiophene monoanion **III.11**. The macrocycle was identified as a brownish yellow coloured band in basic alumina column chromatography and the isolated yield was 11.5%. The composition of the macrocycle was confirmed by High Resolution Mass Spectrometry (HR-MS). It displayed an *m*/*z* value of 972.0159 corresponding to $C_{50}H_{22}F_{10}S_5$ (972.0165) (figure - III.23).

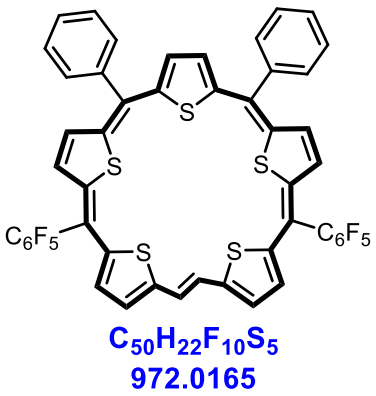

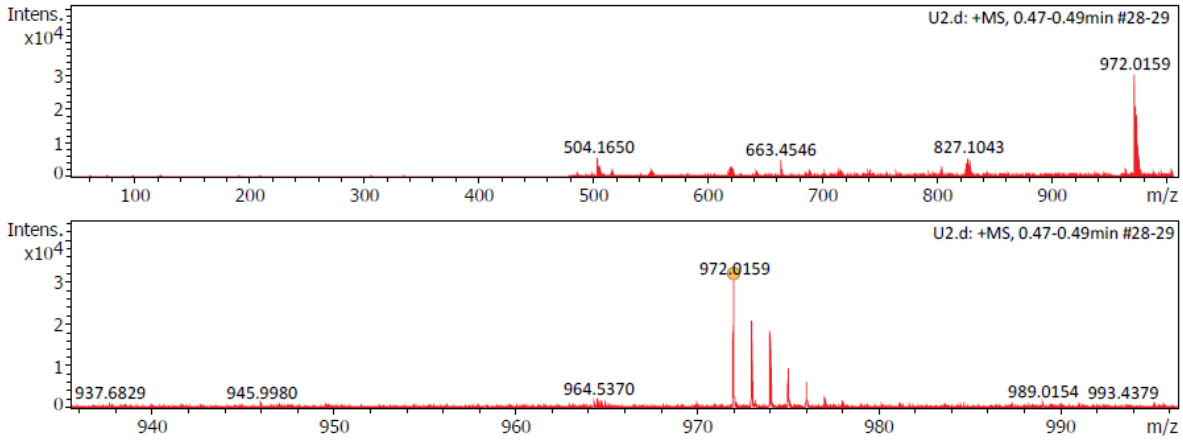

Figure III.23: *HR-ESI-TOF mass spectrum of* ***III.17****.*

III.8.2 ^{1}H NMR study of [26]sapphyrin

[24]sapphyrin, **III.14**, belongs to Huckel's 4nπ electronic system and is antiaromatic in nature. It displayed paratropic ring current in its ^{1}H NMR and from molecular structure it was confirmed with planar conformation. In contrast, [26]sapphyrin (2.1.1.1.1) accounts for 26π-electrons in the π-conjugation path and the macrocycle obeys Huckel's (4n+2)π rule. Therefore it is expected to be aromatic in nature. In its ^{1}H NMR spectrum at room temperature, β-protons of all the thiophene rings were well resolved in the region between δ 5.6 to 9.5 ppm (figure – III.24). Ethylene bridged protons were identified by higher *J-value*, one proton resonate at δ 9.95 ppm having the *J-value* 15.7 Hz and correlating with a proton at δ 6.43 ppm in ^{1}H-^{1}H COSY spectrum (figure – III.25), it confirms the *trans* nature of the double bond and while the phenyl protons resonated between δ 7.27 to 7.4 ppm, signifying an unsymmetrical geometry for the macrocycle. Also, it confirmed the absence of expected diatropic ring current and hence the macrocycle can be either non-aromatic or weakly aromatic in the solution state.

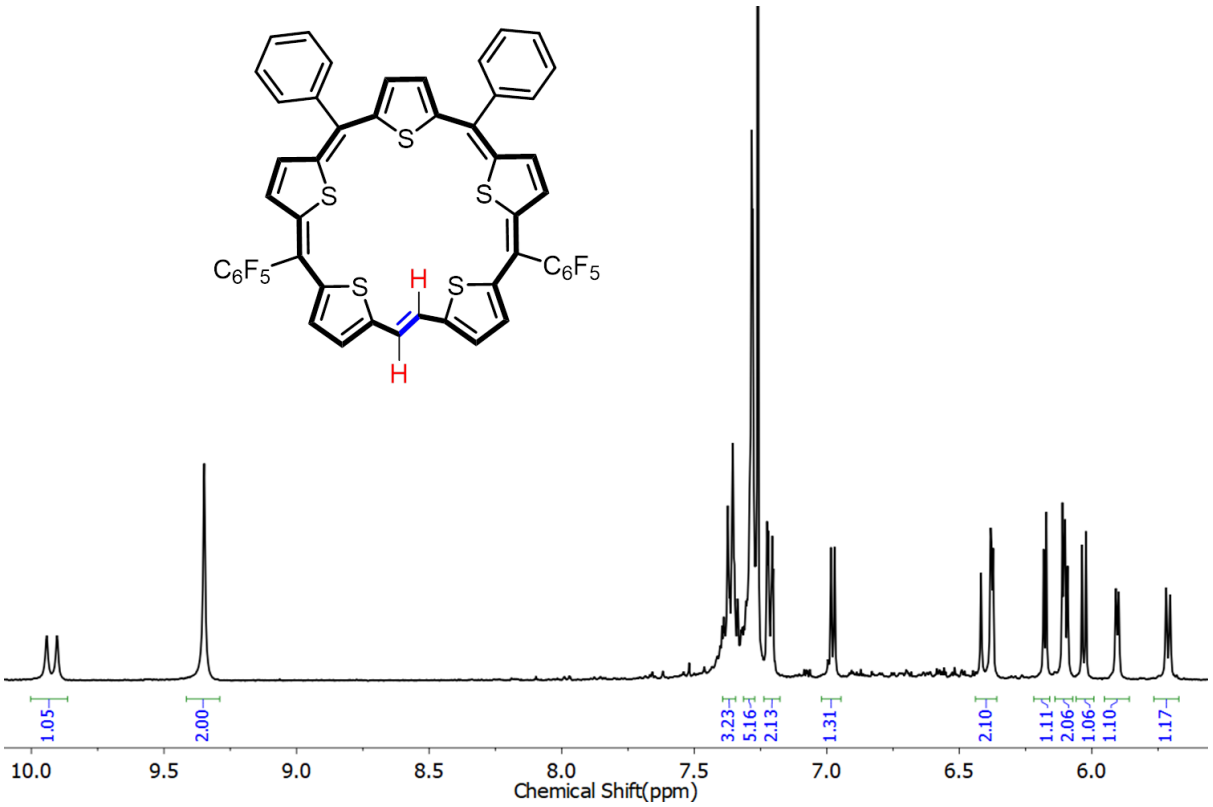

Figure III.24: *^{1}H NMR spectrum of **III.17** in Chloroform-d.*

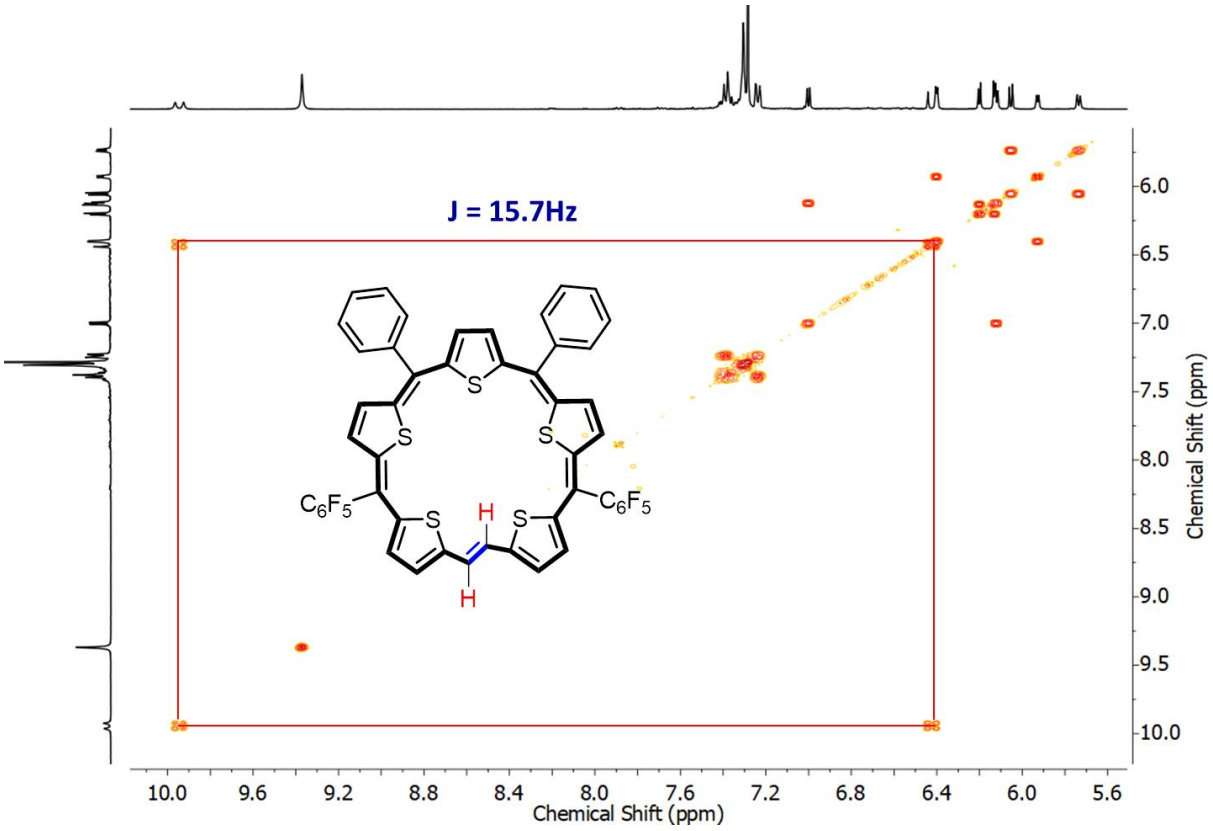

Figure III.25: *^{1}H-^{1}H COSY spectrum of **III.17** in Chloroform-d.*

III.8.3 Electronic absorption and Cyclic Voltammogram studies

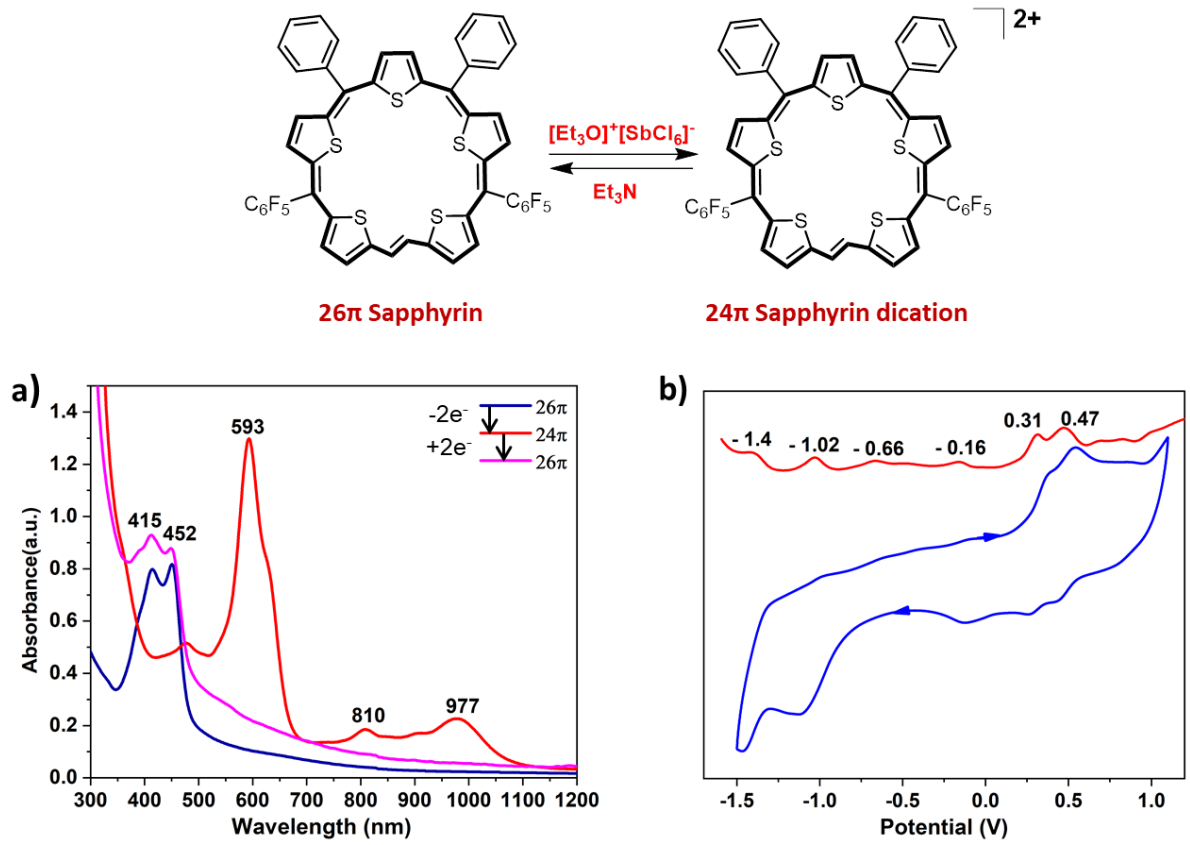

Figure III.26: *a) UV/vis/NIR absorption spectrum of 10^{-5} M solution of **III.17** (26π) and its oxidised species [**III.10**]$^{2+}$ (24 π) recorded in CH_2Cl_2. b) Cyclic voltammogram (CV, blue) and differential pulse voltammogram (DPV, red) of **III.17** in CH_2Cl_2 (with 0.1 M $(Bu)_4NPF_6$ as the supporting electrolyte).*

Ethylene bridged [26]sapphyrin, **III.17**, could be deduced as a non-aromatic macrocycle from its ^{1}H NMR spectrum. The macrocycle has 26π electrons in the global conjugation, and it displayed a doublet like band in the visible region of the electromagnetic spectrum. It displayed absorption maxima at 415 nm (129800) and 452 nm (131900) in dichloromethane (figure – III.26a). Absence of low energy bands suggested non-aromatic character of the macrocycle in the solution state. As observed earlier, because of its non-aromatic character, **III.17** can undergo two-electron ring oxidation from 26π to 24π-dicationic state. Upon the addition of oxidising agents like TFA or $NOBF_4$ or Meerwein's salt, the colour changes from brownish yellow to light pinkish colour suggestive of dicationic species, [**III.17**]$^{2+}$. The oxidized species shows bathochromic shift by more than 150 nm along with higher molar extinction coefficient (figure – III.26a). The suspected dicationic macrocycle displayed a Soret-like band at 593 nm (148020) along with transitions in the lower energy region between 810 (21090) and 977 nm (25770). Further, the [24]sapphyrin dication could be reduced to its neutral state by the addition of suitable reducing agents like triethyl amine or Zinc dust. It's

opto-electronic and redox properties were evaluated by electrochemical methods such as cyclic voltammetry (CV) and spectro-electrochemistry (SEC) studies.

Cyclic voltammogram (CV) and differential pulse voltammogram (DPV) for [26]sapphyrin, **III. 17** confirmed two oxidation potentials at + 0.31 V and + 0.47 V (figure 26b). Further, it also displayed four reduction potentials at - 0.16 V, - 0.66 V, - 1.02 V and – 1.4 V. Based on the potentials estimated from CV studies; spectro-electrochemical studies were conducted to record the absorption maxima at different oxidative potentials. Upon applying the first oxidation potential at + 0.34 V, it displayed absorption at 510 nm suggesting the formation of a 25π radical cation (figure – III.27a). At the second oxidative potential of + 0.6 V, the 25π radical cation was completely oxidized to 24π dicationic species (figure – III.27b). It showed absorption maxima at 593 nm along with shorter bands in the lower region at 810 nm and 977 nm as observed in the chemical oxidation.

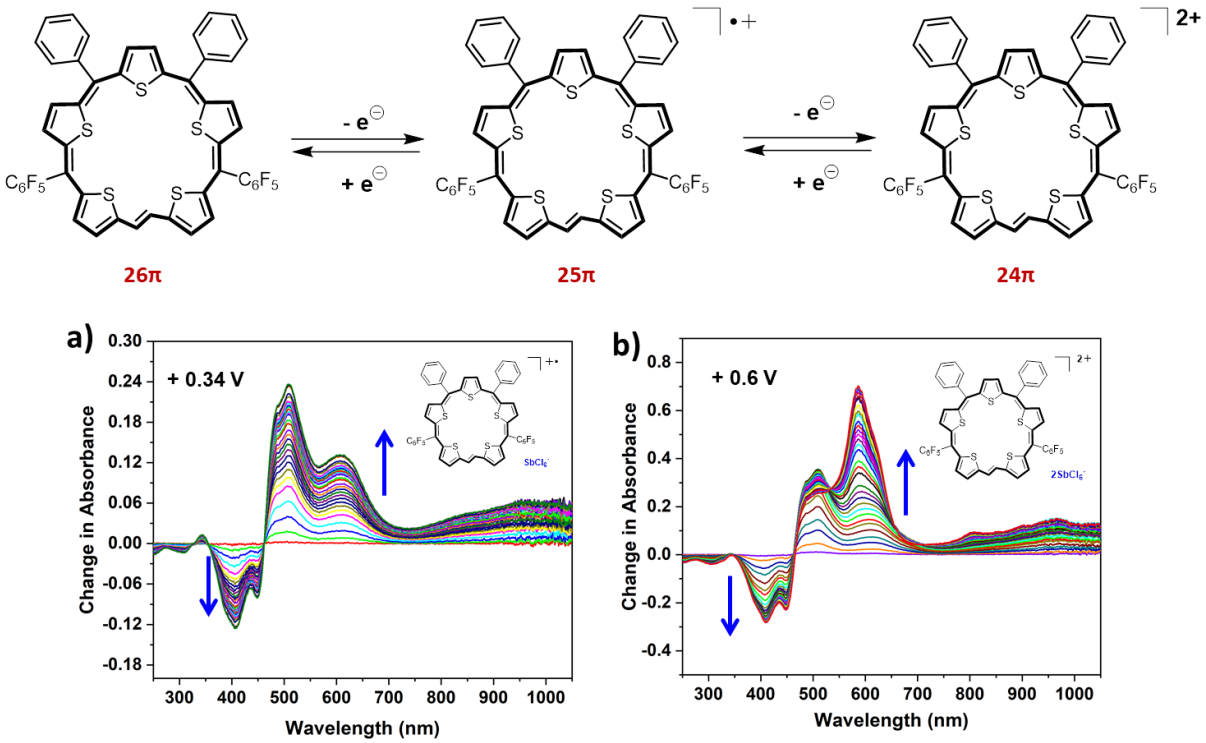

Figure III.27: *Spectro-electro chemistry studies of **III.17**. Change in absorption spectra of **III.17** after applying a potential of + 0.34 V and + 0.6 V, respectively.*

III.9.1 Isolation and Characterisation of [52]decaphyrin

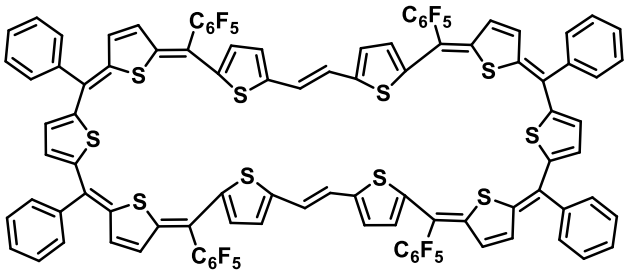

$C_{100}H_{44}F_{20}S_{10}$
1944.0331

Ethylene bridged [52]decaphyrin (2.1.1.1.1.2.1.1.1.1), **III.18**, was identified as a dark violet-blue coloured solution isolated after [26]sapphyrin by repeated basic alumina column and also by size exclusion chromatography in 1.2% yields. The product formation was confirmed by High Resolution Mass Spectrometry (HR-MS), in which macrocycle displayed *m*/*z* value of 1944.0392 corresponding to $C_{100}H_{44}F_{20}S_{10}$ (1944.0331) (figure – III.28).

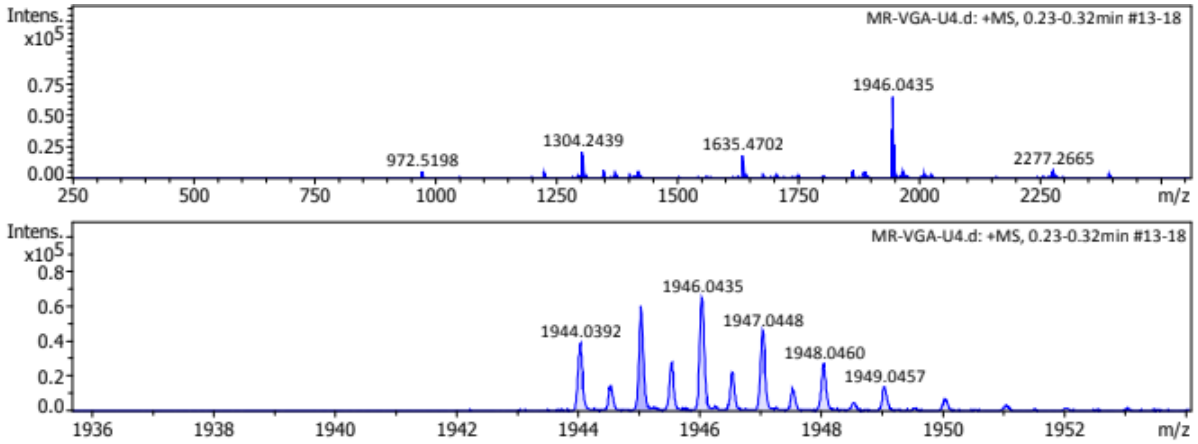

Figure III.28: *HR-ESI-TOF mass spectrum of* ***III.18****.*

III.9.2 ^{1}H NMR study of [52]decaphyrin

Ethylene bridged [52]decaphyrin, **III.18**, accounts for 52π electrons and matches Huckel's antiaromatic system due to 4nπ electron rule. In the ^{1}H NMR, it was expected to show paratropic ring current effect for antiaromatic character. But all protons resonated in the region δ 6.00 to 7.6 ppm at room temperature (figure – III.29). Therefore these chemical shift values do not signify sufficient paratropic ring current effect and hence can be classified as non-antiaromatic macrocycle. As like [48]decaphyrin, this macrocycle can be envisaged to have C_2-axis of symmetry because it displayed only five signals instead of six signals. Among them, four signals correspond to β-protons of all the thiophene rings and one signal

for ethylene protons. Due to less number of signals and also to study its fluxional behaviour variable temperature ^{1}H NMR spectra was recorded up to 220 K (figure – III.30). All the six signals are well resolved at 238 K and macrocycle displayed four doublets and two singlets. All phenyl protons resonated at δ 7.5 ppm. In the ^{1}H-^{1}H correlation spectrum (figure – III.31), four doublets of β-protons of thiophene showed the two correlations to confirm the neighbouring protons from each thiophene unit. From this ^{1}H NMR study, it's clear that akin to [48]decaphyrin, this 52π macrocycle is also expected to adopt a non-planar conformation with ethylene bridges oriented at the centre of the macrocycle.

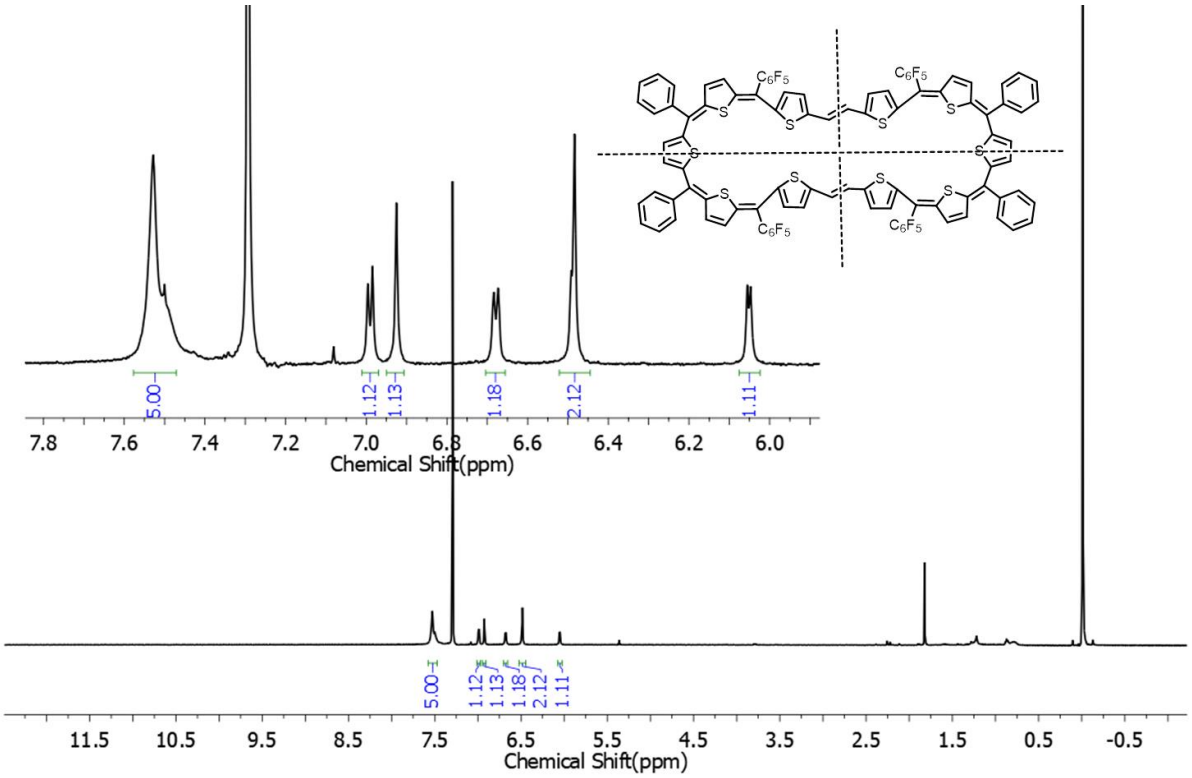

Figure III.29: *^{1}H NMR spectrum of **III.18** in Chloroform-d at 238 K.*

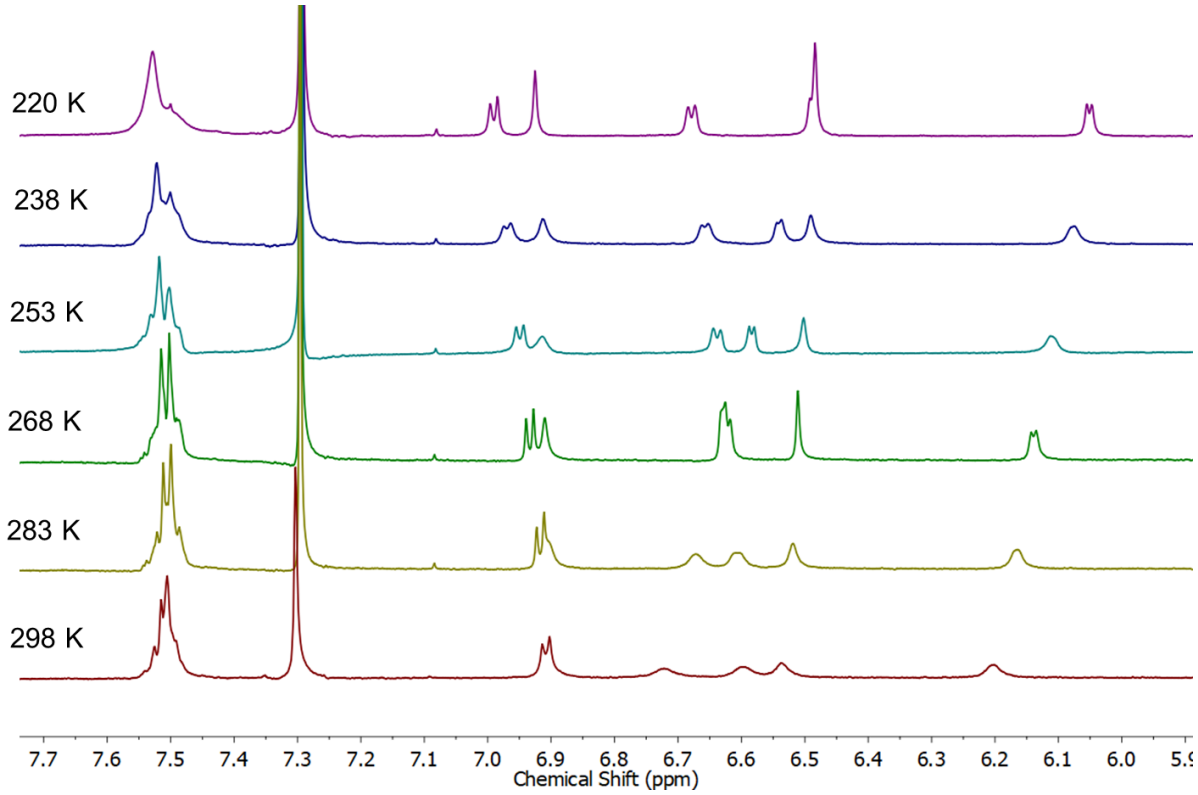

Figure III.30: *Variable temperature ^{1}H NMR spectra of **III.18** in Chloroform-d from 298 K to 220 K.*

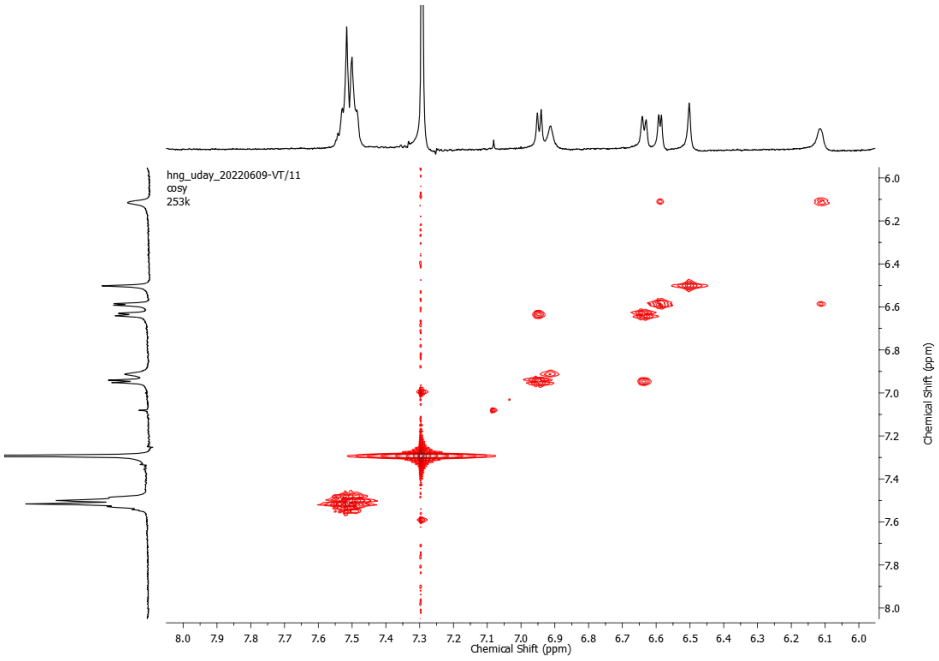

Figure III.31: *^{1}H-^{1}H COSY spectrum of **III.18** in Chloroform-d.*

III.9.3 Electronic absorption studies

In the electronic absorption spectrum [48]decaphyrin, **III.14**, displayed λ_{max} at 581 nm (ε) and the macrocycle was characterized as non-antiaromatic both in solution and solid states. Ethyelene bridged [52]decaphyrin, **III.18**, has four more π-electrons and the macrocycle accounts for 52π electrons in the global conjugation, but displayed non-antiaromatic character in the solution state. In the electronic absorption **III.18** displayed absorption maxima at 583 nm (211900) along with a shorter band at 407 nm (87860) in dichloromethane (figure – III.32). Absence of low energy bands suggested a non-planar conformation of the macrocycle in the solution state. Because of its extended π-conjugation and non-antiaromatic character, the macrocycle can be susceptible for two-electron ring oxidation as observed in previous examples. Addition of oxidising agents like TFA or $NOBF_4$ or Meerwein's salt to **III.18** brought a quick and subtle colour changes from dark violet-blue colour changes to wine red colour. Absorption maxima of the oxidized species showed a red shift by more than 350 nm (figure – III.32) supporting the formation of 50π dicationic species. It displayed an absorption maxima with a broad band at 966 nm (285800) and a shorter band at 1421 nm (1950). [50]decaphyrin dicationic species undergoes a facile reversible oxidation to switch back to its neutral [52]decaphyrin state by the addition of triethyl amine or zinc powder as reducing agents.

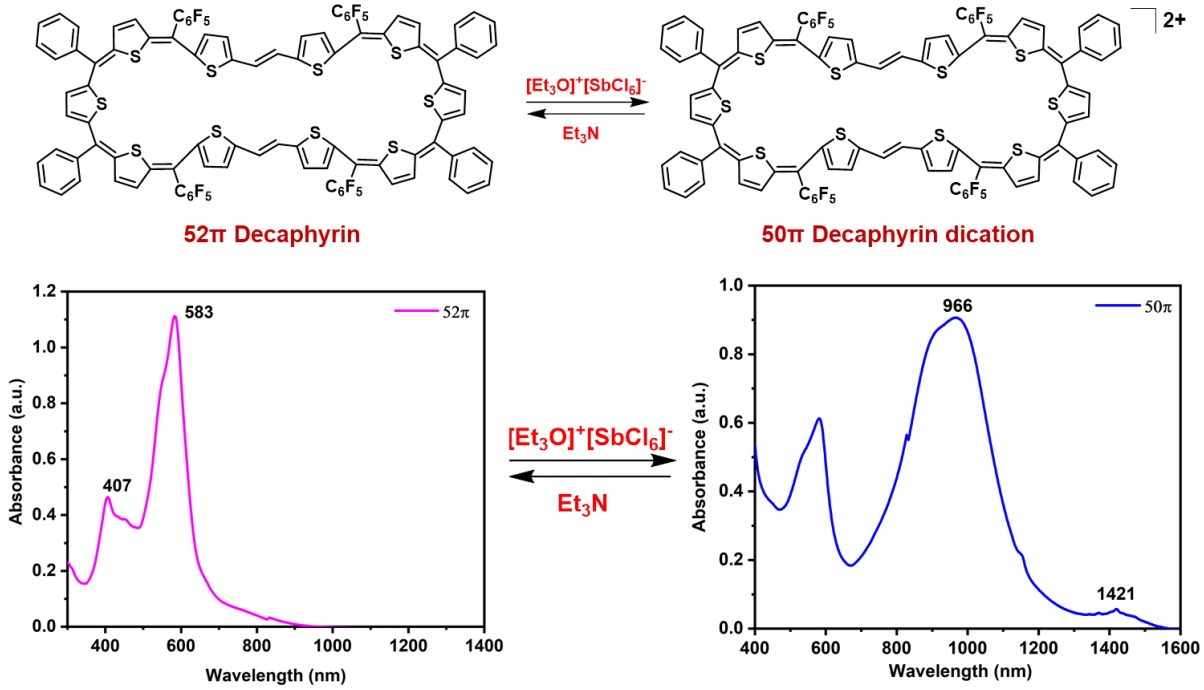

Figure III.32: *UV/vis/NIR absorption spectrum of 10^{-5} M solution of **III.18** (52π) and its oxidised species **[III.18]**$^{2+}$ (50π) recorded in CH_2Cl_2.*

III.10 Conclusions

This chapter describes the successful synthesis of ring contracted 24π antiaromatic pentathia sapphyrin (1.1.1.1.0), **III.10**, and ring expanded ethylene bridged 26π aromatic pentathia sapphyrin (2.1.1.1.1), **III.11**. They are isoelectronic to oxidised state of 24π cyclopentathiophene mono cation, **III.9b**, and reduced state of 26π cyclopentathiophene mono anion, **III.9a**, respectively. ^{1}H NMR spectrum of **III.10** displayed paratropic ring current effect and a planar conformation from single crystal X-ray diffraction studies. It confirms the anti-aromatic nature of the macrocycle and its facile two-electron oxidation to yield the aromatic 22π dicationic species. The oxidized species shows diatropic ring current in ^{1}H NMR to confirm the aromatic nature of the macrocycle. 26π sapphyrin didn't display the expected diatropic ring current in its ^{1}H NMR and macrocycle is classified as non-aromatic in solution state. Both 24π and 26π sapphyrin macrocycles undergo reversible two-electron ring oxidation through the formation of radical cation intermediate confirmed by spectro-electro chemistry studies. 48π decaphyrin (1.1.1.1.0.1.1.1.1.0) and ethylene bridged 52π decaphyrin (2.1.1.1.1.2.1.1.1.1) did not display any significant ring current suggesting that they are non-antiaromatic and non-aromatic in solution state respectively. X-ray crystallographic studies revealed, 48π decaphyrin as a non-planar twisted, 'figure eight' conformation confirming its non-antiaromatic character. 52π decaphyrin displayed the same pattern of ^{1}H NMR as observed in the 48π decaphyrin. It is expected that this macrocycle also adopts 'figure-of-eight' conformation in the solid state. Both macrocycles undergo two-electron reversible ring oxidation to their respective dicationic state. 72π pentadecaphyrin (1.1.1.1.0.1.1.1.1.0.1.1.1.1.0) was the largest expanded macrocycle of this series. However, it did not display significant paratropic ring current effect confirming the non-antiaromatic character in the solution state. Yet, it was also susceptible to undergo reversible two-electron ring oxidation. Its oxidised dicationic species showed a strong red shift in the NIR region of the electromagnetic spectrum.

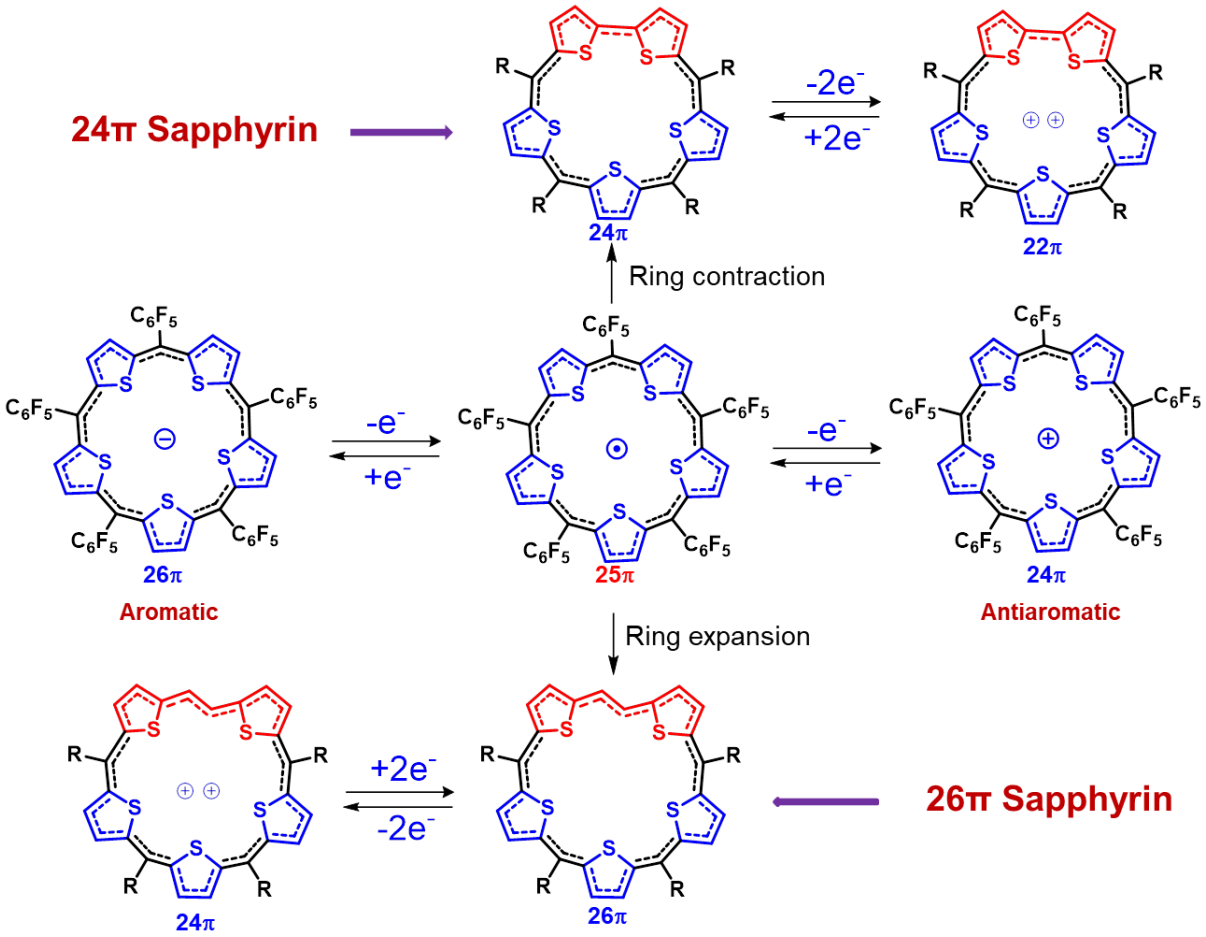

III.11 General Experimental Methods

Column chromatography was performed on silica gel (100-200) in glass columns for the purification of precursors and Macrocycles was isolated through basic alumina column and also by size exclusion chromatography. ^{1}H-NMR spectra were recorded on a Bruker 400 MHz spectrometer. Chemical shifts were reported as the delta scale in ppm relative to $(CH_3)_2CO$ (δ = 2.05 ppm) or CD_2Cl_2 (δ = 5.51 ppm) or $CDCl_3$ (δ = 7.26 ppm) or Tetrahydrofuran-d_8 (δ = 3.58 and 1.73 ppm). Electronic spectra were recorded on a Shimadzu UV-3600 spectrophotometer and a quartz cuvette of path length 1 cm, over the range of 300-2000nm. High Resolution Mass spectra were obtained using WATERS G2 Synapt Mass Spectrometer. Single-crystal diffraction analysis data were collected at 100K with a BRUKER KAPPA APEX II CCD Duo diffractometer (operated at 1500 W power: 50 kV, 30 mA) using graphite-monochromated Mo Kα radiation (λ = 0.71073 Å). In case of disordered solvent molecules, the contributions to the scattering arising from the disordered solvents in the crystal were removed by use of the utility SQUEEZE in the PLATON software package.

Cyclic voltammetry (CV) and Differential pulse voltammetry (DPV) measurements were carried out on a CH electrochemical system using a conventional three-electrode cell in dry CH_2Cl_2 containing 0.1 M tetrabutylammonium perchlorate (TBAP) as the supporting electrolyte. Measurements were carried out under an argon atmosphere. A glassy carbon (working electrode), a platinum wire (counter electrode), and saturated Ag/Ag^+ (reference electrode) were used. The final results were calibrated with the ferrocene/ferrocenium couple.

Materials: Dichloromethane (CH_2Cl_2) was dried by refluxing and distillation over P_2O_5. Tetrahydrofuran (THF) was dried by refluxing and distillation over Sodium metal and benzophenone used as indicator. Thiophene, benzaldehyde and pentafluorobenzaldehyde were freshly distilled prior to use. Other reagents and solvents were of commercial reagent grade and were used without further purification.

Synthesis of 2, 2'-Bithiophene:

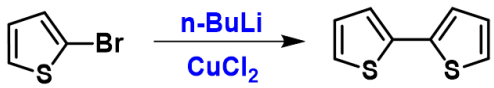

71%

In a flame dried two necks round bottom flask, 2-bromothiophene (1 mmol) was dissolved in the anhydrous diethyl ether under nitrogen atmosphere and takes the temperature to -78 ^{0}C and n-BuLi in hexane (1.2 mmol) was added dropwise. Then reaction mixture allowed stir for 10mins in the same temperature. Then anhydrous $CuCl_2$ (1.5 mmol) was added at -60 ^{0}C in one portion, continued the stirring for one hour. Then the reaction mixture slowly warmed to room temperature and stirring continued overnight. The reaction was quenched by water and followed by extracted with EtOAc and the compound was dried over Na_2SO_4 the product was purified by silica gel column chromatography using hexane as eluent[10]. The product is light blue oil and isolated yield is 71.3%.

^{1}H NMR ($CDCl_3$, 400 MHz): δ 6.99–7.01 (m, 2H), 7.16–7.17 (m, 2H), 7.19–7.20 (m, 2H)

Synthesis of (*E*)-2-[2-(thiophen-2yl) vinyl]thiophene:

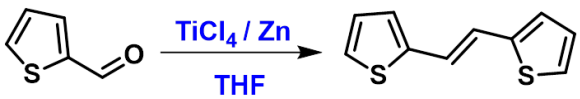

78%

To a flame dried two necks round bottom flask, anhydrous THF was added, followed by TiCl4 was slowly added and the reaction mixture stirred at 0 °C for 20 mins. Later zinc

powder was added portion wise, and the reaction mixture refluxed for one hour. After the reaction mixture cooling to 0 °C, 2-thiophenecarboxaldehyde and pyridine was added. The mixture was refluxed overnight, the reaction quenched by ice water and extracted with ethyl acetate and dried over Na_2SO_4. The residue was purified by column chromatography by silica gel column chromatography and hexane as eluent[11]. The product obtained as white solid and yield was 78%.

^{1}H NMR ($CDCl_3$, 400 MHz): δ 7.18 (d, 2H), δ 7.04 (m, 4H), δ 6.99 (t, 2H).

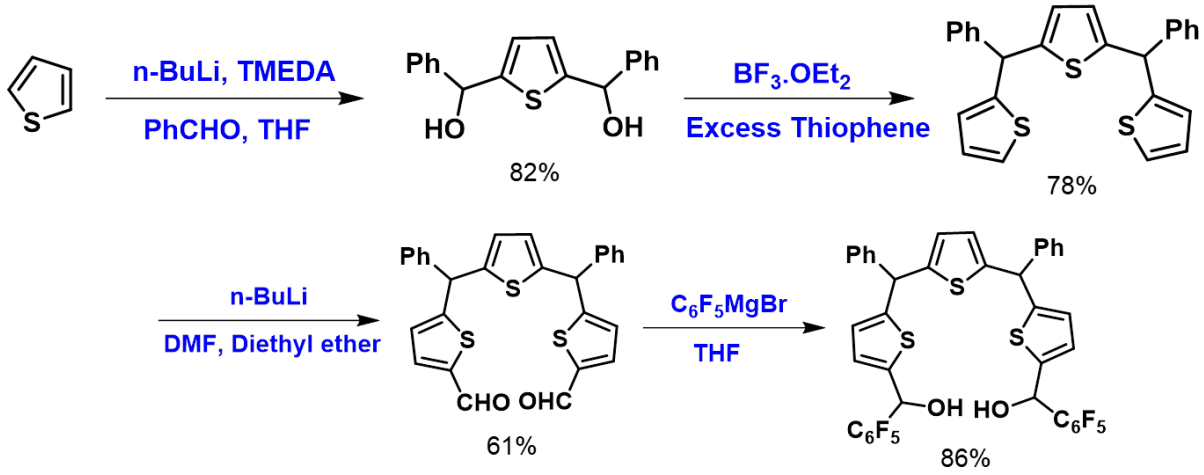

Preparation of 2, 5-Bis(phenylhydroxymethyl)thiophene:

In dry round bottom flask, n-BuLi (2.5 mmol) was added to a solution containing thiophene (1 mmol) in dry n-hexane in nitrogen atmosphere, followed by the addition of TMEDA (2.5 mmol) and reflux the reaction mixture for about one hour, and then cool the reaction mixture to 0 ^{0}C, then benzaldehyde (3 mmol) in THF (25ml) was added dropwise and continued the stirring another three hours. The reaction mixture was quenched by the saturated NH_4Cl and extracted by EtOAc and purifies the diol by recrystallization by dichloromethane/n-hexane combination. The product was white powder and the obtained in 82% yield.

^{1}H NMR ($CDCl_3$, 400 MHz): δ = 7.44-7.45 (m, 4H), 7.34-7.40 (m, 4H), 7.31-7.33 (m, 2H), 6.72 (s, 2H), 5.97 (s, 2H), 2.46 ppm (brs, 2H).

5, 5'-Trithienyldimethane:

Thiophene diol taken in excess of thiophene in a dried round bottom flask and BF3.OEt2 added in dark and stir the reaction for about 30 mins and progress of the reaction confirmed by the thin layer chromatography. Organic compound quenched extracted by dichloromethane and purified through silica column chromatography n-hexane as eluent and product isolated in 78% yield.

^{1}**H NMR** (400 MHz, $CDCl_3$): δ 7.21-7.36 (m, 10H), 7.18 (dd, 2H), 6.95 (d, 2H), 6.81 (m, 2H), 6.61(s, 2H), 5.77 (s, 2H).

5, 5'-Trithienyldimethane-2, 2'-dicarbaldehyde:

In flame dried RB, trithienyldimethane (1.1 mmol) taken in dry diethyl ether in nitrogen atmosphere, n-butyl lithium (5 mmol) was added dropwise to a stirred solution. Dimethylformamide (5 mmol) in diethyl ether was added dropwise with stirring at room temperature, and continued stirring for another three hours. The mixture was quenched by dilute hydrochloric acid and extracted by EtOAc, dried and evaporated. The product was purified by silica column chromatography (20% EA: PE) to give an orange residue at 61% yield.

^{1}**H NMR** (400 MHz, $CDCl_3$): δ 9.81 (2H, s), 7.28-7.33 (10H, m), 7.61 (2H, d), 6.94 (2H, d), 6.66 (2H, s), 5.77 (2H, s).

5, 5'-Trithienyldimethane-2, 2'-bis (perfluorophenyl)dicarbinol:

Trithienyl dialdehyde (1 mmol) taken in dry THF under nitrogen atmosphere and freshly prepared Grignard reagent (C_6F_5MgBr, 2.7 mmol) was added at 0 °C. Stirring was continued for another three hours and the reaction quenched by the saturated NH_4Cl. The reaction mixture extracted to organic layer by ethyl acetate and dried over Na_2SO_4 and the product purified by the silica column chromatography and the isolated brown residue in 86% yield[12].

^{1}H NMR (400 MHz, $CDCl_3$): δ 7.33 -7.26 (5H, m), 7.71 (1H, d), 6.65 (1H, s), 6.61 (1H, s), 6.29 (1H, d), 5.68 (1H, s) 2.81(1H, d).

General synthetic procedure for 24π and 26π Pentathia Sapphyrin and its higher analogues and their dications: In a flame-dried 250mL two neck round bottomed flask, one equivalent of Bithiophene or ethylene bridged bithiophene and 1.2 equivalents of thiophene based tripyrromethane diol were taken and dissolved in 100 ml dry dichloromethane and degassed with N_2 for ten minutes. Then, a catalytic amount of Boron trifluoride diethyl etherate ($BF_3{\cdot}OEt_2$) was added under dark using a syringe. After stirring for two hours, 2.5 equivalents of DDQ were added, opened to air and stirring continued for an additional two hours. The resultant solution was passed through a short bed of basic alumina column. This mixture was concentrated and further purified by basic alumina column chromatography using CH_2Cl_2/Hexane as eluent and Size Exclusion Chromatography (SEC) using Toluene or THF. The dications were generated by the addition of TFA to a solution of the macrocycle in

dichloromethane. Dicationic salt of hexachloroantimonate was prepared as per earlier report[13].

III.10: ^{1}**H NMR** (400 MHz, Chloroform-*d*) δ 7.17 – 7.03 (m, 3H), 6.73 – 6.62 (m, 2H), 5.16 (d, *J* = 3.9 Hz, 1H), 4.81 (d, *J* = 3.9 Hz, 1H), 4.42 (d, *J* = 6.0 Hz, 1H), 4.37 (s, 1H), 4.24 (d, *J* = 6.0 Hz, 1H). **UV/Vis/NIR** (CH_2Cl_2): λ_{max} nm (ε) $Lmol^{-1}cm^{-1}$ = 397 (99760), 430 (150780). **HR-MS** (ESI-TOF): m/z = 946.0003 (found), 946.0009 (Calcd. For $C_{48}H_{20}F_{10}S_5$).

Selected Crystal data of III.10: $C_{48}H_{20}F_{10}S_5$, (M_r = 946.0006), monoclinic, space group *P* $2_1/n$, *a* = 16.227(7), *b* = 14.652(7), *c* = 20.179(9) Å, $\alpha = 90^0$, $\beta = 100.212^0$, $\gamma = 90^0$; *V* = 4721.13 $Å^3$, *Z* = 1, *T* = 100 K , D_{calcd} = 1.053 gcm^{-3}, R_1 = 0.0554 (I > 2sigma (I)), R_w (all data) = 0.097, GOF = 1.001;

[III.10]$^{2+}$: ^{1}**H NMR** (400 MHz, Methylene Chloride-d_2) δ 11.76 (s, 1H), 11.15 (d, 4H), 8.96 – 8.76 (m, 2H), 8.30 (tt, 3H). **UV/Vis/NIR** (CH_2Cl_2): λ_{max} nm (ε) $Lmol^{-1}cm^{-1}$ = 534 (403400), 720 (10890), 805 (37900). **HR-MS** (ESI-TOF): m/z = 472.9995 (found), 473.00045 (Calcd. For $C_{48}H_{20}F_{10}S_5)^{2+}$.

III.14: ^{1}**H NMR** (500 MHz, THF-d_8) δ 7.51 – 7.44 (m, 3H), 7.40 – 7.33 (m, 2H), 7.03 (d, *J* = 4.1 Hz, 1H), 6.61 (d, *J* = 4.1 Hz, 1H), 6.48 (d, *J* = 5.9 Hz, 1H), 6.45 (s, 1H), 6.39 (d, *J* = 5.9 Hz, 1H). **UV/Vis/NIR** (CH_2Cl_2): λ_{max} nm (ε) $Lmol^{-1}cm^{-1}$ = 395 (132100), 581 (167300). **HR-MS** (ESI-TOF): m/z = 1892.0186 (found), 1892.0018 (Calcd. For $C_{96}H_{40}F_{20}S_{10}$).

Selected Crystal data of III.14: $C_{96}H_{40}F_{20}S_{10}$, (M_r = 1892.18), monoclinic, space group *P* $2_1/n$, *a* = 24.838 (8), *b* = 33.241 (11), *c* = 14.229 (5) Å, $\alpha = 90^0$, $\beta = 93.694^0$, $\gamma = 90^0$; *V* = 11723.7(2) $Å^3$, *Z* = 1.2, *T* = 100 K , D_{calcd} = 1.053 gcm^{-3}, R_1 = 0.0654 (I > 2sigma (I)), R_w (all data) = 0.0957, GOF = 1.004;

[III.14]$^{2+}$: UV/Vis/NIR (CH_2Cl_2): λ_{max} nm (ε) $Lmol^{-1}cm^{-1}$ = 487 (297500), 865 (353300), 1133 (37890), and 1287 (60200).

III.15: ^{1}**H NMR** (500 MHz, Acetone-d_6, 238 K) δ 8.17 (d, *J* = 4.2 Hz, 1H), 7.72 (d, *J* = 4.2 Hz, 1H), 7.55 – 7.51 (m, 2H), 7.41 (s, 2H), 7.34 – 7.25 (m, 2H), 7.19 (s, 1H), 7.11 (d, *J* = 4.2 Hz, 1H), 6.98 (d, *J* = 4.2 Hz, 1H), 6.89 (d, *J* = 4.0 Hz, 1H), 6.66 (d, *J* = 3.3 Hz, 1H), 6.56 (d, *J* = 4.1 Hz, 1H), 6.52 (d, *J* = 5.8 Hz, 1H), 6.47 (d, *J* = 4.3 Hz, 1H), 6.45 – 6.39 (m, 2H), 6.31 (d, *J* = 5.8 Hz, 1H), 6.20 (d, *J* = 4.1 Hz, 1H). **UV/Vis/NIR** (CH_2Cl_2): λ_{max} nm (ε) $Lmol^{-1}cm^{-1}$ = 438 (374300), 664 (341100). **HR-MS** (ESI-TOF): m/z = 2838.0103 (found), 2838.0027 (Calcd. For $C_{144}H_{60}F_{30}S_{15}$).

[III.15]$^{2+}$: UV/Vis/NIR (CH_2Cl_2): λ_{max} nm (ε) $Lmol^{-1}cm^{-1}$ = 732 (323200), 1237(450200).

III.17: ^{1}H NMR (400 MHz, Chloroform-*d*) δ 9.94 (d, *J* = 15.7 Hz, 1H), 9.37 (s, 2H), 7.44 – 7.36 (m, 3H), 7.35 – 7.29 (m, 5H), 7.26 – 7.21 (m, 2H), 7.00 (d, *J* = 5.3 Hz, 1H), 6.46 – 6.38 (m, *J* = 15.7, 4.1 Hz, 2H), 6.20 (d, *J* = 4.1 Hz, 1H), 6.13 (dd, *J* = 4.1 Hz, 2H), 6.05 (d, *J* = 5.9 Hz, 1H), 5.93 (d, *J* = 4.1 Hz, 1H), 5.74 (d, *J* = 5.8 Hz, 1H). **UV/Vis/NIR** (CH_2Cl_2): λ_{max} nm (ε) $Lmol^{-1}cm^{-1}$ = 415 (129800), 452(131900). **HR-MS** (ESI-TOF): m/z = 972.0159 (found), 972.0165 (Calcd. For $C_{50}H_{22}F_{10}S_5$).
[III.17]$^{2+}$: UV/Vis/NIR (CH_2Cl_2): λ_{max} nm (ε) $Lmol^{-1}cm^{-1}$ = 593 (148020), 810(21090), and 977 (25770).

III.18: ^{1}H NMR (500 MHz, Chloroform-*d*) δ 7.51 (m, 5H), 6.97 (d, *J* = 5.7 Hz, 1H), 6.91 (s, 1H), 6.66 (d, *J* = 5.7 Hz, 1H), 6.54 (d, *J* = 4.1 Hz, 1H), 6.49 (s, 1H), 6.08 (d, *J* = 4.1 Hz, 1H). **UV/Vis/NIR** (CH_2Cl_2): λ_{max} nm (ε) $Lmol^{-1}cm^{-1}$ = 407 (87860), 583 (211900). **HR-MS** (ESI-TOF): m/z = 1944.0392 (found), 1944.0392 (Calcd. For $C_{100}H_{44}F_{20}S_{10}$).
[III.17]$^{2+}$: UV/Vis/NIR (CH_2Cl_2): λ_{max} nm (ε) $Lmol^{-1}cm^{-1}$ = 966 (285800), 1421 (1950).

III.12 References:

1. Bauer, V. J.; Clive, D. L. J.; King, M. M.; Dolphin, D.; Harris, F. L.; Loder, J.; Wang, S. W. C.; Paine, J. B.; Woodward, R. B. Sapphyrins: Novel Aromatic Pentapyrrolic Macrocycles. *J. Am. Chem. Soc.* **1983**, *105* (21), 6429–6436.
2. Jonathan L. Sessler, Michael J. Cyr, and Vincent Lynch, Synthetic and Structural Studies of Sapphyrin, a 22-ir-Electron Pentapyrrolic "Expanded Porphyrin" *J. Am. Chem. Soc*. **1990**, *112*, 2810-2813.
3. Piotr J. Chmielewski, Lechoslaw Latos-Graiynski, and Krystyna Rachlewicz, 5, 10, 15, 20-Tetraphenylsapphyrin-Identification of a Pentapyrrolic Expanded Porphyrin in the Rothemund Synthesis, *Chem. Eur. J*. **1995**, *1*, 68-73.
4. Tamal Chatterjee, A. Srinivasan, Mangalampalli Ravikanth, and Tavarakere K. Chandrashekar, Smaragdyrins and Sapphyrins Analogues, *Chem. Rev.* **2017**, *117*, 3329−3376.
5. M. J. Broadhurst, R. Grigg and A. W. Johnson, the Synthesis of 22π-Electron Macrocycles. Sapphyrins and Related Compounds, ***J. Chem. Soc., Perkin Trans. 1***, **1972**, 2111-2116.
6. Jerzy Lisowski, Jonathan L. Sessler and Vincent Lynch, Synthesis and X-ray Structure of Selenasapphyrin, *Inorg. Chem*. **1995**, *34*, 3567-3572.
7. Narayanan, S. J.; Sridevi, B.; Chandrashekar, T. K.; Vij, A.; Roy, R. Novel Core-Modified Expanded Porphyrins with Meso-Aryl Substituents: Synthesis, Spectral and Structural Characterization. *J. Am. Chem. Soc.* **1999**, *121* (39), 9053–9068.

8. Alagar Srinivasan, Anand V. G., S. Jeyaprakash Narayanan, Simi K. Pushpan, M. Ravi Kumar, and Tavarekere K. Chandrashekar, Structural Characterization of Meso Aryl Sapphyrins, *J. Org. Chem.* **1999**, *64*, 8693-8697.
9. Gopalakrishna, T. Y.; Reddy, J. S.; Anand, V. G. An Amphoteric Switch to Aromatic and Antiaromatic States of a Neutral Air-Stable 25π Radical. *Angew. Chemie - Int. Ed.* **2014**, *53* (41), 10984–10987.
10. Satapathy, R.; Wu, Y. H.; Lin, H. C. Novel Dithieno-Benzo-Imidazole-Based Pb2+ Sensors: Substituent Effects on Sensitivity and Reversibility. *Chem. Commun.* **2012**, *48* (45), 5668–5670.
11. Peng, S. H.; Tu, W. Y.; Gollavelli, G.; Hsu, C. S. Synthesis of Diketopyrrolopyrrole Based Conjugated Polymers Containing Thieno[3,2-: B] Thiophene Flanking Groups for High Performance Thin Film Transistors. *Polym. Chem.* **2017**, *8* (22), 3431–3437.
12. Reddy, B. K.; Rawson, J.; Gadekar, S. C.; Kögerler, P.; Anand, V. G. A Naphthalene-Fused Dimer of an Anti-Aromatic Expanded Isophlorin. *Chem. Commun.* **2017**, *53* (58), 8211–8214.
13. Rathore, R.; Kumar, A. S.; Lindeman, S. V.; Kochi, J. K. Preparation and Structures of Crystalline Aromatic Cation-Radical Salts. Triethyloxonium Hexachloroantimonate as a Novel (One-Electron) Oxidant. *J. Org. Chem.* **1998**, *63* (17), 5847–5856.
14. Gopalakrishna, T. Y.; Anand, V. G., Reversible Redox Reaction between Antiaromatic and Aromatic States of 32π-Expanded Isophlorins. *Angew. Chem., Int. Ed.* **2014,** *53* (26), 6678-6682.

Chapter IV

Aromaticity in Thieno[3,2-b]thiophene incorporated Expanded Isophlorinoids

IV.1 Introduction

[18]Porphyrin macrocycle is highly tuneable for π-extension by extending the π-conjugation through peripheral modification/fusion, or by including additional heterocyclic units, or by increasing the number of carbons as in vinylogous porphyrinoids.[1] Further, functionalization of heterocyclic units such as pyrrole/ furan/ thiophene, or through fusion or oligomerisation can be employed as building blocks for π-expansion in a porphyrin network. These π-extended macrocycles have attracted significant interest for their potential applications in NIR dyes, NLO materials, as anion binders/sensors, photosensitizers, etc.[2] Among many methods for the π-extension, insertion of fused heterocyclic units like pyrrolopyrrole or furanofuran or thienothiophene in to the macrocyclic system can also alter the aromaticity and significantly decrease the HOMO-LUMO energy gap. Therefore these macrocycles are well known to display absorption maxima in the NIR region of the electromagnetic spectrum.[3]

Thieneo[3,2-b]thiophene heterocyclic unit, fused by two thiophene units accounts for six π-electrons along with two non-bonding electrons. Insertion of thieneothiophene in to porphyrin macrocycle by replacing the pyrrole unit not only extends the π-conjugation but also alters in aromaticity. Rath and co-workers have successfully synthesised three different 22π aromatic porphyrinoids by replacing two pyrrole units with thienothiophene units.[4] They discovered that macrocycle adopts a non-planar geometry due to the steric hindrance induced by the thienothiophene in the centre of macrocycle. Due to the extended π-extension all the three macrocycles displayed absorption maxima in the NIR region. Also they synthesised thienothiophene fused aromatic 30π heteroannulenes, which could sustain a planar conformation along with the thienothiophene unit. Moreover, it displayed diatropic ring current effect as an evidence for the aromatic character of the macrocycle. Further, because of an imine-like pyrrole, macrocycle undergoes protonation to yield the dicationic species which sustained a planar conformation and displayed a red shift in the NIR region.[5] Later, they also synthesised a 32π hexaphyrin bearing two thienothiophene subunits along with six meso-substituents. However, the macrocycle adopted a twisted non-planar conformation in the free base and attained quasi planar conformation upon protonation. These macrocycles also showed conformational fluxionality in free base and also in the protonated species. Due to its extended conjugation, the absorption maxima of free base and the diprotonated species was observed in the NIR region.[6] Similarly, Osuka and co-workers employed the thioenothiophene as an internally bridged moiety in [46]decaphyrin and showed that global

circuits of the macrocycle are doubly twisted and displayed the diatropic ring current along with Huckel's aromatic properties.[7]

Since thienithiophene has not been explored in an isophlorin network, it is expected that replacing a thiophene/ furan/ selenophene/ N-methyl pyrrole by thioenothiophene subunit will alter the aromaticity and affect its electronic properties. It can be envisaged that replacing two heterocyclic units in the macrocycle maintains the aromaticity and benefits in red shifted absorptions. Hence the aim is to synthesize, a 22π isophlorin by incorporating one thienothiophene by replacing the thiophene subunit in an isophlorin. It is well established that tetrathiophene 20π isophlorin, **IV.1**, undergoes a facile two-electron ring oxidation to yield the 18π aromatic dication, **IV.2** (scheme – IV.1a).[8] Now, it has to be evaluated for the possibility to alter the aromatic character without involving redox process. However, structurally it is possible to envisage that replacing the thiophene by thienothiophene adds two extra π-electrons along the conjugated pathway and hence alters the aromaticity (scheme – IV.2b). Another interesting task will be to synthesize a 34π hexaphyrin by maintaining the aromaticity of 30π isophlorin's extended the π-conjugation (scheme – IV.1c).[9] Hence two thiophene units will be replaced by two thienothiophene units to retain the aromatic character of the macrocycle, **IV.5**.

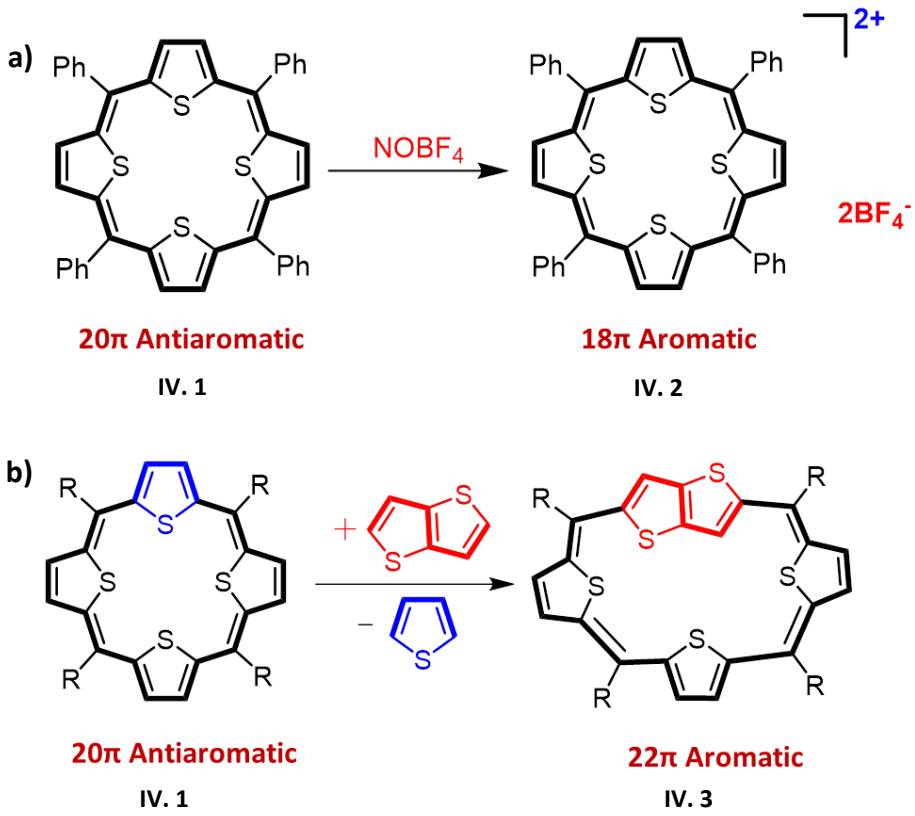

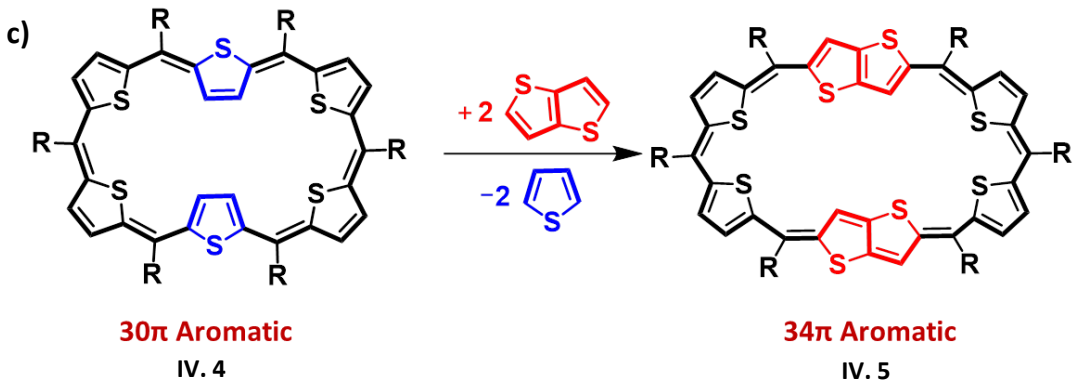

Scheme IV.1: *a) Oxidation of 20π isophlorin to 18π aromatic dication. b) Altering the aromaticity by the incorporation of thienothiophene. c) Extending the π-conjugation of 30π hexaphyrin to 34π hexaphyrin by the insertion of thienothiophene.*

IV.2.1 Synthesis and Characterisation of Thieno[3,2-*b*]thiophene incorporated 22π Isophlorin

Synthesis of thieno[3,2-*b*]thiophene incorporated 22π isophlorin, **IV.3**, was attempted by two different synthetic strategies. In the first synthetic pathway, the thieno[3,2-*b*]thiophene, **IV.6**, was condensed with thiophene based tripyrromethanediol, **IV.7**, in the presence of $BF_3.OEt_2$ under dark and inert conditions in dichloromethane. The mixture was stirred for two hours followed by the addition of DDQ as oxidising agent. Stirring was continued for another two hours open to air to yield the desired macrocycle, **IV.3** (scheme – IV.2). The macrocycle was purified through basic alumina column with DCM/Hexane as the eluent. It was obtained as a dark blue coloured compound in 11% yields. In an alternate strategy, thiophene diol, **IV.9**, was condensed with thieno[3,2-*b*]thiophene based tripyrromethane, **IV.8**, in the presence of $BF_3.OEt_2$ as an acid and DDQ as the oxidant to obtain the macrocycle in 7% isolated yields. The progress of product formation was confirmed by the Thin Layer Chromatography (TLC) and its composition was confirmed by the High Resolution Mass Spectrometry (HR-MS), in which the macrocycle displayed *m/z* value of 919.9844 corresponding to $C_{46}H_{18}F_{10}S_5$ (919.9852) (figure – IV.1).

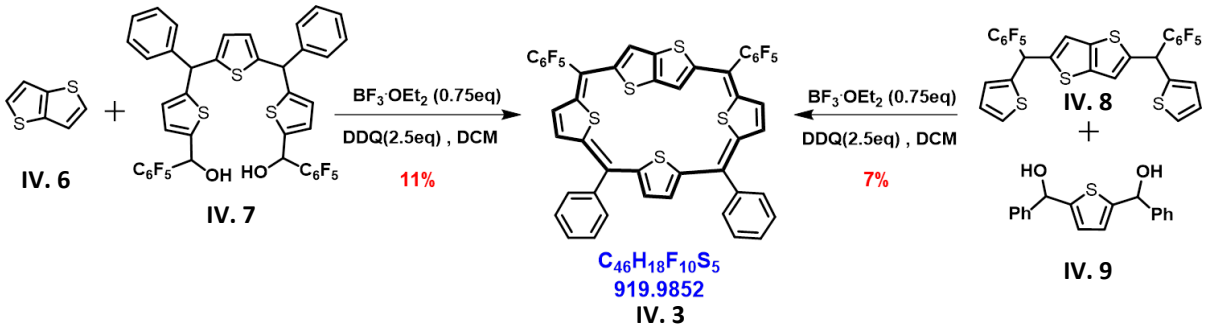

Scheme IV.2: *Synthesis of Thienothiophene incorporated 22π isophlorin **IV.3**.*

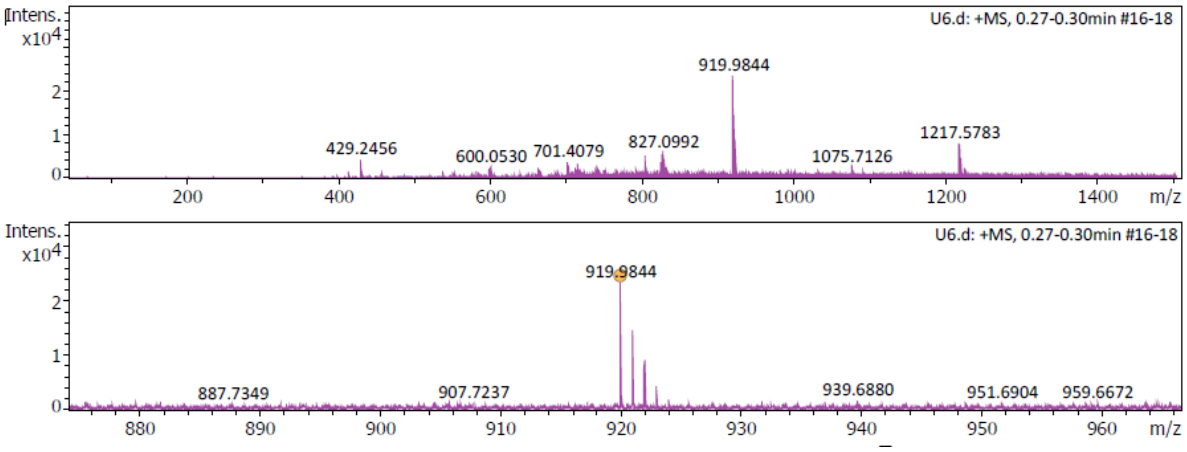

Figure IV.1: *HR-ESI-TOF mass spectrum of **IV.3**.*

IV.2.2 ^{1}H NMR study of 22π Isophlorin

The macrocycle, **IV.3**, has 22 π-electrons in the global conjugation and expected to be aromatic in accordance with Huckel's (4n+2) π electronic rule. It displayed a well resolved ^{1}H NMR spectrum at room temperature and resonances were observed in the region between δ 6.00 to 8.00 ppm (figure – IV.2). These chemical shift values do not signify diatropic ring current as expected of aromatic porphyrinoids suggesting that macrocycle is devoid of aromatic character in the solution state. Insertion of a bulky thienothiophene in the isophlorin network can induce a steric hindrance inside the core of the macrocycle leading to a non-planar structure. In the spectrum, the two thienothiophene β-protons are assigned to the resonance at δ 7.81 ppm, while and thiophene protons correspond to signals at δ 6.1 to 6.4 ppm. The phenyl protons are observed in the region between δ 7.1 to 7.4 ppm. ^{1}H-^{1}H COSY spectrum displayed two correlations (figure – IV.3); one correlation for the two neighbouring thiophene protons (b and c) and second correlation for phenyl protons (e and f).

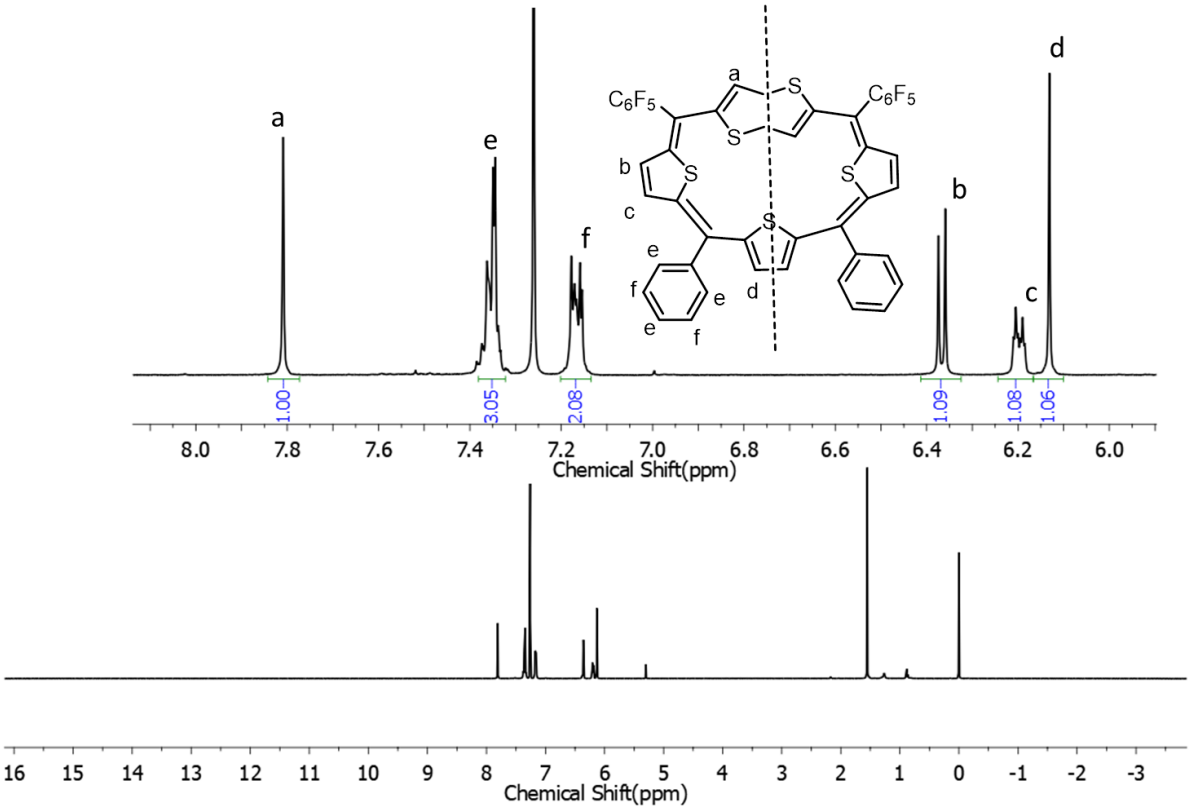

Figure IV.2: *^{1}H NMR spectrum of **IV.3** in Chloroform-d at 298 K.*

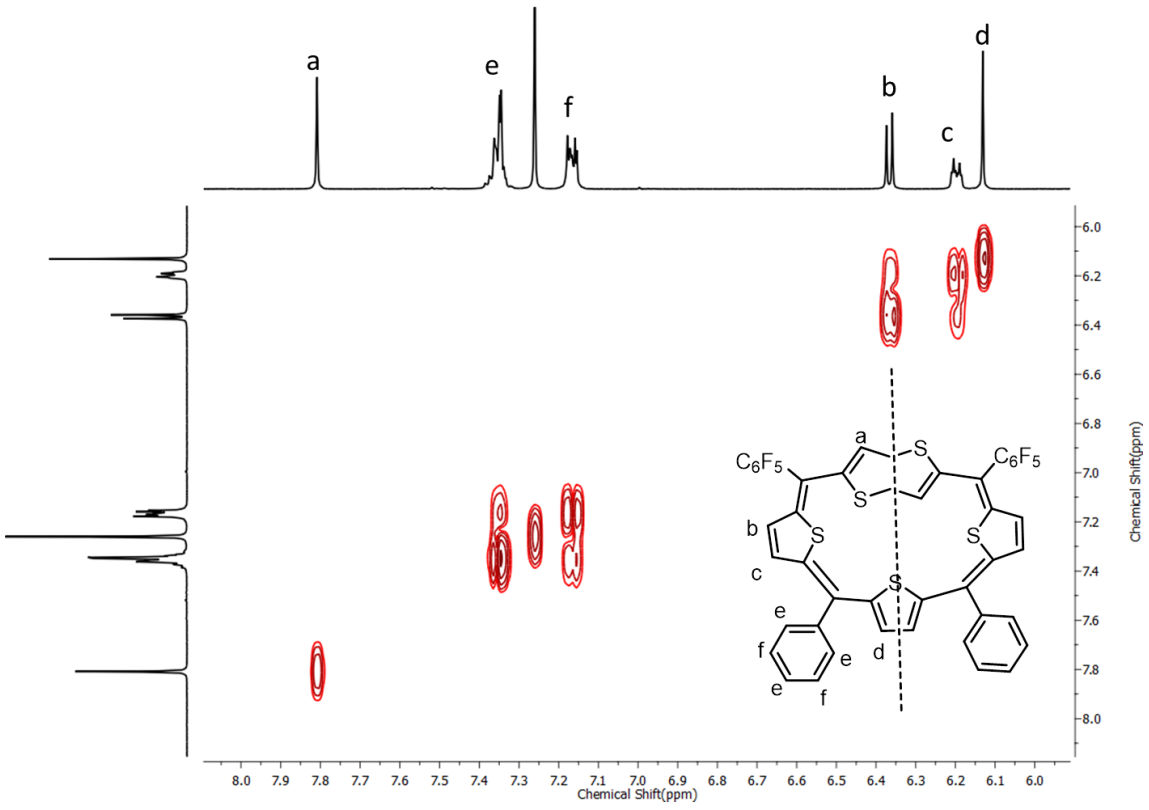

Figure IV.3: *^{1}H-^{1}H COSY spectrum of **IV.3** in Chloroform-d at 298 K.*

IV.2.3 Electronic absorption and Cyclic Voltammogram studies

It is well known that antiaromatic porphyrinoids undergo facile two-electron ring oxidation yield stable aromatic dication.[13] However, aromatic macrocycles are prone to undergo one-electron ring oxidation to yield radical cation species. Yet, two-electron ring oxidation is also possible in (4n+2)π species when macrocycles are either open shell diradical system or if they are characterized as weakly aromatic/non-aromatic in nature. [11]

Even though [22]isophlorin, **IV.3**, belongs to Huckel's aromatic (4n+2) π electron system, the macrocycle did not display diatropic ring current effect in its ^{1}H NMR spectrum and hence suggests non-aromatic character. [22]isophlorin, **IV.3**, is a dark blue coloured macrocycle. In the UV-visible spectrum, it displayed absorption maxima at 398 nm (109900) along with two shorter bands at 576 (27600) and 616 nm (29700) (figure – IV.4). Because of the non-aromatic character, **IV.3** can be expected to undergo facile two-electron ring oxidation to yield the 20π dicatioinic state, [**IV.3**]$^{2+}$. As expected, the addition of oxidising agents like TFA or $NOBF_4$ or Meerwein's salt, the dark blue coloured solution of **IV.3** undergoes a subtle change to yellow brownish along with a bathochromic shift by more than 350 nm (figure – IV.4a). The oxidized species displayed an absorption maximum at 789 nm (535600) along with a less intense band in the lower energy region at 1289 nm (4700). The oxidized species could be reduced back to its free base, by the addition of a suitable reducing agent like triethyl amine or Zinc dust. The opto-electronic and redox properties were evaluated by cyclic voltammetry (CV) and spectro-electrochemistry (SEC) studies.

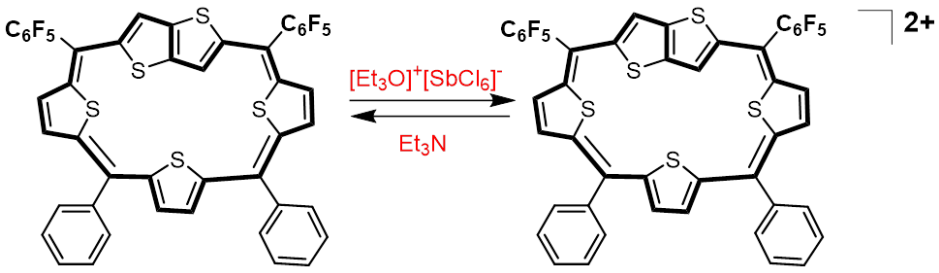

22π Isophlorin **20π Isophlorin dication**

IV. 3 **[IV. 3] $^{2+}$**

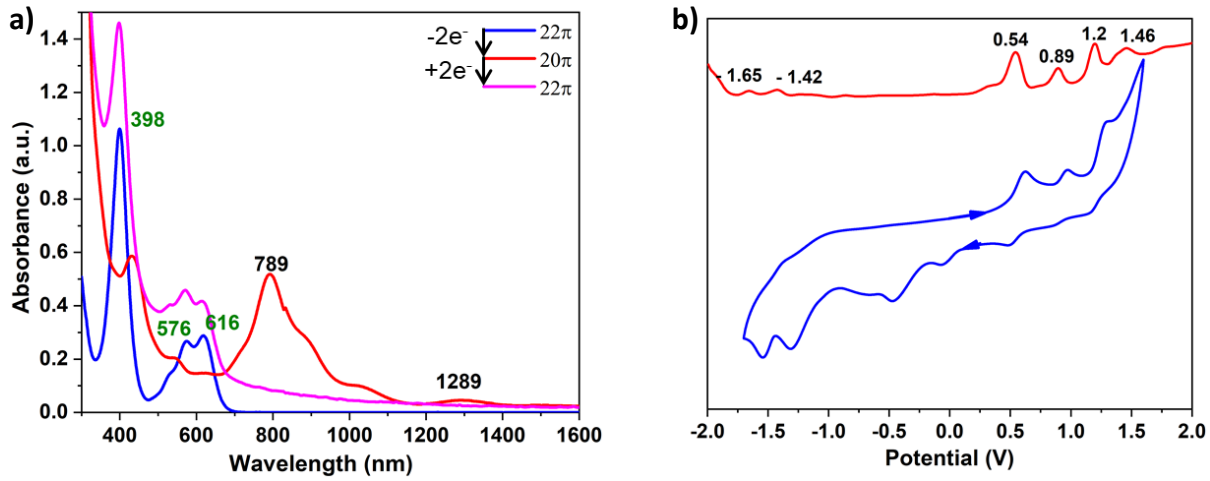

Figure IV.4: *a) UV/vis/NIR absorption spectrum of 10^{-5} M solution of **IV.3** (22π) and its oxidised species [**IV.3**]$^{2+}$ (20π) recorded in CH_2Cl_2. b) Cyclic voltammogram (CV, blue) and differential pulse voltammogram (DPV, red) of IV.3 in CH_2Cl_2 (with 0.1 M $(Bu)_4NPF_6$ as the supporting electrolyte).*

From the Cyclic voltammetry (CV) and differential pulse voltammogram (DPV) [22]isophlorin, **IV.3**, revealed at least four oxidation potentials at +0.54, +0.89, +1.2 and +1.46 V. In addition, two reduction potentials at -1.42 and -1.65 V were also observed (figure – IV.4b). Based on the potential values obtained from cyclic voltammetry, SEC studies were conducted at different oxidation potential. In the SEC studies, upon applying the first oxidation potential at + 0.6 V, 22π isophlorin undergoes one electron ring oxidation to yield 21π radical cation intermediate which displayed an absorption maxima at 446 nm along with doublet like broad band at 787 and 886 nm (figure – IV.5a). On increasing the potential to the second oxidation potential value of + 1 V, the radical cation intermediate gets oxidized to 20π dicationic species. It showed absorption maxima at 788 nm (figure – IV.5b) and this λ_{max} matched the experimental data as observed in electronic absorption from chemically oxidized species. Therefore, it confirms the formation of dicationic species [**IV.3**]$^{2+}$.

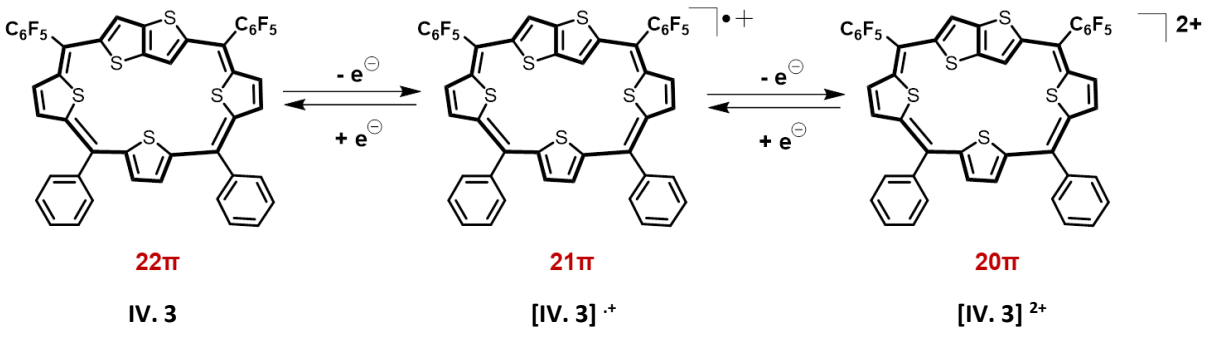

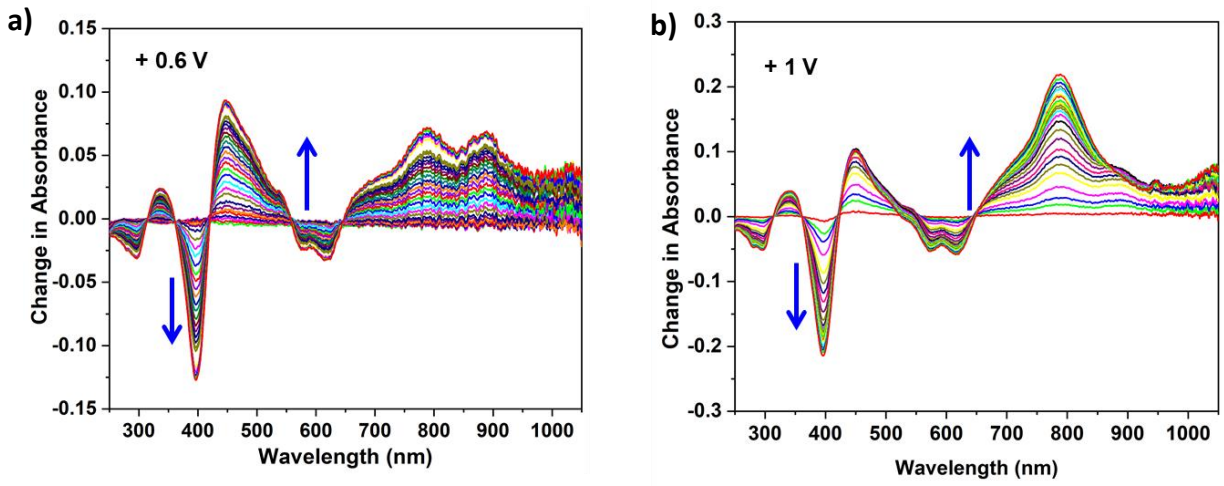

Figure IV.5: *Spectro-electro chemistry studies of IV.3. Change in absorption spectra by change in time of* ***IV.3*** *after applying a potential of + 0.6 V and + 1 V, respectively.*

From the above studies, it is evident that the replacement of a thiophene by thienothiophene alters the aromaticity and redox property of an isophlorin. Therefore, a similar modification in the electronic properties can be expected in a 30π expanded isophlorin if thiophene units are replaced by thienothiophene. Hence an attempt was made to synthesize a hexaphyrin with two thienothiophene units.

IV.3.1 Synthesis and Characterisation of Thieno[3,2-*b*]thiophene incorporated 34π Hexaphyrin

[30]hexaphyrin, **IV.4**, is a planar, rectangular shaped, Huckel's aromatic macrocycle in tune with Huckel's (4n+2)π electronic system. Synthesis of a [34]hexaphyrin, **IV.5**, was attempted by replacing the two thiophene units by fused heterocyclic thienothiophene moieties. Because of 34π electrons, **IV.5** is expected to be a Huckel's aromatic system. The macrocycle was synthesised by condensing thieno thiophene diol, **IV.11**, with thiophene based dipyrromethane, **IV.10**, in dichloromethane in the presence of $BF_3.OEt_2$ under dark and inert conditions (scheme – IV.3). The reaction was stirred for two hours followed by the addition of DDQ as oxidising agent in open atmosphere and continued stirring for additional two hours. The progress of product formation was monitored by the thin layer chromatography. It showed a dark violet-blue coloured band and further supported by MALDI TOF/TOF mass spectrometry. Later, the reaction mixture passed through short bed of basic alumina and further isolated the product by basic alumina column chromatography in 16% yields. The composition of the macrocycle, **IV.5**, was confirmed by the High Resolution Mass Spectrometry (HR-MS), in which the macrocycle displayed an *m*/*z* value of 1318.0104

corresponding to $C_{70}H_{32}F_{10}S_8$ (1318.0110) (figure – IV.6). In an alternate synthetic pathway, it was possible to synthesize the same macrocycle by condensing thieno[3,2-*b*]thiophene based tripyrromethane, **IV.12**, with pentaflurobenzaldehyde, **IV.13**, under similar reaction conditions to obtain the desired macrocycle in 9% isolated yields.

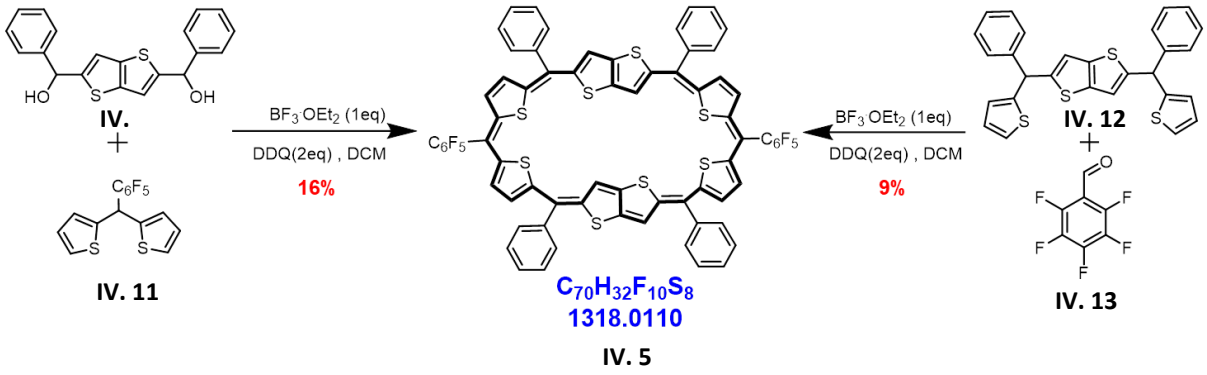

Scheme IV.3: *Synthesis of thienothiophene incorporated 34π hexaphyrin* ***IV.5.***

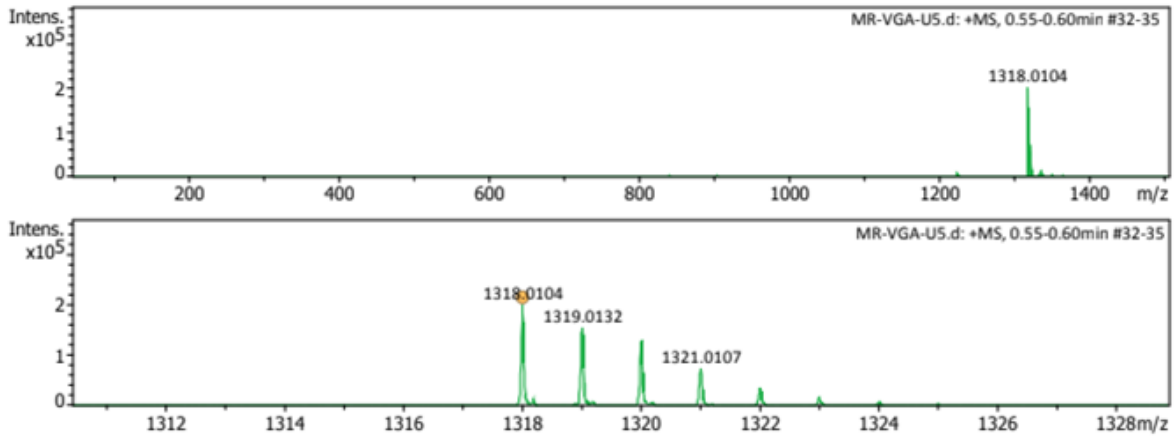

Figure IV.6: *HR-ESI-TOF mass spectrum of* ***IV.5****.*

IV.3.2 ^{1}H NMR study of 34π Hexaphyrin

[30]hexaphyrin, **IV.4**, displayed diatropic ring current effect in its ^{1}H NMR spectrum in support of the aromatic character for the macrocycle. Contrarily, [34]hexaphyrin displayed relatively weaker diatropic ring current effect suggesting poor aromatic character for the macrocycle (figure – IV.7). It was observed that thienothiophene protons resonated as a singlet in the upfield at δ 4.04 ppm and the two thiophene protons resonated in the downfield at δ 9.21 ppm and 9.38 ppm. The phenyl protons were found resonating in the region δ 7.9 to 8.5 ppm. This pattern of ^{1}H NMR signals is relatively similar to that observed for 30π hexaphyrin and hence it suggests a relatively planar conformation with a C_2 axis of symmetry

for the macrocycle, **IV.5**. Since these signals are broad at room temperature, it also hints at possible fluxional nature particularly with the thienothiophene units in the macrocycle.

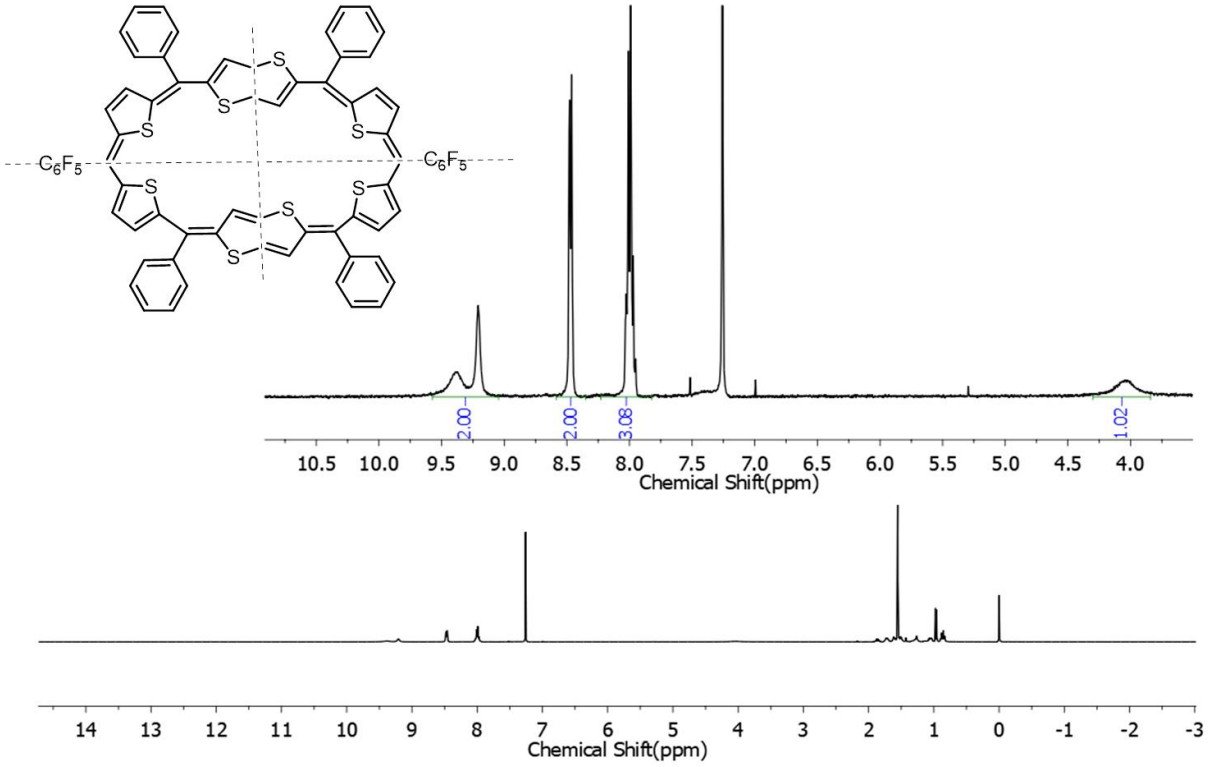

Figure IV.7: *^{1}H NMR spectrum of **IV.5** in Chloroform-d at 298 K.*

IV.3.3 Molecular structure of [34]hexaphyrin

After many efforts, good quality single crystals were grown by solvent diffusion method. Vapours of methanol were diffused into the THF solution of **IV.5** to yield shiny and rod-like shaped crystals. Single crystal X-ray diffraction studies revealed a macrocycle with rectangular shape and a planar conformation (figure – IV.8). Importantly, thioenothiophene heterocyclic units were also aligned to the global planar conformation of the macrocycle. Sulphur of all the thiophene units was oriented towards the macrocyclic centre. This structure supports the observation from ^{1}H NMR studies for a planar molecular structure and confirms that the macrocycle both in solution and solid states has a similar conformation with an aromatic character. However, the observation of only a singlet for the two protons of thienothiophene units suggests the possibility of fluxional character at room temperature. Perhaps, from low temperature ^{1}H NMR studies, it may be possible to distinguish the inner and peripheral hydrogen atoms to analyse the extent of diatropic ring current effect in the 34π macrocycle.

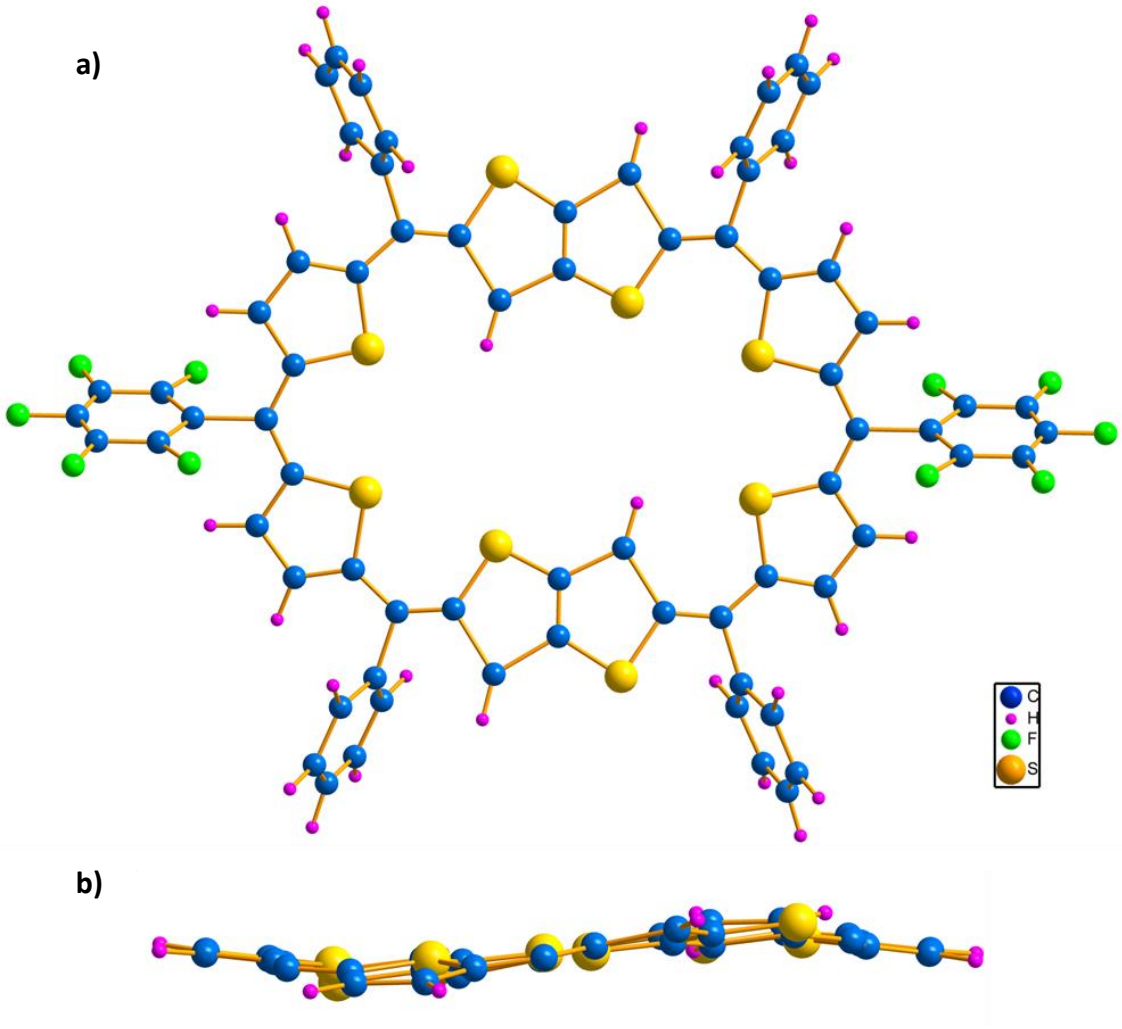

Figure IV.8: *Molecular structure of [34]hexaphyrin (**IV.5**) as determined from single crystal X-ray diffraction. Pentafluorophenyl and phenyl rings are omitted for clarity in the (b) (side view) rows.*

IV.3.4 Electronic absorption and Spectro-Electrochemical studies

[30]hexaphyrin aromatic macrocycle, **IV.4**, displayed a Soret-like band at 551 nm along with the signature Q-type bands in the lower energy region at 670 and 726 nm. Similarly [34]hexaphyrin, **IV.5**, also displayed the sharp intense absorption band at 577 nm (176800) along with bands in the lower energy region between 716 (19800) and 781 nm (20100) (figure – IV.9a). Since aromatic macrocycles are stabilized by the filled orbitals, they invariably resist two-electron ring oxidation. However, it is established that aromatic molecules are privileged to one-electron ring oxidation.[10] Yet, it was observed that $(4n+2)\pi$ non-aromatic [50]decaphyrin macrocycle undergoes reversible two-electron ring oxidation to yield the corresponding anti-aromatic dication due to its non-planar geometry.[11]

Unexpectedly, it was observed that 34π hexaphyrin aromatic macrocycle, **IV.5**, undergoes two-electron ring oxidation to yield that 32π hexaphyrin dication, [**IV.5**]$^{2+}$. Addition of oxidising agents like TFA or $NOBF_4$ or Meerwein's salt induces a subtle colour change from dark violet-blue colour to reddish brown in dichloromethane. This change was also accompanied with a red shift by more than 140 nm. The dicationic species, [**IV.5**]$^{2+}$, showed and λ_{max} at 724 nm (180300) along with less intense and lower energy bands at 967 (10500) and 1095 nm (11700) (figure – IV.9a). The oxidized species could be reduced back to the neutral 34π species by the addition of reducing agents like triethyl amine or zinc powder. Further, its redox properties were studied through electrochemical techniques such as cyclic voltammetry (CV) and spectro-electrochemistry (SEC).

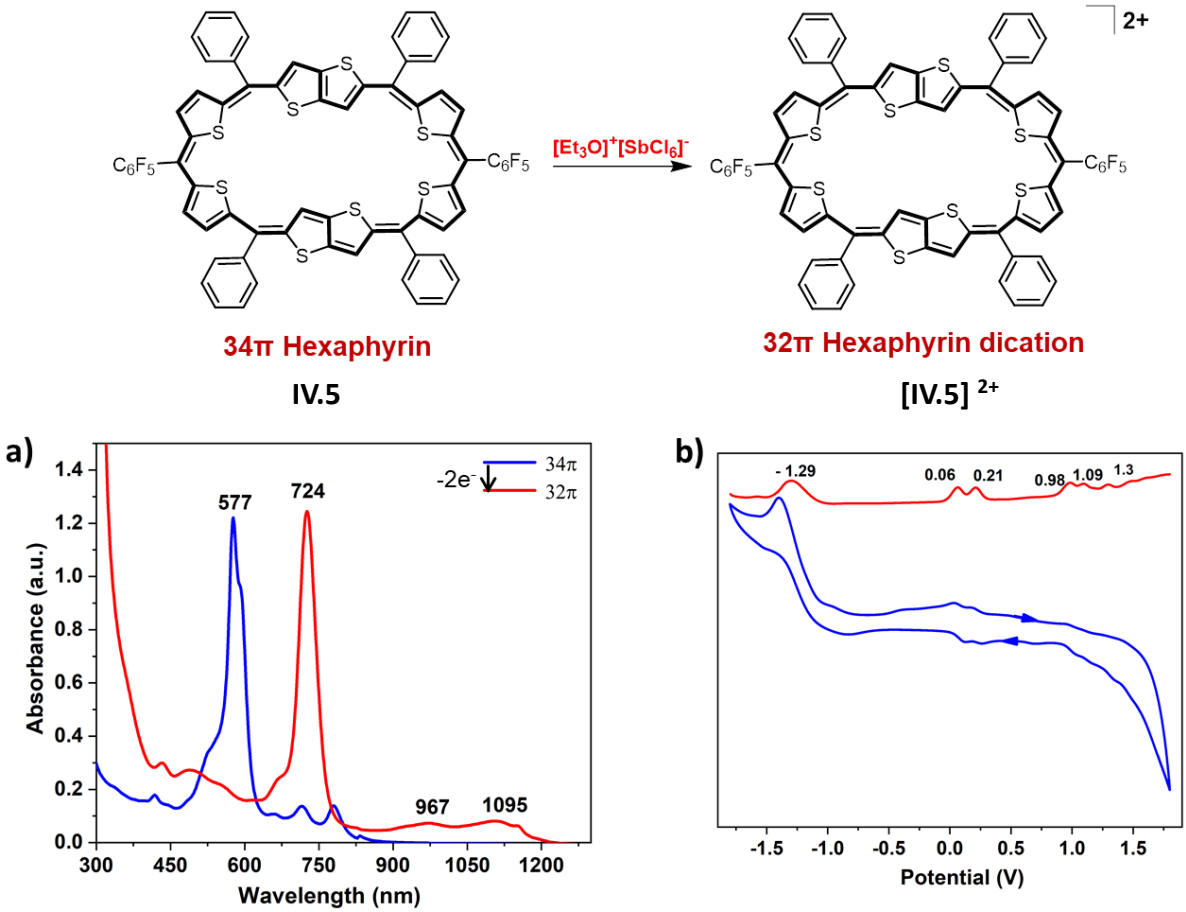

Figure IV.9: *a) UV/vis/NIR absorption spectrum of 10^{-5} M solution of **IV.5** (34π) and its oxidised species [**IV.5**]$^{2+}$ (32π) recorded in CH_2Cl_2. b) Cyclic voltammogram (CV, blue) and differential pulse voltammogram (DPV, red) of IV.5 in CH_2Cl_2 (with 0.1 M $(Bu)_4NPF_6$ as the supporting electrolyte).*

In the Cyclic voltammogram (CV) and differential pulse voltammogram (DPV) studies [34]hexaphyrin, **IV.5**, revealed five oxidation potentials at + 0.06, + 0.21, + 0.98, + 1.09 and +1.3 V along with a solitary reduction potential at – 1.29 V (figure – IV.9b). From the potential values obtained by cyclic voltammetry, spectro-electrochemistry (SEC) studies were carried out by applying the different potentials to record the absorption maxima (figure – IV.10). At the first applied potential of + 0.1 V, 34π macrocycle undergoes a one-electron oxidation to yield a 33π radical cation intermediate which displayed absorption maxima at 623 nm along with a shorter band at 731 nm (figure – IV.10a). Upon applying the second oxidation potential at + 0.26 V SEC the radical cation was oxidized to the 32π dicationic species [**IV.5**]$^{2+}$ which displayed an absorption maxima at 721 nm (figure – IV.10b) exactly matching the chemical oxidation observed from UV-visible spectroscopic study. These observations unequivocally confirms that aromatic [34]hexaphyrin, **IV.5**, undergoes two-electron ring oxidation to yield the 32π dicationic species, [**IV.5**]$^{2+}$.

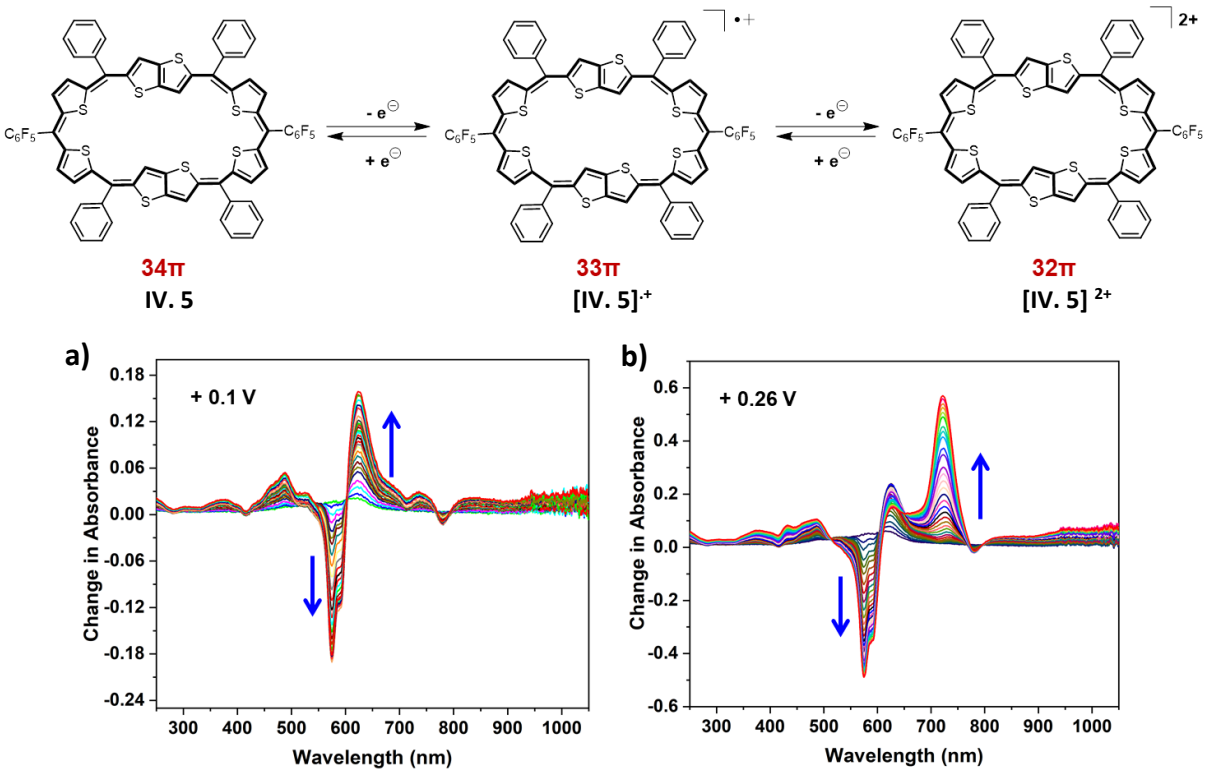

Figure IV.10: *Spectro-electro chemistry studies of **IV.5**. Change in absorption spectra by change in time of IV.5 after applying a potential of + 0.1 V and + 0.26 V, respectively.*

IV.3.5 Computational studies

Theoretical calculations help to understand the aromatic character of the [34]hexaphyrin, **IV.5** as observed in the ^{1}H NMR and X-ray diffraction studies. The estimated NICS (0) value -15.56 ppm, supports the aromatic nature of the macrocycle. AICD plot displayed the clock-wise electron density confirms the diatropic ring current of the macrocycle to substantiate the aromatic character. The extended π-conjugation reflecting in the decreased HOMO-LUMO energy gap of the macrocycle is 1.44 eV.

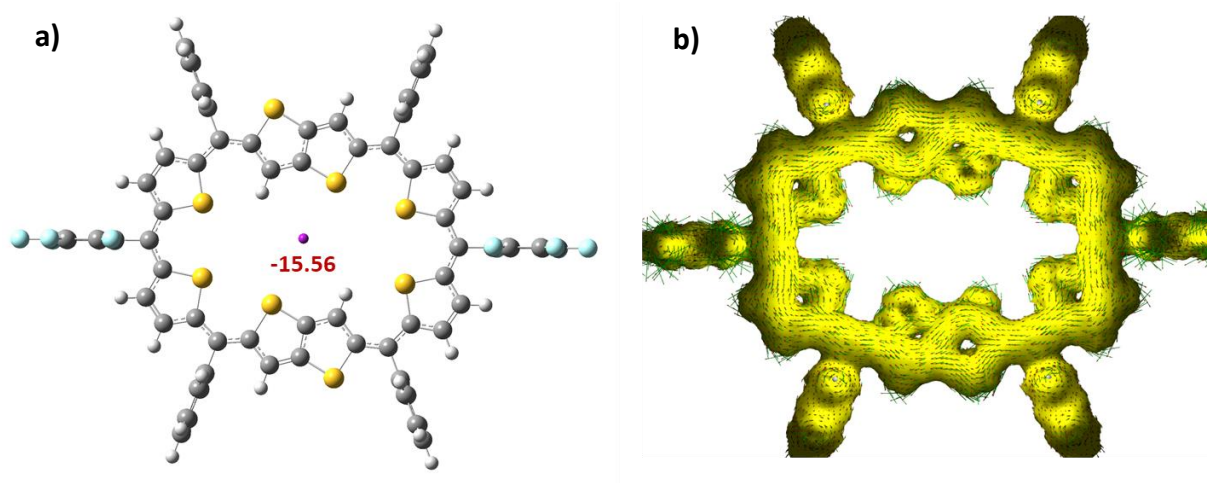

Figure IV.11: *(a) The estimated NICS (0) value mentioned at the centre of the macrocycle **IV.5** and (b) AICD plot of **IV.5** at an isosurface value 0.06 the external magnetic field is applied orthogonal to the macrocyclic plane.*

IV.4 Conclusions

Thieno[3,2-*b*]thiophene is a six-electron fused heterocycle. Its incorporation into any isophlorin system by replacing the thiophene unit alters the aromaticity by extending the π-conjugation. Particularly, it depends on the number of thienothiophene units being included in an isophlorin network. As in the first case, replacing only a thiophene in 4nπ tetrathiophene isophlorin alters the aromaticity to yield a (4n+2)π electrons 22π expanded isophlorin, **IV.3**. On the other hand, replacing two units of thiophenes in a 30π hexaphyrin, **IV.4**, by thienothiophene yielded a (4n+2)π expanded isophlorinod. These finding suggests that replacing an odd thiophene unit alters both the electronic and aromatic characteristics. However, replacing even number of thiophene units yields π-expanded macrocycle while retaining the same aromatic feature. In this chapter, Thieno[3,2-*b*]thiophene incorporated two different aromatic macrocycles, that is 22π isophlorin and 34π hexaphyrin were synthesized and characterized successfully. 22π isophlorin, **IV.3**, represents the smallest aromatic macrocycle in the isophlorin series. ^{1}H NMR studies revealed that the macrocycle is non-aromatic in nature because of the absence of diatropic ring current. By virtue of its non-aromatic character **IV.3** undergoes two-electron ring oxidation to yield 20π dication, through the formation of 21π radical cation intermediate as studied from the SEC studies. Thieno[3,2-*b*]thiophene incorporated 34π hexaphyrin is Huckel's aromatic macrocycle, showed moderate diatropic ring current. Single crystal X-ray diffraction studies revealed a planar conformation evident for the aromatic character of the macrocycle. Noticeably, upon the addition of oxidising agents like TFA or $NOBF_4$ or Meerwein's salt, the macrocycle undergoes two-electron ring oxidation to 32π electronic system, through the formation of 33π radical cation intermediate observed in the SEC studies. These studies suggest that the insertion of thienothiophene units induces a steric hindrance and hence leads to modification of electronic, redox and structural features as attested by spectro-electrochemical studies.

IV.5 General Experimental Methods

3-Bromothiophene-2-carbaldehyde

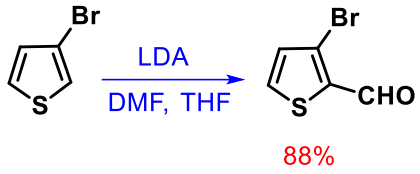

3-bromothiophene (1 mmol) taken in dry THF in a two neck round bottom flask, freshly prepared LDA (1.2 mmol) was added dropwise at 0 ^{0}C, stir the reaction mixture for about 45mins at same temperature and add dry DMF (1.3 mmol) at 0 ^{0}C, continued the reaction for another three hours. Quench the reaction by the addition of 1M HCl and extracted the organic layer by the ethyl acetate. The product was distilled as colourless oil, obtained yield 88 %.

^{1}H NMR (400 MHz, Chloroform-*d*) δ 9.98 (s, 1H), 7.72 (dd, *J* = 5.1 Hz, 1H), 7.15 (dt, *J* = 5.1 Hz, 1H).

Ethyl thieno[3,2-b]thiophene-2-carboxylate

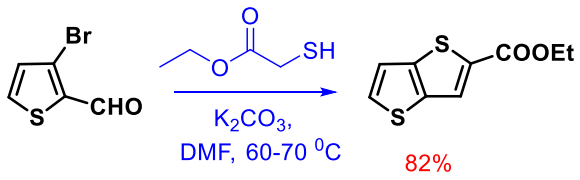

3-Bromothiophene-2-carbaldehyde (1 mmol) added slowly to a reaction mixture containing ethyl 2-sulfanylacetate (1.1 mmol), potassium carbonate (1.5 mmol) in N, N-dimethylformamide at room temperature and stirred the reaction mixture for three days. Quenched the reaction by ice water and extracted the reaction mixture by dichloromethane, dried over Na_2SO_4 and distil the final ester product as colourless oil, obtained yield is 82%.

^{1}H NMR (400 MHz, Chloroform-*d*) δ 7.99 (d, 1H), 7.58 (d, *J* = 5.3 Hz, 1H), 7.37 – 7.22 (d, *J* = 5.3 Hz, 1H), 4.39 (q, *J* = 7.1 Hz, 2H), 1.44 – 1.37 (m, *J* = 7.1 Hz, 3H).

Thieno[3,2-b]thiophene-2-carboxylic acid

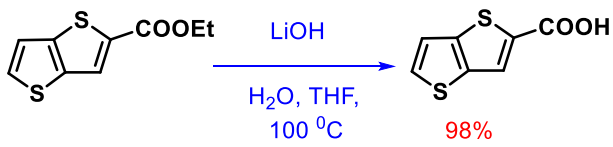

Deesterification was achieved, in a stirred reaction mixture containing the ester (1 mmol), hydrous lithium hydroxide (excess) in Tetrahydrofuran solvent, reflux the reaction mixture for 3 hours, remove the solvent under reduced pressure and wash the residue with the con. HCl, filtered the precipitate and dried product gave the acid and the yield is 98%.

^{1}H NMR (400 MHz, Chloroform-*d*) δ 8.10 (d, 1H), 7.65 (d, J = 5.3 Hz, 1H), 7.32 (dd, J = 5.3, 0.7 Hz, 1H).

Thieno[3,2-b]thiophene

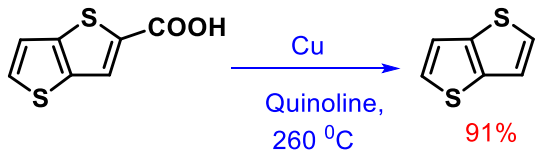

Decarboxylation done in high temperature, acid (1 mmol) and excess of copper powder taken in Quinoline solvent and reflux the reaction mixture up to 260 ^{0}C in silicone oil bath for one hour, when there is no further bubbles of carbon dioxide, take down the temperature to room temperature and remove the quinolone by the addition of repeated acid wash. The product was isolated by the silica gel chromatography using pet ether as eluent. The product obtained in 91% yield as colourless solid. [12]

^{1}H NMR (400 MHz, Chloroform-*d*) δ 7.37 (d, J = 5.0 Hz, 1H), 7.25 (d, J = 5.0 Hz, 1H).

Thieno[3,2-b]thiophene dialdehyde

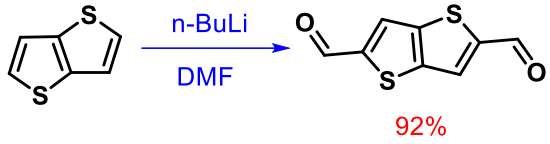

Thienothiophene (1 mmol) and TMEDA (2.3 mmol) dissolved in dry tetrahydrofuran taken in a flame dried two necks of round bottom flask and n-BuLi (2.3 mmol) added dropwise at -78 ^{0}C, after that took the reaction mixture slowly to reflux condition and reflux the reaction mixture to three hours, added the dry DMF (3 mmol) slowly (dissolved in THF) at 0 ^{0}C, continued the reaction for another three hours. Quenched the reaction by 1M HCL; extracted the organic layer by the ethyl acetate. The product highly insoluble in non-polar solvent and then filtered the solid. The product obtained as dark brown solid in 92% yield.

^{1}H NMR (400 MHz, Chloroform-*d*) δ 10.05 (s, 1H), 8.01 (s, 1H).

2, 5-Bis(phenylhydroxymethyl) Thieno[3,2-b]thiophene:

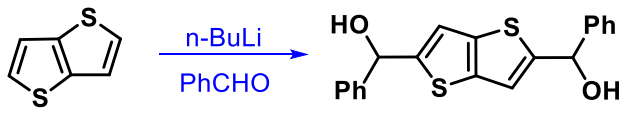

82%

In a flame died round bottom flask, thiophene (1 mmol) and TMEDA (2.3 mmol) dissolved in dry n-hexane and lowering the temperature to -78 ^{0}C, added the n-BuLi (2.3 mmol) to a reaction mixture dropwise. Refluxed the reaction for one hour and cooldown the reaction mixture to 0 ^{0}C, the dropwise addition of benzaldehyde (2.5 mmol taken in THF) and continued the reaction to another three hours in room temperature. Quenched the reaction by saturated NH_4Cl, extracted the reaction mixture by ethyl acetate. The product purified through recrystallization by DCM/n-hexane. The diol obtained as light brown solid in 82% yield.

^{1}H NMR (400 MHz, Chloroform-*d*) δ 7.49 – 7.42 (m, 4H), 7.40 – 7.30 (m, 6H), 6.99 (d, 2H), 6.06 (s, 2H), 1.67 ppm (brs, 2H).

2, 5-Bis(pentafluorophenylhydroxymethyl) Thieno[3,2-b]thiophene:

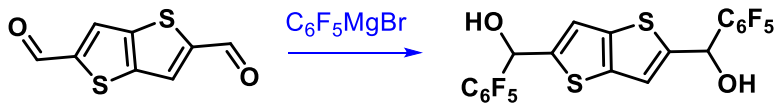

81%

Aldehyde (1 mmol) taken in the dry THF, followed by the addition of freshly prepared C_6F_5MgBr (2.5 mmol) at 0 ^{0}C, continued the reaction for three hours. Then quenched the reaction mixture by the addition of saturated ammonium chloride. Then extracted the reaction mixture by ethyl acetate and recrystallize the reaction mixture by the DCM/ n-hexane combination. The product obtained as light yellowish solid in 81%.

^{1}H NMR (400 MHz, Chloroform-*d*) δ 7.82 (d, 2H), 6.14 (s, 2H), 3.12 ppm (brs, 2H).

2,5-bis (phenyl (thiophen-2-yl) methyl) thieno[3,2-b]thiophene and 2,5-bis (pentafluorophenyl (thiophen-2-yl) methyl) thieno[3,2-b]thiophene:

Thienothiophene diol (1 mmol), dissolved in excess of dry thiophene taken in two neck dry round bottom flask. Slow addition of $BF_3.OEt_2$ (1 mmol) in dark and continued the reaction for half an hour. Reaction progress and product formation confirmed by the thin layer chromatography. The reaction quenched by the water, then extracted the reaction mixture by the dichloromethane solvent, isolated the product by pet ether in silica gel column chromatography.

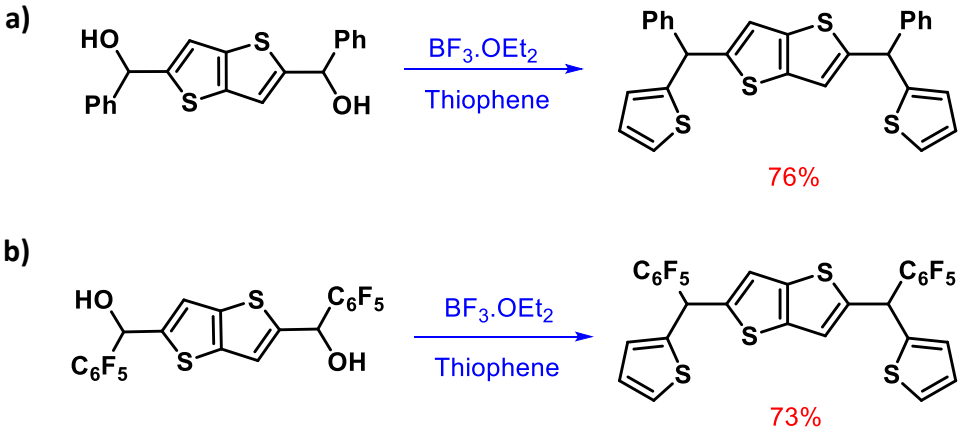

a) **^{1}H NMR** (400 MHz, Chloroform-*d*) δ 7.32 (d, 5H), 7.22 (dd, *J* = 5.1, 1.1 Hz, 1H), 6.94 (dd, *J* = 5.1, 3.5 Hz, 1H), 6.88 (d, 1H), 6.85 (dt, *J* = 3.5, 1.1 Hz, 1H), 5.85 (d, *J* = 1.1 Hz, 1H).

b) **^{1}H NMR** (400 MHz, Chloroform-*d*) δ 7.27 (dd, *J* = 5.1, 1H), 7.07 (d, 1H), 7.01 (d, *J* = 3.4 Hz, 1H), 6.98 (dd, *J* = 5.1, 3.4 Hz, 1H), 6.24 (s, 1H).

Synthesis of thieno[3,2-b]thiophene incorporated 22π isophlorin:

In a dried two neck round bottom flask, thienothiophene (1 mmol) and trithiophene diol (1.2 mmol) dissolved in dry dichloromethane, catalytic amount of $BF_3.OEt_2$ (0.75 mmol) added slowly in the dark and stirred the reaction for two hours. Then an oxidising agent DDQ (2.5 mmol) added and open the reaction to open atmosphere continued the reaction for another two hours, quenched the reaction by few drops of triethyl amine. The reaction mixture passed through the short bed of basic alumina, the reaction mixture was concentrated and further purified by basic alumina column chromatography using CH_2Cl_2/Hexane as eluent, isolated the yield in 11%.

The same product also prepared by condensing the thioenothiophene based tripyrromethane with pentafluorobenzaldehyde in same reaction condition and the isolated yield was 7.3%.

IV.3: ^{1}H NMR (400 MHz, Chloroform-*d*) δ 7.81 (s, 1H), 7.40 – 7.31 (m, 3H), 7.17 (dd, 2H), 6.37 (d, *J* = 6.0 Hz, 1H), 6.20 (dt, *J* = 6.0, 2.1 Hz, 1H), 6.13 (s, 1H). **UV/Vis/NIR** (CH_2Cl_2): λ_{max} nm (ε) $Lmol^{-1}cm^{-1}$ = 398 (109900), 576 (27610) and 619(29780). **HR-MS** (ESI-TOF): m/z = 919.9844 (found), 919.9852 (Calcd. For $C_{46}H_{18}F_{10}S_5$).

[IV.3]$^{2+}$: UV/Vis/NIR (CH_2Cl_2): λ_{max} nm (ε) $Lmol^{-1}cm^{-1}$ = 432 (605990), 792 (535600) and 1289(4750).

Synthesis of thieno[3,2-b]thiophene incorporated 34*π* hexaphyrin:

Thienothiophene diol (1.2 mmol) and thiophene dipyrromethane (1 mmol) dissolved in the dry dichloromethane taken in a 250ml flame dried two necks round bottom flask in nitrogen atmosphere. Catalytic amount of Lewis acid $BF_3.OEt_2$ (0.75 mmol) added in dark and stirred the reaction for two hours and in open atmosphere DDQ (2.5 mmol) was added, continued the reaction for another two hours. Then quenched the reaction by few drops of triethyl amine and passed the reaction mixture through the basic alumina column. Isolated the pure product by basic alumina column using DCM/n-Heaxne as eluent, isolated yield was 16%.

The reaction also possible by condensing the thienothiophene tripyrromethane with pentafluorobenzaldehyde and followed by the same reaction condition, obtained yield was 9%.

IV.5: ^{1}H NMR (400 MHz, Chloroform-*d*) δ 9.30 (d, 2H), 8.65 – 8.32 (m, 2H), 8.14 – 7.89 (m, 3H), 4.04 (s, 1H). **UV/Vis/NIR** (CH_2Cl_2): λ_{max} nm (ε) $Lmol^{-1}cm^{-1}$ = 577 (176800), 716 (19840) and 781 (20130). **HR-MS** (ESI-TOF): m/z = 1318.0104 (found), 1318.0110 (Calcd. For $C_{70}H_{32}F_{10}S_8$).

Selected Crystal data of III.14: $C_{76}H_{32}F_{10}S_8$, (M_r = 1318.12), monoclinic, space group *Cmc2$_1$*, *a* = 41.727 (8), *b* = 10.438 (2), *c* = 18.801 (4) Å, $\alpha = 89.81^0$, $\beta = 90^0$, $\gamma = 90^0$; *V* = 8188.3 (6) $Å^3$, *Z* = 1.2, *T* = 100 K , D_{calcd} = 1.053 gcm^{-3}, R_1 = 0.0654 (I > 2sigma (I)), R_w (all data) = 0.0957, GOF = 1.004;

[IV.5]$^{2+}$: UV/Vis/NIR (CH_2Cl_2): λ_{max} nm (ε) $Lmol^{-1}cm^{-1}$ = 724 (180300), 967(10570) and 1095 (11730).

IV.6 References:

1. Burchard Franck and Ansgar Nonn, Novel Porphyrinoids for Chemistry and Medicine by Biomimetic Syntheses, *Angew, Chem, Int. Ed.*, **1995**, *34*, 1795-1811.
2. Shohei Saito and Atsuhiro Osuka, Expanded Porphyrins: Intriguing Structures, Electronic Properties, and Reactivities, *Angew. Chem. Int. Ed*. **2011**, *50*, 4342 – 4373.
3. Sumit Sahoo, Manik Jana and Harapriya Rath, Tailor-made aromatic porphyrinoids with NIR absorption, *Chem. Commun*., **2022**, *58*, 1834–1859.
4. Harapriya Rath, Abhijit Mallick, Tubai Ghosha and Alok Kalita, Aromatic fused heterocyclic [22] macrocycles with NIR absorption, *Chem. Commun*., **2014**, *50*, 9094—9096.
5. AbhijitMallick, JuwonOh, DonghoKim, and Harapriya Rath, Aromatic Fused [30] Heteroannulenes with NIR Absorption and NIR Emission : Synthesis , Characterization , and Excited-State Dynamics. *Chem.Eur.J.*, **2016**, *22*, 8026–8031.
6. Abhijit Mallick, Juwon Oh, Marcin A. Majewski, Marcin Stępien, Dongho Kim and Harapriya Rath, Protonation Dependent Topological Dichotomy of Core Modified Hexaphyrins: Synthesis, Characterization, and Excited State Dynamics, *J. Org. Chem.*, **2017**, *82*, 556−566.
7. Takanori Soya and Atsuhiro Osuka, Internally Bridged Heckel Aromatic [46]Decaphyrins: (Doubly-Twisted-Annuleno) Doubly-Twisted-Annulene Variants, *Chem. Eur. J*., **2019**, *25*, 5173 – 5176.
8. Masaru Kon-no, John Mack, Nagao Kobayashi, Masahiko Suenaga, Kenji Yoza, and Teruo Shinmyozu, Synthesis, Optical Properties, and Electronic Structures of Fully Core-Modified Porphyrin Dications and Isophlorins, *Chem. Eur. J*., **2012**,*18*, 13361 – 13371.
9. J. Sreedhar Reddy and Venkataramanarao G. Anand, Aromatic Expanded Isophlorins: Stable 30π Annulene Analogues with Diverse Structural Features, *J. Am. Chem. Soc.*, 2009, 131, 42, 15433–15439.
10. Rathore, R.; Kumar, A. S.; Lindeman, S. V.; Kochi, J. K. Preparation and Structures of Crystalline Aromatic Cation-Radical Salts. Triethyloxonium Hexachloroantimonate as a Novel (One-Electron) Oxidant. *J. Org. Chem.*, **1998**, *63* (17), 5847–5856.
11. Hosahalli S. Udaya, Ashokkumar Basavarajappa, Tullimilli Y. Gopalakrishna and Venkataramanarao G. Anand, Topoisomers and aromaticity of a redox active 50p core-modified isophlorinoid, *Chem. Commun*., **2022**, *58*, 13931–13934.
12. Lance S. Fuller, Brian Iddon and Kevin A. Smith, Thienothiophenes. Part 2. Synthesis, metallation and bromine→lithium exchange reactions of thieno[3,2-b]thiophene and its polybromo derivatives, *J. Chem. Soc., Perkin Trans. 1*, **1997**, 3465-3470.

13. Gopalakrishna, T. Y.; Anand, V. G., Reversible Redox Reaction between Antiaromatic and Aromatic States of 32π-Expanded Isophlorins. *Angew. Chem., Int. Ed.* **2014,** *53* (26), 6678-6682.

Summary of the Thesis

This thesis describes a variety of thiophene based expanded isophlorinoids varying from 22π to 80π electrons. All the macrocycles were characterized through spectroscopic techniques to evaluate their (anti)aromatic and non-(anti)aromatic characteristics both in solution and solid states. Expanded porphyrinoids display a variety of non-planar structures and hence deviate from the aromatic characteristics. However they are highly redox active species as attested by proton coupled electron transfer (PCET) reactions because of pyrrole's amine-imine interconversion to switch between aromatic and antiaromatic states. In contrast, non-pyrrolic macrocycles prefer to adopt isophlorin-like framework and undergo facile one/two electron ring oxidation. But a majority of non-pyrrolic systems are limited to eight or less number of heterocyclic units. The present thesis is a synthetic endeavour of expanded non-pyrrolic isophlorin systems. Thiophene is the building block in these systems to study their aromaticity, conformational dynamics and redox chemistry. A novel one-pot condensation of thiophene with pentafluorobenzaldehyde through the modified Rothemund-Lindsey synthetic strategy, yielded a series of thia-isophlorinoids from four to sixteen heterocyclic units corresponding to open shell (4n+1), (4n+3) and closed shell 4n and (4n+2) π-electron systems. In contrast to the typical figure-of-eight conformation, octaphyrin, with 40 π-electrons displayed temperature dependent planar and non-planar conformations in the solution state. But it displayed only planar conformation in the solid state. Remarkably, the 50π decaphyrin macrocycle showed two topoisomers and can adopt to either a unique [6+4] or a near-planar [5+5] conformation depending on the solvent of crystallization. It undergoes facile reversible two-electron ring oxidation to yield the largest planar antiaromatic dication bearing 48 π-electrons. In this series, 60π dodecaphyrin and 70π tetradecaphyrin are the largest isolated macrocycles along its π-electron path. In a modified synthetic approach, pentathia 24π sapphyrin displayed paratropic ring current effect in ^{1}H NMR spectrum. Single crystal X-ray diffraction studies revealed a planar conformation for the macrocycle. In contrast, a 26π pentathia sapphyrin was identified as non-aromatic because macrocycle not display significant diatropic ring current effect in its ^{1}H NMR spectrum. It was observed that these two macrocycles undergo facile two-electron ring oxidation through the formation of radical cation intermediate as confirmed by spectro-elctrochemistry (SEC) studies. The higher analogue 48π decaphyrin adapts to 'figure-of-eight' conformation with non-antiaromatic character. Similarly, 52π decaphyrin was also identified as non-aromatic in nature and both macrocycles undergo two-electron ring oxidation to yield the respective

dicationic species. Thieno[3,2-*b*]thiophene incorporation in isophlorin alters the aromaticity and also extend in the π-conjugation. 22π isophlorin exhibited non-aromatic character as observed from ^{1}H NMR studies. 34π hexaphyrin displayed aromatic character both in solution and solid state. Single crystal X-ray diffraction studies revealed a planar conformation for the 34π macrocycle. Both macrocycles undergo two-electron ring oxidation through the formation of radical cation intermediate as confirmed by the SEC studies. The strength of the anti (aromaticity) was confirmed by NICS and AICD calculations. Cyclic voltammetry studies revealed the redox active nature of these macrocycles with multiple oxidation and reduction potentials. Spectro-electrochemical measurement confirmed facile reversible two-electron ring oxidation and the unstable radical cation intermediate in these macrocyclic systems.